

# Journal of Advances in Information Fusion

A semi-annual archival publication of the International Society of Information Fusion

Regular Papers	Page
Forty Years of Multiple Hypothesis Tracking ..... <i>Chee-Yee Chong, Los Altos, CA, USA</i> <i>Shozo Mori, Sacramento, CA, USA</i> <i>Donald B. Reid, Sunnyvale, CA, USA</i>	131
Multiple-Hypothesis Tracking and Graph-Based Tracking Extensions ..... <i>Stefano P. Coraluppi, Woburn, MA, USA</i> <i>Craig A. Carthel, Woburn, MA, USA</i> <i>Alan S. Willsky, Cambridge, MA, USA</i>	152
Conditions for MHT to be an Exact Bayesian Solution to the Multiple Target Tracking Problem for Target-to-Measurement Association Hypotheses ..... <i>Lawrence D. Stone, Reston, VA, USA</i>	167
Three Mathematical Formalisms of Multiple Hypothesis Tracking ..... <i>Shozo Mori, Sacramento, CA, USA</i> <i>Chee-Yee Chong, Los Altos, CA, USA</i> <i>Kuo-Chu Chang, George Mason University, Fairfax, VA, USA</i>	176
On Indistinguishability and Antisymmetry Properties in Multiple Target Tracking ..... <i>Wolfgang Koch, Fraunhofer FKIE, Wachtberg, Germany</i>	199
Multiscan Implementation of the Trajectory Poisson Multi-Bernoulli Mixture Filter ..... <i>Yuxuan Xia, Chalmers University of Technology, Göteborg, Sweden</i> <i>Karl Granström, Chalmers University of Technology, Göteborg, Sweden</i> <i>Lennart Svensson, Chalmers University of Technology, Göteborg, Sweden</i> <i>Angel F. García-Fernández, University of Liverpool, Liverpool, U.K.</i> <i>Jason L. Williams, Queensland University of Technology, Brisbane, Australia</i>	213

*From the  
Editor-In-Chief*

*Guest Editorial:  
Foreword to the  
Special Issue  
on Multiple-  
Hypothesis  
Tracking*

# INTERNATIONAL SOCIETY OF INFORMATION FUSION

The International Society of Information Fusion (ISIF) is the premier professional society and global information resource for multidisciplinary approaches for theoretical and applied INFORMATION FUSION technologies. Technical areas of interest include target tracking, detection theory, applications for information fusion methods, image fusion, fusion systems architectures and management issues, classification, learning, data mining, Bayesian and reasoning methods.

## JOURNAL OF ADVANCES IN INFORMATION FUSION: December 2019

---

<b>Editor-In-Chief</b>	Uwe D. Hanebeck	Karlsruhe Institute of Technology (KIT), Germany; +49-721-608-43909; uwe.hanebeck@ieee.org
Associate	Stefano Coraluppi	Systems & Technology Research, USA; +1 781-305-4055; stefano.coraluppi@ieee.org
<b>Administrative Editor</b>	David W. Krout	University of Washington, USA; +1 206-616-2589; dkrou@apl.washington.edu
Associate	Ruixin Niu	Virginia Commonwealth University, Richmond, Virginia, USA; +1 804-828-0030; rniu@vcu.edu
Associate	Marcus Baum	Karlsruhe Institute of Technology (KIT), Germany; +49-721-608-46797; marcus.baum@kit.edu

## EDITORS FOR TECHNICAL AREAS

---

<b>Tracking</b>	Paolo Braca	NATO Science & Technology Organization, Centre for Maritime Research and Experimentation, Italy; +39 0187 527 461; paolo.braca@cmre.nato.int
Associate	Florian Meyer	University of California at San Diego, USA, +1 858-246-5016; flmeyer@ucsd.edu
<b>Detection</b>	Pramod Varshney	Syracuse University, Syracuse, New York, USA; +1 315-443-1060; varshney@syr.edu
<b>Fusion Applications</b>	Ben Slocumb	Numerica Corporation; Loveland, Colorado, USA; +1 970-461-2000; bjslocumb@numerica.us
Associate	Ramona Georgescu	United Technologies Research Center, East Hartford, Connecticut, USA; 860-610-7890; georgera@utrc.utc.com
<b>Image Fusion</b>	Lex Toet	TNO, Soesterberg, 3769de, Netherlands; +31 346356237; lex.toet@tno.nl
Associate	Ting Yuan	Mercedes Benz R&D North America, USA; +1 669-224-0443; dr.ting.yuan@ieee.org
<b>High-Level Fusion</b>	Lauro Snidaro	Università degli Studi di Udine, Udine
<b>Fusion Architectures and Management Issues</b>	Chee Chong	BAE Systems, Los Altos, California, USA; +1 650-210-8822; chee.chong@baesystems.com
<b>Classification, Learning, Bayesian and Other Reasoning Methods</b>	Nageswara S. V. Rao	Oak Ridge National Laboratory, USA; +1 865-574-7517;
Associate	Claude Jauffret	Université de Toulon, La Garde, France; + 33 (0) 4 94 14 24 14; jauffret@univ-tln.fr
	Jean Dezert	ONERA, Palaiseau, 91120, France; +33 180386564; jean.dezert@onera.fr

Manuscripts are submitted at <http://jaif.msubmit.net>. If in doubt about the proper editorial area of a contribution, submit it under the unknown area.

## INTERNATIONAL SOCIETY OF INFORMATION FUSION

---

Paulo Costa, *President*

Paulo Costa, *President-elect*

Stefano Coraluppi, *Secretary*

Chee Chong, *Treasurer*

Dale Blair, *Vice President Publications*

David W. Krout, *Vice President Communications*

Lance Kaplan, *Vice President Conferences*

Anne-Laure Jousselme, *Vice President Membership*

Darin Dunham, *Vice President Working Groups*

Uwe Hanebeck, *JAIF EIC*

Roy Streit, *Perspectives EIC*

Journal of Advances in Information Fusion (ISSN 1557-6418) is published semi-annually by the International Society of Information Fusion. The responsibility for the contents rests upon the authors and not upon ISIF, the Society, or its members. ISIF is a California Nonprofit Public Benefit Corporation at P.O. Box 4631, Mountain View, California 94040. **Copyright and Reprint Permissions:** Abstracting is permitted with credit to the source. For all other copying, reprint, or republication permissions, contact the Administrative Editor. Copyright© 2019 ISIF, Inc.

# From the Editor-in-Chief:

December 2019



Chee-Yee Chong



Stefano Coraluppi



Jason Williams

## Guest Editorial: Foreword to the Special Issue on Multiple-Hypothesis Tracking

Welcome to the December 2019 issue of the *Journal of Advances in Information Fusion* (JAIF) published by the International Society for Information Fusion. *Multitarget tracking* (MTT) is an important technical challenge that has featured prominently in these pages since the inception of JAIF in 2006. Of course, the field has a much longer history. Ignoring the earlier foundational mathematical developments, we can perhaps identify the start of the field with the seminal advances to recursive estimation theory due to Kalman [1] and early work on the data association problem due to Sittler [2].

In a paper at the 1978 IEEE Conference on Decision and Control, Donald Reid presented a contribution on *multiple-hypothesis tracking* (MHT) [3]. The subsequent journal article that appeared the following year, in the December 1979 issue of the IEEE TRANSACTIONS ON AUTOMATIC CONTROL, gave visibility to the approach and has been cited widely [4]. MHT is well established as the leading operational methodology for MTT and is at the core of many successful, fielded surveillance systems.

Forty years on, C.-Y. Chong and S. Coraluppi held a special session titled *Forty Years of MHT* at the 2018 International Conference on Information Fusion

(FUSION) that received great interest and participation [5]. This success encouraged us to propose a JAIF special issue on MHT: this December 2019 issue.

So, what has happened in the field from December 1979 to December 2019? We encourage readers to examine the paper by C.-Y. Chong et al. for a panoramic view of many developments, including track-oriented MHT and distributed MHT. The paper by S. Coraluppi et al. focuses on recent graph-based extensions that lead to significant computational gains in certain multisensor settings. The paper by L. Stone focuses on the target-to-measurement association hypothesis, which is different from the measurement-to-measurement hypothesis in standard MHT, showing that this definition provides an exact Bayesian solution to the MTT problem under very general assumptions. The paper by Mori et al. explores alternative mathematical formalisms for MHT.

As with other MTT paradigms, there are limitations to what can be achieved with MHT. A particular challenge is that of merged measurements, for which connections to theoretical physics are explored in the paper by W. Koch. In recent years, a popular formulation of the MTT problem in the research community has emerged via the *random finite set* (RFS) machinery. The paper

by Y. Xia et al. explores multiscan processing in the RFS framework, thus offering an alternative approach to multiple-hypothesis reasoning.

We hope that the readers of this issue will find the contributions to be valuable to review some of the key advances in MTT over the past 40 years, to clarify the theoretical basis for MHT, and to identify new results and directions for promising research.

#### REFERENCES

1. R. Kalman  
"A new approach to linear filtering and prediction problems,"  
*Trans. ASME, Ser. D—J. Basic Eng.*, vol. 82, no. 1, pp. 35–45,  
Mar. 1960.
2. R. Sittler  
"An optimal data association problem in surveillance theory,"  
*IEEE Trans. Mil. Electron.*, vol. 8, no. 2, pp. 125–139,  
Apr. 1964.
3. D. Reid  
"An algorithm for tracking multiple targets," in  
*Proc. IEEE Conf. Decis. Control*, San Diego, CA, 1978.
4. D. Reid  
"An algorithm for tracking multiple targets,"  
*IEEE Trans. Autom. Control*, vol. 24, no. 6, pp. 843–854,  
Dec. 1979.
5. International Society of Information Fusion,  
*Proc. 21st Int. Conf. Inf. Fusion*, Cambridge, U.K., Jul. 2018.

# Forty Years of Multiple Hypothesis Tracking

CHEE-YEE CHONG  
SHOZO MORI  
DONALD B. REID

**Multiple hypothesis tracking (MHT) addresses difficult association problems in multiple target tracking by forming and evaluating data association hypotheses with multiple scans or frames of data. This paper reviews 40 years of MHT research and development since publication of the measurement-oriented MHT journal paper in 1979. It covers hypothesis-oriented and track-oriented MHT, distributed MHT, graph-based association, other MHT research, and the relationship with multitarget filters using random finite sets. It also reviews use of MHT in surveillance and other applications.**

Manuscript received February 16, 2019; revised September 3, 2019; released for publication February 5, 2020.

C.-Y. Chong is an Independent Researcher, Los Altos, CA, USA (E-mail: cychong@ieee.org).

S. Mori is with Systems & Technology Research, Sacramento, CA, USA (E-mail: smori@ieee.org).

D. B. Reid, retired, was with Lockheed Martin, Sunnyvale, CA, USA. He resides in San Jose, CA, USA (E-mail: donreid63@yahoo.com).

1557-6418/19/\$17.00 © 2019 JAIF

## I. INTRODUCTION

Data association is a key component of multiple target tracking (MTT) [1]–[10]. In fact, early papers [11], [12] in MTT frequently include “association” or “correlation” in their titles. The need to utilize multiple frames or scans of data for tracking multiple targets in difficult scenarios was recognized long ago, but early work focused on single target tracks, according to the survey in [1]. The use of multiple data association hypotheses to explain the origins of all measurements first appeared in the late 1970s, with batch solution of the best hypothesis by 0–1 integer programming [13], and recursive evaluation of multiple association hypotheses by computing their probabilities [14], [15]. Almost immediately, multiple hypothesis tracking (MHT) became the standard approach for tracking multiple targets when data association is difficult due to high target density, dense clutter, low probability of detection, etc.

Over the past 40 years, much research has been performed to generalize MHT [16] and address the inherent combinatorial growth in the number of hypotheses [17], [18]. The original measurement-oriented MHT, commonly called hypothesis-oriented MHT (HOMHT), is made practical by efficient algorithms to find the top-ranking hypotheses [19]–[23] and compute the bounds for the highest probabilities [24]. Track-oriented MHT (TOMHT) [17], [25]–[29] has been proposed as a more efficient alternative to the original HOMHT by maintaining association hypotheses at the individual track level and finding the best hypothesis only when needed, using integer programming, multidimensional (MD) assignment, or other methods [30]–[37]. Techniques for finding the top-ranking hypotheses are also available [38], [39].

When sensors are physically distributed, communicating measurements to a centralized tracker is often not feasible due to network bandwidth constraints. A distributed tracking system consists of trackers processing local sensor measurements and sending the results to another tracker for further processing. A distributed version of MHT that communicates hypotheses was proposed in [40]–[43]. Even though communicating hypotheses is not practical, this research identifies issues and techniques for associating tracks with dependent state estimation errors caused by prior communication or common process noise [44]. A more practical approach is communicating tracks from local trackers [45]. When MHT is performed on multiple platforms, the track pictures have to be consistent for distributed decision making [46]. For tracking with a single sensor, MHT is frequently used in a multistage architecture [47], with the first stage removing clutter to generate tracklets [48] of measurements that can be associated with individual targets without ambiguity, and the second stage associating tracklets [49].

Modern fusion systems utilize many sensors to track large numbers of targets. For large-scale tracking

problems, even the most efficient TOMHT implementation suffers from combinatorial explosion. Association graphs have been proposed for implicit representation of all association ambiguities, with tracks represented by paths in the graph, and association hypotheses as sets of feasible paths [50]–[52]. When the track likelihoods satisfy a Markov property, a track likelihood is a product of pairwise association scores and the best hypothesis can be found by efficient graph algorithms [53]–[62]. However, MHT is most useful when the Markov property is not satisfied, e.g., when target feature data are present. Adapting graph-based algorithms for feature-aided association and non-Markov likelihoods is nontrivial [63]–[68].

Standard MHT assumes one-to-one association between measurements. Since this assumption is not valid for some tracking problems, MHT has been adapted to handle unresolved measurements [69], [70], multiple measurements from a single target [71], [72], extended objects [73], and merging and splitting targets [74], [75]. MHT requires data association to be consistent; i.e., measurements in a single scan/frame cannot be associated independently. Probabilistic MHT (PMHT) [76], [77] assumes independent measurement associations even though it has MHT in its name.

The computation complexity of MHT has resulted in much research to investigate other solution techniques. These include Markov chain Monte Carlo (MCMC) for data association [78]–[84] and message passing/belief propagation based on a graphical model of the tracking problem [85]–[88].

Displaying the output of MHT to an operator has to address track switching and jitter resulting from changes in the best or most likely hypothesis. Although MHT output display has not received as much attention as algorithm research, there is some progress in this area [89]–[92].

Detecting a target from a single frame of measurements is difficult when the signal-to-noise ratio is low. Using multiple frames to consider possible target trajectories can increase the probability of detecting targets and reduce false alarm rates. Multiple frame detection is basically track initiation or extraction and has been performed using MHT [93], [94], or with sequential probability ratio tests (SPRTs) [95]–[98].

Random finite set (RFS) for multitarget filtering has been a very active research area in recent years [99], [100]. Since the goal is finding the multitarget state probability density function (pdf), there is no explicit association in the model and filter equations. Thus, RFS-based filters appear to be different from MHT and cannot be used for tracking or forming trajectories, at least in the earlier forms [101]–[104]. Recent research has revealed MHT-like structures [105]–[114] in random set multitarget filters. In addition, MHT can be shown to have a solid theoretic foundation using random set formalisms [115], [116].

MHT is used primarily in defense and security applications where data association is difficult due to the nature of the targets. In particular, MHT is widely used in ocean, maritime, ground, air, and space surveillance [117]–[160]. Sensors include sonar, radar, electro-optical, seismic, etc. Each application domain has different target and sensor characteristics, resulting in different data association problems that MHT has to address. Because of the proliferation of video cameras, video tracking has become a very active area of research [161]–[188]. The nature of the association problem is amenable to efficient solution by graph-based methods. Other applications of MHT involve meteorology, astronomy, text messaging, cyber security, and biological and medical imaging [189]–[202].

This paper reviews key developments in MHT over the past 40 years. It may be viewed as a continuation of the tutorial in 2004 [17], and supplements the MHT chapters in books on tracking and fusion [2]–[10]. A review of this type reflects the limited knowledge and inevitable biases of the authors, especially given the large number of papers related to MHT published in diverse journals and conference proceedings. As of November 2019, [15] had 1530 citations according to IEEE Xplore and 3434 citations according to Google Scholar. Since we cannot include or read all references carefully, we apologize for omissions or misinterpretations and would appreciate any corrections or comments on this paper.

The structure of this paper is as follows. Section II presents target and sensor models, and defines hypotheses and tracks. Sections III and IV present the HOMHT and TOMHT. Section V discusses distributed MHT for single and multiple sensors. Section VI presents a graph model for data association and efficient solutions under the Markov assumption. Section VII discusses relaxation of assumptions and extensions to MHT. Section VIII presents the relationship between MHT and RFS approaches. Section IX lists some applications, and Section X concludes the paper by discussing possible research directions.

## II. MULTIPLE HYPOTHESIS TRACKING

MHT uses target and sensor models to form association hypotheses for the origins of all measurements and computes their probabilities. We use MHT to stand for both multiple hypothesis tracking and multiple hypothesis tracker. The specific meaning should be obvious from the context.

### A. Target and Measurement Models

The number of targets at time  $t$  is  $N_t$ . Each target has a hybrid (continuous–discrete–mixture-valued) state  $x_t$ . Given  $N_t$ , the target states are independent and identically distributed (i.i.d.) Markov processes with transition probability  $f_{t|t'}(x|x')$ .

Suppose there are  $K$  frames or scans of data taken at  $t_1 \leq \dots \leq t_K$ . Each frame consists of  $m_k$  measurements  $Z_k = (z_k^j)_{j=1}^{m_k}$ , where a measurement  $z$  is independently generated from the target state  $x$  by the pdf  $p_M(z|x)$  that may depend on time and the reporting sensor. A target at state  $x$  is independently detected according to a probability  $p_D(x)$ . For each  $k$ , the number of false alarms is  $N_{FAk}$  with some probability distribution density  $p_{FA}(z)$  for their values.

### B. Tracks and Hypotheses

A track  $\tau$  is a sequence of measurement indices  $(j_k)_{k=1}^K$  of cumulative measurements  $Z_{1:K} \triangleq (Z_k)_{k=1}^K$  hypothesized to originate from the same target, where  $j_k = 0$  indicates no measurement or that the target hypothesized by  $\tau$  is undetected. A data association hypothesis  $\lambda$  is a collection of tracks that explains the origins of all measurements. In the MHT literature, it is common practice to refer to data association hypothesis as hypothesis. If the sensor resolution is such that two targets cannot generate one measurement, then two tracks in the same hypothesis cannot share the same measurement.

The definitions of track and hypothesis first appear in [13], which also views a hypothesis as a partition of the cumulative measurements. Data association hypothesis is sometimes called global hypothesis to distinguish it from track hypothesis that concerns only association of measurements with individual targets. We prefer to use global hypothesis to represent the association hypothesis that results from fusing local association hypotheses in distributed tracking.

## III. HYPOTHESIS-ORIENTED MHT

HOMHT recursively generates hypotheses on the origins of measurements and computes the probability of each hypothesis. In the 1970s, there was a lot of interest in correlation techniques for naval ocean surveillance, where association with kinematic data only is difficult because observations or contacts are sparse. Thus, it is useful to use MHT to delay association decisions until good feature data are available. HOMHT consists of recursive generation, evaluation, and management of hypotheses [14], [15].

### A. Hypothesis Generation

Let  $\lambda_{k-1}$  be a hypothesis on the cumulative data  $Z_{1:k-1}$ . Multiple new hypotheses  $\lambda_k$  on  $Z_{1:k}$  are generated by hypothesizing different associations of the measurements in  $Z_k$  with the tracks in  $\lambda_{k-1}$ . A measurement  $z_k^j$  may be associated with an existing track  $\tau_{k-1}^i$  in  $\lambda_{k-1}$ , with a newly detected target, or be hypothesized as a false alarm. A target hypothesized by an existing track  $\tau_{k-1}^i$  in  $\lambda_{k-1}$  may not be detected in  $Z_k$ . This approach is called measurement oriented in [15] because it uses pos-

sible origins of measurements to generate new hypotheses. It is commonly called hypothesis-oriented MHT because of the recursive generation of hypotheses.

### B. Hypothesis Evaluation

Let  $Z$  and  $\bar{Z}$  represent  $Z_{1:k}$  and  $Z_{1:k-1}$ , and  $\lambda$  and  $\bar{\lambda}$  be hypotheses on  $Z$  and  $\bar{Z}$  such that  $\bar{\lambda}$  is the unique predecessor of  $\lambda$ . For a track  $\tau$  in  $\lambda$  and any frame index  $k' \in K$ , let  $Z_{k'|\tau}$  be the measurement in  $Z_{k'}$  specified by  $\tau$ . If  $\tau$  has no measurement in  $Z_{k'}$ , then we say  $Z_{k'|\tau} \triangleq \theta$ , representing a hypothesized nondetection. Let  $Z_{|\tau}$  be the sequence of measurements specified by  $\tau$ . Then, the probability of the hypothesis is evaluated recursively by

$$P(\lambda|Z) = C(Z)^{-1} P(\bar{\lambda}|\bar{Z}) L_k^{FA}(Z_k|\lambda) \prod_{\tau \in \lambda} L_k(Z_{k|\tau}|\bar{Z}_{|\tau}), \quad (1)$$

where  $C(Z)$  is a normalization constant,  $L_k^{FA}(Z_k|\lambda)$  is the likelihood of  $N_{FT}$  hypothesized false alarms given by

$$L_k^{FA}(Z_k|\lambda_k) = \beta_{FAk}^{N_{FT}} \quad (2)$$

with constant false alarm density  $\beta_{FAk}$ , and  $L_k(Z_{k|\tau}|\bar{Z}_{|\tau})$  is the likelihood of associating  $Z_{k|\tau} = z_k^j$  with the predecessor track  $\bar{\tau}$  in  $\bar{\lambda}$ . There are three types of  $L_k(z_k^j|\bar{Z}_{|\tau})$ .

1) Likelihood of  $z_k^j$  from a previously detected target:

$$L_k(z_k^j|\bar{Z}_{|\tau}) = p_{Dk} N(z_k^j - H_k \bar{x}_\tau, B_{k\tau}^j), \quad (3)$$

where  $N(x, P)$  is the zero-mean normal density with covariance  $P$ ,  $H_k$  is the measurement matrix, and  $\bar{x}_\tau$  and  $B_{k\tau}^j$  are the predicted estimate and corresponding error covariance, respectively.

2) Likelihood of previously detected target being undetected:

$$L(\theta|Z_{|\tau}) = 1 - p_{Dk}. \quad (4)$$

3) Likelihood of the hypothesized number  $N_{NT}$  of newly detected target ( $\bar{\tau} \triangleq \phi$ ):

$$L(z_k^j|Z_{|\phi}) = \beta_{NTk}. \quad (5)$$

Equations (1)–(5) define the algorithm in [14] and [15], using Poisson–Gaussian models for target dynamics and sensor measurements. Those likelihoods (2)–(5) are reformulated in [16] for more general target and sensor models, without linearity or Gaussian assumptions. When the number of targets is constant and Poisson distributed, the target states are i.i.d. random processes, and the number of false alarms is Poisson but not uniformly distributed, then the likelihoods are given by the following:

1) False alarm likelihood:

$$L_k^{FA}[Z_k|\lambda] = e^{-\bar{\nu}_{FAk}} \prod_{j \in J_{FAk}(\lambda)} \beta_{FAk}(z_k^j), \quad (6)$$

where  $J_{FAk}(\lambda)$  is the set of measurement indices for the false alarms as hypothesized by  $\lambda$ , and  $\bar{\nu}_{FAk} = \int_{E_M} \beta_{FAk}(z) \mu_M(dz)$  is the expected number of false

alarms in frame  $k$ , with the measure  $\mu_M$  on the measurement space.

2) Likelihood of  $z_k^j$  originating from a previously detected target ( $\bar{\tau} \neq \phi$ ):

$$L_k(z_k^j | \bar{Z}_{|\bar{\tau}}) = \int_X p_{Mk}(z_k^j | x) p_{Dk}(x) p_k(x | \bar{Z}_{|\bar{\tau}}) \mu(dx). \quad (7)$$

3) Likelihood of  $\bar{\tau} \neq \phi$  being undetected:

$$L_k(\theta | \bar{Z}_{|\bar{\tau}}) = \int_X (1 - p_{Dk}(x)) p_k(x | \bar{Z}_{|\bar{\tau}}) \mu(dx). \quad (8)$$

4) Likelihood of  $z_k^j$  originating from a newly detected target:

$$L_k(z_k^j | \bar{Z}_{|\phi}) = \int_X p_{Mk}(z_k^j | x) p_{Dk}(x) \beta_{NT}(x) \mu(dx), \quad (9)$$

where  $\beta_{NTk}(x) = \bar{v}_{NTk} p_k(x | \bar{Z}_{|\phi})$  is the density of undetected targets.

In (7) and (8),  $p_k(x | Z_{|\tau})$  is the track state probability distribution determined by the predecessor track  $\bar{\tau}$  and  $Z$ . When  $x$  is Gaussian, this distribution is represented by means and covariances. The hybrid measure  $\mu$  is introduced to handle the hybrid state with both continuous and discrete variables. For discrete random variables, the integral becomes a summation.

The expected number  $v_{NT}$  of targets that remain undetected through  $k$  frame is calculated from the expected number  $\bar{v}_{NT}$  of undetected targets in  $\bar{Z}$  as

$$v_{NTk} = \bar{v}_{NTk} \int_X [1 - p_{Dk}(x)] p_k(x | \bar{Z}_{|\phi}) \mu(dx). \quad (10)$$

The state distributions for the tracks are updated by

$$p_k(x | Z_{|\tau}) = d^{-1} p_{Mk}(z_k^j | x) p_{Dk}(x) p_k(x | \bar{Z}_{|\bar{\tau}}) \quad (11)$$

for a track  $\tau$  with a detection  $z_k^j$ , and

$$p_k(x | Z_{|\tau}) = d'^{-1} (1 - p_{Dk}(x)) p_k(x | \bar{Z}_{|\bar{\tau}}) \quad (12)$$

for a track  $\tau$  with no detection at frame  $k$ . Equation (12) is also used to compute  $\beta_{NTk}(x)$ , the density of undetected targets. In (11) and (12),  $d$  and  $d'$  are normalizing constants. The likelihoods (2)–(5) are a special case with linear and Gaussian models, and uniform detection probability.

### C. Hypothesis Management or Implementation

Since the number of hypotheses grows rapidly with the number of frames, hypothesis management techniques are needed to make recursive MHT practical [15], [17]. Common techniques are pruning low-probability hypotheses, combining hypotheses with similar tracks, and decomposing targets and measurements into clusters [18] that can be solved independently.

Hypothesis pruning requires finding the hypotheses with the highest probabilities. At first, heuristic methods and search techniques were used, but results were frequently not satisfactory. HOMHT became practical

only after efficient techniques for generating the  $m$ -best hypotheses were developed [19]–[21] using Murty's algorithm [22]. A reformation of the HOMHT [15] with Murty's algorithm is discussed in [23]. A method for estimating the bounds to the hypothesis probabilities is given in [24]. These bounds are useful for validating the correctness of the implementation.

When needed, the probability of a track can be computed as the sum of the probabilities of all hypotheses containing the track. Since it may be very difficult to enumerate and evaluate all hypotheses, track probability calculation is almost always approximate.

## IV. TRACK-ORIENTED MHT

TOMHT is usually claimed to be more efficient than HOMHT because it recursively generates only tracks and finds the best association hypothesis only when needed [17], [25]. Even though [25] is one of the earliest references on the implementation of TOMHT, the concept of TOMHT first appeared in [13], which uses integer programming to find the best hypothesis over a batch of data, and a design for implementation is presented in [26].

### A. Batch Hypothesis Evaluation

The probability of a hypothesis  $\lambda_K$  on the cumulative data  $Z_{1:K}$  can be computed [40] as

$$P(\lambda_K | Z_{1:K}) = C(Z_{1:K})^{-1} l_K^{FA}(Z_{1:K} | \lambda_K) \prod_{\tau \in \lambda_K} l_K(\tau, Z_{1:K}), \quad (13)$$

where  $C(Z_{1:K})$  is a normalizing constant,  $l_K^{FA}(Z_{1:K} | \lambda_K)$  is the likelihood of false alarms, and  $l_K(\tau, Z_{1:K})$  is the likelihood of the track  $\tau$  given by

$$l_K(\tau, Z_{1:K}) = \bar{v} \prod_{k=1}^K \left\{ \int g_k(Z_{k|\tau} | x) p_k(x | Z_{1:(k-1)|\tau}) \mu(dx) \right\} \quad (14)$$

with the generalized likelihood  $g_k(z|x)$  accounting for detection probability, i.e.,

$$g_k(z|x) = \begin{cases} p_{Mk}(z|x) p_{Dk}(x), & \text{if } z \neq \theta, \\ 1 - p_{Dk}(x), & \text{if } z = \theta. \end{cases} \quad (15)$$

Equation (13) assumes that the number of targets is Poisson distributed. Hypothesis evaluation for non-Poisson number of targets is discussed in [27]. This formulation assumes that there are no target births and deaths. Target appearance and disappearance are due to entry into and exit from the sensor field of view. Ref. [28] presents a model with target births that are never detected. The dimensionless scoring of MHT is discussed in [29].

## B. Finding the Best Hypothesis

By suppressing the time index  $K$ , and using the appropriate normalization, (13) becomes

$$P(\lambda|Z) = C(Z)^{-1} \prod_{\tau \in \lambda} l(\tau), \quad (16)$$

where  $C(Z)$  is a normalization constant. The best hypothesis is then the maximum a posteriori (MAP) solution for (16).

1) 0–1 Integer Linear Programming Formulation: Taking the negative logarithm of (16) and ignoring the normalization constant results in the following additive cost:

$$J(\lambda|Z) \triangleq \sum_{\tau \in \lambda} c(\tau), \quad (17)$$

where  $c(\tau) = -\ln l(\tau)$ . The optimization problem is then minimizing (17) subject to the constraint that  $\lambda$  does not have tracks sharing the same reports.

Let  $M$  be the number of tracks and  $c = [c_1, \dots, c_M]^T$  be the  $M$ -dimensional vector with  $c_j = c(\tau_j)$ . A hypothesis  $\lambda$  is represented by the  $M$ -dimensional vector  $x = [x_1, \dots, x_M]^T$ , where  $x_j = 1$  if track  $\tau_j \in \lambda$ , and  $x_j = 0$  otherwise. Then, the MAP solution is given by the integer linear programming problem

$$\begin{aligned} & \text{minimize} && c^T x \\ & \text{subject to} && Ax \leq b \\ & \text{and} && x_j \in \{0, 1\} \text{ for all } j \in \{1, \dots, M\}, \end{aligned} \quad (18)$$

where  $A$  is an  $N \times M$  matrix with  $A_{ij} = 1$  if the report  $z_i$  is included in the track  $\tau_j$ , and  $b$  is a vector of 1's with dimension  $N$  being the number of reports. The constraint  $Ax \leq b$  states that tracks in a single hypothesis cannot share the same reports.

The integer linear programming formulation first appeared in [13], with an NP-hard exact solution. A solution is usually found by relaxing the integer value constraint of  $x_j$  and solving the standard linear programming problem [30]. When the solution is noninteger, branch-and-bound techniques are used.

2) MD Assignment Formulation: The MAP solution can be reformulated as an MD assignment problem [31]–[33]. Let  $j_k$  be the index of measurement  $z_k^{j_k}$  in frame  $k$  and  $z_k^0$  be a dummy measurement representing non-detection. A track hypothesis  $\tau$  can be represented by an indicator function  $\tau_{j_1 \dots j_K}$ , where

$$\tau_{j_1 \dots j_K} = \begin{cases} 1, & \text{if } \tau = ((1, j_1), \dots, (K, j_K)), \\ 0, & \text{otherwise,} \end{cases} \quad (19)$$

and a measurement (index) not in any track is a false alarm.

Let  $c_{j_1 \dots j_K} = c(\tau)$  be the cost of the track  $\tau$ . Then, the minimization of (17) is equivalent to the following MD

assignment problem:

$$\text{minimize} \quad \sum_{j_1=0}^{m_1} \cdots \sum_{j_K=0}^{m_K} c_{j_1 \dots j_K} \tau_{j_1 \dots j_K} \quad (20)$$

$$\text{subject to} \quad \sum_{j_1=0}^{m_1} \cdots \sum_{j_{k-1}=0}^{m_{k-1}} \sum_{j_{k+1}=0}^{m_{k+1}} \cdots \sum_{j_K=0}^{m_K} \tau_{j_1 \dots j_K} = 1 \quad (21)$$

for all  $j_k = 1, 2, \dots, m_k$  and  $k = 1, 2, \dots, K$ . Constraints (21) specify that each measurement can belong to only one track. The cost  $c_{00 \dots 0}$  is defined to be zero. If  $y$  is defined to be the vector formed from all  $\tau_{j_1 \dots j_K}$ , then (20) and (21) have the form of minimize  $c^T y$  subject to  $By = 1$ , which is an integer linear program.

Since the exact solution of MD assignment is NP-hard, approximate solutions are needed. Although there are differences in the specific steps, most approximate MD assignment techniques are based upon Lagrangian relaxation.

TOMHT can be formulated as the maximum weight independent set partition (MWISP) problem [34] with a hypothesis represented by a partition. This approach is not as popular as integer linear programming or MD assignment because the best partition is usually found by a greedy search procedure [35], [36].

## C. Track Management or Implementation

Even though TOMHT is more efficient than HOMHT, the number of tracks still grows rapidly with the number of frames. Since the likelihood and state estimate must be generated for each track, efficient track management is essential. In addition to HOMHT hypothesis management techniques,  $N$ -scan pruning is a common method used in almost all TOMHT algorithms [17], [30]. After a best hypothesis is found, the tracks in the hypothesis are used to prune tracks that do not share ancestor nodes with them. As in HOMHT, clustering decomposes the data association problem into independent problems. An approach for clustering for MD assignment is described in [37].

Unlike HOMHT, TOMHT does not require hypothesis evaluation at each frame. Still it is useful to estimate the probability of the best hypothesis. Techniques for finding the  $m$ -best hypotheses have been developed for both MD assignment [38] and integer programming algorithms [39]. The probabilities of the  $m$ -best hypotheses can be used to compute the probability of a track.

## V. DISTRIBUTED MHT

When sensors are physically distributed, communicating all measurements to a central tracker is often not feasible due to bandwidth constraints. In a distributed tracking system, the local trackers process the local sensor measurements and send the processing results to be fused by another tracker. Even when the sensors are co-located, it is sometimes desirable for each sensor to have

its own tracker to distribute and simplify processing, especially when the sensors are of different types, such as radar and electro-optical.

#### A. Distributed MHT for Multiple Sensors

Distributed tracking must address issues such as what information should be communicated between local trackers, and how trackers process results from other trackers. The first distributed MHT assumes local trackers communicate and fuse local hypotheses and tracks [40]–[43]. Although the approach was demonstrated on a small distributed sensor network and validated using real flight data, communicating multiple hypotheses is not practical because it requires more bandwidth than sending sensor measurements. However, this research addresses the key issues for distributed tracking, such as removal of redundant information in tracks and evaluation of track-to-track association likelihoods. Almost all practical distributed MHT communicate a single hypothesis consisting of high-quality tracks.

The potential of using MHT in a hierarchical tracking architecture was recognized in the early days of MHT. In fact, the ocean surveillance correlation problem that motivated MHT research involves contact reports that are outputs from other systems. If these reports can be converted into measurements with independent errors, then MHT can process them in the usual manner. Otherwise, some form of decorrelation is needed to remove this dependence. The All Source Track and Identity Fuser (ATIF) [30] uses MHT to fuse tracks from multiple sensors. The first version avoids the temporal correlation in the track reports by processing the measurements in the tracks instead of the state estimates. The second version decorrelates the tracks to form equivalent measurements with independent errors. Let  $\hat{x}_{k_1|k_1}^{s,i}$ ,  $P_{k_1|k_1}^{s,i}$ ,  $\hat{x}_{k_2|k_2}^{s,i}$ , and  $P_{k_2|k_2}^{s,i}$  be the state estimates and error covariances of a track  $i$  by sensor  $s$  at times  $k_1$  and  $k_2$  with  $k_2 > k_1$ . Then, the equivalent measurement  $y_{k_2}^{s,i}$  and its covariance  $V_{k_2}^{s,i}$  are given by

$$(V_{k_2}^{s,j})^{-1}y_{k_2} = (P_{k_2|k_2}^{s,i})^{-1}\hat{x}_{k_2|k_2}^{s,i} - (P_{k_1|k_1}^{s,i})^{-1}\hat{x}_{k_1|k_1}^{s,i}, \quad (22)$$

$$(V_{k_2}^{s,j})^{-1} = (P_{k_2|k_2}^{s,i})^{-1} - (P_{k_1|k_1}^{s,i})^{-1}. \quad (23)$$

The equivalent measurement represents the new information contained in the measurements of the track between  $k_1$  and  $k_2$ , and is called tracklet in [48]. In this paper, we will follow the more common definition of tracklet as a short track consisting of measurements from the same target. This equivalent measurement of (22) and (23) is only approximate when the target dynamics have nonzero process noise [44]. The distributed MHT in [45] uses equivalent measurements from passive and active sensors to score association hypotheses.

The concept of data frame or scan is essential to HOMHT or recursive MHT. Since tracklets are not defined at a single observation time, there is no obvi-

ous way of organizing them into frames or scans. Thus, TOMHT is more appropriate for processing tracklets [49]. In particular, TOMHT has a natural formulation as graph-based association discussed in Section VI.

Due to processing differences, communication delays, and failures, the MHT on multiple platforms may produce different results. Conflicting track pictures are problematic when they are used for distributed decision making. An approach for maintaining a single integrated air picture for multiple platforms is developed in [46].

#### B. Multistage MHT for Single Sensor

Multistage processing for single sensor tracking is basically a data compression technique with a front-end tracker that processes the sensor measurements to remove clutter and generate tracks as inputs for the back-end tracker. The back-end tracker usually does some pre-processing such as checking the quality of input tracks and breaking them if necessary [47].

When the front-end tracker generates pure tracklets with little association uncertainty, the inputs to the back-end tracker can be represented by an association graph [50]. Then, the MHT can be solved efficiently if some Markov assumptions are satisfied, as discussed in Section VI.

### VI. GRAPH-BASED ASSOCIATION

Advances in sensing and communication technologies have resulted in surveillance systems with many sensors collecting data on large numbers of targets. For example, ground-based or airborne video sensors are used to track moving vehicles in urban environments. Tracking with kinematic measurements alone is difficult due to high target density, occlusion from buildings, and large amounts of measurements. Thus, target feature observations are needed for accurate association and sparse feature data necessitate the use of MHT to maintain multiple hypotheses until feature observations are received to select the correct hypothesis. The “big data” problem is usually addressed with a hierarchical architecture with sensors generating pure tracklets and a high-level tracker associating the tracklets to form target tracks. The MHT problem can then be represented as an association graph [50], which has efficient solutions under some assumptions [51], [52].

#### A. Association Graph

Representation of tracks as paths over a trellis first appears in [53] and an efficient solution is given in [54]. However, it did not receive much attention in the traditional tracking community until recently even though graph representation of data association is quite standard in video tracking (Section IX-E). The nodes of an association graph are sensor reports that may be individual measurements or tracklets (sequence of measurements associated with same target with high confidence).

Each node is associated with a probability distribution of the state given measurements in the tracklet.

An edge connects two nodes when the reports can be associated with the same target. Two temporally overlapping tracklets from the same sensor cannot be associated. The weight of the edge represents the likelihood of association. Since association is a bidirectional relationship, the association graph is in general undirected. If the tracklets are from the same sensor, the graph is directed with a direction defined by the start or end times of the nodes.

An association graph provides an efficient implicit representation of tracks and hypotheses in MHT. A track is a path in the track graph and an association hypothesis is a set of consistent tracks, where consistency means that no two tracks in a hypothesis can share a single report. If there are no false reports, a hypothesis is a partition of all the reports or a nonoverlapping path cover of all the nodes.

## B. Solution for Markov Association Likelihoods

Let  $\tau = (y_1, \dots, y_k)$  be a track with a tracklet  $\tau_i$  represented by its measurements  $y_i$ . The likelihood of the track  $\tau$  is

$$l(\tau) = \gamma_S(y_1) p_E(y_k) \prod_{i=1}^{k-1} l(y_{i+1}) \prod_{i=1}^{k-1} l(y^i, y_{i+1}), \quad (24)$$

where  $p_E(y_k)$  is the probability of the track ending after  $y_k$ ,  $\gamma_S(y_1)$  depends on the density of the new report  $y_1$ ,  $y^i \triangleq (y_1, \dots, y_i)$  is the partial track with reports up to  $y_i$ ,  $l(y_i)$  is the likelihood of  $y_i$ , and  $l(y^i, y_{i+1})$  is the likelihood of associating  $y_{i+1}$  with  $y^i$ .

1) Markov Likelihoods: The association likelihood satisfies the Markov property if  $p(y_{i+1}|y^i) = p(y_{i+1}|y_1, \dots, y_i) = p(y_{i+1}|y_i)$ . Then, (24) becomes

$$l(\tau) = \gamma_S(y_1) p_E(y_k) \prod_{i=1}^{k-1} l(y_{i+1}) \prod_{i=1}^{k-1} l(y_i, y_{i+1}). \quad (25)$$

The likelihood of a track is now the product of pairwise association likelihoods given by (25). The Markov property is also called the path-independent property because the association of nodes with a path depends only on the last node in the path and is independent of the rest of the path.

The Markov or path-independent property implies  $p(x|y_1, \dots, y_i) = p(x|y_i)$ ; i.e., the previous reports in a track cannot improve the estimate based only on the current report. This is true in tracklet stitching problems with very accurate sensors and fast target dynamics relative to the length of the tracklet [55], e.g., video tracking. The Markov property is not satisfied when the previous reports can improve the estimate computed using only the current report. Examples include raw sensor measurements, feature data, and multisensor reports that can be fused to improve the state estimate.

2) Bipartite Matching Formulation: An association hypothesis  $\lambda$  on the track graph can be represented by  $x_{ij} \in \{0, 1\}$ ,  $i = 1, \dots, N$ ,  $j = 1, \dots, N$ , so that  $x_{ij} = 1$  if the directed edge  $(y_i, y_j)$  is in  $\lambda$  and 0 otherwise. With the Markov assumption, taking the negative logarithm of (16) and ignoring the normalization constant, the cost function for the MAP solution becomes

$$J(x) = \sum_{(i,j) \in E} c_{ij} x_{ij}, \quad (26)$$

where  $c_{ij} = -\ln(l(y_i, y_j)/(\gamma_S(y_j) p_E(y_i)))$  and  $E$  is the set of edges.

The best hypothesis is obtained by finding  $x_{ij} \in \{0, 1\}$  that minimizes (26) subject to the constraints that each node  $i$  can be associated with at most one node  $j$ . This is a bipartite matching or assignment problem. Many efficient algorithms [56] have been developed to find the best matching or assignment. In addition, the  $K$ -best solutions can be found by Murty's algorithm [22].

3) Minimum Cost Network Flow Formulation: The bipartite matching formulation can be converted into the minimum cost network flow (MCNF) formulation. In fact, the MCNF solution first appeared in [54] for finding the best hypothesis for a trellis with the nodes representing radar measurements. However, this approach was ignored for many years because the Markov property does not hold for problems of interest at that time.

This approach was rediscovered with video tracking, which frequently uses a two-level architecture. The first or low level processes video data to form tracklets and the second or high level stitches the tracklets across occlusions or confusions. The tracklet stitching problem usually uses a track graph representation. Since the likelihood of associating a video tracklet with a video track usually depends only on the last tracklet in the track, the Markov property is satisfied and MCNF or bipartite matching algorithms can be used to solve the problem.

Because of this nice computational property, the Markov property is sometimes assumed in problems where it is clearly not valid. For example, [57] uses it for tracking with radar measurements and proposes an iterative approach to improve the solutions generated under the Markov assumption. Another example is multiple sensor track stitching where the path independence assumption is not valid [58]. Graph-based tracking systems with the Markov assumption have been developed and tested on real data involving a graph with several hundred thousand nodes.

The Viterbi data association approach of [53] is further developed for tracking [59]–[61]. A comparison of Viterbi-based and multiple hypothesis-based track stitching is investigated in [62].

## C. Solution for Non-Markov Likelihoods

MHT is most useful when the data from later scans can significantly change the track likelihoods and reduce

the association ambiguity. This is clearly not possible with Markov association likelihoods. The performance of graph-based techniques for track stitching is analyzed in [63].

Graph-based solution for MHT is an active area of research because traditional MHT cannot handle the data volume of modern surveillance systems. While the graph is a good representation of the association problem, standard graph analytic solutions require restrictive assumptions such as the Markov property. Solution of association graphs that violate the Markov assumption is an active research area [52], [64]–[68].

## VII. OTHER MHT RESEARCH

### A. Relaxing Measurement to Target Association Assumptions

Standard MHT assumes that a measurement in a single frame/scan cannot originate from two targets, and a target can generate at most one measurement in a frame/scan. This assumption is violated when low sensor resolution results in unresolved measurements, or high sensor resolution results in multiple measurements per target.

1) **Unresolved Measurements:** One way to handle association of unresolved measurements with multiple tracks is by modeling the unresolved measurements. HOMHT is used in [69] to track closely spaced aircraft with measurements from acoustic sensors. Before measurements are associated with the predicted tracks, track merging hypotheses are formed. The likelihood of associating a measurement with two tracks is computed from the probabilities of track merging and detecting the merged track, and the likelihood of associating the measurement with the detected merged track. The probability of unresolved targets is also a key component in [70], which addresses multiple hypothesis track maintenance for targets flying in close formation.

Unresolved measurements introduce merged track or unresolved track hypothesis in addition to measurement to track association hypothesis. Sophisticated hypothesis management techniques are necessary to make MHT practical for unresolved measurements.

2) **Multiple Measurements:** The sensors in some tracking systems generate multiple measurements per target. One such sensor is the over-the-horizon radar (OTHR), which generates multiple detections arriving over different propagation paths from the same target. Another example is passive coherent localization, which uses a single receiver to detect multiple measurements bouncing off the target from multiple transmitters.

Different MHT modifications have been proposed to address the multiple measurement problem. In [71], multiple measurements are viewed as detections of different modes, with a different measurement equation for each mode. A multiple detection multiple hypothesis tracker

(MD-MHT) is developed to associate the measurements and estimate the mode. The MD-MHT uses MD assignment and its performance is demonstrated for OTHR tracking.

Ref. [72] addresses multiple measurements that are modeled by the same measurement equation. The multiple measurement MHT is based on a generalization of TOMHT recursion to handle repeated measurements. Tracking of multiple extended objects by Poisson multi-Bernoulli mixture (PMBM) filter, which has an MHT-like structure (Section VIII-A.2), is discussed in [73].

3) **Split and Merged Targets:** The targets in some tracking problems may split and merge, resulting in split and merged measurements. An example is tracking clouds that merge and split. Handling target merge and split requires modification of the standard MHT. In addition to new target from birth or first detection, extension of existing track, and false alarms, [74] also considers track split and track merge as possible origins of measurements. A different approach is used in [75], which decomposes the target state into kinematic/attribute state and event. The possible events are birth, death, split, and merge. The MHT has two steps: generating event hypotheses and data association hypotheses.

4) **Probabilistic MHT:** MHT assumes that a target can generate at most one measurement per scan. PMHT [76] uses an assignment model that violates this assumption, and allows measurement/target association to be independent across measurements. With this assumption, the optimization problem is changed from a combinatorial problem requiring solution by integer programming or MD assignment to a continuous optimization problem that can be solved by expectation-maximization algorithms. Even though MHT is in its name, solving the data association problem is not the primary objective of PMHT, which also assumes the number of targets is known. The problems and some solutions of PMHT are discussed in [77].

### B. MCMC Data Association

It is well known that finding the best hypothesis of TOMHT by 0–1 integer linear programming (18) or MD assignment (20), (21) is an NP-hard combinatorial problem. Since MCMC methods [78], [79] can provide polynomial time algorithms to solve the NP-hard problem with sufficient accuracy, it is natural for MCMC to be used for target tracking [80].

In [81] and [82], the MC transition is defined as a combination of five “moves”: 1) birth/death, 2) split/merge, 3) extension/reduction, 4) track update, and 5) track switch. Simulation results show that performance is better than commonly used TOMHT algorithms. MCMC is used to solve a multiple-intelligence (multi-INT) surveillance problem with good reported performance [66].

In [83], three MCMC sampling designs, Metropolis sampling, Metropolis sampling with Boltzmann acceptance probability, and Metropolis–Hasting sampling, are directly applied to the 0–1 linear programming formulation (18) of TOMHT. The results in terms of convergence speed are not very impressive when compared with an open-source mixed-integer linear programming package combining the primal–dual methods with the backup branch-and-bound method. At the suggestion by the late Dr. Jean-Pierre Le Cadre, another sequential Monte Carlo method known as cross entropy method was proposed in [84]. However, no definitive conclusion on the performance improvement was obtained.

### C. Graphical Models for Data Association

Graphical models [85] are efficient representations of joint probability distributions of many random variables by exploiting factorization such as Markov properties. Given such a representation, inference algorithms are used to compute probabilities of specific variables or maximize some probabilities. By representing the MTT with a graphical model, message passing or belief propagation techniques can be used to solve the data association problem.

Ref. [86] presents message passing algorithms for solving a class of MTT problems. Ref. [87] uses a factor graph to represent the TOMHT and variational message passing to estimate the track probabilities. Empirical evaluation shows that track probabilities computed through message passing compare favorably to those obtained by summation over the  $k$ -best hypotheses

Ref. [88] uses an MWISP formulation of TOMHT and represents it by a graphic model. Max-product belief propagation is then used to find the MAP solution.

### D. MHT Output

Designing a good display for a tracking system is always difficult because the information to display depends on the information needs of the operator. Displaying MHT output is particularly challenging. There are two choices: displaying the best (MAP) hypothesis or a combination of hypotheses. Usually the best hypothesis is displayed because finding alternative hypotheses is not easy. However, the tracks in the best hypothesis may change abruptly as the MAP hypothesis changes. This hypothesis hopping is very disconcerting to the operator as it results in track switching and jitter.

One way to generate smooth track estimates is by retrodiction [89], [90]. By introducing a delay and using a “smoothed” hypothesis, the track estimates will have fewer discontinuities. The retrodiction approach is acceptable if the delay is small enough for the mission.

Another approach [91] finds the real-time display of the target state estimates without any delay by minimizing the mean optimal subpattern assignment metric, which is defined in terms of the optimal subpattern as-

signment metric [92]. Since the display involves multiple hypotheses, the target estimates will be smoother.

### E. Multiple Frame Detection and Track Initiation/Extraction

Detecting a target from a single frame of measurements is difficult when the signal-to-noise ratio is low and clutter is high. Multiple frame detection considers multiple candidate trajectories over the multiple frames and selects the best trajectories to detect or extract a target track. Since MHT performs track initiation in addition to track maintenance, it is a natural approach for multiple frame detection. The performance of MHT for track initiation and extraction is assessed in [93] and [94], with probability of establishing a track and number of false tracks as performance metrics.

The detection of small moving objects in a sequence of images is addressed in [95] by multistage hypothesis testing, which is also abbreviated as MHT. To avoid the complexity of standard MHT for target tracking, a sequential probability ratio test (SPRT) [96] is used to sequentially compare the statistics of two decision thresholds. A similar approach is used in [97] to extract tracks of weak but well-separated targets from high interference. More recently, [98] derives a Bayesian SPRT with new target density for track initiation based on the original HOMHT [15] and compares its performance with the classical SPRT [97], both theoretically and with simulations.

## VIII. RELATIONSHIP TO RFSs

Multitarget filtering using random set formalism has been a very active area of research in recent years [99], [100]. In the random set approach, both the multitarget state and measurements are modeled as random sets. More specifically, the multitarget state at time  $t_k$  is the random set  $X_k = \{x_k^1, \dots, x_k^{n_k}\}$  and the measurements, which may be vectors, are the set  $Z_k = \{z_k^1, \dots, z_k^{m_k}\}$ . Although RFSs are basically finite point processes allowing repeated elements, the RFS formalism, which does not allow repeated elements, is much more popular than the finite point process formalism. An appropriate concept of a pdf of an RFS  $X = \{x_1, \dots, x_n\}$  is the  $n$ th-order Janossy measure density function

$$f(\{x_1, \dots, x_n\}) = n!p(n)f_n(x_1, \dots, x_n), \quad (27)$$

where  $p(n)$  is the probability distribution on the number of elements, and  $f_n(x_1, \dots, x_n)$  is the joint pdf given  $n$  elements, which is symmetric or permutable, i.e., for any permutation  $\pi$  on  $\{1, \dots, n\}$ ,  $f_n(x_1, \dots, x_n) = f_n(x_{\pi(1)}, \dots, x_{\pi(n)})$ .

Let  $f_{k|k-1}(X_k|X_{k-1})$  be the RFS state transition pdf, and  $f_M(Z_k|X_k)$  be the RFS measurement likelihood. Then, the multitarget filter can be expressed by the

prediction step

$$f(\mathbf{X}_k|\mathbf{Z}_{1:k-1}) = \int f_{k|k-1}(\mathbf{X}_k|\mathbf{X}_{k-1})f(\mathbf{X}_{k-1}|\mathbf{Z}_{1:k-1})\delta\mathbf{X}_{k-1}, \quad (28)$$

where the integral in (28) is the set integral over the measurable space of all the finite sets, and the update step

$$f(\mathbf{X}_k|\mathbf{Z}_{1:k}) = [f(\mathbf{Z}_{1:k}|\mathbf{Z}_{1:(k-1)})]^{-1}f_M(\mathbf{Z}_k|\mathbf{X}_k)f(\mathbf{X}_k|\mathbf{Z}_{1:k-1}). \quad (29)$$

#### A. MHT-Like Structures in RFS Filters

Since explicit target trajectories or tracks are needed in many applications, there has been much research on deriving MHT from RFS. In particular, RFS filters are shown to have MHT-like structures.

1) Cardinalized Probability Hypothesis Density (CPHD) Filter: The Probability Hypothesis Density (PHD) is the density of the measure defined as the expected number of targets within any measurable set in the target state space. The PHD filter approximates the predicted RFS pdf by a Poisson RFS pdf, at each updating stage, while the CPHD filter approximates it by an i.i.d. cluster RFS, without the Poisson assumption on the number of targets. The PHD filter provides the best Poisson RFS approximation in a Kullback–Leibler divergence sense [101]. Similarly, the CPHD filter provides the best i.i.d. cluster RFS approximation in Kullback–Leibler divergence sense, as proved in [102] and [103].

Neither PHD nor CPHD provides state pdf for each target, and the single-target state pdf cannot be inferred from the peaks of the posterior PHD. There are attempts to relate PHD or CPHD to MHT. For example, [104] shows that the Gaussian mixture CPHD filter is equivalent to MHT for single targets. Each Gaussian component has a predecessor and the sequence of predecessors forms a track.

2) PMBM Filters: A Bernoulli RFS is specified by the probability of existence for an element and a “spatial” pdf for the element if it exists. A multi-Bernoulli RFS is the union of independent Bernoulli RFS components.

The multi-Bernoulli mixture in the PMBM filter represents the posterior density  $f(\mathbf{X}_k|\mathbf{Z}_{1:k})$  over the targets that have ever been detected, with each Bernoulli component representing a track and each mixture component representing a data association hypothesis. The addition of Poisson component represents targets that remain undetected. Thus, it is reasonable to expect that the PMBM filter will have structure similar to MHT [105].

In particular, [106] shows that the hypothesis evaluation equation (3) can be derived from the PMBM filter under the same assumptions of [15], including Gaussian–linear kinematics and no target death, and interpreting the new target density  $\beta_{NT}$  as the unknown target density in [105]. The derivation is based on representation by multi-Bernoulli mixtures. The relationship between

HOMHT and PMBM filter is further analyzed in [107] by representing the multitarget pdf as a mixture of data association hypotheses that generalize the hypotheses of [15] by including undiscovered targets. In addition, new target density is viewed as a birth density. The resulting filter has essentially the same structure as the HOMHT, and the hypothesis probability recursion equation is (3) multiplied by a factor that represents undiscovered targets.

A Gaussian implementation of the PMBM is provided in [108], which also introduces the multi-Bernoulli mixture (MBM) filters. The difference between PMBM filters and MBM filters is that in PMBM filters the birth model is a Poisson point process, while in MBM filters, the birth model is multi-Bernoulli or multi-Bernoulli mixture. The prediction and update equations are analogous with a minor difference in the prediction step.

The PMBM filter does not establish explicit track continuity, which is desirable for MTT. By formulating the MTT problem as an RFS of trajectories [109], [110] derives PMBM trackers that estimate the trajectories, thus providing continuity and structure similar to MHT. Implementation of the trajectory PMBM filter is discussed in [111] and [112].

3) Labeled Multi-Bernoulli Filters: By adding a label to an individual target state, RFS-based filters explicitly maintain track continuity from entire trajectories of consecutive target states with the same label. If one labels the Bernoulli components in the MBM filter, which is a particular case of the unlabeled case, one gets a labeled MBM filter. If the labeled MBM filter is written with (data association) hypotheses in which target existence is deterministic rather than probabilistic, one gets the  $\delta$ -generalized labeled multi-Bernoulli ( $\delta$ -GLMB filter) [108, Sec. IV]. Having deterministic existence in each hypothesis implies an exponential increase in the number of hypotheses (and therefore in the number of data associations to be solved), and is thus not desirable.

$\delta$ -GLMB RFS filters [113], [114] have been used to develop multitarget tracking filters with structure similar to MHT. For example, the update equation for detected targets [86, eqs. (105) and (106)] can be used to illustrate the similarity to MHT. More specifically,

$$\begin{aligned} f(\mathbf{X}_k|\mathbf{Z}_{1:k}) &= \sum_{c_k} P(c_k) f_{c_k}^{\text{LMB}}(\mathbf{X}_k) \\ &= \sum_{c_k} P(c_k) \prod_{l \in L_k} f^{(l, c_k)}(\mathbf{X}_k^l), \end{aligned} \quad (30)$$

where  $L_k$  is the set of detected targets,  $\mathbf{X}_k^l$  is  $\{(x_k^l, l_k^l)\}$ ,  $f^{(l, c_k)}(\mathbf{X}_k^l)$  is a Bernoulli pdf for each label  $l$  in  $L_k$ , and  $c_k$  is a data association vector with entries  $c_k^l$ ,  $l \in L_k$ , and probability  $P(c_k)$ . According to (30), the RFS pdf is the sum of LMB  $f_{c_k}^{\text{LMB}}(\mathbf{X}_k)$  representing the RFS pdf for each data association  $c_k$ , weighted by  $P(c_k)$ , and  $f^{(l, c_k)}(\mathbf{X}_k^l)$  is the track RFS pdf.

## B. RFS Formalisms for MHT

There are some concerns that MHT does not have a solid mathematical foundation because the derivations in [13]–[16] do not use complicated mathematics. In fact, there were even criticisms that MHT is heuristic. These concerns are addressed in [115] and [116], which introduce mathematical formalisms to support a theory for MHT.

In particular, [116] models the set of targets as (i) a random finite sequence, (ii) a finite point process, and (iii) a random finite set, of stochastic processes on the target state space over a given continuous-time interval  $[t_0, \infty)$ . Viewing an individual target as a stochastic process is similar to the use of target trajectories in [110].

Using the standard assumptions on the measurements, the hypothesis evaluation equation is

$$P(\lambda_K | Z_{1:K}) = P(Z_{1:K})^{-1} L_{FAK}(\lambda_K) L_{NDTK}(\#(\lambda_K)) \times \left( \prod_{\tau \in \lambda_K} L_K(\tau) \right), \quad (31)$$

where  $L_K(\tau)$  is the likelihood of a track similar to (14). However,  $L_{FAK}(\lambda_K)$ , the likelihood of false alarms, and  $L_{NDTK}(\#(\lambda_K))$ , the likelihood of the cumulative number of detected targets, are more complicated unless the number of targets and number of false alarms satisfy the Poisson assumption. Note that the hypothesis evaluation equation (31) is the same for all three formalisms.

## IX. APPLICATIONS

MHT has been applied to target tracking problems that require sophisticated methods for data association. Many of these applications are in defense and security, where government regulations and company policies restrict publications, especially on deployed systems. Our review will focus primarily on those published in the open literature. Applications of MHT for tracking ground targets, aircraft, and missiles are already discussed in [17]. We will discuss other applications such as ocean and maritime surveillance, space situational awareness, airborne video surveillance, video tracking, and some unconventional areas.

### A. Ocean and Maritime Surveillance

1) **Ocean Surveillance:** Ocean surveillance is characterized by a huge surveillance region that may cover the entire world. Relative to the size of the surveillance region, there are few targets and they do not move very fast. The tracking problem would be easy except that few sensors provide persistent coverage, resulting in sparse measurements. Since kinematic measurements are not useful for association in many occasions, feature or attribute observations are valuable but not always available. The tracking problem is even more challenging for

submarines because they are designed for stealthy operations.

Naval ocean surveillance was a very active area of research in 1979, with [117] documenting the state of the art around that time. Ref. [118] discusses using MHT of [15] for ocean surveillance with a target state that includes a continuous component representing position, velocity, and emitter parameters, and a discrete component representing attributes such as platform or radar identifications. An architecture for fusion of multisensor ocean surveillance data using MHT is proposed in [119].

Submarine tracking relies largely on acoustic sensors. A multiple hypothesis approach is proposed for concurrent mapping and localization for autonomous underwater vehicles [120]. The MHT approach for tracking with passive and active sonar is discussed in [121]–[124].

2) **Maritime Surveillance:** Maritime surveillance is characterized by a smaller surveillance region and many more sensors than ocean surveillance. However, there are more targets with high maneuverability. Maritime domain awareness requires tracking targets and monitoring their behaviors [125].

One system for port surveillance fuses video and radar data with automatic identification system (AIS) transponder data to form composite fused tracks for all vessels in and approaching the port using MHT. Rule-based and learning-based pattern recognition algorithms are then used to generate alerts [126], [127].

Ref. [128] discusses an MHT at the NATO Undersea Research Centre. An MHT that fuses radar and AIS data is described in [129]. While the targets of interest for ocean and maritime surveillance are surface and subsurface vessels, MHT has been used to estimate the number of beaked whales [130].

### B. Ground Surveillance

Ground surveillance targets include vehicles, people, and animals, with movements in rural or urban environments. Sensors include radar, electro-optical, and others on airborne platforms, as well as ground-based sensors such as seismic.

1) **Ground Moving Target Indicator:** The utility of airborne ground moving target indicator (GMTI) radar for ground surveillance was demonstrated in the first Gulf War of 1991 [131]. The large amount of data produced by GMTI radar overwhelms manual analysis and requires automated tracking algorithms.

Ground target tracking is characterized by large number of targets that may be close to each other. The targets are highly maneuverable with move–stop–move-type behavior and on-road/off-road modes. Because of the observation geometry, the targets may be obscured by terrain. Furthermore, the MTI radar detects targets only when their radial velocities are above the minimum detectable velocity. Coverage gaps and highly maneuverable targets make data association difficult. The

challenges of ground target tracking and available algorithms are discussed in [132].

Ref. [133] describes a U.S. program to develop GMTI tracking algorithms around 2000. The initial phase involved four contractors using HOMHT [134] and TOMHT. The two winning contractors later became the main tracking algorithm developers for ground surveillance in the United States. Other research in GMTI tracking includes [135]–[138].

2) Airborne Video: The targets for tracking with airborne video have similar characteristics to those in GMTI tracking. In addition, airborne video is often used to track people. Some airborne platforms such as the Predator have steerable sensors with narrow field of view, while other platforms have wide-area motion imagery (WAMI) sensors. Since steerable sensors have narrow field of view, accurate tracking is crucial to control the sensor to observe the targets. Thus, MHT is part of a closed-loop system with both tracking and sensor control [139], [140].

A WAMI sensor can detect many targets because of its wide field of view. When used for urban surveillance, occlusion from buildings and high target density makes data association very difficult. Furthermore, the goal of tracking is to produce tracks (trajectories), and not just estimating the locations, which would be very easy for video sensors. Thus, MHT is widely used for airborne video tracking. Approaches include TOMHT with integer programming [141]–[143], MD assignment [144], and graph-based approach [145], [146]. Graph-based approach is particularly applicable because the Markov assumption is valid.

### C. Air and Missile Target Tracking

Air and missile targets have mostly well-defined motion models based on physics, even during maneuvers. Furthermore, sensors such as radar or infrared search and track do not have to contend with the occlusion problem in ground target tracking. However, military targets can fly in close formation, and are designed to escape detection with the help of countermeasures. These are challenges for air and missile target tracking.

The benefit of using MHT for sensor fusion in airborne surveillance systems was recognized very early [147], with performance assessments made in [93] and [94]. MHT algorithms are developed for infrared [148], electronically scanned radar [149], and multisensor air defense [150]. Interacting multiple models are used with MHT to handle target maneuvers [151], [152]. Targets flying in formations are addressed in [153]. More recent research uses MHT with active and passive sensors for the sense and avoid problem [45] and air surveillance system [154], extending earlier MHT work for air traffic control [155].

Missile defense is an important application for MHT [17] because of the high target density, difficult associa-

tion problem for angle-only measurements from space base sensors, and the need for continuous birth to death tracking. However, very little research and development is reported in the open literature. An exception is boost-phase ballistic missile defense using MHT [156].

### D. Space Situational Awareness

Space situational awareness (SSA) is important but difficult due to the large number of satellites and space debris in various orbit regimes. SSA has to discover new objects, catalog and track resident objects, and characterize tracked objects [157]. Since sensors observe space objects with large time gaps, data association is nontrivial. MHT has been recognized as a promising solution to the space object problem [158]–[160].

### E. Video Tracking

Due to the availability of low-cost video cameras, video tracking has been a very active application area for computer vision researchers. The goal of video tracking is to maintain continuous tracks of targets, called objects in the video tracking community, and infer activities and intentions. Object tracking has to address abrupt object motion, changing appearance patterns, nonrigid structures for humans or animals, and occlusions. Association is usually more important than estimation because users can locate the objects on the image.

The association problem among image frames is called correspondence in the computer vision community. Due to object crossing, appearance change, and occlusion, correspondence using only two frames may result in incorrect correspondence. Better tracking results can be obtained if the correspondence is performed over several frames. Thus, MHT is a natural approach for solving the correspondence problem in video tracking.

A Bayesian multiple hypothesis approach for contour grouping, edge and contour segmentation [161], [162] leads to an efficient implementation of HOMHT for video tracking [163], based on finding ranked assignments [20], [21]. This is followed by other research on using MHT for video tracking [164]–[187]. Besides using standard MHT, e.g., [183], most research assumes the Markov assumption to build a track graph and uses efficient solutions such as MCNF. It is interesting to note that most of the research is performed in universities, unlike MHT applications in defense and security performed mostly in companies and government laboratories. The shifting of research to academia is due to easy access to data for algorithm development and testing from community datasets [188] and low-cost camera systems.

### F. Other Nontraditional Applications

In addition to tracking traditional targets such as ships, vehicles, planes, and people, MHT has been used

in other applications where good data association performance requires using multiple frames/scans of data. The following are some examples:

- 1) Ocean eddy current tracking [189].
- 2) Cloud tracking [74], [75].
- 3) Associating asteroid observations [190].
- 4) Solar events tracking [191], [192].
- 5) Tracking text messages and information [193], [194].
- 6) Detection of internet worms [195].
- 7) Cyberattack tracking [196].
- 8) Cellular traffic in living cells [197].
- 9) Tracking in biology and medical images [198]–[202].

## X. CONCLUSION

We have reviewed the main research and development in MHT over the last 40 years. Since MHT is based on a sound mathematical formulation of a real MTT problem, research has focused on relaxing the assumptions of MHT, developing efficient implementations, and applying to problems that require association using multiple frames or scans of data. It is interesting to note that while almost all early research was performed in industry or government laboratories, most recent research is now performed in academia without a strong application focus. We believe future research should be driven by applications, since new problems may require relaxing other assumptions, which in turn requires new algorithms.

Most MHT algorithms assume targets have i.i.d. motion models. The independence assumption is violated when targets move as a group, or when vehicles are moving on a single-lane road. Exploiting this dependence should improve association performance.

MHT is designed to address difficult data association problems by maintaining association hypotheses over multiple frames of data. Experience with real data has shown that when data association is too easy, MHT is not needed, and when data association is too difficult, MHT does not help. Research is needed to predict when MHT is useful, which is related to computing the hypothesis probability distributions. Relating MHT to RFS may also result in algorithms that do explicit data association only when the data are good enough for association to make sense.

Some tracking problems cannot be solved without using sophisticated (or full-fledged) MHT. An example is tracking targets with frequent kinematic measurements and sparse feature observations. In such situations, MHT has to maintain multiple hypotheses until feature data are available for association. Efficient maintenance of hypotheses for long durations is an active area of research.

## REFERENCES

1. Y. Bar-Shalom  
“Tracking methods in a multitarget environment,”  
*IEEE Trans. Autom. Control*, vol. 23, no. 4, pp. 618–626, Aug. 1978.
2. S. S. Blackman  
*Multiple-Target Tracking with Radar Applications*.  
Norwood, MA: Artech House, 1986.
3. Y. Bar-Shalom and T. E. Fortmann  
*Tracking and Data Association*. New York, NY: Academic Press, 1988.
4. Y. Bar-Shalom and X.-R. Li  
*Multitarget–Multisensor Tracking: Principles and Techniques*. Storrs, CT: YBS Publishing, 1995.
5. S. S. Blackman and R. Popoli  
*Design and Analysis of Modern Tracking Systems*.  
Norwood, MA: Artech House, 1999.
6. Y. Bar-Shalom, P. K. Willett, and X. Tian  
*Tracking and Data Fusion: A Handbook of Algorithms*.  
Storrs, CT: YBS Publishing, 2011.
7. S. Challa, M. R. Morelande, D. Mušicki, and R. J. Evans  
*Fundamentals of Object Tracking*. Cambridge, U.K.:  
Cambridge University Press, 2011.
8. L. D. Stone, R. L. Streit, T. L. Corwin, and K. L. Bell  
*Bayesian Multiple Target Tracking*, 2nd ed. Norwood, MA:  
Artech House, 2013.
9. M. Mallick, V. Krishnamurthy, and B.-N. Vo  
*Integrated Tracking, Classification, and Sensor Management: Theory and Applications*. Hoboken, NJ: Wiley, 2012.
10. C.-B. Chang and K.-P. Dunn  
*Applied State Estimation and Association*. Cambridge, MA:  
MIT Press, 2016.
11. R. W. Sittler  
“An optimal data association problem in surveillance theory,”  
*IEEE Trans. Mil. Electron.*, vol. 8, no. 2, pp. 125–139, Apr. 1964.
12. R. Singer and R. Sea  
“New results in optimizing surveillance system tracking and data correlation performance in dense multitarget environments,”  
*IEEE Trans. Autom. Control*, vol. 18, no. 6, pp. 571–582, Dec. 1973.
13. C. Morefield  
“Application of 0–1 integer programming to multitarget tracking problems,”  
*IEEE Trans. Autom. Control*, vol. 22, no. 3, pp. 302–312, Jun. 1977.
14. D. B. Reid  
“An algorithm for tracking multiple targets,”  
in *Proc. IEEE Conf. Decis. Control*, 1978, pp. 1202–1211.
15. D. B. Reid  
“An algorithm for tracking multiple targets,”  
*IEEE Trans. Autom. Control*, vol. 24, no. 6, pp. 843–854, Dec. 1979.
16. S. Mori, C.-Y. Chong, E. Tse, and R. Wishner  
“Tracking and classifying multiple targets without a priori identification,”  
*IEEE Trans. Autom. Control*, vol. 31, no. 5, pp. 401–409, May 1986.
17. S. S. Blackman  
“Multiple hypothesis tracking for multiple target tracking,”  
*IEEE Aerosp. Electron. Syst. Mag.*, vol. 19, no. 1, pp. 5–18, Jan. 2004.
18. J. Roy, N. Duclos-Hindie, and D. Dessureault  
“Efficient cluster management algorithm for multiple-hypothesis tracking,”  
in *Proc. SPIE Signal Data Process. Small Targets*, 1997.

19. R. Danchick and G. E. Newnam  
“A fast method for finding the exact  $N$ -best hypotheses for multitarget tracking,”  
*IEEE Trans. Aerosp. Electron. Syst.*, vol. 29, no. 2, pp. 555–560, Apr. 1993.
20. I. J. Cox and M. L. Miller  
“On finding ranked assignments with application to multitarget tracking and motion correspondence,”  
*IEEE Trans. Aerosp. Electron. Syst.*, vol. 31, no. 1, pp. 486–489, Jan. 1995.
21. I. J. Cox, M. L. Miller, R. Danchick, and G. E. Newnam  
“A comparison of two algorithms for determining ranked assignments with application to multitarget tracking and motion correspondence,”  
*IEEE Trans. Aerosp. Electron. Syst.*, vol. 33, no. 1, pp. 295–301, Jan. 1997.
22. K. G. Murty  
“An algorithm for ranking all the assignments in order of increasing cost,”  
*Oper. Res.*, vol. 16, no. 3, pp. 682–687, 1968.
23. R. Danchick and G. E. Newnam  
“Reformulating Reid’s MHT method with generalised Murty  $K$ -best ranked linear assignment algorithm,”  
*IEE Proc. — Radar, Sonar Navig.*, vol. 153, no. 1, pp. 13–22, Feb. 2006.
24. E. Brekke and M. Chitre  
“Success rates and posterior probabilities in multiple hypothesis tracking,”  
in *Proc. 21st Int. Conf. Inf. Fusion*, Cambridge, U.K., 2018, pp. 949–956.
25. T. Kurien  
“Issues in the design of practical multitarget tracking algorithms,”  
in *Multitarget–Multisensor Tracking: Advanced Applications*, Y. Bar-Shalom  
Ed. Norwood, MA: Artech House, 1989.
26. J. R. Delaney, A. S. Willsky, A. L. Blizt, and J. Korn  
“Tracking theory for airborne surveillance radars,”  
ALPHATECH, Burlington, MA, TR-142, Feb. 1983.
27. S. Mori and C.-Y. Chong  
“Evaluation of data association hypotheses: non-Poisson i.i.d. cases,”  
in *Proc. 7th Int. Conf. Inf. Fusion*, Stockholm, Sweden, 2004.
28. S. Coraluppi and C. A. Carthel  
“If a tree falls in the woods, it does make a sound: Multiple-hypothesis tracking with undetected target births,”  
*IEEE Trans. Aerosp. Electron. Syst.*, vol. 50, no. 3, pp. 2379–2388, Jul. 2014.
29. Y. Bar-Shalom, S. S. Blackman, and R. J. Fitzgerald  
“Dimensionless score function for multiple hypothesis tracking,”  
*IEEE Trans. Aerosp. Electron. Syst.*, vol. 43, no. 1, pp. 392–400, Jan. 2007.
30. S. Coraluppi, C. Carthel, M. Luetzgen, and S. Lynch  
“All-source track and identity fusion,”  
in *Proc. MSS Nat. Symp. Sensor Data Fusion*, 2000.
31. A. Poore and N. Rijavec  
“A Lagrangian relaxation algorithm for multidimensional assignment problems arising from multitarget tracking,”  
*SIAM J. Optim.*, vol. 3, no. 3, pp. 544–563, Aug. 1993.
32. A. B. Poore  
“Multidimensional assignment formulation of data association problems arising from multitarget and multisensor tracking,”  
*Comput. Optim. Appl.*, vol. 3, no. 1, pp. 27–57, Mar. 1994.
33. S. Deb, M. Yeddanapudi, K. Pattipati, and Y. Bar-Shalom  
“A generalized S-D assignment algorithm for multisensor–multitarget state estimation,”  
*IEEE Trans. Aerosp. Electron. Syst.*, vol. 33, no. 2, pp. 523–538, Apr. 1997.
34. D. J. Papageorgiou and M. R. Salpukas  
“The maximum weight independent set problem for data association in multiple hypothesis tracking,”  
in *Optimization and Cooperative Control Strategies*, M. J. Hirsch, C. W. Commander, P. M. Pardalos, and R. Murphey  
Eds. Berlin, Germany: Springer, 2009, pp. 235–255.
35. A. Caponi  
“Polynomial time algorithm for data association problem in multitarget tracking,”  
*IEEE Trans. Aerosp. Electron. Syst.*, vol. 40, no. 4, pp. 1398–1410, Oct. 2004.
36. X. Ren, Z. Huang, S. Sun, D. Liu, and J. Wu  
“An efficient MHT implementation using GRASP,”  
*IEEE Trans. Aerosp. Electron. Syst.*, vol. 50, no. 1, pp. 86–101, Jan. 2014.
37. M. R. Chummun, T. Kirubarajan, K. R. Pattipati, and Y. Bar-Shalom  
“Fast data association using multidimensional assignment with clustering,”  
*IEEE Trans. Aerosp. Electron. Syst.*, vol. 37, no. 3, pp. 898–913, Jul. 2001.
38. R. L. Popp, K. R. Pattipati, and Y. Bar-Shalom  
“ $m$ -Best S-D assignment algorithm with application to multitarget tracking,”  
*IEEE Trans. Aerosp. Electron. Syst.*, vol. 37, no. 1, pp. 22–39, Jan. 2001.
39. E. Fortunato, W. Kremer, S. Mori, C.-Y. Chong, and G. Castanon  
“Generalized Murty’s algorithm with application to multiple hypothesis tracking,”  
in *Proc. 10th Int. Conf. Inf. Fusion*, Quebec City, QC, Canada, 2007.
40. C.-Y. Chong, S. Mori, and K.-C. Chang  
“Distributed multitarget multisensor tracking,”  
in *Multitarget–Multisensor Tracking: Advanced Applications*, Y. Bar-Shalom,  
Ed. Norwood, MA: Artech House, 1989, pp. 247–296.
41. C.-Y. Chong and S. Mori  
“Hierarchical multitarget tracking and classification—A Bayesian approach,”  
in *Proc. Amer. Control Conf.*, 1984, pp. 599–604.
42. C.-Y. Chong, S. Mori, and K.-C. Chang  
“Information fusion in distributed sensor networks,”  
in *Proc. Amer. Control Conf.*, 1985, pp. 830–835.
43. M. E. Liggins, C.-Y. Chong, I. Kadar, M. G. Alford, V. Vannicola, and S. Thomopoulos  
“Distributed fusion architectures and algorithms for target tracking,”  
*Proc. IEEE*, vol. 85, no. 1, pp. 95–107, Jan. 1997.
44. C.-Y. Chong and S. Mori  
“Optimal fusion for non-zero process noise,”  
in *Proc. 16th Int. Conf. Inf. Fusion*, Istanbul, Turkey, 2013.
45. S. Coraluppi et al.  
“Distributed MHT with active and passive sensors,”  
in *Proc. 18th Int. Conf. Inf. Fusion*, Washington, DC, 2015.
46. D. T. Dunham, S. S. Blackman, and R. J. Dempster  
“Multiple hypothesis tracking for a distributed multiple platform system,”  
in *Proc. SPIE Signal Data Process. Small Targets*, 2004.
47. S. Coraluppi and C. Carthel  
“Multi-stage multiple-hypothesis tracking,”  
*J. Adv. Inf. Fusion*, vol. 6, no. 1, pp. 57–67, Jun. 2011.
48. O. E. Drummond  
“Hybrid sensor fusion algorithm architecture and tracklets,”  
in *Proc. SPIE Signal Data Process. Small Targets*, 1997.

49. C.-Y. Chong and S. Mori  
“Multiple hypothesis tracking for processing tracklets,”  
in *Proc. 22nd Int. Conf. Inf. Fusion*, Ottawa, Canada, 2019.
50. C.-Y. Chong, G. Castanon, N. Cooperider, S. Mori,  
R. Ravichandran, and R. Macior  
“Efficient multiple hypothesis tracking by track segment  
graph,”  
in *Proc. 12th Int. Conf. Inf. Fusion*, 2009, pp. 2177–2184.
51. C.-Y. Chong  
“Graph approaches for data association,”  
in *Proc. 15th Int. Conf. Inf. Fusion*, Singapore, 2012,  
pp. 1578–1585.
52. S. P. Coraluppi, C. A. Carthel, G. D. Castañón, and A. S. Willsky  
“Multiple-hypothesis and graph-based tracking for  
kinematic and identity fusion,”  
in *Proc. IEEE Aerosp. Conf.*, 2018.
53. J. K. Wolf, A. M. Viterbi, and G. S. Dixon  
“Finding the best set of  $K$  paths through a trellis with  
application to multitarget tracking,”  
*IEEE Trans. Aerosp. Electron. Syst.*, vol. 25, no. 2,  
pp. 287–296, Mar. 1989.
54. D. A. Castanon  
“Efficient algorithms for finding the  $K$  best paths through a  
trellis,”  
*IEEE Trans. Aerosp. Electron. Syst.*, vol. 26, no. 2,  
pp. 405–410, Mar. 1990.
55. G. Castanón and L. Finn  
“Multi-target tracklet stitching through network flows,”  
in *Proc. Aerosp. Conf.*, 2011.
56. R. K. Ahuja, T. L. Magnanti, and J. B. Orlin  
*Network Flows: Theory, Algorithms, and Applications*.  
Upper Saddle River, NJ: Prentice Hall, 1993.
57. G. Battistelli, L. Chisci, F. Papi, A. Benavoli, A. Farina, and  
A. Graziano  
“Optimal flow models for multiscan data association,”  
*IEEE Trans. Aerosp. Electron. Syst.*, vol. 47, no. 4,  
pp. 2405–2422, Oct. 2011.
58. L. Chen and S. E. Rumbley  
“Track stitching and approximate track association on a  
pairwise-likelihood graph,”  
in *Proc. SPIE Signal Process., Sensor/Inf. Fusion, Target  
Recognit. XXVII*, 2018.
59. B. F. La Scala  
“Viterbi data association tracking using amplitude  
information,”  
in *Proc. 6th Int. Conf. Inf. Fusion*, Stockholm, Sweden, 2004.
60. G. W. Pulford  
“Multi-target Viterbi data association,”  
in *Proc. 9th Int. Conf. Inf. Fusion*, Florence, Italy, 2006.
61. G. W. Pulford and B. F. La Scala  
“Multihypothesis Viterbi data association: Algorithm  
development and assessment,”  
*IEEE Trans. Aerosp. Electron. Syst.*, vol. 46, no. 2,  
pp. 583–609, Apr. 2010.
62. L. van der Merwe and P. de Villiers  
“Comparative investigation into Viterbi based and multiple  
hypothesis based track stitching,”  
*IET Radar, Sonar Navig.*, vol. 10, no. 9, pp. 1575–1582, 2016.
63. S. Mori and C.-Y. Chong  
“Performance analysis of graph-based track stitching,”  
in *Proc. 16th Int. Conf. Inf. Fusion*, Istanbul, Turkey, 2013,  
pp. 196–203.
64. L. Chen and R. Ravichandran  
“A maximum weight constrained path cover algorithm for  
graph-based multitarget tracking,”  
in *Proc. 18th Int. Conf. Inf. Fusion*, 2015, pp. 2073–2077.
65. L. Chen and R. Ravichandran  
“On path cover problems with positive and negative  
constraints for graph-based multitarget tracking,”  
in *Proc. 19th Int. Conf. Inf. Fusion*, Heidelberg, Germany,  
2016, pp. 402–408.
66. S. Coraluppi, C. Carthel, W. Kreamer, and A. Willsky  
“New graph-based and MCMC approaches to multi-INT  
surveillance,”  
in *Proc. 19th Int. Conf. Inf. Fusion*, Istanbul, Turkey, 2016,  
pp. 394–401.
67. J. Fu, J. Sun, and P. Lei  
“Graph-based tracklet stitching with feature information  
for ground target tracking,”  
in *Geo-Spatial Knowledge and Intelligence*, H. Yuan,  
J. Geng, C. Liu, F. Bian, and T. Surapunt  
Eds. Singapore: Springer, 2018, pp. 550–557.
68. S. P. Coraluppi, C. A. Carthel, and A. S. Willsky  
“Multiple-hypothesis tracking and graph-based tracking  
extensions,”  
*J. Adv. Inf. Fusion*, vol. 14, no. 2, Dec. 2019.
69. S. Mori, K.-C. Chang, and C.-Y. Chong  
“Tracking aircraft by acoustic sensors: Multiple hypothesis  
approach applied to possibly unresolved measurements,”  
in *Proc. Amer. Control Conf.*, Minneapolis, MN, 1987.
70. W. Koch and G. Van Keuk  
“Multiple hypothesis track maintenance with possibly  
unresolved measurements,”  
*IEEE Trans. Aerosp. Electron. Syst.*, vol. 33, no. 3,  
pp. 883–892, Jul. 1997.
71. T. Sathyan, T. Chin, S. Arulampalam, and D. Suter  
“A multiple hypothesis tracker for multitarget tracking  
with multiple simultaneous measurements,”  
*IEEE J. Sel. Top. Signal Process.*, vol. 7, no. 3, pp. 448–460,  
Jun. 2013.
72. S. P. Coraluppi and C. A. Carthel  
“Multiple-hypothesis tracking for targets producing  
multiple measurements,”  
*IEEE Trans. Aerosp. Electron. Syst.*, vol. 54, no. 3,  
pp. 1485–1498, Jun. 2018.
73. K. Granstrom, M. Fatemi, and L. Svensson  
“Poisson multi-Bernoulli conjugate prior for multiple  
extended object estimation,” arXiv:1605.06311v6.
74. C. B. Storlie, T. C. M. Lee, J. Hannig, and D. Nychka  
“Tracking of multiple merging and splitting targets: A  
statistical perspective,”  
*Stat. Sin.*, vol. 19, no. 1, pp. 1–52, Jan. 2009.
75. A. Makris and C. Prieur  
“Bayesian multiple-hypothesis tracking of merging and  
splitting targets,”  
*IEEE Trans. Geosci. Remote Sens.*, vol. 52, no. 12,  
pp. 7684–7694, Dec. 2014.
76. R. L. Streit and T. E. Luginbuhl  
“Probabilistic multi-hypothesis tracking,” Naval Undersea  
Warfare Center Div., Newport, RI, NUWC-NPT Tech. Rep.  
10,428, Feb. 1995.
77. P. Willett, Y. Ruan, and R. Streit  
“PMHT: Problems and some solutions,”  
*IEEE Trans. Aerosp. Electron. Syst.*, vol. 38, no. 3,  
pp. 738–754, Jul. 2002.
78. W. R. Gilks, S. Richardson, and D. Spiegelhalter  
*Markov Chain Monte Carlo in Practice*. Boca Raton, FL:  
CRC Press, 1995.
79. M. Jerrum and A. Sinclair  
“The Markov chain Monte Carlo method: An approach to  
approximate counting and integration,”  
in *Approximation Algorithms for NP-Hard Problems*,  
D. S. Hochbaum  
Ed. Boston, MA: PWS Publishing Co., 1997, pp. 482–  
520.
80. N. Bergman and A. Doucet  
“Markov chain Monte Carlo data association for target  
tracking,”

- in *Proc. IEEE Int. Conf. Acoust., Speech, Signal Process.*, 2000.
81. S. Oh, S. Russell, and S. Sastry  
“Markov chain Monte Carlo data association for general multiple-target tracking problems,”  
in *Proc. 43rd IEEE Conf. Decis. Control*, 2004.
  82. S. Oh, S. Russell, and S. Sastry  
“Markov chain Monte Carlo data association for multi-target tracking,”  
*IEEE Trans. Autom. Control*, vol. 54, no. 3, pp. 481–497, Mar. 2009.
  83. S. Mori and C.-Y. Chong  
“Markov chain Monte Carlo method for evaluating multi-frame data association hypotheses,”  
in *Proc. 11th Int. Conf. Inf. Fusion*, Cologne, Germany, 2008.
  84. S. Mori and C. Chong  
“Cross-entropy method for  $K$ -best dependent-target data association hypothesis selection,”  
in *Proc. 13th Int. Conf. Inf. Fusion*, Edinburgh, U.K., 2010.
  85. M. I. Jordan  
“Graphical models,”  
*Stat. Sci.*, vol. 19, no. 1, pp. 140–155, Feb. 2004.
  86. F. Meyer et al.  
“Message passing algorithms for scalable multitarget tracking,”  
*Proc. IEEE*, vol. 106, no. 2, pp. 221–259, Feb. 2018.
  87. A. Frank, P. Smyth, and A. Ihler  
“Beyond MAP estimation with the track-oriented multiple hypothesis tracker,”  
*IEEE Trans. Signal Process.*, vol. 62, no. 9, pp. 2413–2423, May 2014.
  88. Q. Li, J. Sun, and W. Sun  
“An efficient multiple hypothesis tracker using max product belief propagation,”  
in *Proc. 20th Int. Conf. Inf. Fusion*, Xi’an, China, 2017.
  89. W. Koch  
“Retrodiction for Bayesian multiple-hypothesis/multiple-target tracking in densely cluttered environment,”  
in *Proc. SPIE Signal Data Process. Small Targets*, 1996.
  90. W. Koch  
“Fixed-interval retrodiction approach to Bayesian IMM-MHT for maneuvering multiple targets,”  
*IEEE Trans. Aerosp. Electron. Syst.*, vol. 36, no. 1, pp. 2–14, Jan. 2000.
  91. D. F. Crouse, P. Willett, and Y. Bar-Shalom  
“Developing a real-time track display that operators do not hate,”  
*IEEE Trans. Signal Process.*, vol. 59, no. 7, pp. 3441–3447, Jul. 2011.
  92. D. Schuhmacher, B. Vo, and B. Vo  
“A consistent metric for performance evaluation of multi-object filters,”  
*IEEE Trans. Signal Process.*, vol. 56, no. 8, pp. 3447–3457, Aug. 2008.
  93. K.-C. Chang, S. Mori, and C.-Y. Chong  
“Performance evaluation of a multiple-hypothesis multi-target tracking algorithm,”  
in *Proc. 29th IEEE Conf. Decis. Control*, 1990.
  94. K.-C. Chang, S. Mori, and C.-Y. Chong  
“Evaluating a multiple-hypothesis multitarget tracking algorithm,”  
*IEEE Trans. Aerosp. Electron. Syst.*, vol. 30, no. 2, pp. 578–590, Apr. 1994.
  95. S. D. Blostein and T. S. Huang  
“Detecting small, moving objects in image sequences using sequential hypothesis testing,”  
*IEEE Trans. Signal Process.*, vol. 39, no. 7, pp. 1611–1629, Jul. 1991.
  96. A. Wald  
*Sequential Analysis*. New York, NY: Wiley, 1947.
  97. G. V. Keuk  
“Sequential track extraction,”  
*IEEE Trans. Aerosp. Electron. Syst.*, vol. 34, no. 4, pp. 1135–1148, Oct. 1998.
  98. E. Wilthil, E. Brekke, and O. Asplin  
“Track initiation for maritime radar tracking with and without prior information,”  
in *Proc. 21st Int. Conf. Inf. Fusion*, Cambridge, U.K., 2018.
  99. R. P. S. Mahler  
*Statistical Multisource–Multitarget Information Fusion*. Norwood, MA: Artech House, 2007.
  100. R. P. S. Mahler  
*Advances in Statistical Multisource–Multitarget Information Fusion*. Norwood, MA: Artech House, 2014.
  101. R. P. S. Mahler  
“Multitarget Bayes filtering via first-order multitarget moments,”  
*IEEE Trans. Aerosp. Electron. Syst.*, vol. 39, no. 4, pp. 1152–1178, Oct. 2003.
  102. Á. F. García-Fernández and B. Vo  
“Derivation of the PHD and CPHD filters based on direct Kullback–Leibler divergence minimization,”  
*IEEE Trans. Signal Process.*, vol. 63, no. 21, pp. 5812–5820, Nov. 2015.
  103. J. L. Williams  
“An efficient, variational approximation of the best fitting multi-Bernoulli filter,”  
*IEEE Trans. Signal Process.*, vol. 63, no. 1, pp. 258–273, Jan. 2015.
  104. M. Ulmke, O. Erdinc, and P. Willett  
“Gaussian mixture cardinalized PHD filter for ground moving target tracking,”  
in *Proc. 10th Int. Conf. Inf. Fusion*, Quebec City, QC, Canada, 2007.
  105. J. L. Williams  
“Marginal multi-Bernoulli filters: RFS derivation of MHT, JIPDA, and association-based member,”  
*IEEE Trans. Aerosp. Electron. Syst.*, vol. 51, no. 3, pp. 1664–1687, Jul. 2015.
  106. E. F. Brekke and M. Chitre  
“The multiple hypothesis tracker derived from finite set statistics,”  
in *Proc. 20th Int. Conf. Inf. Fusion*, Xi’an, China, 2017.
  107. E. Brekke and M. Chitre  
“Relationship between finite set statistics and the multiple hypothesis tracker,”  
*IEEE Trans. Aerosp. Electron. Syst.*, vol. 54, no. 4, pp. 1902–1917, Aug. 2018.
  108. Á. F. García-Fernández, J. L. Williams, K. Granström, and L. Svensson  
“Poisson multi-Bernoulli mixture filter: Direct derivation and implementation,”  
*IEEE Trans. Aerosp. Electron. Syst.*, vol. 54, no. 4, pp. 1883–1901, Aug. 2018.
  109. L. Svensson and M. Morelande  
“Target tracking based on estimation of sets of trajectories,”  
in *Proc. 17th Int. Conf. Inf. Fusion*, Salamanca, Spain, 2014.
  110. K. Granström, L. Svensson, Y. Xia, J. Williams, and A. F. Garcia-Fernandez  
“Poisson multi-Bernoulli mixture trackers: Continuity through random finite sets of trajectories,”  
in *Proc. 21st Conf. Inf. Fusion*, Cambridge, U.K., 2018.
  111. Y. Xia, K. Granström, L. Svensson, and Á. F. García-Fernández  
“An implementation of the Poisson multi-Bernoulli mixture trajectory filter via dual decomposition,”  
in *Proc. 21st Int. Conf. Inf. Fusion*, Cambridge, U.K., 2018.

112. Y. Xia, K. Granström, L. Svensson, A. F. Garcia-Fernandez, and J. L. Williams  
“Multi-scan implementation of the trajectory Poisson multi-Bernoulli mixture filter,”  
*J. Adv. Inf. Fusion*, vol. 14, no. 2, Dec. 2019.
113. B.-T. Vo and B.-N. Vo  
“Labeled random finite sets and multi-object conjugate priors,”  
*IEEE Trans. Signal Process.*, vol. 61, no. 13, pp. 3460–3475, Jul. 2013.
114. B.-N. Vo, B.-T. Vo, and D. Phung  
“Labeled random finite sets and the Bayes multi-target tracking filter,”  
*IEEE Trans. Signal Process.*, vol. 62, no. 24, pp. 6554–6567, Dec. 2014.
115. S. Mori, C.-Y. Chong, and K.-C. Chang  
“Three formalisms of multiple hypothesis tracking,”  
in *Proc. 19th Int. Conf. Inf. Fusion*, Heidelberg, Germany, 2016, pp. 727–734.
116. S. Mori, C.-Y. Chong, and K.-C. Chang  
“Three mathematical formalisms of multiple hypothesis tracking,”  
*J. Adv. Inf. Fusion*, vol. 14, no. 2, Dec. 2019.
117. H. L. Wiener, W. W. Willman, J. H. Kullback, and I. R. Goodman  
“Naval Ocean-Surveillance Correlation Handbook, 1978,”  
Naval Res. Lab., Washington, DC, NRL Rep. 8340, Oct. 1979.
118. D. B. Reid  
“The application of multiple target tracking theory to ocean surveillance,”  
in *Proc. 18th IEEE Conf. Decis. Control*, 1979.
119. C. L. Bowman and M. S. Murphy  
“An architecture for fusion of multisensor ocean surveillance data,”  
in *Proc. 20th IEEE Conf. Decis. Control*, 1981.
120. C. M. Smith and J. J. Leonard  
“A multiple-hypothesis approach to concurrent mapping and localization for autonomous underwater vehicles,”  
in *Field and Service Robotics*, A. Zelinsky Ed. London, U.K.: Springer, 1998, pp. 237–244.
121. S. Coraluppi and C. Carthel  
“Multi-hypothesis sonar tracking,”  
in *Proc. 4th Int. Conf. Inf. Fusion*, Montreal, Canada, 2001.
122. S. Coraluppi and C. Carthel  
“Distributed tracking in multistatic sonar,”  
*IEEE Trans. Aerosp. Electron. Syst.*, vol. 41, no. 3, pp. 1138–1147, Jul. 2005.
123. S. Coraluppi and C. Carthel  
“Advances in active sonar tracking,”  
in *Proc. 14th Eur. Signal Process. Conf.*, 2006.
124. S. Coraluppi, C. Carthel, and A. Coon  
“An MHT approach to multi-sensor passive sonar tracking,”  
in *Proc. 21st Int. Conf. Inf. Fusion*, Cambridge, U.K., 2018.
125. M. Balci and R. Pegg  
“Towards global maritime domain awareness—Recent developments and challenges,”  
in *Proc. 9th Int. Conf. Inf. Fusion*, Florence, Italy, 2006.
126. N. A. Bomberger, B. J. Rhodes, M. Seibert, and A. M. Waxman  
“Associative learning of vessel motion patterns for maritime situation awareness,”  
in *Proc. 9th Int. Conf. Inf. Fusion*, Florence, Italy, 2006.
127. M. Seibert et al.  
“SeeCoast port surveillance,”  
in *Proc. Photon. Port Harbor Secur. II*, 2006, vol. 6204.
128. C. Carthel, S. Coraluppi, and P. Grignan  
“Multisensor tracking and fusion for maritime surveillance,”  
in *Proc. 10th Int. Conf. Inf. Fusion*, Quebec City, QC, Canada, 2007.
129. E. Liland  
“AIS aided multi hypothesis tracker,” Master’s thesis, Norwegian Univ. Sci. Technol., Trondheim, Norway, 2017.
130. O. Gerard, C. Carthel, and S. Coraluppi  
“Estimating the number of beaked whales using an MHT tracker,”  
in *Proc. 2008 New Trends Environ. Monit. Passive Syst.*, Hyeres, French Riviera, France, 2008, pp. 1–6.
131. J. N. Entzminger, C. A. Fowler, and W. J. Kenneally  
“JointSTARS and GMTI: Past, present and future,”  
*IEEE Trans. Aerosp. Electron. Syst.*, vol. 35, no. 2, pp. 748–761, Apr. 1999.
132. C.-Y. Chong, D. Garren, and T. P. Grayson  
“Ground target tracking—A historical perspective,”  
in *Proc. IEEE Aerosp. Conf.*, 2000.
133. D. R. Kirk, T. Grayson, D. Garren, and C.-Y. Chong  
“AMSTE precision fire control tracking overview,”  
in *Proc. IEEE Aerosp. Conf.*, 2000.
134. P. J. Shea, T. Zadra, D. Klamer, E. Frangione, R. Brouillard, and K. Kastella  
“Precision tracking of ground targets,”  
in *Proc. IEEE Aerosp. Conf.*, 2000.
135. R. J. Dempster, S. S. Blackman, and T. S. Nichols  
“Combining IMM filtering and MHT data association for multitarget tracking,”  
in *Proc. 29th Southeastern Symp. Syst. Theory*, 1997.
136. W. Koch  
“GMTI-tracking and information fusion for ground surveillance,”  
in *Proc. SPIE Signal Data Process. Small Targets*, 2001.
137. J. Koller and M. Ulmke  
“Multi hypothesis track extraction and maintenance of GMTI sensor data,”  
in *Proc. 7th Int. Conf. Inf. Fusion*, Philadelphia, PA, 2005.
138. D. Svensson, J. Wintenby, and L. Svensson  
“Performance evaluation of MHT and GM-CPHD in a ground target tracking scenario,”  
in *Proc. 12th Int. Conf. Inf. Fusion*, Seattle, WA, 2009.
139. P. O. Arambel, J. Silver, J. Krant, M. Antone, and T. Strat  
“Multiple-hypothesis tracking of multiple ground targets from aerial video with dynamic sensor control,”  
in *Proc. SPIE Signal Process., Sensor Fusion, Target Recognit. XIII*, 2004.
140. P. O. Arambel and M. Antone  
“Multiple target tracking with a steerable airborne video sensor,”  
in *Proc. SPIE Signal Process., Sensor Fusion, Target Recognit. XV*, 2006.
141. M. Keck, L. Galup, and C. Stauffer  
“Real-time tracking of low-resolution vehicles for wide-area persistent surveillance,”  
in *Proc. 2013 IEEE Workshop Appl. Comput. Vis.*, 2013.
142. P. Bendich et al.  
“Topological and statistical behavior classifiers for tracking applications,”  
*IEEE Trans. Aerosp. Electron. Syst.*, vol. 52, no. 6, pp. 2644–2661, Dec. 2016.
143. R. Spraul, C. Hartung, and T. Schuchert  
“Persistent multiple hypothesis tracking for wide area motion imagery,”  
in *Proc. 2017 IEEE Int. Conf. Image Process.*, 2017.
144. B. Uz Kent, M. J. Hoffman, and A. Vodacek  
“Integrating hyperspectral likelihoods in a multidimensional assignment algorithm for aerial vehicle tracking,”  
*IEEE J. Sel. Top. Appl. Earth Obs. Remote Sens.*, vol. 9, no. 9, pp. 4325–4333, Sep. 2016.

145. A. G. A. Perera, C. Srinivas, A. Hoogs, G. Brooksby, and W. Hu  
“Multi-object tracking through simultaneous long occlusions and split-merge conditions,”  
in *Proc. Conf. Comput. Vis. Pattern Recognit.*, 2006.
146. Y. Z. Gürbüz, O. Can, and A. A. Alatan  
“Roadesic distance: Flow-aware tracklet association cost for wide area surveillance,”  
in *Proc. IEEE Int. Conf. Image Process.*, 2017.
147. D. E. Iverson, K.-C. Chang, and C.-Y. Chong  
“Performance assessment for airborne surveillance systems incorporating sensor fusion,”  
in *Proc. SPIE Signal Data Process. Small Targets*, 1989.
148. S. S. Blackman, R. J. Dempster, and T. J. Broida  
“Multiple hypothesis track confirmation for infrared surveillance systems,”  
*IEEE Trans. Aerosp. Electron. Syst.*, vol. 29, no. 3, pp. 810–824, Jul. 1993.
149. G. Van Keuk  
“Multihypothesis tracking with electronically scanned radar,”  
*IEEE Trans. Aerosp. Electron. Syst.*, vol. 31, no. 3, pp. 916–927, Jul. 1995.
150. T. Wigren, E. Sviestins, and H. Egnell  
“Operational multi-sensor tracking for air defense,”  
in *Proc. 1st Aust. Data Fusion Symp.*, 1996.
151. S. S. Blackman, R. J. Dempster, M. T. Busch, and R. F. Popoli  
“IMM/MHT solution to radar benchmark tracking problem,”  
*IEEE Trans. Aerosp. Electron. Syst.*, vol. 35, no. 2, pp. 730–738, Apr. 1999.
152. W. Koch  
“Generalized smoothing for multiple model/multiple hypothesis filtering: Experimental results,”  
in *Proc. Eur. Control Conf.*, 1999.
153. G. Van Keuk  
“MHT extraction and track maintenance of a target formation,”  
*IEEE Trans. Aerosp. Electron. Syst.*, vol. 38, no. 1, pp. 288–295, Jan. 2002.
154. A. Thite and A. Mishra  
“Optimized multi-sensor multi-target tracking algorithm for air surveillance system,”  
in *Proc. 2nd Int. Conf. Adv. Elect., Electron., Inf., Commun. Bioinf.*, 2016.
155. R. A. Hoogendoorn and W. H. L. Neven  
“ARTAS: Multisensor tracking in an ATC environment,”  
Nat. Aerosp. Lab., Emmeloord, The Netherlands, NLR TP 97657, 1997.
156. B. Rakdham, M. Tummala, P. E. Pace, J. B. Michael, and Z. P. Pace  
“Boost phase ballistic missile defense using multiple hypothesis tracking,”  
in *Proc. IEEE Int. Conf. Syst. Syst. Eng.*, 2007.
157. J. A. Kennewell and B.-N. Vo  
“An overview of space situational awareness,”  
in *Proc. 16th Int. Conf. Inf. Fusion*, Istanbul, Turkey, 2013.
158. A. B. Poore and J. T. Horwood  
“Multiple hypothesis correlation for space situational awareness,” Numerica Corp., Loveland, CO, Final Tech. Rep., Aug. 2011.
159. S. M. Gadaleta, J. T. Horwood, and A. B. Poore  
“Short arc gating in multiple hypothesis tracking for space surveillance,”  
in *Proc. SPIE Sensors Syst. Space Appl. V*, 2012.
160. N. Singh, J. T. Horwood, J. M. Aristoff, A. B. Poore, C. Sheaff, and M. K. Jah  
“Multiple hypothesis tracking (MHT) for space surveillance: Results and simulation studies,”  
in *Proc. Adv. Maui Opt. Space Surveillance Technol. Conf.*, 2013.
161. I. J. Cox, J. M. Rehg, and S. Hingorani  
“A Bayesian multiple hypothesis approach to contour grouping,”  
in *Proc. Eur. Conf. Comput. Vis.*, 1992.
162. I. J. Cox, J. M. Rehg, and S. Hingorani  
“A Bayesian multiple-hypothesis approach to edge grouping and contour segmentation,”  
*Int. J. Comput. Vis.*, vol. 11, no. 1, pp. 5–24, Aug. 1993.
163. I. J. Cox and S. L. Hingorani  
“An efficient implementation and evaluation of Reid’s multiple hypothesis tracking algorithm for visual tracking,”  
in *Proc. 12th Int. Conf. Pattern Recognit.*, 1994.
164. T.-J. Cham and J. M. Rehg  
“A multiple hypothesis approach to figure tracking,”  
in *Proc. Conf. Comput. Vis. Pattern Recognit.*, 1999.
165. C. Stauffer  
“Estimating tracking sources and sinks,”  
in *Proc. Conf. Comput. Vis. Pattern Recognit.*, 2003.
166. A. Y. S. Chia, W. Huang, and L. Li  
“Multiple objects tracking with multiple hypotheses graph representation,”  
in *Proc. 18th Int. Conf. Pattern Recognit.*, 2006.
167. H. Jiang, S. Fels, and J. J. Little  
“A linear programming approach for multiple object tracking,”  
in *Proc. IEEE Conf. Comput. Vis. Pattern Recognit.*, 2007.
168. V. K. Singh, B. Wu, and R. Nevatia  
“Pedestrian tracking by associating tracklets using detection residuals,”  
in *Proc. IEEE Workshop Motion Video Comput.*, 2008.
169. K. O. Arras, S. Grzonka, M. Luber, and W. Burgard  
“Efficient people tracking in laser range data using a multi-hypothesis leg-tracker with adaptive occlusion probabilities,”  
in *Proc. IEEE Int. Conf. Robot. Autom.*, 2008.
170. L. Zhang, Y. Li, and R. Nevatia  
“Global data association for multi-object tracking using network flows,”  
in *Proc. IEEE Conf. Comput. Vis. Pattern Recognit.*, 2008.
171. J. Xing, H. Ai, and S. Lao  
“Multi-object tracking through occlusions by local tracklets filtering and global tracklets association with detection responses,”  
in *Proc. IEEE Conf. Comput. Vis. Pattern Recognit.*, 2009.
172. Z. Wu, N. I. Hristov, T. H. Kunz, and M. Betke  
“Tracking-reconstruction or reconstruction-tracking? Comparison of two multiple hypothesis tracking approaches to interpret 3D object motion from several camera views,”  
in *Proc. Workshop Motion Video Comput.*, 2009.
173. A. Azim and O. Aycard  
“Multiple pedestrian tracking using Viterbi data association,”  
in *Proc. IEEE Intell. Veh. Symp.*, 2010.
174. X. Yu and A. Ganz  
“Global identification of tracklets in video using long range identity sensors,”  
in *Proc. 7th IEEE Int. Conf. Adv. Video Signal Based Surveillance*, 2010.
175. J. Berclaz, F. Fleuret, E. Turetken, and P. Fua  
“Multiple object tracking using  $K$ -shortest paths optimization,”  
*IEEE Trans. Pattern Anal. Mach. Intell.*, vol. 33, no. 9, pp. 1806–1819, Sep. 2011.

176. H. Pirsiavash, D. Ramanan, and C. C. Fowlkes  
“Globally-optimal greedy algorithms for tracking a variable number of objects,”  
in *Proc. IEEE Conf. Comput. Vis. Pattern Recognit.*, 2011.
177. W. Brendel, M. Amer, and S. Todorovic  
“Multiobject tracking as maximum weight independent set,”  
in *Proc. IEEE Conf. Comput. Vis. Pattern Recognit.*, 2011.
178. Z. Wu, T. H. Kunz, and M. Betke  
“Efficient track linking methods for track graphs using network-flow and set-cover techniques,”  
in *Proc. Conf. Comput. Vis. Pattern Recognit.*, 2011.
179. L. Lin, Y. Lu, Y. Pan, and X. Chen  
“Integrating graph partitioning and matching for trajectory analysis in video surveillance,”  
*IEEE Trans. Image Process.*, vol. 21, no. 12, pp. 4844–4857, Dec. 2012.
180. A. A. Butt and R. T. Collins  
“Multi-target tracking by Lagrangian relaxation to min-cost network flow,”  
in *Proc. IEEE Conf. Comput. Vis. Pattern Recognit.*, 2013.
181. H. B. Shitrit, J. Berclaz, F. Fleuret, and P. Fua  
“Multi-commodity network flow for tracking multiple people,”  
*IEEE Trans. Pattern Anal. Mach. Intell.*, vol. 36, no. 8, pp. 1614–1627, Aug. 2014.
182. T. Linder and K. O. Arras  
“Multi-model hypothesis tracking of groups of people in RGB-D data,”  
in *Proc. 17th Int. Conf. Inf. Fusion*, Salamanca, Spain, 2014.
183. C. Kim, F. Li, A. Ciptadi, and J. M. Rehg  
“Multiple hypothesis tracking revisited,”  
in *Proc. IEEE Int. Conf. Comput. Vis.*, 2015.
184. B. Wang, G. Wang, K. L. Chan, and L. Wang  
“Tracklet association by online target-specific metric learning and coherent dynamics estimation,”  
*IEEE Trans. Pattern Anal. Mach. Intell.*, vol. 39, no. 3, pp. 589–602, Mar. 2017.
185. M. Manafifard, H. Ebadi, and H. A. Moghaddam  
“Appearance-based multiple hypothesis tracking,”  
*Image Commun.*, vol. 55, no. C, pp. 157–170, Jul. 2017.
186. O. Birbach and U. Frese  
“A multiple hypothesis approach for a ball tracking system,”  
in *Computer Vision Systems*, M. Fritz, B. Schiele, and J. H. Piater Eds. Berlin, Germany: Springer, 2009, pp. 435–444.
187. X. Zhou, L. Xie, Q. Huang, S. J. Cox, and Y. Zhang  
“Tennis ball tracking using a two-layered data association approach,”  
*IEEE Trans. Multimedia*, vol. 17, no. 2, pp. 145–156, Feb. 2015.
188. “MOT challenge.” [Online]. Accessed: Feb. 15, 2019. Available: <https://motchallenge.net/>.
189. J. H. Faghmous et al.  
“Multiple hypothesis object tracking for unsupervised self-learning: An ocean eddy tracking application,”  
in *Proc. 23th AAAI Conf. Artif. Intell.*, 2013.
190. J. Kubica, A. Moore, A. Connolly, and R. Jedicke  
“A multiple tree algorithm for the efficient association of asteroid observations,”  
in *Proc. 11th ACM SIGKDD Int. Conf. Knowl. Discov. Data Mining*, New York, NY, 2005.
191. D. Kempton, K. G. Pillai, and R. Angryk  
“Iterative refinement of multiple targets tracking of solar events,”  
in *Proc. 2014 IEEE Int. Conf. Big Data*, Washington, DC, 2014.
192. D. J. Kempton and R. A. Angryk  
“Tracking solar events through iterative refinement,”  
*Astron. Comput.*, vol. 13, pp. 124–135, Nov. 2015.
193. G. V. Cybenko and C. Alberola  
“Tracking with text-based messages,”  
*IEEE Intell. Syst.*, vol. 14, no. 4, pp. 70–78, 1999.
194. S. Aja-Fernández, C. Alberola-López, and G. Cybenko  
“A fuzzy MHT algorithm applied to text-based information tracking,”  
*IEEE Trans. Fuzzy Syst.*, vol. 10, pp. 360–374, Jul. 2002.
195. V. H. Berk, G. V. Cybenko, and R. S. Gray  
“Early detection of active Internet worms,”  
in *Managing Cyber Threats: Issues, Approaches, and Challenges*, V. Kumar, J. Srivastava, and A. Lazarevic Eds. Boston, MA: Springer US, 2005, pp. 147–180.
196. S. Schwoegler, J. Holsopple, S. Blackman, and M. J. Hirsch  
“On the application of multiple hypothesis tracking to the cyber domain,”  
in *Proc. 14th Int. Conf. Inf. Fusion*, Chicago, IL, 2011.
197. J. H. P. Broeke et al., “Automated quantification of cellular traffic in living cells,”  
*J. Neurosci. Methods*, vol. 178, no. 2, pp. 378–384, Apr. 2009.
198. L. Feng, Y. Xu, Y. Yang, and X. Zheng  
“Multiple dense particle tracking in fluorescence microscopy images based on multidimensional assignment,”  
*J. Struct. Biol.*, vol. 173, no. 2, pp. 219–228, Feb. 2011.
199. N. Chenouard, I. Bloch, and J. Olivo-Marin  
“Multiple hypothesis tracking in microscopy images,”  
in *Proc. 2009 IEEE Int. Symp. Biomed. Imag.: From Nano to Macro*, 2009.
200. N. Chenouard, I. Bloch, and J. Olivo-Marin  
“Multiple hypothesis tracking for cluttered biological image sequences,”  
*IEEE Trans. Pattern Anal. Mach. Intell.*, vol. 35, no. 11, pp. 2736–2750, Nov. 2013.
201. E. Cheng, Y. Pang, Y. Zhu, J. Yu, and H. Ling  
“Curvilinear structure tracking by low rank tensor approximation with model propagation,”  
in *Proc. IEEE Conf. Comput. Vis. Pattern Recognit.*, 2014.
202. L. Liang, H. Shen, P. De Camilli, and J. S. Duncan  
“A novel multiple hypothesis based particle tracking method for clathrin mediated endocytosis analysis using fluorescence microscopy,”  
*IEEE Trans. Image Process.*, vol. 23, no. 4, pp. 1844–1857, Apr. 2014.

**Chee-Yee Chong** received the S.B., S.M., and Ph.D. degrees in electrical engineering from the Massachusetts Institute of Technology, Cambridge, MA, USA, in 1969, 1970, and 1973, respectively. He was with the Electrical Engineering Faculty, Georgia Tech, Atlanta, GA, USA, until 1980, when he moved to Silicon Valley to join Advanced Decision Systems, which was acquired by Booz Allen Hamilton in 1991. In 2003, he joined ALPHATECH, which was acquired by BAE Systems, and stayed until 2013. He is currently an independent researcher and consultant. He has been involved in all levels of information fusion, including Bayesian multiple hypothesis tracking, optimal track fusion and association, close loop tracking with sensor resource management, analytical model to predict association performance, Bayesian networks for situation assessment, hard and soft data fusion, and graph approaches for data association. He is particularly interested in combining model-based and learning-based approaches for robust data fusion in mission-critical systems. He co-founded the International Society of Information Fusion (ISIF), and served as its President in 2004. He was general Co-chair for the 12th International Conference on Information Fusion held in Seattle, WA, USA, in 2009. He was Associate Editor for the IEEE TRANSACTIONS ON AUTOMATIC CONTROL and *Information Fusion*, and is an Associate Editor for *Journal of Advances in Information Fusion* published by ISIF. He received the ISIF Yaakov Bar-Shalom Award for a Lifetime of Excellence in Information Fusion in 2016.



**Shozo Mori** received the B.S. degree in electric engineering from Waseda University, Tokyo, Japan, in 1970, the M.S. degree in control engineering from Tokyo Institute of Technology, Tokyo, Japan, in 1972, and the Ph.D. degree in engineering economic systems from Stanford University, Stanford, CA, USA, in 1983. He is currently a Consultant with Systems & Technology Research (STR), Sacramento, CA, USA. He was with Advanced Decision & Information Systems (later acquired by Booz-Allen & Hamilton), Mountain View, CA, USA, from 1980 to 1991, Tiburon Systems (later acquired by Texas Instruments, and then by Raytheon Company), San Jose, CA, USA, from 1992 to 1999, Information Extraction & Transport, Arlington, VA, USA, from 2000 to 2003, ALPHATECH (later acquired by BAE Systems), Burlington, MA, USA, from 2003 to 2013, and STR, Woburn, MA, USA, from 2013 to present. His current research interests include multiple target tracking, particularly as applications of theories of random finite sets and finite point processes, distributed data fusion problems in various domains, and applications of theories of information processing and multiple-person decision systems to economic and social system analysis. He is an IEEE Life Member. He was a member of Program Committee for MSS National Sensor and Data Fusion Symposium, and an Area/Assistant Editor for the IEEE TRANSACTIONS ON SYSTEMS, MAN, AND CYBERNETICS, IEEE TRANSACTIONS ON AEROSPACE AND ELECTRONIC SYSTEMS, and *Journal of Advances in Information Fusion* published by the International Society of Information Fusion. He was the recipient of 2016 Joseph Mignogna Data Fusion Award.





**Donald B. Reid** was born in Washington, DC, USA, on March 29, 1941, and grew up there and in the Maryland and Virginia suburbs, graduating from Falls Church High School in 1959. In 1963, he graduated from the U.S. Military Academy, West Point, NY, USA, and was commissioned into the U.S. Air Force. After receiving a master's degree from Stanford University, Stanford, CA, USA, in 1965, he was stationed at Vandenberg AFB involved in the test and launch of satellites. He returned to Stanford University and received the Ph.D. degree in 1972 with Professor Arther E. Bryson as thesis supervisor. He then joined the Institute for Defense Analysis (IDA), Arlington, VA, USA, and was involved in various military-related studies. In 1976, he joined the Lockheed Palo Alto Research Labs, and led a small group doing research on target tracking with applications to tracking military units over open terrain as well as ocean surveillance. One notable report was "An Algorithm for Tracking Multiple Targets," which presents the multiple hypothesis tracking algorithm. During 1981–1984 and 1986–1989, he worked in West Germany. From 1990 to 1999, he worked on the Milstar Communications Satellite. During 2000–2003 and 2005–2008, he worked in England. From 2008 until his retirement in 2011 from Lockheed Martin, he worked in Sunnyvale, CA, USA, on the Milstar, AEHF, and SBIRS programs, primarily on the attitude determination and control systems. He currently lives in San Jose, CA, USA, and is the proud father of three daughters and seven grandchildren, and husband of Carole Cooke Reid.

# Multiple-Hypothesis Tracking and Graph-Based Tracking Extensions

STEFANO P. CORALUPPI  
CRAIG A. CARTHEL  
ALAN S. WILLISKY

**This paper reviews key elements in the development of *multiple-hypothesis tracking* (MHT), a leading paradigm for multitarget tracking, as well as *graph-based tracking* (GBT), a scalable version of MHT that has proven effective in kinematic track stitching applications. We introduce a novel MHT/GBT algorithm that we denote as *multi-INT GBT* (MI-GBT). It provides computational benefits over classical MHT, while allowing for static components of the target state that classical GBT does not. Thus, the MI-GBT provides an effective method for multisensor feature-aided track fusion with disparate sensors. We quantify the improved performance over the MHT solution in Monte Carlo studies.**

Manuscript received January 28, 2019; revised May 8, 2019, October 30, 2019, and November 5, 2019; released for publication February 5, 2020.

Refereeing of this contribution was handled by Jason L. Williams.

S. P. Coraluppi and C. A. Carthel are with Systems and Technology Research, 600 West Cummings Park, Woburn, MA 01801, USA (E-mail: Stefano.Coraluppi@STRResearch.com, Craig.Carthel@STRResearch.com).

A. S. Willisky is with the Department of Electrical Engineering, Massachusetts Institute of Technology, 77 Massachusetts Avenue, Cambridge, MA 02139, USA (E-mail: willisky@mit.edu).

1557-6418/19/\$17.00 © 2019 JAIF

## I. INTRODUCTION

Many approaches have been developed to address the *multitarget tracking* (MTT) problem, whereby an unknown and time-varying set of objects is to be tracked while contending with unknown measurement origin, missed detections, and false alarms [1]. *Multiple-hypothesis tracking* (MHT) was first posed in hypothesis-oriented form [2] and was later shown to admit hypothesis factorization (assuming Poisson-distributed births and clutter) and a more efficient track-oriented formulation [3], consistent with the *integer linear program* (ILP) framework of the MTT problem that had been proposed previously [4].

The ILP can be solved via relaxation approaches [5]–[7], and distributed processing can provide performance and robustness advantages in many settings [8]–[10]. The MHT paradigm has been generalized to consider object births without detection, enabling improved performance in dim-target settings [11]. More recently, extension to allow for multiple measurements per target per scan has been developed to deal with extended objects and multipath phenomena [12], [13].

When a simplifying Markovian (path-independence) assumption may be invoked, significant computational gains can be achieved. In the *hypothesis-oriented MHT* (HO-MHT) context, the simplified formulation may be solved by use of the Viterbi algorithm on an expanded trellis [14]. The more general treatment, with missed detections and clutter, was addressed in a series of papers culminating in [15]. Application of the approach to track-level inputs is discussed in [16]. While these are valuable contributions, unfortunately these approaches do not scale well when the numbers of measurements and targets are large. Also, these papers do not contend with target birth and death phenomena, which appear somewhat cumbersome to include.

Shortly after the publication of [14], the same simplification was introduced in the track-oriented MHT (TO-MHT) context [17]. This established the *graph-based tracking* (GBT) paradigm for MTT. The approach is not generally adopted for remote-sensing applications (e.g., sonar or radar tracking), since the Markovian assumption is too strong in these settings. Nonetheless, GBT for track maintenance with missed detections and clutter is developed in [18]. Perhaps more significantly, application of GBT to track-level inputs is discussed in [19]; this represents an important contribution in that, for track-level kinematic data, the Markovian assumption is quite appropriate.

In some settings, the Markovian assumption inherent in both Viterbi and GBT methods is not appropriate. Indeed, some elements of the target state vector, e.g., object size, color, etc., may be fixed or slowly varying. In such cases, measurement sequences do not exhibit a path-independence property, except when these slowly varying elements are always observed. Accordingly, when feature measurements are temporally

TABLE I  
Assumptions and Some Solution Approaches for MTT

Assumptions	General	Partially Markov data	Markov data
General	HO-MHT [2]	Not investigated	Viterbi [14]
Poisson targets and clutter	TO-MHT [3]	MI-GBT [22]	GBT [17]

sparse, until recently it was necessary to resort to MHT solutions.

Recent work has extended the GBT approach to deal with feature states. In [20], a novel GBT multicommodity flow approach is discussed. The approach assumes a known number of objects, a unique object of each type, single-sensor data, and a batch-processing formulation. The methodology is promising in that it leads to a much smaller ILP than with an MHT approach. In [21] and [22], we develop a similar approach—the *multi-INT GBT* (MI-GBT)—for the general multisensor MTT problem, with a temporally sparse identity sensor and one or more kinematic sensors. Refs. [21] and [22] discuss as well a *Markov chain Monte Carlo* (MCMC) approach for the multi-INT (i.e., disparate-sensor) track fusion problem that builds on the work in [23]; for our application with sparse identity data, MCMC provides a promising approach to solution refinement. Related investigations of generalized GBT methods include [24] and [25].

Most recently, in [26] we relax the unique-type assumption in the MI-GBT, allowing for multiple objects of each type, and explore performance for multitarget track maintenance. Here, we discuss a sliding-window approach to ILP formation and resolution, enabling scalable processing of lengthy scenarios that are otherwise computationally prohibitive with earlier, batch-processing solution methods.

Table I provides a summary view of some paradigms for the MTT problem, focusing on hard data association and labeled target tracking. (See [1] and [27] for a discussion of other methods.) Given the computational advantages of the TO-MHT approach that avoids the global-hypothesis enumeration inherent in HO-MHT, we have chosen not to investigate a hybrid HO-MHT/Viterbi approach. This paper makes further progress on the MI-GBT that provides a hybrid TO-MHT/GBT paradigm that exploits path independence when possible, and introduces hypothesis branching when necessary to contend with identity data.

This paper is organized as follows. In Section II, we review salient elements of MHT. Section III discusses both MHT and MI-GBT for the multi-INT track fusion problem with sparse identity data, allowing for multiple objects of each type and with sliding-window processing. Section IV describes performance results for MI-GBT compared to the MHT baseline solution. We establish the superior performance characteristics of

MI-GBT over both GBT and MHT. Conclusions are provided in Section V.

## II. MULTIPLE-HYPOTHESIS TRACKING

In MTT, we seek a set of trajectories over a sequence of times  $t^k = (t_1, \dots, t_k)$  that we may denote compactly by  $X^k$ . Each trajectory in this set has a time of birth, an evolution in target state space, and (possibly) a time of death. Hence, we are interested in identifying the time evolution of an unknown (and time-varying) number of objects. We observe a sequence of sets of measurements  $Z^k = (Z_1, \dots, Z_k)$ . The usual simplifying assumption in the MTT problem formulation is that, with each sensor scan, each target gives rise to at most one measurement. It is not known which measurement originates from which object, and there are as well false measurements that are not target originated.

### A. MAP Estimation and Hypothesis-Oriented MHT

In statistical estimation theory, it is well established that minimization of the Bayes risk with an underlying cost function that penalizes all estimation errors uniformly is achieved with the conditional mode. Stated another way, the minimum probability of error estimator is given by the *maximum a posteriori* (MAP) estimator [28]. However, use of the MAP criterion for the MTT problem, when applied directly to  $p(X^k|Z^k)$ , is conceptually problematic [29, pp. 494–500].

One may explicitly consider an explanation for the data, i.e., to specify which measurements are to be rejected as false and how target-originated measurements are to be associated. Let us denote by  $q^k$  one such global hypothesis or explanation. This leads to a probabilistic conditioning approach and the following expression for the multitarget posterior probability distribution  $p(X^k|Z^k)$ <sup>1</sup>:

$$p(X^k|Z^k) = \sum_{q^k} p(X^k|Z^k, q^k) p(q^k|Z^k). \quad (1)$$

Note that, for any MTT problem of reasonable size, the space of global hypotheses—and hence the summation in Eq. (1)—is enormous.

The MHT paradigm addresses both the conceptual difficulty associated with MAP estimation applied to  $p(X^k|Z^k)$  and the computational difficulty associated with the representation given by Eq. (1). In particular, MHT seeks the MAP global hypothesis  $\hat{q}^k$  and conditions on this global hypothesis to estimate the set of target trajectories while discarding competing global hypotheses. This is captured in the following equations:

$$\hat{q}^k = \arg \max_{q^k} p(q^k|Z^k), \quad (2)$$

<sup>1</sup>Equation (1) is a conceptual expression; a more rigorous treatment with the *random finite set* formalism may be found in [30].

$$\hat{X}^k = \arg \max_{X^k} p(X^k | Z^k, \hat{q}^k). \quad (3)$$

Note that  $X^k$  is representative of a set of trajectories, each with a time of birth, an evolution in state space, and (possibly) a time of death. We will not discuss here the random finite set treatment of the MTT problem; see [29] and [30] for more details.

Solving Eq. (3) entails the solution to a set of smoothing problems. Most MTT approaches include recursive filtering but do not focus on trajectory smoothing. Indeed, while useful for output reporting, trajectory smoothing does not aid in data association; i.e., it does not contribute to solving Eq. (2).

Though solving Eq. (2) is not conceptually problematic, it remains computationally prohibitive. In practice, most MHT implementations consider a sliding-window formulation and *resolve* (i.e., select) global hypotheses with some delay. Having solved Eq. (2), solving Eq. (3) amounts to solving a set of filtering problems with no measurement-origin uncertainty. It is often beneficial to decouple data association and track extraction (see [31]).

Computational and real-time constraints require that we adopt a recursive formulation of  $p(q^k | Z^k)$ . The following expression may be derived:

$$p(q^k | Z^k) = \frac{p(Z_k | Z^{k-1}, q^k) p(q^k | q^{k-1}) p(q^{k-1} | Z^{k-1})}{p(Z_k | Z^{k-1})}. \quad (4)$$

This is the global-hypothesis recursion that expresses  $p(q^k | Z^k)$  as a function of  $p(q^{k-1} | Z^{k-1})$  and the current scan of data  $Z_k$ .

## B. Track-Oriented MHT

Though useful, the recursion in Eq. (4) is generally intractable in the sense that the space of global hypotheses is quite large. Fortunately, under some simplifying assumptions, namely, a Poisson-distributed number of target births and false alarms at each scan, the posterior probability of a global hypothesis  $p(q^k | Z^k)$  may be expressed as a product over local (or *track*) hypotheses associated with  $q^k$ .

The Poisson assumption is reasonable in many settings. We consider a continuous-time process with exponentially distributed target interarrival (birth) times with parameter  $\lambda_b$ , and exponentially distributed target lifetime with parameter  $\lambda_\chi$ . Discrete-time statistics may be readily obtained, leading to a Poisson distributed number of births with mean  $\mu_b(t)$  and death probability  $p_\chi(t)$  over an interval of duration  $t$ :

$$\mu_b(t) = \frac{\lambda_b}{\lambda_\chi} (1 - e^{-\lambda_\chi t}), \quad (5)$$

$$p_\chi(t) = 1 - e^{-\lambda_\chi t}. \quad (6)$$

For simplicity, in the following we will omit the time interval  $t$  and use the birth rate and death probability

$\mu_b$  and  $p_\chi$ , respectively. Note that the Poisson birth process has an intuitively appealing independence property, whereby the numbers of births in temporally nonoverlapping intervals are independent random variables [32]. Similarly, the Poisson false alarm assumption (with mean  $\Lambda$ ) characterizes clutter statistics in many application domains. For target-originated measurements, we assume that, at each scan, each target is detected with probability  $p_d$ .

Let  $\tau$  be the number of tracks in the parent global hypothesis  $q^{k-1}$  at time  $t_{k-1}$ , let  $r = |Z_k|$  be the number of measurements in the current scan at time  $t_k$ , and let  $b$ ,  $\chi$ , and  $d$  be the number of target births, deaths, and measurement updates in global hypothesis  $q^k$  at time  $t_k$ , respectively.

We now express the global-hypothesis recursion given by Eq. (4) in detail. First, let us consider the factor  $p(q^k | q^{k-1})$ . For this, we introduce the auxiliary variable  $\psi_k$  that specifies the number of births  $b$ , the number of target deaths  $\chi$ , and the number of targets with measurement update  $d$ . We use the following conditioning approach that relies on  $\psi_k$ :

$$p(q^k | q^{k-1}) = p(\psi_k | q^{k-1}) p(q^k | q^{k-1}, \psi_k). \quad (7)$$

The first factor in Eq. (7) denotes the probability of observing  $b$  target births,  $\chi$  deaths, and  $d$  measurement updates from  $\tau$  targets, and  $r - d - b$  false alarms (to account for all remaining measurements). This may be written as follows, noting that we rely on 1) the Poisson distribution to account for  $b$  (detected) births and  $r - d - b$  false alarms, as well as 2) the binomial distribution for the probability of observing some number of successes in a set of independent trials—this is relevant to the factors that account for  $\chi$  deaths from  $\tau$  targets and  $d$  detections from the surviving  $\tau - \chi$  targets:

$$\begin{aligned} p(\psi_k | q^{k-1}) &= \binom{\tau}{\chi} p_\chi^\chi (1 - p_\chi)^{\tau - \chi} \cdot \binom{\tau - \chi}{d} \\ &\times p_d^d (1 - p_d)^{\tau - \chi - d} \cdot \frac{(p_d \mu_b)^b \exp(-\mu_b)}{b!} \\ &\cdot \frac{\Lambda^{r-d-b} \exp(-\Lambda)}{(r - d - b)!}. \end{aligned} \quad (8)$$

The second factor in Eq. (7) denotes the probability of a particular global hypothesis, conditioned on the parent hypothesis and on the cardinalities associated with  $\psi_k$ . As all association probabilities have the same *a priori* probabilities, this factor can be written as follows. Note that the denominator terms quantify the number of ways of selecting the target deaths, the number of ways of selecting which tracks to update, the number of ways of selecting measurements and assigning them to tracks (where ordering matters), and the number of ways of selecting birth measurements among the remaining  $r - d$

measurements.

$$p(q^k | q^{k-1}, \psi_k) = \frac{1}{\binom{\tau}{\chi} \binom{\tau - \chi}{d} \binom{r!}{(r-d)!} \binom{r-d}{b}}. \quad (9)$$

Combining Eqs. (8) and (9) according to Eq. (7) yields

$$p(q^k | q^{k-1}) = \left\{ \frac{\exp(-\mu_b - \Lambda) \Lambda^r}{r!} \right\} p_\chi^\chi \cdot ((1 - p_\chi)(1 - p_d))^{\tau - \chi - d} \left( \frac{(1 - p_\chi) p_d}{\Lambda} \right)^d \times \left( \frac{p_d \mu_b}{\Lambda} \right)^b. \quad (10)$$

The factor  $p(Z_k | Z^{k-1}, q^k)$  in Eq. (4) accounts for the probability of observing a set of measurements given a global hypothesis. It is a product over filter residual scores; hence, it may be written as follows, where, under  $q^k$ ,  $J_d$  is the set of track update measurements,  $J_{fa}$  is the set of false alarms,  $J_b$  is the set of target birth measurements,  $f(\cdot | Z^{k-1}, q^k)$  is the conditional probability distribution of a target measurement (with no conditioning in the case of object birth), and  $f_{fa}(\cdot)$  is the distribution of false alarms in measurement space:

$$p(Z_k | Z^{k-1}, q^k) = \prod_{z_j \in J_d} f(z_j | Z^{k-1}, q^k) \prod_{z_j \in J_b} f(z_j) \cdot \prod_{z_j \in J_{fa}} f_{fa}(z_j). \quad (11)$$

Equations (10) and (11) may be substituted into Eq. (4), resulting in the following TO-MHT recursion, in which we denote by  $C$  the factor that is common to all global hypotheses. (This common factor need not be computed for MAP estimation, and indeed its evaluation would rely on  $p(Z_k | Z^{k-1})$ , requiring summation over all global hypotheses.) The restriction that each measurement be used at most once in track formation, and that all measurements be accounted for, is captured in Eq. (12c), where  $J_Z$  is the set of indices for measurement set  $Z_k$ .

$$p(q^k | Z^k) = p_\chi^\chi ((1 - p_\chi)(1 - p_d))^{\tau - \chi - d} \cdot \prod_{j \in J_d} \frac{(1 - p_\chi) p_d f(z_j | Z^{k-1}, q^k)}{\Lambda f_{fa}(z_j)} \cdot \prod_{j \in J_b} \frac{p_d \mu_b f(z_j)}{\Lambda f_{fa}(z_j)} \cdot C \cdot p(q^{k-1} | Z^{k-1}), \quad (12a)$$

$$C = \frac{\left\{ \frac{\exp(-\mu_b - \Lambda) \Lambda^r}{r!} \right\} \prod_{z_j \in Z_k} f_{fa}(z_j)}{p(Z_k | Z^{k-1})}, \quad (12b)$$

$$J_d \cap J_b = \emptyset, \quad J_d \cap J_{fa} = \emptyset, \quad J_b \cap J_{fa} = \emptyset, \quad J_d \cup J_b \cup J_{fa} = J_Z. \quad (12c)$$

Equation (12) is of fundamental importance in that it factors the global hypothesis score into (dimensionless) track scores. Accordingly, it is unnecessary to consider each global hypothesis probability explicitly. Indeed, up to the hypothesis-independent factor  $C$ , a global hypothesis probability may be evaluated as a product over local hypothesis factors. This in turn allows the determination of  $\hat{q}^k$ , the solution to Eq. (2), without explicit enumeration of global hypotheses.

Thus, the TO-MHT formalism results in an ILP, with an objective function that may be expressed compactly by Eq. (13), where the cost  $c_i$  associated with track hypothesis  $x_i$  results from statistics-associated targets and sensors; the variable  $x_i \in \{0, 1\}$  may be understood as an indicator variable that corresponds to selecting a track hypothesis when setting  $x_i = 1$ . The sum is over all track hypotheses within a hypothesis reasoning window:

$$J = \sum_i c_i x_i, \quad (13)$$

$$Ax \leq b. \quad (14)$$

In addition to the objective, the ILP includes constraints captured by Eq. (14) that require that each measurement be used at most once in track formation, and that each resolved track from the start of the reasoning window be accounted for.

### III. MULTI-INT TRACK FUSION

Section II described TO-MHT (hereafter, MHT) for detection-level MTT. We now consider the MTT problem, downstream of single-sensor trackers. That is, upstream association decisions have been made, and we assume negligible residual false alarms. The challenge is to perform correct track association over time and across sensors. We assume that tracks are composed of sequences of measurements, so that optimal filtering can be performed without the need to contend with correlated state estimates due to common target process noise [27]. We are interested in both real-time and forensic settings. The principal challenge is how to contend with temporally sparse identity information that is crucial to exploit for high-performance association decisions. After providing some modeling details, we will first discuss the conventional MHT solution and then describe the MI-GBT approach.

#### A. Some Modeling Details

As noted earlier, we model target existence via a Poisson birth–death process; see Eqs. (5) and (6). For simplicity, we will discuss our work in the context of linear Gaussian dynamics and measurements, though the solution methodologies are applicable more broadly. (The model described here is what we use for the simulation results in Section IV.) Specifically, we will assume independent target dynamics according to a stable,

stationary generalization to *nearly constant velocity* (NCV) motion, as given by a second-order *Ornstein–Uhlenbeck* (OU) process [33].

Each object is of a fixed type, with a probability distribution over the finite set of types given by the vector  $p_{\text{type}}$ , with element  $p_{\text{type}}(i)$  being the probability that an object is of type  $i$ . We may handle unique objects of type  $i$  by using a small value for  $p_{\text{type}}(i)$ . This modeling approach is more robust than disallowing multiple objects, as the multiplicity is sometimes necessary to contend with potentially erroneous sliding-window association decisions. Also, all objects must be of some type; hence, we generally include the type “other” to include all those that are not of specific interest.

Kinematic tracks are composed of linear measurements with additive Gaussian noise with  $v_k \sim N(0, R_k)$ :

$$y_k = C_k x_k + v_k. \quad (15)$$

As noted earlier in the MHT derivation, at each scan targets are detected with probability  $p_d$ . For simplicity, we do not consider motion-dependent (or, more generally, state-dependent) detection statistics. Further, we do not consider identity-dependent detection statistics, as when objects of certain types are easier to detect than others.

We assume that identity sensors differ from kinematic sensors in two key respects. First, we assume a low revisit time between scans; hence, the identity detections are not associated over time. Second, detections include both kinematic information and precise target-type information. The type information is highly informative but does not provide association information, as there may be multiple objects of the same type. Detection and localization quality ( $p_d$  and  $R_k$ ) differ for kinematic and identity sensors. We do not consider false alarms from the identity sensor; this is reasonable in settings where *automatic target recognition* is performed to provide object-type information and to reject spurious detections.

## B. MHT Approach

The detection-level TO-MHT recursion given by Eq. (12) yields a dimensionless likelihood ratio associated with each track hypothesis. Normalization is with respect to a null hypothesis whereby all measurements are false alarms. For a track with index  $i$ , the negative log of this score yields the coefficient  $c_i$  in the objective function to be minimized, as given by Eq. (13).

For track-level association, since all tracks (including identity singleton tracks) are assumed to be target originated, we do not normalize with respect to the same null hypothesis. We may still utilize dimensionless track scores by normalizing with respect to another null hypothesis, whereby all tracks are unassociated.

Let  $z_j$  represent a track (i.e., a sequence of previously associated measurements) and let  $L(z^n)$  denote

the track likelihood associated with a sequence of tracks  $z^n = (z_1, \dots, z_n)$ . Note that  $L(z^n)$  is the (unnormalized) local hypothesis contribution to the global hypothesis probability. If this sequence corresponds to the  $i$ th track hypothesis, we may express the coefficient  $c_i$  in Eq. (13) as follows:

$$c_i = -\log L(z^n). \quad (16)$$

The likelihood  $L(z^n)$  accounts for target birth, a sequence of detection and missed-detection events, and (possibly) a target death. This score can be computed recursively based on the following probabilistic conditioning:

$$L(z^n) = L(z_1) \prod_{j=2, \dots, n} L(z_j | z^{j-1}). \quad (17)$$

We may alternatively adopt a dimensionless track score as given by the following. This is advantageous when solving Eq. (13) with fast greedy track selection methods, in lieu of a relaxation approach.

$$c_i = -\log \frac{L(z^n)}{\prod_{j=1, \dots, n} L(z_j)}. \quad (18)$$

As with detection-level MHT, most nontrivial track fusion problems entail hypothesis-space reduction via sliding-window processing. That is, with some temporal delay, we resolve ambiguity and identify a single global hypothesis by solving an appropriately defined ILP as in Eq. (13). Then, we ingest further data for processing, and solve a new ILP. The hypothesis tree depth is generally identified as the number of scans of data ( $n$ -scan) between the resolved time and current time [12], [31]. *Global nearest-neighbor* (GNN) processing corresponds to  $n$ -scan = 0 [27].

The MHT track fusion capability is quite general and allows for an arbitrary number of kinematic and identity sensor inputs. Key assumptions include target independence (both existence and dynamics) and correct (but not necessarily complete) upstream association decisions. Hence, we may associate multiple tracks from the same sensor, provided there is no scan with measurements from more than one track.

## C. GBT Approach

Computational simplifications may be achieved if local (track) hypotheses satisfy a path-independence assumption, whereby the track likelihood may be factored with pairwise contributions to the likelihood.

The fundamental path-independence assumption that we introduce is appropriate for single-sensor kinematic track-level data. Again, let  $z_j$  represent a track (i.e., a sequence of previously associated measurements) and let  $L(z^n)$  denote the track likelihood associated with a sequence of tracks. The path-independence assumption

amounts to the following:

$$\begin{aligned} L(z^n) &= L(z_1) \prod_{i=2, \dots, n} L(z_i | z^{i-1}) \\ &\approx L(z_1) \prod_{i=2, \dots, n} L(z_i | z_{i-1}). \end{aligned} \quad (19)$$

The path-independence assumption enables a graph-based representation of the MTT problem with pairwise costs derived from conditional likelihoods.

Under the GBT formalism, we consider a set of kinematic tracks that we represent by a set of nodes  $V$ . We consider also source and sink nodes, denoted by  $v_0$  and  $v_\infty$ , respectively. We define the augmented set of nodes by  $\bar{V} = V \cup \{v_0, v_\infty\}$ . We consider a directed graph  $G = (\bar{V}, A)$ , where  $A$  is a set of edges. For each feasible edge  $(i, j) \in A$ , i.e., with no temporal overlap between the corresponding tracks, we define the cost  $c_{ij}$  by the negative log conditional likelihood:

$$c_{ij} = -\log L(v_j | v_i). \quad (20)$$

Note that the likelihood  $c_{0j} = L(v_j | v_0) = L(v_j)$  accounts for target birth. As all track likelihoods account already for target death, we have  $L(v_\infty | v_i) = 1$ .

The kinematic GBT formulation leads to the following ILP:

$$J = \sum_{(i,j) \in A} c_{ij} x_{ij}, \quad (21)$$

$$x_{ij} \in \{0, 1\} \quad \forall (i, j) \in A, \quad (22)$$

$$\sum_{i:(i,j) \in A} x_{ij} = 1 \quad \forall v_j \in V, \quad (23)$$

$$\sum_{j:(i,j) \in A} x_{ij} = 1 \quad \forall v_i \in V. \quad (24)$$

We seek the solution that minimizes the objective (21) subject to constraints (22)–(24). Equations (23) and (24) ensure that all nodes be used exactly once, and that flow balance be achieved.

The resulting MAP estimation problem for global hypothesis  $q^k$  is over a smaller space than MHT. Indeed, here a second form of factorization is invoked in addition to that of TO-MHT, based on Eq. (19). By exploiting this factorization, we avoid the enumeration of track hypotheses; rather, the ILP is posed over pairwise-association variables.

A nice feature of the single-sensor GBT formulation is that it results in an ILP with special structure: it may be expressed as a *min-cost network flow* (MCNF) problem or, equivalently, as a *bipartite matching* problem. Thus, the problem admits an integer solution and faster solution than a general ILP [34].

As with MHT, we may wish to define dimensionless scores analogous to Eq. (18). Here, we may adopt the

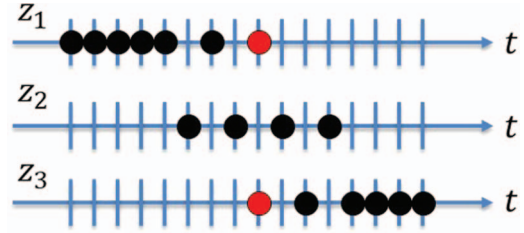


Fig. 1. Tracks  $z_1$  and  $z_3$  cannot originate from the same target, as there is a scan where both have a measurement (shown in red). Avoiding the association in GBT requires a strict condition for pairwise-association feasibility.

following in lieu of Eq. (20):

$$c_{ij} = -\log \frac{L(v_j | v_i)}{L(v_j)} = -\log \frac{L(v_i, v_j)}{L(v_j) L(v_i)}. \quad (25)$$

Note that the requirement for association feasibility mentioned above—no temporal overlap between the corresponding tracks—is stricter than that in MHT. This is necessary due to the pairwise nature of track scoring. Consider the example in Fig. 1. MHT computes  $L(z^3)$  precisely; it must necessarily be zero since tracks  $z_1$  and  $z_3$  share a relevant sensor scan. On the other hand, GBT would allow for the association of the tracks since pairwise feasibility is maintained, were we not to impose the stricter *no temporal overlap* condition.

Indeed, GBT will assume  $L(z^3) \approx L(z_3 | z_2) L(z_2 | z_1) L(z_1)$ . In this example, both  $L(z_3 | z_2)$  and  $L(z_2 | z_1)$  are nonzero, while  $L(z^3)$  must be zero. Hence, the approximation is potentially poor for temporally overlapping tracks, not due to a poor kinematic filtering approximation but rather due to an incorrect accounting for measurement-cardinality information.

#### D. MI-GBT Approach

We wish to leverage the GBT approach while allowing for multiple kinematic and identity sensors, as well as for identity tracks that violate the Markovian assumption on the data.

Let us first address the need to process multiple sensors, as illustrated in Fig. 2. We do so by exploiting MHT processing with a dedicated kinematic-fusion stage, yielding a single, fused kinematic sensor feed. Only nontemporally overlapping fused tracks (i.e., the strict condition above) will be feasibly associated in downstream MI-GBT processing.

It is worth emphasizing that kinematic processing may introduce undesired measurement association errors. This is not problematic when one or more objects remain in close proximity. On the other hand, when a group of objects splits into two or more, it is important to fragment kinematic-only tracks to enable high-confidence stitching in downstream processing, with the aid of identity-sensor data.

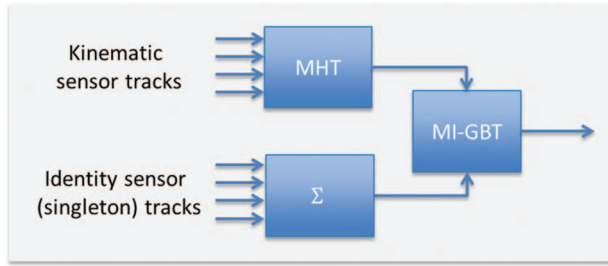


Fig. 2. The MI-GBT is seemingly more restrictive as it requires a single kinematic and identity feed. However, this can be addressed with preprocessing that exploits MHT kinematic tracking, as well as the recasting of multiple-measurement identity tracks as unassociated measurements of a vanishingly small type probability, all due to one sensor.

Likewise, there may be multiple identity sensors. However, since we assume single-measurement identity tracks, there is no loss of generality in considering all tracks as originating from a single identity sensor. For identity measurements that potentially observe different aspects of the target state, e.g., object color, object size, etc., we may recast the formulation as a single identity sensor with vector-valued measurements. For simplicity, here we consider scalar object types.

It is important to note that the *unionizing* operation on identity measurements preserves the scan structure of the data. That is, if two identity sensors have sensor scans at the same time, the two scans are kept distinct for downstream processing. The point-target assumption remains crucial as in MHT; i.e., we have at most one measurement per target per scan.

The second need is to handle identity measurements that violate the Markovian approximation in Eq. (29). Indeed, while past kinematic tracks are not relevant to future kinematic association scores, the same is not true for identity tracks that specify the object type. Our approach will be to define an ILP that corresponds to a *multilayer* graph, one for each object type. Path independence holds within a layer of the track, but not across layers. Before defining the ILP, we show an illustrative example.

The advantage of the architecture in Fig. 2 is that we exploit the MHT for what it performs well, namely, multisensor kinematic tracking where small hypothesis tree depths are effective. We defer the disparate-sensor fusion problem, where MHT is severely challenged computationally, to generalized GBT processing.

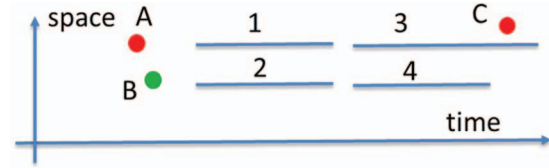


Fig. 3. A multi-INT track fusion example.

#### E. MHT and MI-GBT Structure

Consider the notional example in Fig. 3. We have an unknown number of objects giving rise to three identity tracks and four kinematic tracks, indicating that there are red and green objects present.

For simplicity of exposition, we assume a forensic surveillance problem, in the sense that all data have been received at the processing center. This enables a compact representation of the association spaces associated with competing solution approaches, with nodes representing input track. Regardless of whether online or forensic analysis is to be performed, the data-association process will necessarily rely on sliding-window processing for computational tractability.

Under the simplifying assumption of no never-observed objects (the usual assumption in MHT), there are at most seven objects present, and there are at least two targets (one red, one green). The MAP solution will depend on target and sensor statistical assumptions, and on the measured data themselves. The corresponding data structure associated with TO-MHT processing may be represented as illustrated in Fig. 4. Note that, for simplicity, we have expressed each path in the MHT track forest as a sequence of tracks. This is not fully reflective of the actual processing sequence, since data are ingested and processed in proper time order. As an example, in the leftmost path, some measurements associated with track 3 follow track C. Track filtering and scoring is performed in proper time sequence.

The MAP solution associated with MHT processing will be that set of paths that accounts for all the data, while minimizing the sum of negative log likelihoods as in Eq. (26). Alternatively, we may use likelihood ratios as in Eq. (28).

Figs. 5 and 6 illustrate the GBT and MI-GBT graphs, respectively. For simplicity, in both graphs we have not drawn the termination node, nor the termination edges from each node to the termination node. (There is no edge directly from the birth node to the termination node.) By default, all edges are *directed* (downward), ex-

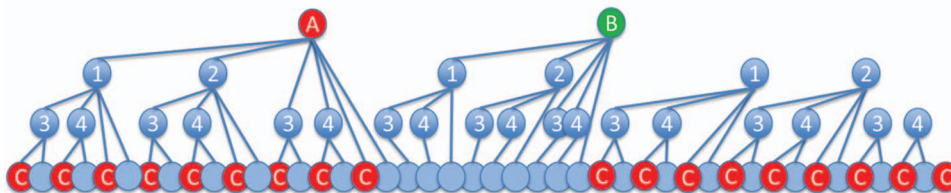


Fig. 4. MHT track forest for the example in Fig. 3.

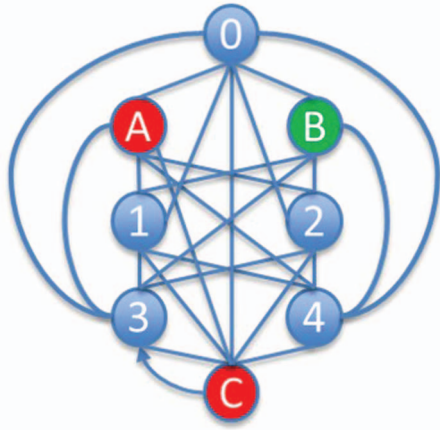


Fig. 5. GBT graph topology for the example in Fig. 3. While the representation supports computationally efficient solutions, these cannot exploitation crucial object-type information.

cept where explicitly denoted, i.e., the second edge between track 3 and node C.

There are several points to note. First, while much more compact than the MHT structure, the GBT graph topology does not allow for exploitation of target-type information (except for the lack of an edge directly connecting node B and node C). There is too much simplification in the problem formulation, so that feature information cannot help the data-association process. Indeed, target-type information does not satisfy the Markovian property that applies to kinematic data.

The MI-GBT structure is more compact than that of MHT, due to the simplifying path-independence assumption. Thus, for instance, each node associated with track 4 is a sufficient representation of kinematic information on the target, without the need for expressing from whence the target originates. At the same time, it is crucial to maintain graph layers (or subgraphs) associated with distinct object types. No flow is permitted between subgraphs, except for flow from the null subgraph to the object-type subgraphs.

The null subgraph captures objects for which no object-type information is known. In the example, these objects may well be red or green—we do not know. Col-

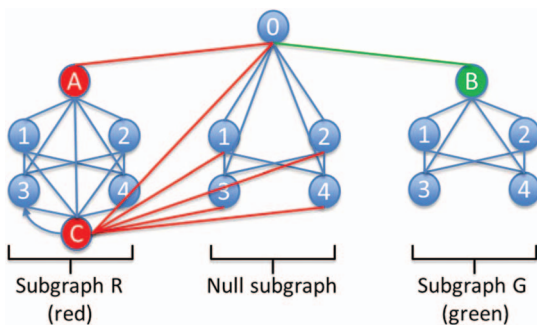


Fig. 6. MI-GBT graph topology for the example in Fig. 3. Colored edges indicate when type information is inserted into a tracking solution. Constraints in the ILP ensure that equivalent vertices are used only once.

ored edges indicate associations where type information is introduced.

The MI-GBT topology distinguishes between nonoverlapping tracks and overlapping (nested) tracks. Indeed, the only temporal overlap that we allow is that between kinematic and identity tracks. This requires the use of double (directional) edges between such tracks when there is temporal overlap. Either both or neither is to be selected.

In the example in Fig. 3, there is temporal overlap between track 3 and track C; hence, if these are associated, we want flow from track 3 to track C, and then from track C to track 3. In this manner, track 3 is relevant to (kinematic) association with any preceding or subsequent tracks, while track C is not. Indeed, it is always the identity track that is temporally nested in the kinematic track, not vice versa.

There is an interesting question of how best to break the symmetry whereby flow might in principle go into track C, then to track 3, and then back to track C. This is not admissible and can be avoided by introducing an inequality constraint that forces flow into node 3 of subgraph R, if the cycle from track 3 to track C is active.

Note that the return flow from track C to track 3 must necessarily be in subgraph R, since the object of interest is necessarily of type R (red). Note also that, for tracks 1, 2, and 4, there is no need for bidirectional flow to any identity track, since none of these identity tracks is temporally nested in these kinematic tracks. Thus, in particular, if there is association between one of the tracks (1, 2, 4) with track C, any associations with subsequent tracks would be from track C.

The data fusion that the MI-GBT permits—that between kinematic tracks and single-measurement identity tracks—does pose a potential hazard. Indeed, we must introduce a mechanism to specifically disallow the fusion of multiple identity measurements at the same time with the same kinematic track. Once more, this can be achieved with a suitable inequality constraint.

The need for this constraint emphasizes a fundamental limitation of graph-based reasoning. It is inherently myopic, in the sense that it reasons only over pairwise-association scores. While this is reasonable for kinematic information, it is not so for cardinality information whereby we wish to disallow fusion of multiple measurements at the same time from the same sensor, hence the need for the constraints noted above. Nor is pairwise reasoning sufficient to exploit object-type information, hence the need for the expanded (multilayer) graph structure in MI-GBT that conventional GBT lacks.

Sliding-window  $n$ -scan processing to resolve global hypotheses may be performed on the MI-GBT data structure, in analogous fashion to how it is performed in MHT [1].

As an extension to the example above, consider the scenario in Fig. 7, where we observe an additional kinematic track. The corresponding MI-GBT topology is given in Fig. 8.

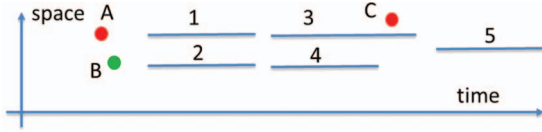


Fig. 7. An extension to the previous multi-INT example.

## F. MI-GBT ILP

While our ILP implementation corresponds to the illustration in Fig. 6 (or Fig. 8, for the larger example), it will be easier to describe the ILP associated with the equivalent representation illustrated in Fig. 9. In practice, we prefer the structure in Fig. 6 as we only spawn subgraphs when identity tracks of the corresponding type are to be processed, and not earlier. There is a one-to-one correspondence between the two representations.

Let us denote by  $V$  the set of kinematic tracks, and by  $v_0$  and  $v_\infty$  the source and sink vertices, respectively. We denote by  $W_k$  the set of identity (singleton) tracks of type  $k$ , with  $k = 1, \dots, K$ .

In the MI-GBT, each kinematic track node may appear on multiple graph subgraphs (or layers). It will appear on all layers if spatial and kinematic gating are not performed; we assume it does so, for ease of presentation. On the other hand, each identity track appears only in one graph layer, e.g., red measurements only in the red layer, etc. We denote by  $\tilde{V}_k = V \cup W_k \cup \{v_0, v_\infty\}$  the set of vertices in the  $k$ th subgraph  $G_k$ , and by  $A_k$  the set of edges in subgraph  $G_k$ , i.e.,  $G_k = (\tilde{V}_k, A_k)$ .  $G_0$  is the null subgraph, where no identity tracks are present. The full set of identity tracks is given by  $W = \bigcup_{k=1, \dots, K} W_k$ . We have  $W_0 = \emptyset$ , as there are no null-type identity measurements.

Recall that in Eq. (25), pairwise scores were indexed by two tracks. Now we have a third index to account for object type. Letting  $K$  be the number of object types, and denoting by  $k = 0$  the null index (i.e., no object-type information), we have the following, where the likelihood function is understood not to include any contribution from object type. Note there is no need for edges with

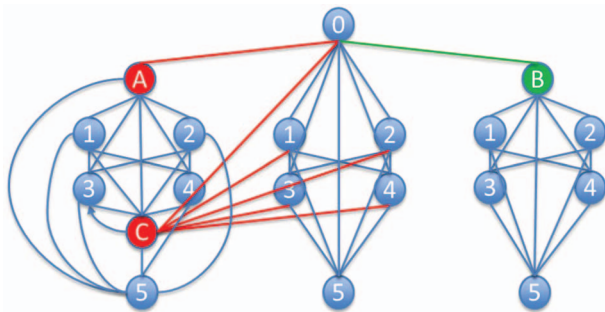


Fig. 8. The MI-GBT topology for the scenario in Fig. 7. Constraints in the ILP ensure that equivalent vertices are used only once.

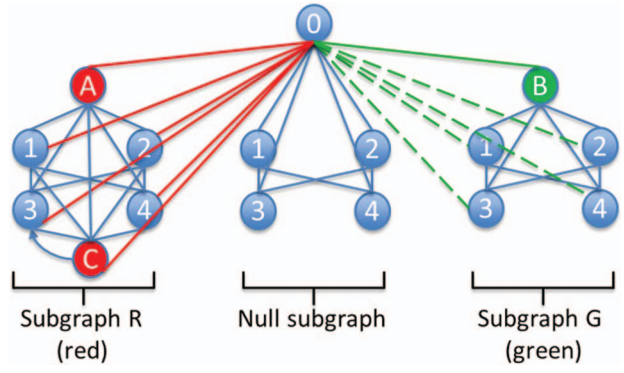


Fig. 9. An equivalent MI-GBT graph topology for the example in Fig. 3. Constraints in the ILP ensure that equivalent vertices are used only once. While our implementation matches the topology of Fig. 6, the ILP is easier to describe for this topology. Dashed edges are not strictly necessary (the solution will not include these edges) but are included for completeness.

$i = j$ .

$$c_{ijk} = \begin{cases} -\log L(v_j), & i = 0, k = 0, \\ -\log(p_{\text{type}}(k) L(v_j)), & i = 0, k \neq 0, \\ -\log L(v_j | v_i), & i \neq 0, j \neq 0, \\ 0, & j = 0. \end{cases} \quad (26)$$

As before, we may alternatively use dimensionless track score based on likelihood ratios. In this case, we have the following:

$$c_{ijk} = \begin{cases} 0, & i = 0, k = 0, \\ -\log p_{\text{type}}(k), & i = 0, k \neq 0, \\ -\log \frac{L(v_j | v_i)}{L(v_j)}, & i \neq 0, j \neq 0, \\ 0, & j = 0. \end{cases} \quad (27)$$

Using either Eq. (26) or Eq. (27), we may then express the ILP as follows:

$$J = \sum_{k=0, \dots, K} \sum_{(i, j, k) \in A_k} c_{ijk} x_{ijk}, \quad (28)$$

$$x_{ijk} \in \{0, 1\} \quad \forall (i, j, k) \in A_k, \quad k = 0, \dots, K, \quad (29)$$

$$\sum_{k=0, \dots, K} \sum_{i: (i, j, k) \in A_k} x_{ijk} = 1 \quad \forall v_j \in V \cup W, \quad (30)$$

$$\sum_{j: (i, j, k) \in A_k} x_{jik} - \sum_{j: (i, j, k) \in A_k} x_{ijk} = 0 \quad \forall v_i \in V \cup W_k, \quad k = 0, \dots, K. \quad (31)$$

We seek the solution that minimizes the objective (28) subject to conditions (29)–(31). Equation (30) ensures that all nodes be used exactly once. Equation (31) ensures that flow balance be achieved in each track node in each subgraph.

Additional constraints are needed to complete the ILP formulation. Indeed, in Section III-E we identified two concerns that must be addressed via appropriate

constraints. The first is that identity track  $v_j$  may be temporally nested within track  $v_i$ , so that both edge variables  $x_{ijk}$  and  $x_{jik}$  are defined for  $k = 1, \dots, K$ . In this case, we must ensure that both edge variables (or neither) are set to unity in subgraph  $G_k$ . Furthermore, if both are set to unity, there must be flow into  $v_i$  from another node in addition to  $v_j$ . This ensures that, in  $G_k$ , flow is into  $v_i$  from  $v_i$  to  $v_j$  and back, and out of  $v_i$ . This is captured in the following constraints:

$$(j, i, k) \in A_k \Rightarrow x_{ijk} = x_{jik} \quad \forall (i, j, k) \in A_k, \\ k = 1, \dots, K, \quad (32)$$

$$(j, i, k) \in A_k, v_j \in W_k \Rightarrow \sum_{l:(l,i,k) \in A_k \setminus (j,i,k)} x_{lik} \geq x_{ijk}, \\ k = 1, \dots, K. \quad (33)$$

A second concern is that we must exclude the association of multiple identity tracks in the same scan with the same kinematic track. This would violate the modeling assumption of at most one detection per target per scan. This can be achieved with an inequality constraint whereby for each identity-sensor scan and each (relevant) kinematic track at most one edge variable is unity.

Each identity scan is at a time  $t_m \in t^n$ , with  $t^n$  the sequence of identity-sensor scan times. Let us denote by  $W(t_m)$  the corresponding set of identity (singleton) tracks. For each kinematic track  $v_i \in V$ , one or both of two cases apply, depending on whether the end of the kinematic track temporally precedes or follows the identity scan at time. Thus, we have

$$\forall v_i \in V, \forall t_m \in t^n, \begin{cases} \sum_{k=1, \dots, K} \sum_{j:(i,j,k) \in A_k, v_j \in W(t_m)} x_{ijk} \leq 1, \\ \sum_{k=1, \dots, K} \sum_{j:(j,i,k) \in A_k, v_j \in W(t_m)} x_{jik} \leq 1. \end{cases} \quad (34)$$

It is worth emphasizing that the MI-GBT solution is fully specified by the ILP defined by Eqs. (28)–(34). The graphical illustrations shown in Figs. 6, 8, and 9 are pictorial aids, but do not capture the required optimization constraints.

### G. Solution Complexity

It is useful to have an approximate, analytical assessment of the computational complexity associated with MHT, GBT, and MI-GBT solutions to the multi-INT problem. Here, we estimate the size of the ILP associated with these paradigms. We denote by  $\dim(x)$  the length of the solution vector in the objective—Eqs. (13), (21), and (28), respectively.

Given  $m$  sets of  $|V|$  tracks, and with  $|W|$  identity types, the GBT problem size is  $|x| = O(m|V|^2)$ , while the MI-GBT problem size is  $|x| = O(m|V|^2(1 + |W|))$ . Both compare favorably to the (track-oriented) MHT approach, for which problem size is  $|x| =$

$O(|V|^{m+1}(1 + |W|))$ . The solution time associated with the ILP is problem size dependent. Empirically, we observe low-order polynomial times as a function of the solution vector, typically  $O(|x|^n)$  with small  $n$  for MHT and MI-GBT solutions based on LP relaxation, and  $O(|x|^3)$  for the GBT based on MCNF or an equivalent bipartite matching formulation [34].

The MI-GBT provides a good trade-off with its ability to exploit object-type information (like MHT) while maintaining an efficient pairwise-cost formalism (like GBT). For a given hypothesis depth ( $n$ -scan), MHT will generally outperform MI-GBT. Likewise, for a given hypothesis depth, GBT will incur lower computational effort. We anticipate that, in disparate-sensor settings where kinematic Markovian assumptions are appropriate, MI-GBT will yield a better complexity versus performance operating curve than both MHT (which *does the right thing*, at great expense) and GBT (which cannot exploit type information).

## IV. SIMULATION RESULTS

We now explore the performance of MHT and MI-GBT approaches to multi-INT track fusion. We focus on a simplified version of the general problem while including the key challenge that exposes the differences between the MHT, GBT, and MI-GBT solutions. This will allow us to gain intuition regarding the relative strengths of the methods. It will be of interest to conduct more general MTT performance analysis in subsequent studies.

We consider a fixed number of targets, with no target births or deaths. We assume high track-level detection performance. We simplify the problem further by assuming equivalent-measurement processing that leads to single-measurement kinematic tracks. Thus, our problem may be viewed as one for which we observe a sequence of measurement sets, each containing a detection on all targets, with no false measurements.

We assume that the identity sensor reports twice, at the start and at the end of the scenario. In the interim, we have a number of kinematic scans, each containing positional measurements on all targets. The identity sensor includes precise object-type information with each positional measurement. In general, there are multiple objects of each type, so the association of measurements from the two identity-sensor scans is not known.

We consider GBT, MHT, and MI-GBT solutions to this data-association problem. Ultimately, even for this simplified problem, one would want to compare GBT, MHT, and MI-GBT solutions for a common processing load. Since the computational complexity of MHT grows significantly as a function of scenario duration, we limit processing to an  $n$ -scan = 0 solution (i.e., no hypothesis depth) that amounts to GNN processing.

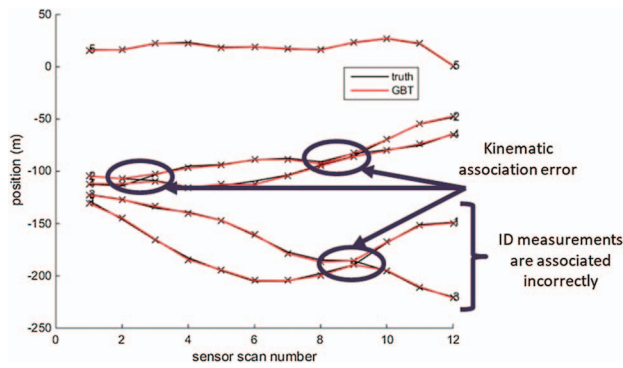


Fig. 10. GBT processing is more error-prone than MHT in kinematic association, due to the fundamental path-independence approximation that degrades kinematic-filtering accuracy. In the 1D case, GBT tracks never cross. Note that ID associations may violate type information: target 1 is of type A and target 3 is of type B.

Figs. 10–12 illustrate one realization of 1D target trajectories (black lines), measurement data (black cross symbols), and GBT, MHT, and MI-GBT solutions. Target motion is according to our stable, stationary second-order OU process that generalizes the standard NCV motion. Indeed, note that the positional spread of the trajectories remains roughly the same over time; the same is true in velocity space. Positional measurements include additive Gaussian noise.

The first and last sensor scans are provided by the ID sensor. We consider a five-target scenario. Targets 1 and 2 are of type A, targets 3 and 4 are of type B, and target 5 is of type C. The ID sensor does not exhibit object-type measurement error, but the association of target measurements of the same type is unknown.

It is instructive to consider aspects of the solutions as illustrated in these figures. Note that the GBT solution incurs errors when targets cross, since the solution trajectories do not do so. This can be readily understood, as the GBT reasons over pairwise costs. In the 1D case, it is costly to associate measurements in such a way as to alter the relative ordering of the tracks.

The GBT solution cannot exploit ID information except when there are sequential ID-sensor scans. Hence,

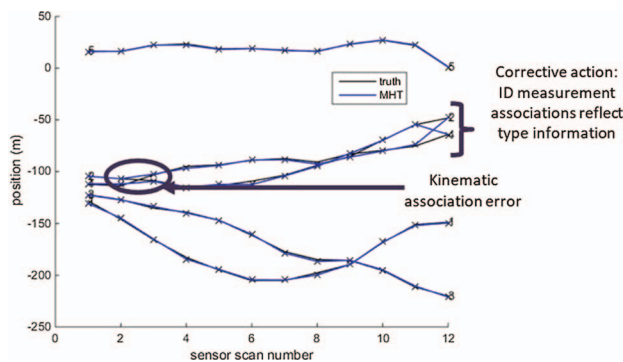


Fig. 11. MHT performs effective kinematic association but is ultimately myopic as it cannot exploit ID measurements that are in the distant future. ID information is part of the track state and, thus, corrective action is taken when prior association errors are detected.

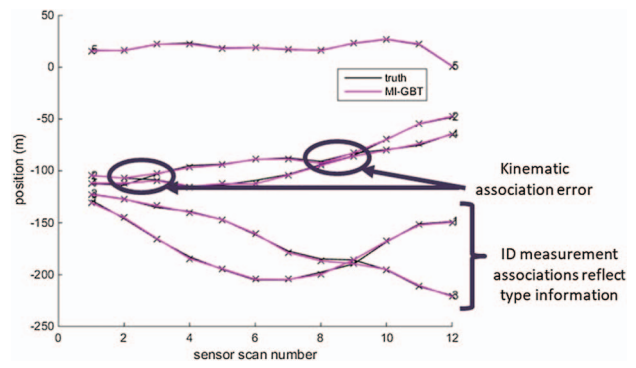


Fig. 12. MI-GBT may perform association errors when consistent with available ID data, but yields solutions that exploit all available ID measurements.

when there are kinematic-sensor scans between ID-sensor scans, the association of ID measurements is error-prone. Unlike the GBT solution, the MHT solution relies on recursive filtering so that crossing targets are handled properly in most cases. Corrective action is taken when the second ID-sensor scan is received. Note that full corrective action with MHT may not be possible when kinematic gating disallows sufficiently unlikely associations.

The MI-GBT solution struggles with multiple target crossing in the absence of ID data, but it maintains ID information and is able to deal effectively with single-crossing events between ID reports. More importantly, the MI-GBT exploits ID data in performing associations with the second scan of ID-sensor data. Hence, ID measurement associations do not violate type information, and this is achieved without the corrective action that MHT exhibits. For the same computational load, deeper hypothesis reasoning is possible.

Of course, for sufficiently temporally distant ID measurements, MI-GBT will also require corrective action. Note also that, when focusing only on the MI-GBT tracking solution for targets of the same type, no track crossing occurs. This behavior is consistent with what we observe in the overall solution with all tracks in the GBT solution.

Due to the nonunique nature of target-type measurements, some incorrect ID measurement association decisions are performed by MHT and MI-GBT. Figs. 13 and 14 illustrate a scenario for which both MHT and MI-GBT incorrectly associate some ID measurements, when these are of the same type. We highlight a track that starts with a measurement on target 1, and ultimately associates with one on target 2. Note that both targets are of type A; hence, this error cannot be excluded.

In all cases, the final tracking solution for all paradigms (GBT, MHT, and MI-GBT) includes trajectory smoothing based on the forward-backward implementation of the Kalman smoother. This provides improved localization accuracy that is appropriate for

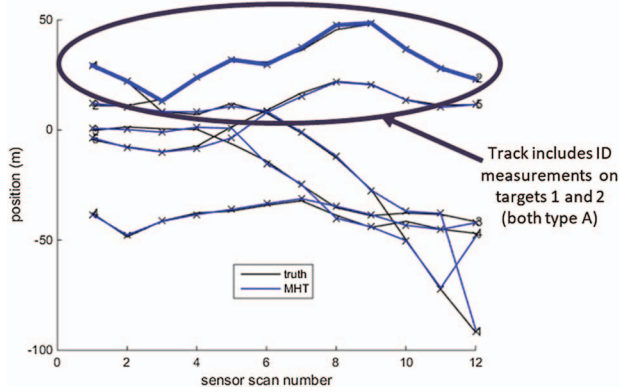


Fig. 13. ID measurement association error in MHT processing, due to common target type (targets 1 and 2).

forensic problems where maintaining small processing latency is not crucial. When it is, this postprocessing step may be omitted.

Figs. 15 and 16 provide performance as a function of the number of kinematic-sensor scans. Note that, with an increasing number of scans, correct measurement association decisions become harder, for all solution approaches. Indeed, the value of temporally distinct identity measurements is more limited than when temporally close identity measurements are available. There are at least two ways that this can be understood. First, knowledge of future location of a target has little bearing on data-association decisions, when the future time is in the distant future. Second, there are typically a larger number of ambiguous object-crossing events over a longer time horizon, providing many similarly scoring tracking solutions. The increasing difficulty of the MTT problem can be seen empirically in the fact that performance under *all* solution paradigms degrades as a function of the number of kinematic-sensor scans, as these lack target-type information.

We compare against a clairvoyant (ideal) algorithm for which measurement association is known *a priori*. We consider both the average track localization error and the fraction of correct data-association decisions.

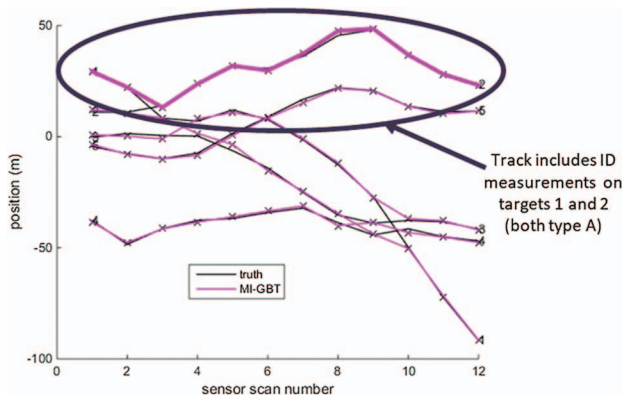


Fig. 14. ID measurement association error in MI-GBT processing, due to common target type (targets 1 and 2).

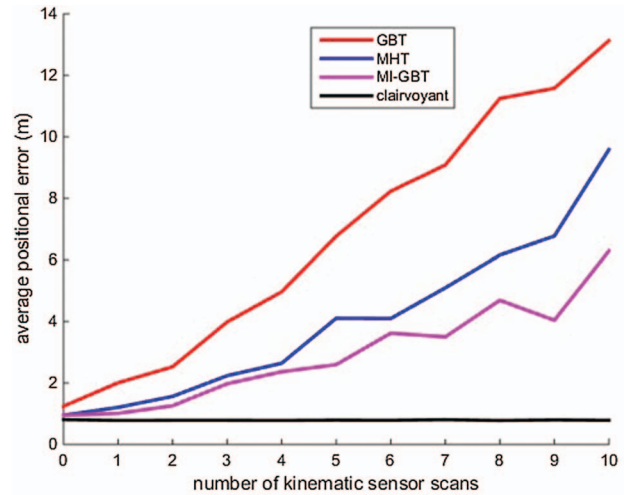


Fig. 15. Positional error of solutions: MI-GBT is best.

Results are based on 100 Monte Carlo realizations for each scenario duration.

These results on idealized scenarios provide confidence in the significant potential of MI-GBT processing for multi-INT surveillance, even when ID measurement associations are only partially constrained. The full MI-GBT solution accounts as well for birth/death phenomena and missed detections. A key enhancement relative to our early work is to relax the unity-flow constraint on the number of objects of each type. In so doing, it is crucial to express ID measurements as nodes in the multilayer graph topology.

## V. CONCLUSION

This paper introduces an efficient, generalized GBT scheme for multi-INT track fusion that yields promising performance against an MHT baseline. Crucially, our scheme allows for object identity measurements via a multilayer graph approach, while exploiting kinematic path independence. As such, the approach may be

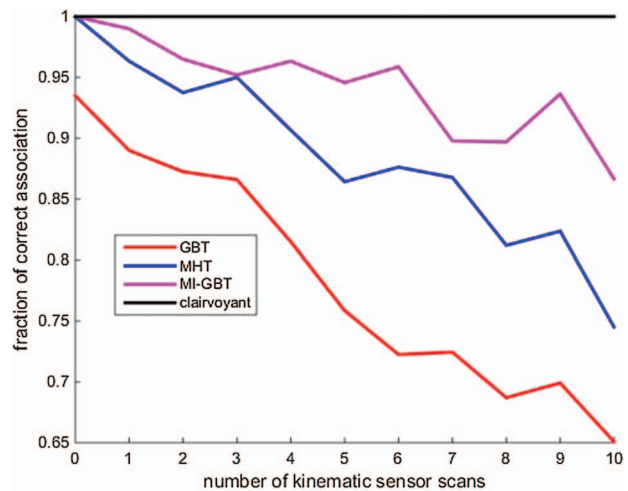


Fig. 16. Association accuracy of solutions: MI-GBT is best.

thought of as a hybrid GBT/MHT approach to data association. We allow for an arbitrary number of objects of each type and achieve scalability via sliding-window hypothesis resolution as is commonly performed in MHT.

It is important to emphasize that our proposed graph-based multisensor fusion algorithm is not fully general, in the sense that we do not directly handle an arbitrary number of kinematic and identity sources. Rather, we rely on upstream processing (see again Fig. 2) and assume a single (consolidated) kinematic source and a single (consolidated) identity source. Further, we do not consider fusion of temporally overlapping kinematic tracks (see again Fig. 1), and we assume singleton (single-measurement) identity tracks. Nonetheless, our work offers promising performance benefits over classical MHT technology in this restricted setting.

In ongoing work, we are investigating use of the MI-GBT on scenarios that exhibit *move-stop-move* target motion cycles and motion-sensitive kinematic sensors. Additionally, further analysis is needed to address slowly varying (nonstatic) feature states and noisy feature measurements.

#### REFERENCES

1. B.-N. Vo, M. Mallick, Y. Bar-Shalom, S. Coraluppi, R. Osborne, R. Mahler, and B.-T. Vo  
“Multitarget tracking,”  
in *Wiley Encyclopedia of Electrical and Electronics Engineering*. Hoboken, NJ: Wiley-IEEE, 2015.
2. D. Reid  
“An algorithm for tracking multiple targets,”  
*IEEE Trans. Autom. Control*, vol. 24, no. 6, pp. 843–854, Dec. 1979.
3. T. Kurien  
“Issues in the design of practical multitarget tracking algorithms,”  
in *Multitarget–Multisensor Tracking: Advanced Applications*, Y Bar-Shalom  
Ed. Norwood, MA: Artech House, 1990.
4. C. Morefield  
“Application of 0–1 integer programming to multitarget tracking problems,”  
*IEEE Trans. Autom. Control*, vol. 22, no. 3, pp. 302–312, Jun. 1977.
5. S. Coraluppi, C. Carthel, M. Luetzgen, and S. Lynch  
“All-source track and identity fusion,”  
in *Proc. MSS Nat. Symp. Sensor Data Fusion*, San Antonio, TX, USA, Jun. 2000.
6. A. Poore and N. Rijavec  
“A Lagrangian relaxation algorithm for multidimensional assignment problems arising from multitarget tracking,”  
*SIAM J. Optim.*, vol. 3, no. 3, pp. 544–563, 1993.
7. P. Storms and F. Spieksma  
“An LP-based algorithm for the data association problem in multitarget tracking,”  
in *Proc. 3rd Int. Conf. Inf. Fusion*, Paris, France, Jul. 2000.
8. C.-Y. Chong, G. Castañón, N. Coopriider, S. Mori, R. Ravichandran, and R. Macior  
“Efficient multiple hypothesis tracking by track segment graph,”

- in *Proc. 12th Int. Conf. Inf. Fusion*, Seattle, WA, USA, Jul. 2009.
9. S. Coraluppi, C. Carthel, W. Kreamer, G. Titi, and J. Vasquez  
“Advanced multi-stage multiple-hypothesis GMTI tracking,”  
in *Proc. MSS Nat. Symp. Sensor Data Fusion*, Gaithersburg, MD, USA, Jun. 2016.
10. S. Coraluppi, C. Carthel, B. Zimmerman, T. Allen, J. Douglas, and J. Muka  
“Multi-stage MHT with airborne and ground sensors,”  
in *Proc. IEEE Aerosp. Conf.*, Big Sky, MT, USA, Mar. 2018.
11. S. Coraluppi and C. Carthel  
“If a tree falls in the woods, it does make a sound: Multiple-hypothesis tracking with undetected target births,”  
*IEEE Trans. Aerosp. Electron. Syst.*, vol. 50, no. 3, pp. 2379–2388, Jul. 2014.
12. S. Coraluppi and C. Carthel  
“Multiple-hypothesis tracking for targets producing multiple measurements,”  
*IEEE Trans. Aerosp. Electron. Syst.*, vol. 54, no. 3, pp. 1485–1498, Jun. 2018.
13. T. Sathyan, T.-J. Chin, S. Arulampalam, and D. Suter  
“A multiple hypothesis tracker for multitarget tracking with multiple simultaneous measurements,”  
*IEEE J. Sel. Topics Signal Process.*, vol. 7, no. 3, pp. 448–460, Jun. 2013.
14. J. Wolf, A. Viterbi, and G. Dixon  
“Finding the best set of  $K$  paths through a trellis with application to multitarget tracking,”  
*IEEE Trans. Aerosp. Electron. Syst.*, vol. 25, no. 2, pp. 287–295, Mar. 1989.
15. G. Pulford and B. La Scala  
“Multihypothesis Viterbi data association: Algorithm development and assessment,”  
*IEEE Trans. Aerosp. Electron. Syst.*, vol. 46, no. 2, pp. 583–609, Apr. 2010.
16. L. van der Merwe and J. de Villiers  
“A comparative investigation into Viterbi based and multiple hypothesis based track stitching,”  
*IET Radar, Sonar Navigation*, vol. 10, no. 9, pp. 1575–1582, Dec. 2016.
17. D. Castañón  
“Efficient algorithms for finding the  $K$  best paths through a trellis,”  
*IEEE Trans. Aerosp. Electron. Syst.*, vol. 26, no. 2, pp. 405–410, Mar. 1990.
18. G. Battistelli, L. Chisci, F. Papi, A. Benavoli, A. Farina, and A. Graziano  
“Optimal flow models for multiscan data association,”  
*IEEE Trans. Aerosp. Electron. Syst.*, vol. 47, no. 4, pp. 2405–2422, Oct. 2011.
19. G. Castañón and L. Finn  
“Multi-target tracklet stitching through network flows,”  
in *Proc. IEEE Aerosp. Conf.*, Big Sky, MT, USA, Mar. 2011.
20. H. Shirit, J. Berclaz, F. Fleuret, and P. Fua  
“Multi-commodity network flow for tracking multiple people,”  
*IEEE Trans. Pattern Anal. Mach. Intell.*, vol. 36, no. 8, pp. 1614–1627, Aug. 2014.
21. S. Coraluppi, C. Carthel, G. Castañón, and A. Willsky  
“Multiple-hypothesis and graph-based tracking for kinematic and identity fusion,”  
in *Proc. IEEE Aerosp. Conf.*, Big Sky, MT, USA, Mar. 2018.
22. S. Coraluppi, C. Carthel, W. Kreamer, and A. Willsky  
“New graph-based and MCMC approaches to multi-INT surveillance,”  
in *Proc. 19th Int. Conf. Inf. Fusion*, Heidelberg, Germany, Jul. 2016.
23. S. Oh, S. Russell, and S. Sastry

- “Markov chain Monte Carlo data association for multi-target tracking,”  
*IEEE Trans. Aerosp. Electron. Syst.*, vol. 54, no. 3, pp. 481–497, Mar. 2009.
24. L. Finn and P. Kingston  
“Unifying multi-hypothesis and graph-based tracking with approximate track automata,”  
in *Proc. IEEE Aerosp. Conf.*, Big Sky, MT, USA, Mar. 2019.
  25. T. Tran, J. Foley, G. Godfrey, and J. Ferry  
“Graph-based multi-INT tracklet stitching,”  
in *Proc. MSS Nat. Symp. Sensor Data Fusion*, Springfield, VA, USA, Oct. 2018.
  26. S. Coraluppi, C. Carthel, and A. Willsky  
“Graph-based tracking with uncertain ID measurement associations,”  
*Proc. 22nd Int. Conf. Inf. Fusion*, Ottawa, Canada, Jul. 2019.
  27. Y. Bar-Shalom, P. Willett, and X. Tian  
*Tracking and Data Fusion: A Handbook of Algorithms*.  
Storrs, CT: YBS Publishing, 2011.
  28. V. Poor  
*An Introduction to Signal Detection and Estimation*. Berlin, Germany: Springer, 1988.
  29. R. Mahler  
*Statistical Multisource--Multitarget Information Fusion*.  
Norwood, MA: Artech House, 2007.
  30. J. Williams  
“Marginal multi-Bernoulli filters: RFS derivation of MHT, JIPDA, and association-based member,”  
*IEEE Trans. Aerosp. Electron. Syst.*, vol. 51, no. 3, pp. 1664–1687, Jul. 2015.
  31. S. Coraluppi and C. Carthel  
“Track management in multiple-hypothesis tracking,”  
in *Proc. 10th IEEE Sensor Array Multichannel Signal Process. Workshop*, Sheffield, U.K., Jul. 2018.
  32. A. Papoulis  
*Probability, Random Variables, and Stochastic Processes*.  
New York, NY: McGraw-Hill, 1991.
  33. S. Coraluppi and C. Carthel  
“Stability and stationarity in target kinematic modeling,”  
in *Proc. IEEE Aerosp. Conf.*, Big Sky, MT, USA, Mar. 2012.
  34. C.-Y. Chong  
“Graph approaches for data association,”  
in *Proc. 15th Int. Conf. Inf. Fusion*, Singapore, Jul. 2012.



**Stefano P. Coraluppi** received the B.S. degree in electrical engineering and mathematics from Carnegie Mellon University, Pittsburgh, PA, USA, in 1990, and the M.S. and Ph.D. degrees in electrical engineering from the University of Maryland, College Park, MD, USA, in 1992 and 1997, respectively. He is currently a Chief Scientist with Systems and Technology Research, Woburn, MA, USA. He has held research positions with ALPHATECH, Inc. (1997–2002), the NATO Undersea Research Centre (2002–2010), Compunetix, Inc. (2010–2014), and STR (since 2014). His primary research interests are multitarget tracking and multisensor data fusion. He serves on the Board of Governors of the IEEE Aerospace and Electronic Systems Society (AESS) and the Board of Directors of the International Society of Information Fusion (ISIF). He is Associate Editor-in-Chief for both the *IEEE Transactions on Aerospace and Electronic Systems* and the *ISIF Journal of Advances in Information Fusion*. He is a Senior Member of IEEE.



**Craig A. Carthel** received the B.S. degree in physics and mathematics, and the M.S. and Ph.D. degrees in mathematics from the University of Houston, Houston, TX, USA, in 1988, 1992, and 1995, respectively, where he did research in numerical analysis and optimization theory. He is currently a Lead Scientist with Systems and Technology Research, Woburn, MA, USA. From 1995 to 1997, he was with the Institute for Industrial Mathematics, Johannes Kepler University, Linz, Austria, where he worked on parameter identification and inverse problems. From 1998 to 2002, he was a Senior Mathematician with AlphaTech, Inc., Burlington, MA, USA, where he worked on image processing, multisensor data fusion, and ground target tracking. From 2002 to 2010, he was a Senior Scientist with the NATO Undersea Research Centre, La Spezia, Italy, where he worked on military operations research, simulation, optimization, and data fusion problems associated with maritime environments. From 2010 to 2014, he was a Principal Scientist with Compunetix, Inc., Monroeville, PA, USA. In 2006, he was the Technical Program Chair for FUSION 2006.

**Alan S. Willsky** received the S.B. and Ph.D. degrees from the Department of Aeronautics and Astronautics, Massachusetts Institute of Technology, Cambridge, MA, USA, in 1969 and 1973, respectively. In 1973, he joined the faculty of Department of Electrical Engineering and Computer Science, Massachusetts Institute of Technology, continued full time through June 2014, and continues now as Edwin Sibley Webster Professor (retired). He served in leadership roles and from 2009 to 2014 as Director of the Laboratory for Information and Decision Systems. He has held visiting positions with Imperial College London (1977), Universite de Paris-Sud (1980–1981), and INRIA (1988). He was a founder, member of the Board of Directors, and Chief Scientific Consultant with AlphaTech, Inc. (where his work on statistical signal processing found applications in a variety of domains including multiobject tracking) and served for 4 years as a member of the U.S. Air Force Scientific Advisory Board. He has authored more than 220 journal papers and 375 conference papers, as well as 2 books, including the widely used undergraduate text *Signals and Systems*. He has received numerous awards, including the 1975 American Automatic Control Council Donald P. Eckman Award, the 1980 IEEE Browder J. Thompson Memorial Award and 1979 ASCE Alfred Noble Prize (both for a *Proceedings of the IEEE* paper on control-signal processing synergies), the 2004 IEEE Donald G. Fink Prize Paper Award (for a widely cited paper in the *Proceedings of the IEEE* that provided a survey and tutorial on multiscale statistical models for signal and image processing), a number of other best paper awards, and an honorary doctorate from Université de Rennes. He has given numerous plenary and keynote lectures at major meetings and received the 2009 Technical Achievement Award from the IEEE Signal Processing Society as well as the 2014 IEEE Signal Processing Society Award. In 2010, he was elected to the National Academy of Engineering and he is the recipient of the 2019 IEEE Jack S. Kilby Signal Processing Medal. His early work on methods for failure detection in dynamic systems is still widely cited and used in practice, and his research on statistical and multiresolution and curve-evolution methods has found application in diverse fields, including target tracking, computer vision, biomedical image analysis, oceanographic remote sensing, and groundwater hydrology. He is a Life Fellow of IEEE.



# Conditions for MHT to be an Exact Bayesian Solution to the Multiple Target Tracking Problem for Target-to-Measurement Association Hypotheses

LAWRENCE D. STONE

**This paper finds conditions under which multiple hypothesis tracking (MHT) is an exact Bayesian solution to the multiple target tracking problem for target-to-measurement association hypotheses. The crucial condition is that measurements arrive in scans from one or more sensors, but otherwise the conditions are minimally restrictive. In order to produce a computationally feasible implementation of MHT, some approximations must be made, but this true is for any (existing) method of producing an exact Bayesian solution. Limiting the number of hypotheses considered is an example of such an approximation. This paper is motivated by recent claims that MHT is not theoretically rigorous or “Bayes optimal.”**

Manuscript received January 5, 2019; revised November 13, 2019; released for publication February 5, 2020.

Refereeing of this contribution was handled by Chee-Yee Chong.

The author is with Metron Inc., 1818 Library Street, Reston, VA 20190, USA. E-mail: stone@metsci.com

1557-6418/19/\$17.00 © 2019 JAIF

## I. INTRODUCTION

This paper, which is based on [1], considers the question of when multiple hypothesis tracking (MHT) is an exact Bayesian solution to the multiple target tracking problem for target-to-measurement association hypotheses, or, more succinctly, when is it exact Bayesian. By exact, we mean that MHT produces the correct Bayesian posterior distribution on the targets and their states. Recently, there have been claims that MHT is not theoretically rigorous or “Bayes optimal” (see [2, Sec. 10.72] and [3]). Ref. [4, Sec. VII] observes that if the random finite set (RFS) version of multiple target tracking is exact Bayesian, then so are certain special cases of MHT that can be derived from the RFS formulation. However, this begs the question as to whether the RFS formulation is exact Bayesian and whether more general versions of MHT are exact Bayesian.

Note, a target-to-measurement association hypothesis is different from a measurement-to-measurement association hypothesis that is used in the standard MHT formulation.

In this paper, we explore the question of when MHT is exact Bayesian by first stepping back a bit and considering a more general definition of MHT than is generally used (see, e.g., [4], [5], and [6]). The plan of this paper is to proceed from general versions of MHT to the specific until we arrive at the most commonly used notions of MHT. This approach has two virtues. First, it shows that the notion and validity of an MHT decomposition (defined below) is more general than the usual notion of MHT. Second, it highlights the special assumptions needed to produce the most common and useful forms of MHT.

In classical multiple target tracking, the problem is divided into two steps: association and estimation. Step 1 associates measurements with targets. Step 2 uses the measurements associated with each target to produce an estimate of that target’s state. Complications arise when there is more than one reasonable way to associate measurements with targets. MHT approaches this problem by forming association hypotheses to explain the source of the measurements. We consider the situation where each hypothesis assigns the measurements to targets or false measurements. For each association hypothesis, MHT computes the probability that the hypothesis is correct and the conditional probability distribution on the joint target state given the hypothesis is correct. The Bayesian posterior is a mixture of the conditional joint target state distributions weighted by the association probabilities. This is the *MHT decomposition* of the multiple target tracking problem.

Theoretically, there are other decompositions that could be used. For example, one could use any set of mutually exclusive and exhaustive conditions for the decomposition. What makes the MHT decomposition special and important is that it is *useful*. Each element (hypothesis) of an MHT decomposition specifies which

measurements are associated with which targets and which are associated with false measurements. Under a hypothesis, the multiple target tracking problem becomes a much more tractable problem. Usually it becomes a set of  $n$  single target tracking problems, where  $n$  is the number of targets specified by the hypothesis. The MHT decomposition transforms a difficult and daunting multiple target tracking problem into a set of problems we know how to solve. This was Reid’s key insight [5].

While MHT is the most widely used method for solving multiple target tracking problems, multiple target tracking is not limited to the classical case described above. Section II-C includes a brief discussion of multiple target tracking when the notion of associating measurements with targets is not meaningful.

Reid [5] formulated the initial version of MHT that was later generalized by Mori et al. [6]. Since then, many versions and implementations of MHT have been developed (see [4]).

Many of the technical results presented in this paper are based on results from [7, Ch. 4]. However, the emphasis in this paper is on identifying conditions under which MHT is an exact Bayesian solution to multiple target tracking.

We show that the crucial condition ensuring that MHT is exact Bayesian is that measurements arrive in scans as defined below. The additional conditions required for this result are minimally restrictive. Thus, the MHT decomposition is exact Bayesian for a wide class of tracking problems. In order to produce a computationally feasible implementation, some approximations must be made, but this is true of any (existing) method of producing an exact Bayesian solution. In MHT, the number of association hypotheses grows exponentially in the number of measurements, so a typical approximation is to limit the number of hypotheses considered. In addition, it is customary to display only the tracks resulting from the highest probability association hypothesis and treat them as the “tracking solution.”

Section II provides the basic definitions that we use for multiple target tracking. Section III proves the basic result on the validity of the MHT decomposition. The reader will note in this section that we use a more general definition of MHT than is usual. In particular, the various versions of MHT discussed in [4] are all special cases of this definition. Section IV presents additional assumptions that allow the MHT decomposition to be performed recursively, and Section V gives assumptions under which the target state distributions, conditioned on an association hypothesis, are independent. Section VI provides a summary of these assumptions. Section VII provides some conclusions.

## II. MULTIPLE TARGET TRACKING

We employ a continuous–discrete formulation of tracking where the target motion takes place in continuous time, but the measurements are received at a dis-

crete sequence  $0 \leq t_1 \leq \dots \leq t_K$  of possibly random times. We represent a single target’s state and its motion through the target state space  $S$  in terms of a stochastic process  $\{X(t); t \geq 0\}$ , where  $X(t)$  is the target state at time  $t$ . The target state can have both continuous and discrete components. In addition to kinematic components, there can be components that correspond to “features” such as color or frequency and source level of an emission. Target motion can include changes in nonkinematic as well as kinematic components.

### A. Multiple Target Motion Process

The multiple target tracking problem begins at  $t = 0$ . The total number of targets is unknown but bounded by  $\bar{N}$ , which is known. We assume a known bound on the number of targets because it allows us to simplify the presentation and produces no restriction in practice. It is possible to remove this restriction but that would add complications without adding capability. We add an additional state  $\phi$  to the target state space  $S$ . If a target is not present in  $S$ , we say that it is in state  $\phi$ . Let  $S^+ = S \cup \{\phi\}$  be the augmented state space for a single target and  $\mathbf{S}^+ = S^+ \times \dots \times S^+$  be the joint target state space where the product is taken  $\bar{N}$  times. This is a vector formulation of the multiple target tracking motion model. Each component (target) can be indistinguishable from the others, or if there is prior knowledge some components can have different motion models. Both are possible but neither is required. In the case where the targets are indistinguishable, the component labels are arbitrary. The notion of including a state such as  $\phi$  to represent target not present in  $S$  has precedent in the works of [8], [9], [10], [11], and [12].

Our prior knowledge about the targets and their “movements” through the state space  $\mathbf{S}^+$  is given by a stochastic process  $\mathbf{X} = \{\mathbf{X}(t); t \geq 0\}$ , where  $\mathbf{X}(t) = (X_1(t), \dots, X_{\bar{N}}(t))$  is the state of the system at time  $t$  and  $X_n(t) \in S^+$  is the state of target  $n$  at time  $t$ . The term “state of the system” means the joint state of all the targets. If  $X_n(t) = \phi$ , then target  $n$  is not present in  $S$  at time  $t$ . The motion model can allow for targets to arrive (transition from  $\phi$  to  $S$ ) and depart (transition from  $S$  to  $\phi$ ) as time progresses.

### B. Multiple Target Likelihood Functions

**Definition.** A *measurement* is a function of a sensor response.

A sensor response that has crossed a specified threshold and is used to provide an estimate of a target’s position is an example of a measurement. A measurement can be a multivariate function of the sensor response. An example is a peak-picking algorithm that identifies the number of peaks that cross a threshold and their locations. Another example of a measurement is the sensor response itself. This is the identity function applied

to the sensor response to yield the measurement. An example of this is the acoustic times series received at a hydrophone over an interval of time.

Let the random variable  $Y(t, j)$  be the measurement from sensor  $j$  at time  $t$ . Measurements from sensor  $j$  take values in the measurement space  $\Psi_j$  that may be different for each sensor. We define the *multiple target likelihood function*  $l_j$  for sensor  $j$  at time  $t$  as follows:

$$l_j(t, y|\mathbf{s}) = \Pr\{Y(t, j) = y | \mathbf{X}(t) = \mathbf{s}\} \text{ for } y \in \Psi_j, \mathbf{s} \in \mathbf{S}^+. \quad (1)$$

Note that this likelihood depends on the *system state*  $\mathbf{s}$  at time  $t$ . The system state gives the state of each target. If a target is not present, its state is  $\phi$ . If false measurements are possible, then a model for these must be defined and used in the calculation of (1). Note that we use  $\Pr$  to mean probability or probability density, whichever is appropriate.

Suppose we have obtained measurements at the discrete times  $0 \leq t_1 \leq \dots \leq t_K \leq t$ . Let the random variable  $\mathbf{Y}_k$  be the set of measurements received at time  $t_k$  and  $\mathbf{y}_k$  denote a value of  $\mathbf{Y}_k$ . We extend (1) to define

$$L_k(\mathbf{y}_k|\mathbf{s}) = \Pr\{\mathbf{Y}_k = \mathbf{y}_k | \mathbf{X}(t_k) = \mathbf{s}\} \text{ for } \mathbf{s} \in \mathbf{S}^+. \quad (2)$$

$L_k(\mathbf{y}_k|\cdot)$  is the multitarget likelihood function for the measurement set  $\mathbf{Y}_k = \mathbf{y}_k$ . If the sensor responses are correlated or there are restrictions such as a target can generate at most one measurement in a set, then these must be taken into account in computing this likelihood function.

Let  $\mathbf{Y}_{1:K} = (\mathbf{Y}_1, \mathbf{Y}_2, \dots, \mathbf{Y}_K)$  and  $\mathbf{y}_{1:K} = (\mathbf{y}_1, \dots, \mathbf{y}_K)$ . These are the measurement sets received at the times  $\{t_1, \dots, t_K\}$ .

Define

$$\begin{aligned} \mathbf{L}(\mathbf{y}_{1:K}|\mathbf{s}_1, \dots, \mathbf{s}_K) \\ = \Pr\{\mathbf{Y}_{1:K} = \mathbf{y}_{1:K} | X(t_1) = \mathbf{s}_1, \dots, X(t_K) = \mathbf{s}_K\}. \end{aligned} \quad (3)$$

We assume that the distribution of the measurements at the times  $\{t_1, \dots, t_K\}$  depends only on the system states at these times. That is,

$$\Pr\{\mathbf{Y}_{1:K} = \mathbf{y}_{1:K} | \mathbf{X}(u), 0 \leq u \leq t\} = \mathbf{L}(\mathbf{y}_{1:K}|\mathbf{s}_1, \dots, \mathbf{s}_K), \quad (4)$$

where  $\mathbf{s}_k = \mathbf{X}(t_k)$  for  $k = 1, \dots, K$ .

Let

$$q(\mathbf{s}_1, \dots, \mathbf{s}_K) = \Pr\{\mathbf{X}(t_1) = \mathbf{s}_1, \dots, \mathbf{X}(t_K) = \mathbf{s}_K\}.$$

Then, the posterior distribution on the multiple target state at time  $t_K$  given  $\mathbf{Y}_{1:K} = \mathbf{y}_{1:K}$  is

$$\begin{aligned} p(t_K, \mathbf{s}_K | \mathbf{y}_{1:K}) &= \frac{\Pr\{\mathbf{Y}_{1:K} = \mathbf{y}_{1:K} \text{ and } \mathbf{X}(t_K) = \mathbf{s}_K\}}{\Pr\{\mathbf{Y}_{1:K} = \mathbf{y}_{1:K}\}} \\ &= \frac{\int \mathbf{L}(\mathbf{y}_{1:K}|\mathbf{s}_1, \dots, \mathbf{s}_K) q(\mathbf{s}_1, \dots, \mathbf{s}_K) d\mathbf{s}_1 \cdots d\mathbf{s}_{K-1}}{\int \mathbf{L}(\mathbf{y}_{1:K}|\mathbf{s}_1, \dots, \mathbf{s}_K) q(\mathbf{s}_1, \dots, \mathbf{s}_K) d\mathbf{s}_1 \cdots d\mathbf{s}_K}, \end{aligned} \quad (5)$$

where the integral in the numerator of (5) is over the system states at the first  $K - 1$  measurement times and the integral in the denominator is over these states at the first  $K$  times.

### C. Bayes–Markov Recursion

If the motion model is Markovian so that

$$q(\mathbf{s}_1, \dots, \mathbf{s}_K) = \int_{\mathbf{S}^+} q_0(\mathbf{s}_0) \prod_{k=1}^K q_k(\mathbf{s}_k | \mathbf{s}_{k-1}) d\mathbf{s}_0 \quad (6)$$

where

$$q_0(\mathbf{s}) = \Pr\{\mathbf{X}(0) = \mathbf{s}\},$$

$$q_k(\mathbf{s}_k | \mathbf{s}_{k-1}) = \Pr\{\mathbf{X}(t_k) = \mathbf{s}_k | \mathbf{X}(t_{k-1}) = \mathbf{s}_{k-1}\},$$

and the likelihood function in (4) factors so that

$$\mathbf{L}(\mathbf{y}_{1:K}|\mathbf{s}_1, \dots, \mathbf{s}_K) = \prod_{k=1}^K L_k(\mathbf{y}_k|\mathbf{s}_k),$$

then the following Bayes–Markov recursion holds:

$$\begin{aligned} p(t_K, \mathbf{s}_K | \mathbf{y}_{1:K}) \\ = \frac{L_k(\mathbf{y}_K|\mathbf{s}_K) \int_{\mathbf{S}^+} q(\mathbf{s}_K|\mathbf{s}_{K-1}) p(t_{K-1}, \mathbf{s}_{K-1} | \mathbf{y}_{1:K-1}) d\mathbf{s}_{K-1}}{\int_{\mathbf{S}^+} L_k(\mathbf{y}_K|\mathbf{s}_K) \int_{\mathbf{S}^+} q(\mathbf{s}_K|\mathbf{s}_{K-1}) p(t_{K-1}, \mathbf{s}_{K-1} | \mathbf{y}_{1:K-1}) d\mathbf{s}_{K-1} d\mathbf{s}_K}. \end{aligned}$$

Observe that the above recursion does not require the notion of measurement association. The process of performing multiple target tracking with or without measurement association is called *unified tracking* in [13]. Ref. [13, Ch. 5] gives examples where two targets are tracked in a case where the notion of association is not meaningful. In some cases, the targets are indistinguishable and in others not. When association is not meaningful, standard MHT is not applicable to the multiple target tracking problem.

An example where association is not meaningful involves a fixed array of passive omnidirectional acoustic hydrophones. The measurement received at the sensor at time  $t$  is the vector of complex amplitudes (as a function of frequency) of the acoustic time series received at the hydrophones of the array at time  $t$ . When there is more than one target present, the signals from all targets are received and acoustically summed at each hydrophone so that it does not make sense to associate the measurement with a single target. The maximum posterior probability penalty function (MAP-PF) algorithm, described in [7, Ch. 6], uses the Bayes–Markov recursion above to perform multiple target tracking using these measurements without association or thresholding to produce contacts. By avoiding thresholding, one can utilize more information and provide better tracking solutions than if one is limited to using thresholded data (e.g., called contacts). The MAP-PF algorithm has been applied to a number of operational problems (see [7, Ch. 6, refs. 1–5]).

One can sometimes force the problem into an MHT framework, but the results are suboptimal. In particular, the results are not Bayes optimal. Ref. [13, Sec. 5.3.2]

gives an illustration of this and the resulting degradation of the tracking performance that results.

Ref. [13, Ch. 5] shows that MHT can be derived as a special case of unified tracking that motivates the name because the above recursion provides a unified approach to tracking with or without measurement association.

### III. MULTIPLE HYPOTHESIS TRACKING

We take a more expansive definition of MHT than is normally the case—see [4], for example. In particular, we do not require targets to be indistinguishable, or false measurements to be Poisson distributed. We do not require that the target motion processes be independent or Markovian. In addition, Gaussian assumptions are not required. We *do require* that measurements arrive in scans as defined below.

A global measurement association hypothesis, defined more precisely in Section III-A, assigns all measurements received up to a given time to targets or false measurements. These hypotheses are target-to-measurement hypotheses, which are different from measurement-to-measurement association hypotheses used in the standard MHT formulation.

**Definition.** An *MHT* is a tracker that computes the posterior distribution on system state as follows. It identifies all possible global measurement association hypotheses and calculates their probabilities of being true, computes the conditional target state distributions given each hypothesis, and forms the posterior distribution as a mixture of the conditional target state distributions weighted by the association hypothesis probabilities. This is called the *MHT decomposition*.

In Section III-B, we show that under the conditions assumed in Sections II-A and II-B and the assumption that measurements come in scans, the MHT decomposition produces the exact Bayesian posterior on system state. That is, it is the exact Bayesian solution, theoretically correct, and “Bayes optimal.”

However, the MHT decomposition will be of limited use unless the conditional target state distributions can be computed recursively and the target state random variables are independent given a global measurement association hypothesis. Sections IV and V provide conditions under which these are true.

#### A. Scans and Global Measurement Association Hypotheses

**Definition.** A set of measurements at time  $t_k$  is a *scan* if each measurement is generated by at most one target and each target generates at most one measurement. We also require that the association of measurements in different scans is independent.

Note that this definition means that not every measurement is a scan by itself.

**Assumption.** We assume measurements arrive in scans.

Some of these measurements may be false measurements, i.e., not generated by a target, and some targets may not produce measurements on a given scan. Let

$G_j$  = set of measurements in the  $j$ th scan,

$G(1 : k)$  = set of measurements in the first  $k$  scans

$$= \bigcup_{j=1}^k G_j.$$

**Definition.** A *global measurement association hypothesis*  $h$  on  $G(1 : k)$  is a mapping  $h : G(1 : k) \rightarrow \{0, 1, \dots, \bar{N}\}$  such that

$h(m) = n > 0$  means measurement  $m$  is associated with target  $n$ ,

$h(m) = 0$  means measurement  $m$  is associated with a false measurement,

and no target has more than one measurement per scan associated with it.

Let  $H(k)$  = set of global measurement association hypotheses on  $G(1 : k)$ . A hypothesis  $h \in H(k)$  partitions  $G(1 : k)$  into disjoint subsets

$$\Psi_k(n) = \{m \in G(1 : k) : h(m) = n\} \text{ for } n = 0, 1, \dots, \bar{N},$$

where  $\Psi_k(n)$  is the subset of measurements associated with target  $n$  for  $n > 0$  and  $\Psi_k(0)$  is the subset of measurements associated with false measurements.

#### B. MHT Decomposition

MHT calculates the posterior distribution on system state at time  $t_K$  given the global measurement association hypothesis  $h$  is true and the probability  $\alpha(h|\mathbf{y}_{1:K})$  that hypothesis  $h$  is true given  $\mathbf{Y}_{1:K} = \mathbf{y}_{1:K}$  for each  $h \in H(K)$ . Specifically, it computes

$$p(t_K, \mathbf{s}_K | h \wedge \mathbf{y}_{1:K}) = \Pr\{\mathbf{X}(t_K) = \mathbf{s}_K | h \wedge \mathbf{Y}_{1:K} = \mathbf{y}_{1:K}\} \quad (7)$$

and

$$\alpha(h|\mathbf{y}_{1:K}) = \Pr\{h|\mathbf{Y}_{1:K} = \mathbf{y}_{1:K}\} = \frac{\Pr\{h \wedge \mathbf{Y}_{1:K} = \mathbf{y}_{1:K}\}}{\Pr\{\mathbf{Y}_{1:K} = \mathbf{y}_{1:K}\}}, \quad (8)$$

where  $\wedge$  denotes conjunction. The Bayesian posterior is given by

$$p(t_K, \mathbf{s}_K | \mathbf{y}_{1:K}) = \sum_{h \in H(K)} p(t_K, \mathbf{s}_K | h \wedge \mathbf{y}_{1:K}) \alpha(h|\mathbf{y}_{1:K}). \quad (9)$$

Equation (9) is the MHT decomposition. The validity of this decomposition depends only on the assumptions in Sections II-A, II-B, and III-A. Thus, MHT is an exact Bayesian solution under very general assumptions. The main restriction is that measurements must arrive in scans. However, in most cases, we require more assumptions to compute MHT solutions.

#### IV. RECURSIVE MHT ASSUMPTIONS

In this section, we add assumptions that allow us to compute the MHT decomposition recursively. We assume the motion model is Markovian in the joint state space and that

$$\mathbf{L}(\mathbf{y}_{1:K}|\mathbf{s}_1, \dots, \mathbf{s}_K) = \prod_{k=1}^K L_k(\mathbf{y}_k|\mathbf{s}_k). \quad (10)$$

Let the Markov transition function be denoted by

$$q_k(\mathbf{s}_k|\mathbf{s}_{k-1}) = \Pr\{\mathbf{X}(t_k) = \mathbf{s}_k | \mathbf{X}(t_{k-1}) = \mathbf{s}_{k-1}\} \text{ for } k \geq 1$$

and  $q_0$  be the probability (density) function for  $\mathbf{X}(0)$ . Then, we can compute the posterior distribution in (5) using the classic Bayes–Markov recursion as follows.

*Initial distribution:*

$$p(t_0, \mathbf{s}_0) = q_0(\mathbf{s}_0) \text{ for } \mathbf{s}_0 \in \mathbf{S}^+. \quad (11)$$

For  $k \geq 1$  and  $\mathbf{s}_k \in \mathbf{S}^+$ ,

$$\begin{aligned} p^-(t_k, \mathbf{s}_k|\mathbf{y}_{1:k-1}) &= \int q_k(\mathbf{s}_k|\mathbf{s}_{k-1})p(t_{k-1}, \mathbf{s}_{k-1}|\mathbf{y}_{1:k-1})d\mathbf{s}_{k-1}, \\ L_k(\mathbf{y}_k|\mathbf{s}_k) &= \Pr\{\mathbf{Y}_k = \mathbf{y}_k | \mathbf{X}(t_k) = \mathbf{s}_k\}, \\ p(t_k, \mathbf{s}_k|\mathbf{y}_{1:k}) &= \frac{1}{C} L_k(\mathbf{y}_k|\mathbf{s}_k)p^-(t_k, \mathbf{s}_k|\mathbf{y}_{1:k-1}), \end{aligned} \quad (12)$$

where

$$C = \int L_k(\mathbf{y}_k|\mathbf{s}_k)p^-(t_k, \mathbf{s}_k|\mathbf{y}_{1:k-1})d\mathbf{s}_k.$$

##### A. Scan and Global Measurement Association Hypotheses

For the  $k$ th scan of measurements  $\mathbf{y}_k$ , let  $M_k$  = number of measurements in the scan.

**Definition.** A function  $\gamma : \{1, \dots, M_k\} \rightarrow \{0, \dots, \bar{N}\}$  is a *scan association hypothesis* if  $\gamma(m) = n > 0$  means measurement  $m$  is associated with target  $n$ ,  $\gamma(m) = 0$  means measurement  $m$  is associated with a false measurement, and no two measurements are assigned to the same positive number (target).

Let

$\Gamma_k$  = the set of all scan association hypotheses on scan  $Y_k$ .

A global measurement association hypothesis  $h_K \in H(K)$  is composed of  $K$  scan association hypotheses  $\{\gamma_1, \dots, \gamma_K\}$ , where  $\gamma_k$  is the association hypothesis for the  $k$ th scan. The global measurement association hypothesis  $h_K$  is an extension of  $h_{K-1} = \{\gamma_1, \dots, \gamma_{K-1}\} \in H(K-1)$ . That is,  $h_K$  is composed of  $h_{K-1}$  with  $\gamma_K$  appended. We write this as  $h_K = h_{K-1} \wedge \gamma_K$ .

1) **Scan Association Likelihood Function:** Define the scan association likelihood function

$$\begin{aligned} \ell_k(\mathbf{y}_k|\gamma \wedge \mathbf{s}_k) &= \Pr\{\mathbf{Y}_k = \mathbf{y}_k | \gamma \wedge \mathbf{X}(t_k) = \mathbf{s}_k\} \text{ for} \\ \mathbf{s}_k \in \mathbf{S}^+ \text{ and } \gamma \in \Gamma_k. \end{aligned} \quad (13)$$

The conditioning on the right-hand side of (13) means that we are conditioning on the scan association hypothesis  $\gamma$  as well as the system state  $\mathbf{s}_k$ .

As a function of  $\mathbf{s}_k$ , the likelihood of the scan measurement computed in (13) accounts for the probability of detecting the targets with which measurements are associated, failing to detect the remaining targets, and the false measurements. The likelihood function for the scan  $\mathbf{Y}_k = \mathbf{y}_k$  is

$$L_k(\mathbf{y}_k|\mathbf{s}_k) = \sum_{\gamma \in \Gamma_k} \ell_k(\mathbf{y}_k|\gamma \wedge \mathbf{s}_k) \Pr\{\gamma\} \text{ for } \mathbf{s}_k \in \mathbf{S}^+, \quad (14)$$

where on the right-hand side of (14) we assume that the (prior) probability of a scan association does not depend on the system state.

2) **Global Measurement Association Likelihood Function:** From (10), it follows that conditioned on  $h \in H(K)$ , the likelihood of the measurements received at times  $t_1, \dots, t_K$  depends only on the system state values at those times. Specifically, the global measurement association likelihood function  $l$  is

$$\begin{aligned} l(\mathbf{y}_{1:K}|h \wedge (\mathbf{s}_1, \dots, \mathbf{s}_K)) \\ &= \Pr\{\mathbf{Y}_{1:K} = \mathbf{y}_{1:K} | h \wedge \mathbf{X}(t_u) = \mathbf{s}_u; 0 \leq u \leq t_K\} \\ &= \Pr\{\mathbf{Y}_{1:K} = \mathbf{y}_{1:K} | h \wedge \mathbf{X}(t_k) = \mathbf{s}_k; k = 1, \dots, K\}. \end{aligned} \quad (15)$$

We assume that the scan association likelihoods are independent given  $h \wedge (\mathbf{s}_1, \dots, \mathbf{s}_K)$ , so that

$$l(\mathbf{y}_{1:K}|h \wedge (\mathbf{s}_1, \dots, \mathbf{s}_K)) = \prod_{k=1}^K \ell_k(\mathbf{y}_k|\gamma_k \wedge \mathbf{s}_k). \quad (16)$$

Finally, we assume that the prior probability of the global measurement association hypothesis  $h$  is equal to the product of the prior probabilities of its constituent scan association hypotheses. Specifically,

$$\Pr\{h_K\} = \prod_{k=1}^K \Pr\{\gamma_k\}, \text{ where } h = \{\gamma_1, \dots, \gamma_K\}. \quad (17)$$

*Association probabilities:* Define

$$C(h_0) = 1 \text{ and } C(h_K) = \Pr\{h_K \wedge \mathbf{Y}_{1:K} = \mathbf{y}_{1:K}\} \text{ for } K \geq 1. \quad (18)$$

Ref. [7, Sec. 4.5.1] shows that

$$\begin{aligned} C(h_K) &= C(h_{K-1}) \Pr\{\gamma_K\} \\ &\times \int \ell_K(\mathbf{y}_K|\gamma_K \wedge \mathbf{s}_K) p^-(t_K, \mathbf{s}_K|h_{K-1} \wedge \mathbf{y}_{1:K-1}) d\mathbf{s}_K \end{aligned} \quad (19)$$

and that the probability of the global measurement association  $h \in H(K)$  being correct given  $\mathbf{y}_{1:K}$  is

$$\alpha(h|\mathbf{y}_{1:K}) = \frac{C(h)}{\sum_{h' \in H(K)} C(h')}. \quad (20)$$

## B. Recursive Calculation of MHT Decomposition

Under the above assumptions, ref. [7, Sec. 4.2.5] shows how the conditional target state distribution in (7) and the association hypothesis probabilities in (8) may be calculated recursively. This allows us to calculate the MHT decomposition in (9) in a recursive fashion.

## V. INDEPENDENT MHT

In this section, we give additional assumptions that assure that the conditional target state distributions are independent so that  $p(t_K, \mathbf{s}_K | h \wedge \mathbf{y}_{1:K})$  in (9) equals the product of independent probability distributions on the  $\bar{N}$  possible targets. In this case, the MHT decomposition in (9) becomes

$$\begin{aligned} p(t_K, \mathbf{s}_K | \mathbf{y}_{1:K}) &= \sum_{h \in H(K)} \alpha(h | \mathbf{y}_{1:K}) p(t_K, \mathbf{s}_K | h \wedge \mathbf{y}_{1:K}) \\ &= \sum_{h \in H(K)} \alpha(h | \mathbf{y}_{1:K}) \prod_{n=1}^{\bar{N}} p_n(t_K, x_n | h \wedge \mathbf{y}_{1:K}) \\ &\quad \text{for } \mathbf{s}_K = (x_1, \dots, x_{\bar{N}}) \in \mathbf{S}^+, \end{aligned} \quad (21)$$

where  $p_n(t_K, \cdot | h \wedge \mathbf{y}_{1:K})$  is the marginal distribution on target  $n$ . If target  $n$  is not present at time  $t_K$  under hypothesis  $h$ , then  $p_n(t_K, \phi | h \wedge \mathbf{y}_{1:K}) = 1$ .

## A. Conditionally Independent Association Likelihoods

**Definition.** The likelihood of a scan  $\mathbf{Y}_k = \mathbf{y}_k$  obtained at time  $t_k$  is *conditionally independent* if and only if for all scan association hypotheses  $\gamma \in \Gamma_k$ ,

$$\begin{aligned} \ell_k(\mathbf{y}_k | \mathbf{s}_k = (x_1, \dots, x_{\bar{N}}) \wedge \gamma) \\ &= \Pr\{\mathbf{Y}_k = \mathbf{y}_k | \gamma \wedge \mathbf{X}(t_k) = (x_1, \dots, x_{\bar{N}})\} \\ &= g_0^\gamma(\mathbf{y}_k) \prod_{n=1}^{\bar{N}} g_n^\gamma(\mathbf{y}_k, x_n) \end{aligned} \quad (22)$$

for some functions  $g_n^\gamma$ ,  $n = 0, \dots, \bar{N}$ , where  $g_0^\gamma$  can depend on the scan measurements but not  $\mathbf{s}_k$ . For  $n > 0$ ,  $g_n^\gamma(\mathbf{y}_k, \cdot)$  is typically the likelihood function for the measurement in  $\mathbf{y}_k$  that is associated with target  $n$ , which may be no measurement, and  $g_0^\gamma(\mathbf{y}_k)$  is the probability of receiving the false measurements and measurements generated by targets as specified by the scan association hypothesis  $\gamma$ .

## B. Independence Theorem

Under the assumptions of conditional independence of the scan association likelihood functions and independence of the target motion models, MHT decomposes the multiple target tracking problem into  $\bar{N}$  independent single target problems by conditioning on a global measurement association hypothesis. Let  $q_k^n(s_{n,k} | s_{n,k-1})$  be the transition function at time  $t_k$  for target  $n$  for  $n = 1, \dots, \bar{N}$ . The following theorem and proof are from [7].

**Independence theorem.** *Suppose the prior target motion processes are mutually independent so that the multiple target transition function factors as follows:*

$$q_k(\mathbf{s}_k | \mathbf{s}_{k-1}) = \prod_{n=1}^{\bar{N}} q_k^n(s_{n,k} | s_{n,k-1}) \quad (23)$$

*and the scan association likelihood functions are conditionally independent. Then, the posterior system state distribution conditioned on a global measurement association hypothesis is the product of independent distributions on the targets' states.*

**Proof.** Let  $\mathbf{Y}_{1:K} = \mathbf{y}_{1:K}$  be the scan measurements that are received at times  $0 \leq t_1 \leq \dots \leq t_K \leq t$ . Recall that  $H(k)$  is the set of all global measurement association hypotheses on the first  $k$  scans. We wish to show for  $k = 1, \dots, K$  that

$$\begin{aligned} p(t_k, \mathbf{s}_k | h \wedge \mathbf{y}_{1:K}) &= \prod_{n=1}^{\bar{N}} p_n(t_k, x_n | h \wedge \mathbf{y}_{1:K}) \text{ for } h \in H(k) \\ \text{and } \mathbf{s}_k &= (x_1, \dots, x_{\bar{N}}) \in \mathbf{S}^+, \end{aligned} \quad (24)$$

where

$$\begin{aligned} p_n(t_k, x_n | h \wedge \mathbf{y}_{1:K}) &= \Pr\{X_n(t_k) = x_n | h \wedge \mathbf{Y}_{1:K} = \mathbf{y}_{1:K}\} \\ &\quad \text{for } x_n \in \mathbf{S}^+ \text{ and } n = 1, \dots, \bar{N}. \end{aligned}$$

We will prove the theorem by induction.

$k = 1$ : We first show that (24) holds for  $k = 1$ . By the independence of the prior target motion processes,

$$p(0, \mathbf{s}) = \prod_{n=1}^{\bar{N}} p_n(0, x_n) \text{ for } \mathbf{s} = (x_1, \dots, x_{\bar{N}}) \in \mathbf{S}^+,$$

where  $p_n(0, \cdot)$  is the initial state distribution on target  $n$ . Since the motion models for the targets are independent, the joint distribution at time  $t_1$  before updating for the scan of measurements  $\mathbf{Y}_1 = \mathbf{y}_1$  is

$$p^-(t_1, \mathbf{s}_1) = \prod_{n=1}^{\bar{N}} p_n^-(t_1, x_n) \text{ for } \mathbf{s}_1 = (x_1, \dots, x_{\bar{N}}) \in \mathbf{S}^+,$$

where  $p_n^-(t_1, \cdot)$  is the motion-updated distribution for target  $n$  at time  $t_1$ . A global measurement association hypothesis,  $h \in H(1)$ , is equal to a scan association hypothesis  $\gamma \in \Gamma_1$ . By the conditional independence assumption, the likelihood function for the scan  $\mathbf{Y}_1$  factors into functions that depend only on the state of a single target and are independent of the state of the other targets.

To compute the posterior given  $\mathbf{Y}_1 = \mathbf{y}_1$  and the association  $h = \gamma$ , we follow the recursion in (11) and (12) that clearly holds when we condition on a measurement association hypothesis. We multiply the motion-updated multiple target distribution at time  $t_1$  by the likelihood function for  $\mathbf{Y}_1 = \mathbf{y}_1$ , both conditioned on  $\gamma$ , to obtain

$$\begin{aligned} p(t_1, \mathbf{s}_1 | \gamma \wedge \mathbf{y}_1) &\propto g_0^\gamma(\mathbf{y}_1) \prod_{n=1}^{\bar{N}} g_n^\gamma(\mathbf{y}_1, x_n) \prod_{n=1}^{\bar{N}} p_n^-(t_1, x_n) \\ &\propto g_0^\gamma(\mathbf{y}_1) \prod_{n=1}^{\bar{N}} [g_n^\gamma(\mathbf{y}_1, x_n) p_n^-(t_1, x_n)] \\ &\quad \text{for } \mathbf{s}_1 = (x_1, \dots, x_{\bar{N}}) \in \mathbf{S}^+. \end{aligned} \quad (25)$$

We obtain  $p_n(t_1, x_n | \gamma \wedge \mathbf{y}_1)$ , the marginal distribution on the state of target  $n$ , by integrating the right-hand side of (25) over all components except  $x_n$  and normalizing to obtain a probability distribution. The result is

$$p_n(t_1, x_n | \gamma \wedge h_1) \propto g_n^\gamma(\mathbf{y}_1, x_n) p_n^-(t_1, x_n) \\ \text{for } n = 1, \dots, \bar{N},$$

and we see that (24) holds for  $k = 1$ .

$k$  implies  $k + 1$ : Suppose that (24) holds for the first  $k$  scans. Consider a global measurement association hypothesis  $h_{k+1} \in H(k+1)$ . Then,  $h_{k+1} = \{h_k \wedge \gamma\}$  for some hypothesis  $h_k \in H(k)$  and scan hypothesis  $\gamma \in \Gamma_{k+1}$ . Define

$$p^-(t_{k+1}, \cdot | h_k \wedge \mathbf{y}_{1:k}) = \text{distribution on } \mathbf{X}(t_{k+1}) \\ \text{given } h_k \wedge \mathbf{y}_{1:k}.$$

This distribution is obtained by performing the motion and information updates for the first  $k$  scans and the motion update only from time  $t_k$  to  $t_{k+1}$ . For target  $n$ , we define

$$p_n^-(t_{k+1}, \cdot | h_k \wedge \mathbf{y}_{1:k}) = \text{distribution on } X_n(t_{k+1}) \text{ given } \\ h_k \wedge \mathbf{y}_{1:k}.$$

By assumption, the target motion processes are independent. From this and the fact that (24) holds for  $k$ , we have

$$p^-(t_{k+1}, \mathbf{s}_{k+1} | h_k \wedge \mathbf{y}_{1:k}) = \prod_n p_n^-(t_{k+1}, x_n | h_k \wedge \mathbf{y}_{1:k}).$$

To obtain the posterior system state distribution at time  $t_{k+1}$ , we multiply  $p^-(t_{k+1}, \mathbf{s}_{k+1} | h_k \wedge \mathbf{y}_{1:k})$  by the scan likelihood function conditioned on  $\gamma_{k+1}$  to obtain

$$p(t_{k+1}, \mathbf{s}_{k+1} | h_{k+1} \wedge \mathbf{y}_{1:k+1}) \\ = \frac{1}{C} g_0^{\gamma_{k+1}}(\mathbf{y}_{k+1}) \prod_n g_n^{\gamma_{k+1}}(\mathbf{y}_{k+1}, x_n) \prod_n p_n^-(t_{k+1}, x_n | h_k \wedge \mathbf{y}_{1:k}) \\ = \frac{1}{C} g_0^{\gamma_{k+1}}(\mathbf{y}_{k+1}) \prod_n g_n^{\gamma_{k+1}}(\mathbf{y}_{k+1}, x_n) p_n^-(t_{k+1}, x_n | h_k \wedge \mathbf{y}_{1:k}) \\ \text{for } \mathbf{s}_{k+1} = (x_1, \dots, x_{\bar{N}}) \in \mathbf{S}^+.$$

This shows that if (24) holds for  $k$ , then it is true for  $k + 1$ . Since we have shown that (24) holds for  $k = 1$ , the theorem is proved by mathematical induction.

## VI. SUMMARY OF ASSUMPTIONS

In this section, we provide a summary of the assumptions we made to ensure the validity of the MHT decomposition, the recursive computation of the MHT decomposition, and the independence of the posterior distributions on the targets given a global measurement association hypothesis. In each case, MHT produces an exact Bayesian solution. The assumptions are cumulative; e.g., the assumptions in Section VI-B implicitly include those in Section VI-A.

### A. Assumptions for Validity of MHT Decomposition

- *Continuous discrete formulation*: Targets move in continuous time but measurements are received at a discrete set of times  $\{t_1, \dots, t_K\}$ .
- *Target evolution*: Prior knowledge of the motion of the targets in state space is specified by a stochastic process.
- *Scan assumption*: Measurements are received in scans at the discrete times  $\{t_1, \dots, t_K\}$ .
- Measurements at  $t_k$  depend only on system state at  $t_k$ , and we can calculate the multiple target likelihood function in (3).

### B. Assumptions for Recursive Computation of MHT Decomposition

- Target motion process is Markovian in system state.
- Measurement likelihood functions factor over scans:

$$L(\mathbf{y}_{1:K} | \mathbf{s}_1, \dots, \mathbf{s}_K) = \prod_{k=1}^K L_k(\mathbf{y}_k | \mathbf{s}_k), \\ l(\mathbf{y}_{1:K} | h \wedge (\mathbf{s}_1, \dots, \mathbf{s}_K)) = \prod_{k=1}^K \ell_k(\mathbf{y}_k | \gamma_k \wedge \mathbf{s}_k).$$

- Prior on global measurement association hypotheses factors:

$$\Pr\{h\} = \prod_{k=1}^K \Pr\{\gamma_k\}, \quad \text{where } h = \{\gamma_1, \dots, \gamma_K\}.$$

### C. Assumptions for Independent Conditional Target State Distributions

- Prior motion models are independent, i.e.,

$$q_k(\mathbf{s}_k | \mathbf{s}_{k-1}) = \prod_{n=1}^{\bar{N}} q_k^n(s_{n,k} | s_{n,k-1}).$$

- Scan likelihood functions are conditionally independent, i.e.,

$$\ell_k(\mathbf{y}_k | \gamma \wedge \mathbf{s}_k = (x_1, \dots, x_{\bar{N}})) = g_0^\gamma(\mathbf{y}_k) \prod_{n=1}^{\bar{N}} g_n^\gamma(\mathbf{y}_k, x_n).$$

### D. Comments

Looking at the assumptions for the validity of the MHT decomposition in Section VI-A, we see that only the scan assumption puts any substantial restriction on the class of problems for which MHT is the exact Bayesian solution. The assumptions in Sections VI-B and VI-C make explicit the assumptions made in most multiple target tracking problems to make them more computationally tractable. Most versions of MHT make the further assumption that the false alarm process is Poisson and that the motion and measurement models are linear Gaussian, at least approximately, so that a Kalman filter can be used to calculate target state distributions.

## VII. CONCLUSIONS

From the above discussion, we see that the MHT decomposition produces the exact Bayesian solution to the multiple target tracking problem for target-to-measurement hypotheses under quite general assumptions. The main requirement is that measurements arrive in scans. In order to compute the decomposition recursively and to obtain independent conditional target distributions, we add the Markovian and independence assumptions given in Sections IV and V. Section VI summarizes these assumptions. Although the MHT decomposition applies to a great many multiple target tracking problems, it does not apply to all of them. Both unified fusion of [13, Ch. 5] and the RFS approach of [2] deal with problems beyond the purview of MHT.

Because the number of global measurement association hypotheses grows exponentially in the number of measurements received, implementation of an MHT algorithm requires approximations such as limiting the number of global association hypotheses or using a track-oriented approach (see [4]). This problem is not unique to MHT. All (existing) methods of producing an exact Bayesian solution require approximations of some sort to produce a computationally feasible algorithm for even modestly complex multiple target tracking problems.

## REFERENCES

1. L. D. Stone  
“Conditions for MHT to be an exact Bayesian solution to the multiple target tracking problem,” in *Proc. 21st Int. Conf. Inf. Fusion*, Cambridge, UK, 2018.
2. R. Mahler  
*Statistical Multisource–Multitarget Information Fusion*. Norwood, MA: Artech House, 2007.
3. R. Mahler  
“Measurement to track association and finite-set statistics,” arXiv:17101.07078v1, Jan. 5, 2017.
4. C. Y. Chong, S. Mori, and D. R. Reid  
“Forty years of multiple hypothesis tracking—A review of key developments,” in *Proc. 21st Int. Conf. Inf. Fusion*, Cambridge, UK, 2018.
5. D. B. Reid  
“An algorithm for tracking multiple targets,” *IEEE Trans. Autom. Control*, vol. 24, no. 6, pp. 843–854, Dec. 1979.
6. S. Mori, C. Y. Chong, E. Tse, and R. P. Wishner  
“Tracking and classifying multiple targets without a priori identification,” *IEEE Trans. Autom. Control*, vol. 31, no. 5, pp. 401–409, May 1986.
7. L. D. Stone, R. L. Streit, T. L. Corwin, and K. L. Bell  
*Bayesian Multiple Target Tracking*, 2nd ed. Boston, MA: Artech House, 2014.
8. R. E. Bethel and R. G. Rakka  
“Optimum time delay detection and tracking,” *IEEE Trans. Aerosp. Electron. Syst.*, vol. 26, no. 5, pp. 700–712, Sep. 1990.
9. S. B. Colegrove, A. W. Davis, and J. K. Ayliff  
“Track initiation and nearest neighbors incorporated into probabilistic data association,” *J. Elect. Electron. Eng.*, vol. 6, pp. 191–198, Sep. 1986.
10. G. E. Kopec  
“Formant tracking using hidden Markov models and vector quantization,” *IEEE Trans. Acoust., Speech, Signal Process.*, vol. 34, no. 4, pp. 709–729, Aug. 1986.
11. D. Musicki, R. Evans, and S. Stankovic  
“Integrated probabilistic data association,” *IEEE Trans. Autom. Control*, vol. 39, no. 6, pp. 1237–1241, Jun. 1994.
12. R. L. Streit and R. F. Barrett  
“Frequency line tracking using hidden Markov models,” *IEEE Trans. Acoust., Speech, Signal Process.*, vol. 38, no. 4, pp. 586–598, Apr. 1990.
13. L. D. Stone, C. A. Barlow, and T. L. Corwin  
*Bayesian Multiple Target Tracking*, 1st ed. Boston, MA: Artech House, 1999.



**Lawrence D. Stone** received the B.S. degree in mathematics from Antioch College, Yellow Springs, OH, USA, in 1964, and the M.S. and Ph.D. degrees in mathematics from Purdue University, West Lafayette, IN, USA, in 1966 and 1967, respectively. He is currently a Chief Scientist at Metron Inc. In 1986, he produced the probability maps used to locate the *SS Central America* that sank in 1857, taking millions of dollars of gold coins and bars to the ocean bottom one and one-half miles below. In 2010, he led the team that produced the probability distribution that guided the French to the location of the underwater wreckage of Air France Flight AF447. He was one of the primary developers of the Search and Rescue Optimal Planning System used by the Coast Guard since 2007 to plan searches for people missing at sea. He continues to work on a number of detection and tracking systems for the United States Navy. He has coauthored the books *Bayesian Multiple Target Tracking*, 2nd ed. (2014) and *Optimal Search for Moving Targets* (2016). He is a member of the National Academy of Engineering and a Fellow of the Institute for Operations Research and Management Science (INFORMS). He was a recipient of the Jacinto Steinhardt Award from the Military Applications Section of INFORMS in recognition of his applications of operations research to military problems, and Lanchester Prize from the Operations Research Society of America in 1975 for his text *Theory of Optimal Search*.

# Three Mathematical Formalisms of Multiple Hypothesis Tracking

SHOZO MORI  
CHEE-YEE CHONG  
KUO-CHU CHANG

**This paper describes three mathematical formalisms, each of which provides a solid foundation for developing multiple hypothesis tracking (MHT) theories and algorithms, as solutions to detection-based multiple target tracking (MTT) problems. The three formalisms are 1) random finite sequence (RFSeq), 2) finite point process (FPP), and 3) random finite set (RFSet) formalisms. We will discuss equivalencies and some subtle differences among them. In addition, we will discuss theoretical consequences of various assumptions on MHT hypothesis evaluation, as well as recent RFSet-based MTT algorithm developments claiming relationship to MHT.**

Manuscript received February 1, 2019; revised June 14, 2019, September 22, 2019, November 9, 2019; released for publication February 5, 2020.

Refereeing of this contribution was handled by Jason L. Williams.

S. Mori is with Systems & Technology Research, Sacramento, CA, 95823, USA (E-mail: smori@ieee.org).

C.-Y. Chong is an Independent Researcher, Los Altos, CA, 94024, USA (E-mail: cychong@ieee.org).

K.-C. Chang is with the Department of Systems Engineering and Operations Research (SEOR), George Mason University, Fairfax, VA, 22030, USA (E-mail: kchang@gmu.edu).

1557-6418/19/\$17.00 © 2019 JAIF

## I. INTRODUCTION

This paper is generally concerned with *multiple target tracking* (MTT) problems, as defined in [1]–[3], i.e., problems of tracking a generally unknown number of objects, called *targets*,<sup>1</sup> based on noisy data. Specifically, we are concerned with a particular class of MTT problems, where the information is provided by generally multiple sensors in terms of finite sets of noisy measurements, called *target detections*,<sup>2</sup> without any explicit indication of their origins. This class of problems is sometimes referred to as *point target tracking*, due to the fact that each target is modeled as a point in a target state space, or each target appears and is detected as a point in a sensor measurement space. It may also be referred to as *tracking small targets*,<sup>3</sup> for the same reason. Our focus is on a particular class of solutions based on systematic generation and evaluation of multiple *data association hypotheses*, which hypothesize the number of detected targets and partition the set of all the acquired detections according to their hypothesized common origins, customarily referred to as *multiple hypothesis tracking* (MHT).<sup>4</sup>

To the best of our knowledge, various approaches to MTT problems were first comprehensively described in an MTT survey paper [4]. It referenced the two seminal works: one by C. L. Morefield [5] and the other by D. B. Reid [41] (the work of which was subsequently published as [6]).<sup>5</sup> These two works constitute, in our opinion, the first two significant MHT developments. In [5], C. L. Morefield established the MHT foundation by defining *association hypotheses*, each of which is a set of *tracks*, and proposed the best hypothesis selection using a zero–one integer linear programming algorithm. D. B. Reid, in [6], presented a recursive MHT algorithm that propagates and evaluates multiple tracks and hypotheses, both recursively. Subsequently in [7], a generalized recursive MHT algorithm was developed, as a Bayesian optimal solution, showing the optimality as a clear theoretical consequence of mathematical models of targets and sensors, and a set of statistical assumptions, complementing the developments by Morefield [5] and Reid [6].

Generation and evaluation of multiple hypotheses are often considered as an intermediate step toward Bayesian estimation<sup>6</sup> of the states of an unknown number of targets. However, in some applications, the Bayesian estimation of measurement-to-measurement (data-to-data) association is of primary interest and

<sup>1</sup>In MTT, a target is a generic name for any *object* to be tracked.

<sup>2</sup>Also called *contacts*, *returns*, or simply *measurements* or *observations*.

<sup>3</sup>As opposed to *extended targets* with possibly multiple observations from each single target.

<sup>4</sup>In MHT, by *hypotheses* we always mean data association hypotheses.

<sup>5</sup>The introduction section of [6] contains an excellent summary of the early works on MTT problems.

<sup>6</sup>By *Bayesian estimation*, we mean a process to obtain analytical or numerical expressions of the conditional probability distributions of the states to be estimated, conditioned by available data (information).

an important task by itself. In that regard, the MHT has maintained a unique and important realm within the MTT universe. The evolution of various MHT and MHT-related MTT algorithms over the last 40 years was extensively and comprehensively described in [8], and will not be repeated in this paper. It is not the objective of this paper to describe and compare various MHT algorithms, or to discuss related implementation issues, or to present yet another new algorithm. Instead, our objective is to present three different mathematical formalisms, any one of which provides a solid theoretical foundation to support MHT concept and algorithm developments.

The three formalisms are 1) *random finite sequence* (RFSeq) formalism, 2) *finite point process* (FPP) formalism, and 3) *random finite set* (RFSet) formalism. These three are seemingly quite distinct from each other on the surface, but essentially equivalent to each other in a specific sense, as we discuss in this paper. We will define MHT problem in each formalism, with precise mathematical definitions to commonly used terms that have been often loosely defined, such as “originate from,” “associated with,” “assigned to,” “tracks,” “hypotheses,” etc. We hope that, showing the uses of these three formalisms, side by side, we will be able to present a clear and precise picture of the past, and the potential future MHT developments. An earlier version of this paper was presented in [9], to which we added some analyses on specific consequences of commonly used assumptions, and our perspectives on relations of a selected set of recently developed RFSet-based MTT algorithms to MHT.

The rest of the paper is organized as follows: Section II presents the three mathematical formalisms for MTT, including all the relevant mathematical concepts in algebra, topology, and probability theories. Section III introduces target and sensor models, in the three formalisms, and defines data association hypotheses, to form a standard MHT problem. Section IV discusses generation and evaluation of association hypotheses, and describes the optimal Bayesian solution to MHT problem, in each of the three formalisms, under a set of commonly used assumptions. It is followed by Section V that discusses relationship of the MHT solution of Section IV with a selected set [36]–[39] of recently developed RFSet-based MTT algorithms. We will state our concluding remarks in Section VI.

## II. THREE MATHEMATICAL FORMALISMS

We define MTT as a process of estimating the states of a generally unknown number of objects, called targets, generally changing their states over time with given stochastic dynamics, based on information collected by generally multiple sensors on regular or irregular observation schedules. As we often do, in this paper, any target is identified with its state, i.e., a point in a state space  $E$ , which we assume is a *locally compact Hausdorff space*

*satisfying the second axiom of countability* (LCHC2)<sup>7</sup> [10]. Any countable set with discrete topology, as well as any Euclidean space, is LCHC2. Let  $\mathcal{B}$  be the collection of Borel sets in  $E$ , i.e., the smallest  $\sigma$ -algebra containing all the open sets in  $E$ , and we assume that a  $\sigma$ -finite measure  $\mu$  on the measurable space  $(E, \mathcal{B})$  is given. Throughout this paper, we will maintain the measure set  $(E, \mathcal{B}, \mu)$  as the target state space. To track  $n$  targets,  $(x_1, \dots, x_n)$ , each in  $E$ , we use the state space defined as

the  $n$ th-order direct product  $E^n = \overbrace{E \times \dots \times E}^{n \text{ times}}$  with the direct product topology (inheriting LCHC2), the direct product  $\sigma$ -algebra  $\mathcal{B}_n$ , and the direct product measure  $\mu^n$ .

The measure space  $(E^n, \mathcal{B}_n, \mu^n)$  with a fixed  $n$  provides us with a natural basis for the generalization<sup>8</sup> of the *probabilistic data association* (PDA) ( $n = 1$  [12]) and the *joint PDA* (JPDA) ( $n \geq 1$  [13]) algorithms to track a fixed number  $n$  of targets, each of which has its existence established, as target state  $x_i$  within the joint state<sup>9</sup>  $(x_i)_{i=1}^n$ , and is given a unique distinct *a priori identification*  $i \in \{1, \dots, n\}$ . The main focus of this paper is, however, to present mathematical formalisms to provide a basis for tracking *targets without a priori identification* in the sense that 1) the number  $n$  of targets is generally unknown a priori and 2) given  $n$ , any particular ordering of the joint states  $(x_i)_{i=1}^n$  is arbitrary. These facts necessitate 1) considering all the possible numbers  $n$  (any non-negative integer) of targets and 2) requiring any particular joint target state probability distribution to be *permutable* or *symmetric*, which is an important aspect of this class of MTT that we are exclusively concerned with in this paper.

**Remark 1 (Notations: Finite Sequences and Finite Sets):**  $(x_i)_{i=1}^n \in E^n$  is shorthand<sup>10</sup> of  $(x_1, \dots, x_n)$ , a finite sequence in space  $E$  with length  $n$ , or an  $n$ -tuple of points in  $E$ . Sometimes, it will be necessary to use a nested expression to shorten  $((y_{11}, \dots, y_{1m_1}), \dots, (y_{K1}, \dots, y_{Km_K}))$  as  $((y_{kj})_{j=1}^{m_k})_{k=1}^K$  with double-indexed variables  $y_{kj}$ . We also use continuous index, e.g.,  $(x_t)_{t \in [t_0, \infty)} \in E^{[t_0, \infty)}$  for a function defined on time index set  $[t_0, \infty)$ . If the index set  $I$  is a finite set, by  $(x_i)_{i \in I}$ , we mean a function  $x$  defined on  $I$ , but we may also mean a sequence  $(x_{i_1}, \dots, x_{i_n})$  with an arbitrary enumeration  $(i_1, \dots, i_n)$  of set  $I$ . By  $\{x_i\}_{i=1}^n$ , we mean  $\{x_i\}_{i=1}^n = \bigcup_{i=1}^n \{x_i\}$ , which is a set of  $n$  elements if  $x_i$ 's are all distinct, where  $\{x\}$  is the singleton with only single element  $x$ .

<sup>7</sup>Also known as *locally compact Hausdorff second-countable* topological space. See Remark 2, later in this section, for more explanations on the meaning of this choice of the state space as the basis of our paper.

<sup>8</sup>See Remark 6 in Section III-C, for more comments on PDA and JPDA algorithms, and their generalizations.

<sup>9</sup>See Remark 1.

<sup>10</sup>We consciously avoided the notation such as  $(x_i)_{i=1:n}$  or  $x_{1:n}$ , in favor of  $(x_i)_{i=1}^n$ , since  $1:n$  or  $n:m$ , used as a “colon” MATLAB syntax, is also used for a one-to-many or a many-to-many relationship in database designs, while  $(x_i)_{i=1}^n$  is universally used in the mathematical literature (although  $(x_i)_{i=1}^n$  is used instead in [28]).

**Remark 2 (LCHC2):** If an LCHC2 space is a vector space, the local compactness implies a finite dimension [11, Th. 1.22, p. 17], so that we are excluding any infinite-dimensional state space in this paper. On the other hand, the countability implies being metrizable and separable (having a countable, dense subset) [10, Ch. 6, p. 241]. Non-Euclidean examples include a hybrid space (direct product of a Euclidean space (e.g., for kinematic states) and a finite set (e.g., for discrete attribute states)), an ellipsoidal surface (for surface ship tracking), other one- or two-dimensional manifolds (e.g., for targets in road networks), Lie group  $SO(3)$  (coupled with Lie algebra  $so(3)$ ), the space of unit quaternions for attitude estimation, etc. Thus, it seems to us that this LCHC2 assumption may specify a necessary mathematical sphere for us to cover for all the application domains that we, engineers, may be interested in, beyond familiar Euclidean spaces. On the other hand, we understand that this LCHC2 assumption allows us to almost “freely” use familiar notions of conditional probability distributions, densities, Bayes rules, stochastic processes, etc., without fear of any mathematical pathology.

#### A. RFSeq Formalism

Randomness of the number  $n$  of targets forces us to consider all the spaces  $E^n$ , for  $n = 0, 1, 2, \dots$ , together, as the direct-sum space<sup>11</sup>  $\bigcup_{n=0}^{\infty} E^n$ , using the standard convention  $E^0 = \{\theta\}$  with the symbol<sup>12</sup>  $\theta$  for the sequence of the zero length, signifying “nothing,” or in our case “no target.” Algebraically,  $\bigcup_{n=0}^{\infty} E^n$  is the *free monoid* (FM) generated by  $E$  (as the set of its alphabets [14]<sup>13</sup>), with the concatenation operator  $*$  as an associative binary operator, defined by  $(x_i)_{i=1}^n = (x_i)_{i=1}^{n'} * (x_i)_{i=n'+1}^n$  for any  $0 \leq n' \leq n$  and any  $(x_i)_{i=1}^n \in E^n$  with the identity element  $\theta$ . Topologically,  $\bigcup_{n=0}^{\infty} E^n$  is also an LCHC2 with the direct-sum topology, which induces the direct-sum  $\sigma$ -algebra  $\bigcup_{n=0}^{\infty} \mathcal{B}_n$ , where each  $\mathcal{B}_n$  is  $\sigma$ -algebra of Borel sets in  $E^n$ , which allows the direct-sum measure  $\sum_{n=0}^{\infty} \mu^n$  on it.

Then, we can define an RFSeq as a random element  $X$  on the measurable space  $(\bigcup_{n=0}^{\infty} E^n, \bigcup_{n=0}^{\infty} \mathcal{B}_n)$ . Although, in general, we may not know a priori how many targets exist or we have to track, the number  $n$  of all the targets (at least potentially to be detected) is always *finite*, but often with no known a priori upper limit. For each  $n = 0, 1, 2, \dots$ , let  $p_n$  be the probability of the number<sup>14</sup> of targets being  $n$ , and given any  $n$ , let the joint

<sup>11</sup>We assume  $E \neq \emptyset$  so that  $E^n \neq \emptyset$  for any  $n$ , yet we have  $E^n \cap E^{n'} = \emptyset$  for any  $n \neq n'$ .

<sup>12</sup> $\theta \notin E$  ( $E^0 = \{\theta\}$ ) is used as a special symbol (for the empty sequence) throughout this paper. It is also considered as a function whose domain, image (range or codomain), and graph are all the empty set.

<sup>13</sup>A semigroup is a nonempty set with an associative binary operator. A monoid is a semigroup with an identity (unit) element.

<sup>14</sup>We generally assume that the number  $n$  of targets is constant, for the reasons explained by Remark 5 in Section III-A.

probability distribution of the  $n$ -tuple of target states,  $(x_i)_{i=1}^n \in E^n$ , be  $F^{(n)}$ , called the  *$n$ th-order probability distribution* ( $n$ -PDist), so that we can model targets, as a whole, by an RFSeq  $X$ , with<sup>15</sup>  $F^{(n)}(B) = \text{Prob}\{X \in B | \ell(X) = n\}$  for each  $n$  and for each  $B \in \mathcal{B}_n$ .

Our assumption that the targets are without a priori identification is translated into the assumption that, for each  $n$ ,  $F^{(n)}$  is *permutable*,<sup>16</sup> in the sense  $F^{(n)}(B) = F^{(n)}(\pi_a^{(n)}(B))$  for every  $B \in \mathcal{B}_n$  and every  $a \in A_n$ , where  $A_n$  is the set of all the permutations on  $\{1, \dots, n\}$ , and  $\pi_a^{(n)}((x_i)_{i=1}^n) \stackrel{\text{def}}{=} (x_{a(i)})_{i=1}^n$  for any  $(x_i)_{i=1}^n \in E^n$  and any  $a \in A_n$ . If each permutable probability measure  $F^{(n)}$  is absolutely continuous with respect to the product measure  $\mu^n$ , its Radon–Nikodym derivative  $f^{(n)}$ , called the  *$n$ th-order probability density* ( $n$ -PD), is also permutable, in the sense that  $f^{(n)}(\pi_a^{(n)}(x)) = f^{(n)}(x)$  for all  $x \in E^n$ , for any  $a \in A_n$ .

#### B. FPP Formalism

In [15, Ch. 5, p. 111], an RFSeq  $(x_i)_{i=1}^n \in E^n$  with  $(p_n, F^{(n)})_{n=0}^{\infty}$  is called an FPP if each  $n$ -PDist  $F^{(n)}$  is permutable, and is characterized by a sequence  $(\mathcal{J}^{(n)})_{n=0}^{\infty}$  of measures, each of which,  $\mathcal{J}^{(n)}$ , is a finite measure on  $(E^n, \mathcal{B}_n)$ , defined by  $\mathcal{J}^{(n)}(B) = n! p_n F^{(n)}(B)$  for each  $B \in \mathcal{B}_n$ , called the  *$n$ th-order Janossy measure* ( $n$ -JM).<sup>17</sup> If  $n$ -JM<sup>18</sup>  $\mathcal{J}^{(n)}$  is absolutely continuous with respect to the product measure  $\mu^n$ , its Radon–Nikodym derivative  $J^{(n)}$  is called the  *$n$ th-order Janossy density* ( $n$ -JD), which we can write as  $J^{(n)}(x) = n! p_n f^{(n)}(x)$  for every  $x \in E^n$ , with  $n$ -PD  $f^{(n)}$  of each  $n$ -PDist  $F^{(n)}$ . Obviously, every  $n$ -JM  $\mathcal{J}^{(n)}$  is permutable, and so is any  $n$ -JD  $J^{(n)}$  if it exists.

In this paper, as well as in [9] and [16], however, we present an alternative but equivalent FPP formalism: For each  $n$  and each  $x \in E^n$ , let the equivalence class in  $E^n$ , obtained by ignoring the ordering of  $x = (x_i)_{i=1}^n$ , be  $[x]$ , i.e.,  $[x] \stackrel{\text{def}}{=} \{\pi_a^{(n)}(x) | a \in A_n\}$  with  $\pi_a^{(n)}$  and  $A_n$ , as defined earlier. For each  $n$ , let us *symbolically* denote  $E^n/n! = \{[x] | x \in E^n\}$ , using “ $n!$ ” only as a symbol in place of equivalence classes “[ $\cdot$ ]” or relation “ $\sim$ .”

<sup>15</sup>For any  $x \in \bigcup_{n=0}^{\infty} E^n$ , by  $\ell(x)$  we mean the length of finite sequence  $x$  in  $E$ , i.e.,  $\ell(x) = n \Leftrightarrow x \in E^n$ , and  $\ell(\theta) = 0$ .

<sup>16</sup>Synonymous to *symmetric* (permutation-symmetric), *exchangeable*, *interchangeable*, etc. See Remark 3.

<sup>17</sup>According to [15], the term *Janossy measure* originated from [17] that references [18]. It is indicated [15, p. 124] that the constant  $n!$  in its definition, as it distinctly appears in (1)–(4) also, is included to be *advantageous in simplifying combinatorial formulae*, so that, in a sense, this constant  $n!$  uniquely identifies the  $n$ -JM, the  $n$ -JD, and the JMD (introduced later), distinguishing themselves from other concepts.

<sup>18</sup>In this paper, we use superscripts ( $n$ ) for  $n$ -PDist  $F^{(n)}$ ,  $n$ -PD  $f^{(n)}$ ,  $n$ -JM  $\mathcal{J}^{(n)}$ , and  $n$ -JD  $J^{(n)}$ , to signify the fact that they are applied to the  $n$ th-order product space  $E^n$ , although, customarily, subscripts are used instead as in  $F_n, f_n, \mathcal{J}_n$ , and  $J_n$ .

$E^n/n!$  is a quotient space induced by the quotient map<sup>19</sup>  $\varphi_n : x \mapsto [x]$  for each  $n$ . We may call  $[(x_i)_{i=1}^n]$  an *un-ordered  $n$ -tuple*, while  $(x_i)_{i=1}^n$  is an *ordered  $n$ -tuple*.

Algebraically, we may call  $\bigcup_{n=0}^{\infty} E^n/n!$  the *free commutative monoid* (FCM)<sup>20</sup> generated by  $E$  with the commutative operation  $*$  defined by  $[x] * [x'] = [x * x']$  for every  $(x, x') \in E^n \times E^{n'}$ , and the identity element  $[\theta] = \{\theta\}$ . Topologically, each  $E^n/n!$  is a quotient topological space. Since each coordinate permutation  $\pi_a^{(n)}$  is a homeomorphism (and hence a continuous open map), every open set in  $E^n/n!$  can be written as the image  $\varphi_n(B)$  of an open set  $B$  in  $E^n$ , and hence each  $E^n/n!$  is LCHC2, and so is their direct sum  $\bigcup_{n=0}^{\infty} E^n/n!$ , with the  $\sigma$ -algebra  $\bigcup_{n=0}^{\infty} \mathcal{B}_n/n!$  of Borel sets in it. We may consider  $\bigcup_{n=0}^{\infty} E^n/n!$  as the quotient space through the map  $\varphi : \bigcup_{n=0}^{\infty} E^n \rightarrow \bigcup_{n=0}^{\infty} E^n/n!$  defined by  $\varphi(x) = \varphi_n(x)$  for each  $x \in E^n$  ( $n > 0$ ), and  $\varphi(\theta) = \varphi_0(\theta) = [\theta] = \{\theta\}$ .

Finally, an FPP can be defined as a random element  $X$  on a measurable space  $(\bigcup_{n=0}^{\infty} E^n/n!, \bigcup_{n=0}^{\infty} \mathcal{B}_n/n!)$ , with PDist  $\Phi$  such that

$$\begin{aligned} \Phi\left(\bigcup_{n=0}^{\infty} \varphi(B_n)\right) &= \text{Prob}\left\{X \in \bigcup_{n=0}^{\infty} \varphi(B_n)\right\} \\ &= \sum_{n=0}^{\infty} p_n F^{(n)}(\varphi_n^{-1}(\varphi_n(B_n))) \\ &= \sum_{n=0}^{\infty} \frac{1}{n!} \mathcal{J}^{(n)}(\varphi_n^{-1}(\varphi_n(B_n))) \end{aligned} \quad (1)$$

for any  $(B_n)_{n=0}^{\infty} \in \prod_{n=0}^{\infty} \mathcal{B}_n$ . Since each coordinate permutation  $\pi_a^{(n)}$  is measurable, every measurable set  $\mathbf{B} \in \bigcup_{n=0}^{\infty} \mathcal{B}_n/n!$  in  $\bigcup_{n=0}^{\infty} E^n/n!$  can be expressed as  $\bigcup_{n=0}^{\infty} \varphi(B_n)$  with some  $(B_n)_{n=0}^{\infty} \in \prod_{n=0}^{\infty} \mathcal{B}_n$ . The first equality of (1), therefore, simply states the definition of PDist  $\Phi$  of a random element  $X$ , i.e.,  $\Phi(\mathbf{B}) = \text{Prob}\{X \in \mathbf{B}\}$  for any  $\mathbf{B} \in \bigcup_{n=0}^{\infty} \mathcal{B}_n/n!$ . The second equality of (1) means that, given PDist  $\Phi$  of FPP  $X$ , there exists a series  $(p_n, F^{(n)})_{n=0}^{\infty}$  of probabilities and permutable  $n$ -PDists such that<sup>21</sup>  $p_n = \Phi(E^n/n!) = \text{Prob}\{\ell(X) = n\}$  for every  $n$ , and  $p_n F^{(n)}(\varphi_n^{-1}(B_n)) = \Phi(B_n)$  for every  $B_n \in \mathcal{B}_n/n!$ . It also implies that PDist  $\Phi$  is uniquely defined by a PDist  $(p_n)_{n=0}^{\infty}$  and any permutable  $n$ -PDists  $F^{(n)}$  for each  $n$ . The third equality is nothing but the definition of each  $n$ -JM. For each  $n$  and each measurable set  $B_n = \varphi_n(B_n)$  in  $E^n/n!$ , event  $\{X \in B_n\}$  can be viewed as the event  $\bigcup_{a \in A_n} \{x \in \varphi_n^{-1}(B_n)\}$ , where  $x$  is an arbitrary enumeration of  $X$ . We should note  $\varphi_n^{-1}(\varphi_n(B_n)) = \bigcup_{a \in A_n} \pi_a^{(n)}(B_n)$ , which is the set of all the enumerations of equivalence classes in  $B_n = \varphi_n(B_n)$ .

Using the collection  $(E^n, \mathcal{B}_n, \mu^n)_{n=0}^{\infty}$  of the measure spaces, we can define a positive linear functional

<sup>19</sup>Also known as identification map, natural map, canonical surjection map, canonical projection map, etc. In topological algebra [19],  $E^n/n!$  is called the  $n$ th-order symmetric product of  $E$ ,  $\text{SP}^n(E)$ .

<sup>20</sup>Cf. [47, Sec. I.6.3, p. 16], for definition of *free commutative semigroup*, which becomes FCM when given an identity element.

<sup>21</sup>For any  $[x] \in \bigcup_{n=0}^{\infty} E^n/n!$ , the length  $\ell(x)$  of any element in the equivalent class  $[x]$  is the same, so that we let  $\ell([x]) = \ell(x)$ . We have  $\Phi(\bigcup_{n=0}^{\infty} E^n/n!) = \sum_{n=0}^{\infty} \Phi(E^n/n!) = \sum_{n=0}^{\infty} p_n = 1$ .

$\mathcal{L}$ , defined on a set of bounded measurable functionals  $\psi$ , and a measure  $\mathcal{M}$ , both on measurable set  $(\bigcup_{n=0}^{\infty} E^n/n!, \bigcup_{n=0}^{\infty} \mathcal{B}_n/n!)$ , such that we have<sup>22</sup>

$$\begin{aligned} \mathcal{L}(\psi) &= \int_{\bigcup_{n=0}^{\infty} E^n/n!} \psi(X) \mathcal{M}(dX) \\ &= \sum_{n=0}^{\infty} \frac{1}{n!} \int_{E^n} \psi(\varphi(x)) \mu^n(dx), \end{aligned} \quad (2)$$

where  $\mathcal{M}(B_n) = \mu^n(\varphi_n^{-1}(B_n))/n!$  for every  $B_n \in \mathcal{B}_n/n!$ , for each  $n$ . We may call the measure space  $(\bigcup_{n=0}^{\infty} E^n/n!, \bigcup_{n=0}^{\infty} \mathcal{B}_n/n!, \mathcal{M})$ , derived from the state measure space  $(E, \mathcal{B}, \mu)$  in this way, the *quotient measure space* (QMS).

It follows from (1) and (2) that, if each  $n$ -JM  $\mathcal{J}^{(n)}$  of (1) has  $n$ -JD  $J^{(n)}$ , then PDist  $\Phi$  has the density  $\phi$ , i.e., the Radon–Nikodym derivative of  $\Phi$ , with respect to the measure  $\mathcal{M}$ , which we call the *Janossy–Mahler density* (JMD), defined as  $\phi(\varphi_n(x)) = J_n(x)$  for every  $x \in E^n$ , for each  $n$ , such that

$$\begin{aligned} \Phi(\varphi(\bigcup_{n=0}^{\infty} B_n)) &= \int_{\varphi(\bigcup_{n=0}^{\infty} B_n)} \phi(X) \mathcal{M}(dX) \\ &= \sum_{n=0}^{\infty} \frac{1}{n!} \int_{\varphi_n^{-1}(\varphi_n(B_n))} \phi(\varphi_n(x)) \mu^n(dx) \end{aligned} \quad (3)$$

for any  $(B_n)_{n=0}^{\infty} \in \prod_{n=0}^{\infty} \mathcal{B}_n$ .

**Remark 3 (FM, FCM, FPP, and JMD):** To call a random element on FM<sup>23</sup> an RFSeq, and a random element on FCM an FPP, is our own “invention,” which had most probably not seen before our preliminary paper [9] (or its predecessor [16]) was published. The introduction of FM and FCM (or its variation), however, appeared in [15] and [23]. In [15, p. 129], FM  $\bigcup_{n=0}^{\infty} E^n$  is called the *canonical probability space*, and an FPP as a random element in the quotient space  $\bigcup_{n=0}^{\infty} E^n/n!$  is also suggested. In [23], FM  $\bigcup_{n=0}^{\infty} E^n$  is called the *population state space*, and a version of FCM,  $\bigcup_{n=0}^{\infty} E^n/n!$ , the *symmetric population state space*. Furthermore, in [23], what we call an FPP was called a *symmetric point process*, while what we call an RFSeq was called simply a *point process*,<sup>24</sup> reflecting the distinction caused by the “commutativity” or “permutability,”<sup>25</sup> or lack of it.

Both in [15, Ch. 5, p. 111] and [23], we may say that an FPP is defined through a series of  $n$ -PDist or  $n$ -JM,

<sup>22</sup>We use the convention that  $\int_{E^0} q(\xi) \mu^0(\xi) = q(\theta) \mu^0(E^0) = q(\theta)$  for any functional  $q$  on  $(E^0, \mathcal{B}_0) = (E^0, \{\emptyset, E^0\}) = (\{\theta\}, \{\emptyset, \{\theta\}\})$ .

<sup>23</sup>By replacing the target indices by the discrete time indices, an FM can be used as a mathematical model for a discrete-time dynamical process with a variable *end-of-the-process time*, as shown in [21].

<sup>24</sup>According to [23], the term “point process” is attributed to [24].

<sup>25</sup>In [23], the permutability is treated as synonymous to “indistinguishability,” which, in our opinion, is misleading to a degree, because, for example, two targets, as realizations of two random points, which do not share the same state, can always be “distinguished,” even when the distributions are “identical” and “independent.” We would prefer that the distinction is considered as “targets with and without *a priori* identifications,” rather than “distinguishability” and “indistinguishability.”

rather than a random element itself. A traditional definition of an FPP is, however, as a *random counting measure*<sup>26</sup> [22, Def. 1.1, p. 4], which can represent possibly countably many points. In our MTT applications, however, we do not need to consider any set of countably many points, and therefore, we may say that our definition of FPP, without ever considering a random measure, is justified.<sup>27</sup> A counting measure representation  $\mathcal{N}$  of an FPP  $X = [(x_i)_{i=1}^n]$ , as a random measure on  $(E, \mathcal{B})$ , can be defined as  $\mathcal{N}(B) = \sum_{i=1}^n \mathbb{I}(x_i; B)$  for each  $B \in \mathcal{B}$ , with an arbitrary enumeration  $(x_i)_{i=1}^n$  of FPP  $X$ , where  $\mathbb{I}$  is the generic indicator function defined as  $\mathbb{I}(\xi; A) = 1$  if  $\xi \in A$  and zero otherwise for any set  $A$ .

We call the probability density  $\phi$  that appears in (3) in our FPP formalism, as well as in the RFSet formalism described later in this section, the JMD, because of 1) its obvious relation to the Janossy densities  $n$ -JDs,  $(J^{(n)})_{n=0}^\infty$ , through  $\phi(\varphi(x)) = J^{(n)}(x)$  for any  $x \in E^n$ , and 2) our understanding that the PD  $\phi$  was first introduced by Dr. R. P. S. Mahler as a single function, as opposed to a series  $(J^{(n)})_{n=0}^\infty$  of functions, in his *finite set statistics* (FISST) formalism [25]–[27]. The JMD  $\phi$  is called the *multiobject density function* in [25, Sec. 11.3.3, p. 360] and [26, Sec. 3.2.4, p. 62], and the *global probability density function* in [27, Sec. 4.3.3, p. 162].

### C. RFSet Formalism

For each  $n > 0$ , let  $\mathcal{F}_n(E) = \{X \subseteq E \mid 0 < \#(X) \leq n\}$  and  $\tilde{\mathcal{F}}_n(E) = \{X \subseteq E \mid \#(X) = n\}$ . Then, with  $\mathcal{F}_0 = \tilde{\mathcal{F}}_0 = \{\emptyset\}$ ,  $\mathcal{F}(E) = \bigcup_{n=0}^\infty \mathcal{F}_n(E) = \bigcup_{n=0}^\infty \tilde{\mathcal{F}}_n(E)$  is the collection of all the finite sets in the state space  $E$ . Algebraically, we may call  $\mathcal{F}(E)$  the *free idempotent commutative monoid* (FICM) with the set-theoretic union<sup>28</sup> as the binary operator on it. For each  $n > 0$ , redefine the quotient map  $\varphi_n$  as  $\varphi_n : E^n \rightarrow \mathcal{F}_n(E)$  with  $\varphi_n((x_i)_{i=1}^n) = \{x_i\}_{i=1}^n$ . It makes  $\mathcal{F}_n(E)$  a quotient topological space that is an LCHC2 with its open sets as the collections of the images  $\varphi_n(B)$  of all the open sets  $B$  in  $E^n$ .  $\mathcal{F}(E)$  is also LCHC2 as the quotient space induced by the redefined map  $\varphi : \bigcup_{n=0}^\infty E^n \rightarrow \mathcal{F}(E)$  with  $\varphi(x) = \varphi_n(x)$  for all  $x \in E^n$  and  $\varphi(\emptyset) = \varphi_0(\emptyset) = \emptyset$ .

An RFSet  $X$  can then be defined as a random element on measurable set  $(\mathcal{F}(E), \mathcal{B}(\mathcal{B}))$ , where  $\mathcal{B}(\mathcal{B})$  is the  $\sigma$ -algebra of Borel sets in quotient topological

<sup>26</sup>A counting measure  $\mu$  on any measurable space  $(E, \mathcal{B})$  is an integer-valued functional defined by  $\mu(B) = \#(B)$  for each  $B \in \mathcal{B}$ . By  $\#(A)$ , we mean the cardinality of (the number of elements in) any set  $A$ , throughout this paper.

<sup>27</sup>In [15, p. 131], it is stated: “The main difficulty with this (Moyal’s) approach from our point of view is that it does not extend readily to random measures, which require for their own sake and for applications in later chapter.”

<sup>28</sup>The union operator  $\cup$  on  $\mathcal{F}(E)$  is associative and commutative with the empty set as the unit element.  $\mathcal{F}(E)$  is also idempotent, i.e., every  $X \in \mathcal{F}(E)$  is an idempotent, because  $X * X = X \cup X = X$ . Cf. [47, Sec. I.6.3, p. 16], for definition of *free idempotent commutative semigroup*, which becomes FICM when given an identity element.

space  $\mathcal{F}(E)$ . As the PDist  $\Phi$  of RFSet  $X$ , (1) holds for any  $(B_n)_{n=0}^\infty \in \prod_{n=0}^\infty \mathcal{B}_n$ , with the  $n$ -PDist  $F^{(n)}$  (and  $n$ -JM  $\mathcal{J}^{(n)} = n!p_n F^{(n)}$ ) and the redefined quotient map  $\varphi$ . Exactly in parallel to FPP formalism, through the redefined quotient map  $\varphi$ , we can redefine  $\mathcal{L}$  as the positive linear bounded functional on the space of bounded measurable functionals  $\psi$  on the measurable space  $(\mathcal{F}(E), \mathcal{B}(\mathcal{B}))$ , and the measure  $\mathcal{M}$  on the measurable space  $(\mathcal{F}(E), \mathcal{B}(\mathcal{B}))$ , as (2), and the JMD  $\phi$  with respect to the redefined measure space  $(\mathcal{F}(E), \mathcal{B}(\mathcal{B}), \mathcal{M})$ , as (3).

The *idempotency* of the FICM  $\mathcal{F}(E)$ , however, poses some peculiar problems: For example, a multidimensional point,  $(x_i)_{i=1}^n$  in  $E^n$  with  $n > 1$ , is mapped into a single point in  $\mathcal{F}(E)$ , when its elements are all identical, i.e.,  $x_1 = \dots = x_n$ . One way to avoid this peculiarity is to “ignore” such coincidences. Namely, we may assume that the set  $D_n \stackrel{\text{def}}{=} \{(x_i)_{i=1}^n \in E^n \mid x_i = x_{i'} \text{ for some } i \neq i'\}$  of  $n$ -tuples with any repeated elements, which we call the *diagonal set in  $E^n$* , has the zero product measure, i.e.,  $\mu^n(D_n) = 0$ . We can then define the JMD  $\phi$  in RFSet formalism by  $\phi(\varphi((x_i)_{i=1}^n)) = \phi(\{x_i\}_{i=1}^n) = J^{(n)}((x_i)_{i=1}^n)$  for every  $(x_i)_{i=1}^n \in E^n$ , for each  $n$ .

However, in case where the state space  $E$  is countable with discrete topology<sup>29</sup> and counting measure  $\mu$ ,  $\mu^2(D_2) = 0$  implies  $\mu(E) = 0$ , which is obviously not desirable. To remedy the situation, we need to modify (2) and (3) slightly as

$$\left\{ \begin{array}{l} \mathcal{L}(\psi) = \int_{\mathcal{F}(E)} \psi(X) \mathcal{M}(dX) \\ = \sum_{n=0}^{\infty} \frac{1}{n!} \int_{E^n} \psi(\varphi(x)) \tilde{\mu}_n(dx) \\ \Phi(\varphi(\bigcup_{n=0}^{\infty} B_n)) = \int_{\varphi(\bigcup_{n=0}^{\infty} B_n)} \phi(X) \mathcal{M}(dX) \\ = \sum_{n=0}^{\infty} \frac{1}{n!} \int_{\varphi^{-1}(\varphi(B_n))} \phi(\varphi(x)) \tilde{\mu}_n(dx) \end{array} \right. \quad (4)$$

using the modified measure,<sup>30</sup>  $\tilde{\mu}_n(B) = \mu^n(B \setminus D_n)$  for every  $B \in \mathcal{B}_n$ , for each  $n$ , to make  $\tilde{\mu}_n(D_n) = 0$  without affecting any product measure  $\mu^n$ , with  $\mathcal{M}(\varphi(B)) = \tilde{\mu}_n(\varphi^{-1}(\varphi(B)))/n!$  for any  $B \in \mathcal{B}_n$ , and with the JMD in RFSet formalism by  $\phi(\varphi((x_i)_{i=1}^n)) = \phi(\{x_i\}_{i=1}^n) = J^{(n)}((x_i)_{i=1}^n)$  for every  $(x_i)_{i=1}^n \in E^n$ . With this modification, each component  $\tilde{\mathcal{F}}_n$  of FICM  $\mathcal{F}(E)$  as the direct sum  $\mathcal{F}(E) = \bigcup_{n=0}^\infty \tilde{\mathcal{F}}_n(E)$  becomes the image of the quotient map  $\varphi_n$  in the  $\tilde{\mu}_n$ -a.e. sense. In the rest of this paper, whenever the RFSet formalism is used, we assume we are using the modified measures  $\tilde{\mu}_n$ ’s, as in (4).

When  $E$  is countable with the discrete topology and the counting measure  $\mu$ , the measure  $\mathcal{M}$  defined in (4), using  $\tilde{\mu}_n$ ’s, becomes a counting measure on  $(\mathcal{F}(E), \mathcal{B}(\mathcal{B}))$ , where  $\mathcal{B}(\mathcal{B})$  becomes the power set of a

<sup>29</sup>Namely, every subset  $B$  of  $E$  is an open set, and hence,  $\sigma$ -algebra of Borel sets  $\mathcal{B}$  is the power set of  $E$ .

<sup>30</sup>By “ $\setminus$ ” we mean the set-theoretic subtraction operator, i.e.,  $A \setminus B = \{a \in A \mid a \notin B\}$ .

countable set<sup>31</sup>  $\mathcal{F}(E)$ , so that the JMD  $\phi$ , which is the Radon–Nikodym derivative of the probability distribution  $\Phi$  with respect the counting measure  $\mathcal{M}$ , becomes the probability mass function (PMF). In such a case, for example, when we define data association, as an RFSet in Section III-C, we will use the generic symbol<sup>32</sup> “ $P$ ” (instead of  $\phi$ ) for such JMD that is nothing but a PMF.

We call the measure space  $(\mathcal{F}(E), \mathbb{B}(\mathcal{B}), \mathcal{M})$  derived from the state measure space  $(E, \mathcal{B}, \mu)$  for RFSet formalism the QMS. We also call  $(\bigcup_{n=0}^{\infty} E^n/n!, \bigcup_{n=0}^{\infty} \mathcal{B}_n/n!, \mathcal{M})$  for FPP formalism QMS. If disambiguation is necessary, we will use FCM-QMS or FICM-QMS.

**Remark 4 (QMS):** In Section II-B and II-C, we defined the FCM-QMS and FICM-QMS for FPP and RFSet formalisms, respectively, through the quotient map  $\varphi$ , with which we defined the quotient topology and the *quotient measure*  $\mathcal{M}$ . An alternative, but an equivalent, way to construct these measure spaces may be possible directly from the linear functionals  $\mathcal{L}$ , defined in (2) or (4), first applied to an appropriate small class of functionals  $\psi$ , and then appropriately extended to construct measurable sets and measures, as shown in [28, Ch. 16, p. 419] and [29]. In [25]–[27], what we have defined as RFSet formalism in this paper is called FISST formalism, in which the integral in (4) is called the *set integral*, as its core concept, as we understand. We may interpret the FISST formalism as the one in which the set integral plays this role to construct the appropriate measure space  $(\mathcal{F}(E), \mathbb{B}(\mathcal{B}), \mathcal{M})$ .

As mentioned in [25, Appendix F, p. 711], FICM  $\mathcal{F}(E)$  can be topologized by the relative (subspace) topology as the subset of the space  $\mathcal{C}(E)$  of the closed sets in  $E$ , with *Fell–Matheron topology*<sup>33</sup> [40, p. 3; 45, p. 398]. Since the quotient map  $\varphi$  is continuous in this topology [20, Prop. 2.4, p. 156], the quotient topology (with which we have introduced RFSet formalism) is stronger<sup>34</sup> than the Fell–Matheron topology. The FISST formalism established in [25]–[27] motivated our definition of an FPP as a random element taking values in FCM  $\bigcup_{n=0}^{\infty} E^n/n!$ .

In summary, among the three formalisms, the equivalence between RFSeq and FPP is rather obvious. Instead of calling an RFSeq  $(x_i)_{i=1}^n$  with permutable  $n$ -PDists an FPP, we call a random element on FCM  $\bigcup_{n=0}^{\infty} E^n/n!$  an FPP, forcing the permutability on the state space algebraic structure rather than on the  $n$ -PDists. By doing so,

<sup>31</sup>The countability of  $E$  implies the countability of  $\mathcal{F}(E)$  under the axiom of countable choice.

<sup>32</sup>As a general “rule,” we use the symbols,  $F$  and  $f$ , for PDist and PD in  $E$  ( $F^{(n)}$  and  $f^{(n)}$  for  $E^n$ ),  $P$  and  $p$  for the probability or the PMF for the discrete, or density function of random elements of mixed nature, and  $\phi$  for the JMD for FPP or RFSet formalism.

<sup>33</sup>Also known as hit-or-miss topology. With this topology,  $\mathcal{C}(E)$  is a compact Hausdorff space satisfying the second axiom of countability [40, Th. 1-2-1, p. 3], and  $\mathcal{F}(E)$  is dense in  $\mathcal{C}(E)$  [40, Cor. 2, p. 7].

<sup>34</sup>Hence, our introductions of the linear functional  $\mathcal{L}$  and the measure  $\mathcal{M}$  are consistent with the Fell–Matheron topology.

we put an FPP and an RFSet into almost equivalence, with the same JMD concept. The difference between an FPP and an RFSet is, however, that the former allows *repeated elements*, while the latter does not. An FPP that does not allow any repeated elements is called a *simple* FPP, and it is shown in [15, Prop. 5.4.V, p. 138], the necessary and the sufficient condition for the “simpleness” is  $\mathcal{J}^{(n)}(D_n) = 0$ ; i.e., the  $n$ -JM of the diagonal set  $D_n$  is zero. In this sense, we may say an RFSet is just a simple FPP.

We should note that the target state space  $E$  may be a finite set itself, e.g., when the original state space is approximated by a set of small rectangular cells, as in the target model used in [30]. In that case, it would be *unreasonable* to prohibit any two targets from occupying a single state, so that RFSet formalism becomes inadequate,<sup>35</sup> while FPP formalism may become a perfect alternative. This *idempotency* peculiarity becomes apparent also when we consider the union of two independent RFSets, as we see below.

#### D. Concatenation, Union, Superposition, and Convolution

As a foundation for MHT, the binary operation on FM, FCM, or FICM, i.e., concatenation or unionization, of random elements, plays crucial roles. Let  $X_1$  and  $X_2$  be two independent RFSets, i.e., two independent random elements in  $(\mathcal{F}(E), \mathbb{B}(\mathcal{B}), \mathcal{M})$ , with JMDs  $\phi_1$  and  $\phi_2$ , respectively. Then, as described in [25, Sec. 11.5.3, p. 385], JMD  $\phi$  of the union  $X = X_1 \cup X_2$  can be written as

$$\phi(X) = \sum_{X_1 \subseteq X} \phi_1(X_1)\phi_2(X \setminus X_1), \quad (5)$$

which holds true only when each product measure  $\tilde{\mu}_{n_1} \times \tilde{\mu}_{n_2}$  of the modified measures satisfies<sup>36</sup>  $(\tilde{\mu}_{n_1} \times \tilde{\mu}_{n_2})(D_{n_1+n_2}) = 0$ . This condition, guaranteeing that  $X_1 \cap X_2 = \emptyset$  with probability 1, is satisfied if  $\mu^n(D_n) = 0$ , e.g., when target state space  $E$  has a *continuous* component such as a Euclidean component.

In FPP formalism, which lacks the idempotency, for any two independent FPPs,  $[(x_{1i})_{i=1}^{n_1}]$  and  $[(x_{2i})_{i=1}^{n_2}]$ , with JMDs  $\phi_1$  and  $\phi_2$ , respectively, the JMD  $\phi$  of the concatenation  $[(x_{1i})_{i=1}^{n_1}] * [(x_{2i})_{i=1}^{n_2}] = [(x_{1i})_{i=1}^{n_1} * (x_{2i})_{i=1}^{n_2}]$  can always be written as

$$\phi([(x_i)_{i=1}^n]) = \sum_{I \subseteq \{1, \dots, n\}} \phi_1([(x_i)_{i \in I}])\phi_2([(x_i)_{i \in \{1, \dots, n\} \setminus I}]), \quad (6)$$

which is translated into the case where the  $n$ -JD of the two RFSeqs with permutable  $n$ -PDists, with  $n$ -JDs,

<sup>35</sup>In [25, Appendix E, p. 705], it is indicated that the *idempotency* issues should be resolved by the concept of *multisets*.

<sup>36</sup>In Section II-C, we defined  $\tilde{\mu}_n(B) = \mu^n(B \setminus D_n)$ , which does not necessarily imply  $(\tilde{\mu}_{n_1} \times \tilde{\mu}_{n_2})(D_{n_1+n_2}) = 0$ , because  $\tilde{\mu}_{n_1+n_2} = \tilde{\mu}_{n_1} \times \tilde{\mu}_{n_2}$  does not hold necessarily.

$$(J_1^{(n_1)})_{n_1=0}^\infty \text{ and } (J_2^{(n_2)})_{n_2=0}^\infty, \text{ is } (J^{(n)})_{n=0}^\infty, \text{ as}$$

$$J^{(n)}((x_i)_{i=1}^n) = \sum_{I \subseteq \{1, \dots, n\}} J_1^{(\#(I))}((x_i)_{i \in I}) J_2^{(n-\#(I))}((x_i)_{i \in \{1, \dots, n\} \setminus I}). \quad (7)$$

For the rest of this paper, we will denote the right-hand side of (5) for RFSet formalism, or of (6) for FPP formalism, by the *convolution*  $\phi_1 \otimes \phi_2$  of two JMDs  $\phi_1$  and  $\phi_2$ . This convolution can be extended to  $N$  independent RFSets or FPPs as  $\phi_1 \otimes \dots \otimes \phi_N$ , in an obvious way. When two independent FPPs are represented by random measures  $\mathcal{N}_1$  and  $\mathcal{N}_2$ , the random measure representation  $\mathcal{N}$  of the concatenation (the union) is simply the sum  $\mathcal{N} = \mathcal{N}_1 + \mathcal{N}_2$ , which is called the *superposition* of two FPPs with  $\mathcal{N}_1$  and  $\mathcal{N}_2$  [42, Ch. 5.1, p. 152].

### III. TARGET AND SENSOR MODELS, AND DATA ASSOCIATION HYPOTHESES

Whenever the word MHT is mentioned in the context of MTT, we understand that by a ‘‘hypothesis’’ we mean a *data association hypothesis*, which is the core concept of the MHT. The ultimate goal of any MHT algorithm is to estimate the target states, in either one of the three formalisms described in the previous section, while generation, evaluation, and maintenance of association hypotheses may constitute various intermediate algorithmic steps. In some applications, however, determination of correlation or relations among the data in terms of their origins, retroactively in many cases, is of primary interests and importance. In this section, after describing a general class of target and sensor models for the rest of this paper, association hypotheses will be defined as possible realizations of an RFSet, called *data association*, or simply *association*, in a discrete space.

#### A. Target Model: Set of Stochastic Processes

Unlike almost all the target models in RFSet (FISST) formalism [25]–[27] where a set of an unknown number of targets is modeled as a stochastic process on FICM, i.e., the collection  $\mathcal{F}(E)$  of finite sets in a given target state space  $E$ , our target model assumes that

**(A1) [Target Model]:** The set of targets, as a whole, is modeled as 1) an RFSeq  $((x_i(t))_{t \in [t_0, \infty)})_{i=1}^n$ , 2) an FPP  $[((x_i(t))_{t \in [t_0, \infty)})_{i=1}^n]$ , or 3) an RFSet  $\{(x_i(t))_{t \in [t_0, \infty)}\}_{i=1}^n$ , of stochastic processes on space  $E$ , over a continuous time interval  $[t_0, \infty)$ , with the probability  $p_n = P(n)$  of the number of targets being  $n$  with a finite mean, so that, for each  $n$ , for any  $N$ -tuple,  $(s_\kappa)_{\kappa=1}^N \in [t_0, \infty)^N$ , of distinct times, 1) RFSeq  $((x_i(s_\kappa))_{\kappa=1}^N)_{i=1}^n$  has permutable  $n$ -PDist  $F^{(n)}(\cdot; (s_\kappa)_{\kappa=1}^N)$  and  $n$ -JM  $\mathcal{J}^{(n)}(\cdot; (s_\kappa)_{\kappa=1}^N)$  on  $(E^{Nn}, \mathcal{B}_{Nn}, \mu^{Nn})$  with  $n$ -PD  $f^{(n)}(\cdot; (s_\kappa)_{\kappa=1}^N)$  and  $n$ -JD  $J^{(n)}(\cdot; (s_\kappa)_{\kappa=1}^N)$ , 2) FPP  $[((x_i(s_\kappa))_{\kappa=1}^N)_{i=1}^n]$  has PDist<sup>37</sup>

<sup>37</sup>We are using the same notations for the PDist  $\Phi$ , and the JMD  $\phi$  for both the FPP and RFSet formalisms. Distinction should be clear

$\Phi(\cdot; (s_\kappa)_{\kappa=1}^N)$  on  $(\bigcup_{n=0}^\infty E^{Nn}/n!, \bigcup_{n=0}^\infty \mathcal{B}_{Nn}/n!, \mathcal{M}_N)$  with JMD  $\phi(\cdot; (s_\kappa)_{\kappa=1}^N)$ , or 3) RFSet  $\{(x_i(s_\kappa))_{\kappa=1}^N\}_{i=1}^n$  has PDist  $\Phi(\cdot; (s_\kappa)_{\kappa=1}^N)$  on  $(\mathcal{F}(E^N), \mathcal{B}(\mathcal{B}_N), \mathcal{M}_N)$  with JMD  $\phi(\cdot; (s_\kappa)_{\kappa=1}^N)$ , where  $\mathcal{M}_N$  is the measure defined by (2) or (4) (for FPP or RFSet formalism) with  $E$  replaced by  $E^N$ .

**Remark 5 (Birth–Death Target Models):** There are two significant departures of our target model from the commonly used target models: 1) Targets are modeled as an RFSeq, an FPP, or an RFSet of stochastic processes, each on the target state space  $(E, \mathcal{B}, \mu)$ , over a continuous time interval  $[t_0, \infty)$ , rather than a single stochastic process on FM  $\bigcup_{n=0}^\infty E^n$  or FCM  $\bigcup_{n=0}^\infty E^n/n!$  or FICM  $\mathcal{F}(E)$ , and 2) the (generally unknown, and hence random) number  $n$  of targets is *constant* over the entire time interval  $[t_0, \infty)$ . We contend that condition 1 is necessary to define data association hypotheses as hypotheses of the *true* association sharing the same origins, to avoid any possibility of target *identities* from *ever* being *switched* by the symmetrization as a consequence of using the FPP or the RFSet formalisms. We believe that condition 2 can be defended from a ‘‘first principle’’ point of view, as we argue in the following.

A *real* birth or death of any target occurs only under very limited circumstances, most probably in battlefield type of environments, where, e.g., missiles are launched or vehicles are destroyed. Even missiles before being launched, however, may exist as ground targets. A destroyed vehicle may be still called a damaged vehicle, or a wreckage, with its existence intact, even if it is dead. In many cases, an emergence of a persistent track is at least partly a result of sensor management, and should not be confused with a target birth,<sup>38</sup> which should be a part of a purely target behavioral model, independent of any sensor.

In most realistic situations, what we call new targets (or newly born targets) are actually those that had remained undetected (and hence existed) but were detected for the first time by a sensor that is capable of detecting them. For the implementation of MHT algorithms, therefore, the issue becomes how to calculate the track initiation likelihood, or the newly detected target likelihood, as discussed in [35] as implementation of track-oriented MHT, or in [36] as a part of overall algorithm complexity as discussed in connection with the RFSet-based algorithms. When hypotheses are evaluated recursively, as discussed in Section III-C, the issue is how to calculate the density of newly detected targets

from the context. In FPP or RFSet formalism, Assumption A1 implies  $\Phi(E^{Nn}/n!; (s_\kappa)_{\kappa=1}^N) = p_n$  or  $\Phi(\mathcal{F}_n(E^N); (s_\kappa)_{\kappa=1}^N) = p_n$ .

<sup>38</sup>In our opinion, a typical example of this type of confusion can be seen in an assertion made in [2, p.327]: ‘‘A true target is most generally defined to be an object that will persist in the tracking volume for at least several scans.’’ Although ‘‘many’’ true targets may be persistent in any tracking volume (if it is well defined and well designed), we may not know generally, a priori, any ‘‘true’’ target would appear at any time in any portion of any tracking volume, depending on particular *sensor management strategies*.

in the sensor measurement space (as discussed in [41]). In our opinion, the target birth–death model has more often been used for the convenience of the algorithms than for faithfully modeling the targets’ behaviors and the sensor detection capabilities.

Moreover, the constant number  $n$  can be justified even when the target birth–death is indeed supported by some legitimate reality, by counting all the targets that ever exist in a given time interval, e.g.,  $[t_0, \infty)$ , and by including the augmented discrete states, such as {unborn, alive, dead}, at any given time, with an appropriate target dynamics, within the framework of *multiple models* [46].

## B. Sensor Model: Random Assignments and False Alarms

Our sensor model defines available information in the form of a sequence  $y_k, k = 1, 2, \dots$ , of *measurement frames*,<sup>39</sup> each of which,  $y_k = (y_{kj})_{j=1}^{m_k}$ , is an RFSeq, in an appropriate measurement space<sup>40</sup>  $E_{Mk}$  with an appropriate measure to let us properly define the  $m_k$ -PD, composed of  $m_k$  measurements,  $y_{kj}$ ’s, collected at the same time  $t_k$  ( $t_0 \leq t_1 \leq t_2 \leq \dots$ ) by the same sensor.<sup>41</sup>

The uncertainty of the origin of each measurement  $y_{kj}$  is modeled by an unobservable RFSet  $a_k$  of pairs of integers in  $\{1, \dots, n\} \times \{1, \dots, m_k\}$ , given the number  $n$  of the targets and the number  $m_k$  of the measurements in frame  $k$ , called the *target-to-measurement assignment* or simply *target assignment* at frame  $k$ . Let the domain and the image (range) of  $a_k$  be denoted by  $\text{Dom}(a_k) = \{i | (i, j) \in a_k \text{ for some } j\}$ , and  $\text{Im}(a_k) = \{j | (i, j) \in a_k \text{ for some } i\}$ . Then, 1)  $i \in \text{Dom}(a_k)$  means the  $i$ th target is *detected* at frame  $k$ , 2)  $(i, j) \in a_k$  means<sup>42</sup> the  $j$ th measurement of frame  $k$  *originates from* the  $i$ th target, and 3)  $j \notin \text{Im}(a_k)$  means the  $j$ th measurement of frame  $k$  is a *false alarm* (that does not originate from any target).

Throughout the rest of this paper, we maintain the following two assumptions for each frame  $k$ :

**(A2) [No Merged or Split Measurement]:** There is no *merged measurement*, i.e.,  $\#\{(i, j) \in a_k\} = 1$  for any  $j \in \text{Im}(a_k)$ , and there is no *split measurement*, i.e.,  $\#\{j | (i, j) \in a_k\} = 1$  for any  $i \in \text{Dom}(a_k)$ .

**(A3) [Measurement Ordering]:** Given the number  $m_k$  of measurements and given the set  $\text{Dom}(a_k)$  of indices of detected targets at frame  $k$ , the target assignment  $a_k$  is independent of the target states at time  $t_k$ , and all the  $m_k! / (m_k - \#\text{Dom}(a_k))!$  possible realizations of  $a_k$ , under Assumption A2, are equally probable.

<sup>39</sup>Synonymous to scans, measurement sets, data sets, etc.

<sup>40</sup>We generally assume each measurement space  $E_{Mk}$  is also LCHC2 so that its conditional PD is well defined as the likelihood function that is a measurable function of the state  $X(t_k)$  in  $\bigcup_{n=0}^{\infty} E^n$  or  $\bigcup_{n=0}^{\infty} E^n/n!$  or  $\mathcal{F}(E)$ . The measurement space  $E_{Mk}$  is essentially the field of view of the sensor for frame  $k$ , and hence should be compact, or at least bounded.

<sup>41</sup>Generally, one of the multiple sensors.

<sup>42</sup>We also write  $a_k(i) = j$  to mean  $(i, j) \in a_k$ , under Assumption A2.

Assumption A2 makes each target assignment  $a_k$  a one-to-one function, while Assumption A3 is to best reflect the fact that the actual process of how each sensor orders the measurements  $(y_{kj})_{j=1}^{m_k}$  might be very complex and different from sensor to sensor, making any ordering of the measurements not informative.

One of the most basic assumptions for any dynamical state estimation problem to be tractable is *conditional independence* of information. In our MTT cases, that assumption is translated into the conditional independence of the pair  $(y_k, a_k)$  of observations  $y_k$  and unobservable target assignments  $a_k$ , for  $k = 1, 2, \dots$

**(A4) [Conditional Independence]:** For any sequence  $(y_k, a_k)_{k=1}^K$  of measurement frames and target assignments, we have

$$\begin{aligned} & P\left((y_k, a_k)_{k=1}^K \mid \varphi\left(\left((x_i(t))_{t \in [t_0, \infty)}\right)_{i=1}^n\right)\right) \\ &= \prod_{k=1}^K P\left(y_k, a_k \mid \varphi\left(\left(x_i(t_k)\right)_{i=1}^n\right)\right), \end{aligned} \quad (8)$$

where  $\varphi(x) = x$  for RFSeq formalism,  $\varphi(x) = [x]$  for FPP formalism, and  $\varphi((x_i)_{i=1}^n) = \{x_i\}_{i=1}^n$  for RFSet formalism, while  $\varphi(\left((x_i(t))_{t \in [t_0, \infty)}\right)_{i=1}^n)$  should be understood as the  $\sigma$ -algebra of events generated by the RFSeq, the FPP, or the RFSet of the entire stochastic processes, modeling targets according to each formalism.

In (8), and in many of subsequent equations, to avoid excessive notational complexities, we will use  $P$  or  $p$  as the generic symbol for any conditional or unconditional PD whenever its usage will not generate any confusion. However, we should remember that, when the usage of symbol  $P$  involves any discrete RFSet such as the target assignment  $a_k$  (and also the data association  $\lambda_{k,K}$ , defined in Section III-C), its PD is the JMD with respect to the counting measure on the space of subsets of a countable space, and, as discussed in Section II-C, is actually the PMF.

Under Assumption A2, therefore, Assumption A3 can be written as a conditional PMF

$$\begin{aligned} & P(a_k | m_k, \text{Dom}(a_k), X(t_k)) \\ &= P(a_k | m_k, \#\text{Dom}(a_k)) = \frac{(m_k - \#\text{Dom}(a_k))!}{m_k!} \end{aligned} \quad (9)$$

for each frame  $k$ , where  $X(t_k)$  is the target state set in any of the three formalisms. With a straightforward Bayesian expansion, we can write each scan-wise *extended* likelihood function on the right-hand side of (8) as<sup>43</sup>

$$\begin{aligned} & P\left((y_{kj})_{j=1}^{m_k}, a_k \mid \varphi\left(\left(x_i(t_k)\right)_{i=1}^n\right)\right) = \frac{(m_k - \#\text{Dom}(a_k))!}{m_k!} \\ & P\left((y_{kj})_{j=1}^{m_k} \mid a_k, m_k, \varphi\left(\left(x_i(t_k)\right)_{i=1}^n\right)\right) \\ & P\left(m_k \mid \text{Dom}(a_k), \varphi\left(\left(x_i(t_k)\right)_{i=1}^n\right)\right) \\ & P\left(\text{Dom}(a_k) \mid \varphi\left(\left(x_i(t_k)\right)_{i=1}^n\right)\right), \end{aligned} \quad (10)$$

<sup>43</sup> $P((y_{kj})_{j=1}^{m_k}, a_k | X)$  is the conditional joint PD for RFSeq  $(y_{kj})_{j=1}^{m_k}$  in  $E_{Mk}$  and RFSet  $a_k$  on the space of pairs of integers. Whenever we use any RFSeq such as  $(y_{kj})_{j=1}^{m_k}$ , we need to remember that the length  $m_k$  is a random variable, so that we have  $P((y_{kj})_{j=1}^{m_k}) = P((y_{kj})_{j=1}^{m_k} | m_k)P(m_k)$ .

the right-hand side of which consists of four factors: 1) the equal probability of each realization of assignment  $a_k$  given only set  $\text{Dom}(a_k)$  of indices for detected targets, and the number  $m_k$  of measurements, as shown by (9), 2) the PD of the values of the measurements  $(y_{kj})_{j=1}^{m_k}$  in  $E_{Mk}$ , given the number  $m_k$  of the measurements and their origins specified by  $a_k$ , 3) the probability of the number of false alarms of being  $m_{FAk}$  that is equal to  $m_k - \#(\text{Dom}(a_k))$  under Assumption A2, and 4) the joint probability of detection/nondetection of the  $n$  targets.

We should note that, although each measurement frame  $y_k = (y_{kj})_{j=1}^{m_k}$  is modeled as an ordered set (i.e., RFSeq), the assignment is defined on an arbitrarily chosen enumeration of the targets, modeled by RFSeq with permutable  $n$ -PDist, or FPP, or RFSet of stochastic processes. Consequently, in (8) and (10),  $(x_i(t_k))_{i=1}^n$  means target states with an enumeration that is arbitrary but consistent throughout all the measurement frames that we model.

By summing out the assignment  $a_k$  in (10), we obtain the measurement frame likelihood function in the *ordinary sense* as

$$\begin{aligned} P\left((y_{kj})_{j=1}^{m_k} \mid \varphi((x_i(t_k))_{i=1}^n)\right) &= \frac{1}{m_k!} \sum_{a_k \in \bar{\mathcal{A}}(\{1, \dots, n\}, \{1, \dots, m_k\})} \\ P\left((y_{kj})_{j=1}^{m_k} \mid a_k, m_k, \varphi((x_i(t_k))_{i=1}^n)\right) & \\ (m_{FAk}!) P(m_{FAk} \mid \text{Dom}(a_k), \varphi((x_i(t_k))_{i=1}^n)) & \\ P(\text{Dom}(a_k) \mid \varphi((x_i(t_k))_{i=1}^n)), & \end{aligned} \quad (11)$$

where  $m_{FAk} = m_k - \#(\text{Dom}(a_k))$  and  $\bar{\mathcal{A}}$  (as well as  $\mathcal{A}$  that will be used later) is the symbol for the space of one-to-one functions, which we may call *assignment functions*, defined, for any pair of finite sets  $I$  and  $J$ , as

$$\begin{cases} \mathcal{A}(I, J) \stackrel{\text{def}}{=} \left\{ a : I \rightarrow J \mid I = \text{Dom}(a) \text{ and} \right. \\ \left. \#(\text{Dom}(a)) = \#(\text{Im}(a)) \right\}, \\ \bar{\mathcal{A}}(I, J) \stackrel{\text{def}}{=} \left\{ a : D \rightarrow J \mid D = \text{Dom}(a) \subseteq I \text{ and} \right. \\ \left. \#(\text{Dom}(a)) = \#(\text{Im}(a)) \right\}. \end{cases} \quad (12)$$

It is significant that we define each measurement frame  $(y_{kj})_{j=1}^{m_k}$  as an RFSeq (not as an FPP or an RFSet) so that we can call each measurement as the “ $j$ th” measurement at the “ $k$ th” frame, to define data association hypotheses in the next section. Apparently, both sides of (11) are permutable with respect to the index  $j \in \{1, \dots, m_k\}$  of measurements  $(y_{kj})_{j=1}^{m_k}$ , as well as with respect to the index  $i \in \{1, \dots, n\}$  of targets  $(x_i(t_k))_{i=1}^n$ , as the likelihood function and hence  $(y_{kj})_{j=1}^{m_k}$  can be considered as an FPP or RFSet with conditional JMD  $\phi_{Mk}([(y_{kj})_{j=1}^{m_k} \mid [(x_i(t_k))_{i=1}^n]])$  in FPP formalism, or  $\phi_{Mk}(\{y_{kj}\}_{j=1}^{m_k} \mid \{x_i(t_k)\}_{i=1}^n)$  in RFSet formalism, dropping  $1/m_k!$  from (11), reflecting the fact that the *order* of the measurements does not bear any information.

## C. Association and Association Hypotheses

*Measurement-to-measurement* or *data-to-data* or simply *data association*  $\lambda_K$  over given cumulative frames  $(y_k)_{k=1}^K = ((y_{kj})_{j=1}^{m_k})_{k=1}^K$  is defined, from the multiframe target assignment  $(a_k)_{k=1}^K$ , as

$$\lambda_K = \left\{ \bigcup_{k=1}^K \{(k, j) \mid (i, j) \in a_k\} \mid i \in \bigcup_{k=1}^K \text{Dom}(a_k) \right\}. \quad (13)$$

We should note that we define the data association  $\lambda_K$ , not as a partition of the cumulative measurements themselves  $(y_k)_{k=1}^K = ((y_{kj})_{j=1}^{m_k})_{k=1}^K$ , but rather as a partition of the cumulative set of measurement indices,  $I_K \stackrel{\text{def}}{=} \bigcup_{k=1}^K \{k\} \times \{1, \dots, m_k\}$ . Each component of  $\lambda_K$  constitutes the indices of all the measurements originating from the same target, so that  $\#(\lambda_K)$  targets are detected in  $(y_k)_{k=1}^K$ , implying  $\#(\lambda_K) \leq n$ , while its complement  $I_K \setminus (\bigcup \lambda_K)$  is the set of all the measurement indices for false alarms in  $(y_k)_{k=1}^K$ . We call any realization of association  $\lambda_K$  a *data association hypothesis*<sup>44</sup> or simply an *association hypothesis* or a *hypothesis*. As a consequence of Assumption A2, the set  $\Lambda_K$  of all the association hypotheses on  $(y_k)_{k=1}^K$  is given by

$$\Lambda_K = \left\{ \lambda \subseteq \mathcal{T}_K \setminus \{\emptyset\} \mid \begin{array}{l} \tau \cap \tau' = \emptyset \text{ for any} \\ (\tau, \tau') \in \lambda \times \lambda \text{ such that } \tau \neq \tau' \end{array} \right\}, \quad (14)$$

where

$$\mathcal{T}_K \stackrel{\text{def}}{=} \left\{ \tau \subseteq I_K \mid \begin{array}{l} \#(\{j \in \{1, \dots, m_k\} \mid (k, j) \in \tau\}) \leq 1 \\ \text{for any } k \in \{1, \dots, K\} \end{array} \right\}, \quad (15)$$

each member of which is called a *track* on  $(y_k)_{k=1}^K$ ; i.e., each hypothesis is a *consistent* (i.e., *nonoverlapping*) set of nonempty tracks.

In Section IV, we will describe issues concerning generation of data association hypotheses, and their evaluation under additional sets of assumptions, completing our definition of MHT in the three mathematical formalisms, which is the main goal of this paper.

**Remark 6 (Hypotheses):** As we call any possible realization of the data association, i.e., an RFSet, a data association hypothesis, we may call any possible realization of target assignment  $a_k$  for each frame  $k$ , i.e., any element in  $\bar{\mathcal{A}}(\{1, \dots, n\}, \{1, \dots, m_k\})$ , a *target-to-measurement assignment hypothesis*. The latter type of hypotheses was introduced in the context of the PDA [12] and JPDA [13] algorithms, assuming a fixed number of targets, predating the development of the MHT. In [2, Sec. 7.5.2, p. 431] and [3, Sec. 4.2, p. 113], multiple-scan, non-Gaussian extension of the JPDA algorithms is discussed. In [3, Sec. 4.1.1, p. 109], in order to model an unknown number of

<sup>44</sup>Also known as data-to-data or measurement-to-measurement association hypothesis. We are using two different terms, “association” and “assignment,” to make a clear distinction between two random sets  $\lambda_K$  and  $a_k$ .

targets, it was proposed to augment target space  $E$  to  $E \cup \{\theta\}$ , where “ $\theta$ ” is the “target does not exist” state, and to use the joint state space  $(E \cup \{\theta\})^N$  with a fixed number  $N$  (that serves as a priori upper bound  $N$  on the number of targets), within the extended JPDA context mentioned earlier.

As seen in (13), each association hypothesis  $\lambda \in \Lambda_K$  can be viewed as an equivalence class of multiframe target assignment hypotheses  $(a_k)_{k=1}^K \in \prod_{k=1}^K \mathcal{A}(\{1, \dots, n\}, \{1, \dots, m_k\})$ , the equivalence defined through the permutation of the target indices. Given the number  $n$  of targets and cumulative frames  $(y_k)_{k=1}^K$ , through (13), each multiframe target assignment  $(a_k)_{k=1}^K$  is uniquely determined by a pair  $(\lambda, \alpha)$  of data association  $\lambda \in \Lambda_K$  and *track-to-target assignment* (or simply *track assignment*)  $\alpha \in \mathcal{A}(\lambda, \{1, \dots, n\})$  so that we have  $\tau = \bigcup_{k=1}^K \{(k, a_k(\alpha(\tau))) | \alpha(\tau) \in \text{Dom}(a_k)\}$  for any  $\tau \in \lambda_K$ . The target permutability, assumed by Assumption A1, implies that, given  $((y_k)_{k=1}^K, \lambda_K, n)$ , every realization of track assignment  $\alpha$  in  $\mathcal{A}(\lambda, \{1, \dots, n\})$  is equally probable. Moreover, in FPP or RFSet formalism, any *arbitrary enumeration* of the targets in (8)–(13) can be viewed as another random assignment from the set of targets,  $X = [(x_i)_{i=1}^n]$  or  $X = \{x_i\}_{i=1}^n$ , to its index set  $\{1, \dots, n\}$  with  $n = \ell(X)$  or  $n = \#(X)$ , i.e., a random element in  $\mathcal{A}(X, \{1, \dots, n\})$ .

**Remark 7 (Merged and Split Measurements):** For many sensors, the no-merged-or-split-measurement assumption (A2) is a reasonable assumption. It is very likely that any occasional violation of this assumption may be helped out by an effective *recovery* algorithm. On the other hand, there have been many efforts to generate and probabilistically evaluate, explicitly, merge/split measurement hypotheses, e.g., [34] (merged measurements) and [35] (split measurements).

#### IV. HYPOTHESIS GENERATION AND EVALUATION

To our best knowledge, the concept of the data association hypothesis, the core of the MHT, as described in the previous section, was first clearly defined in [5], in terms of tracks and hypotheses, together with an algorithm for selecting the single best (*most probable* or *maximum a posteriori probability*) hypothesis in a batch-data-processing mode. Subsequently, an algorithm for simultaneously generating and evaluating tracks and hypotheses, using recursive formulas, was first systematically and comprehensively described in [6]. In this section, we discuss hypothesis generation, and hypothesis evaluation under commonly used assumptions, using the three formalisms described in Section II, and the target/sensor models defined in Section III, which we may view as a form of generalizations of the results described in [5]–[7].

##### A. Hypothesis Generation and Management

For any pair  $((y_k)_{k=1}^{K_1}, (y_k)_{k=1}^{K_2})$  of cumulative frames such that  $K_1 < K_2$ , we call a track  $\tau_1 \in \mathcal{T}_{K_1}$  a *prede-*

*cessor* of a track  $\tau_2 \in \mathcal{T}_{K_2}$  (or  $\tau_2$  is a *successor* of  $\tau_1$ ) if  $\tau_1 = \{(k, j) \in \tau_2 | k \leq K_1\}$  (including the case  $\tau_1 = \emptyset$ ). We call a hypothesis  $\lambda_1 \in \Lambda_{K_1}$  a *predecessor* of a hypothesis  $\lambda_2 \in \Lambda_{K_2}$  (or  $\lambda_2$  is a *successor* of  $\lambda_1$ ) if, for each track  $\tau_2 \in \lambda_2$ , there exists a (necessarily unique) predecessor  $\tau_1$  in  $\lambda_1$  or otherwise track  $\tau_2$  has an empty predecessor  $\tau_1 = \emptyset$  in  $\mathcal{T}_{K_1}$ . Then, both cumulative collections of tracks and hypotheses,  $\bigcup_{k=1}^K \mathcal{T}_k$  and  $\bigcup_{k=1}^K \Lambda_k$ , respectively, form arborescent (tree) directed graphs through the predecessor–successor relations. For each hypothesis  $\lambda \in \Lambda_{K_2}$  and each track  $\tau \in \mathcal{T}_{K_2}$ , we denote their unique predecessors in  $\Lambda_{K_1}$  and  $\mathcal{T}_{K_1}$  by  $\lambda_{|K_1}$  and  $\tau_{|K_1}$ , respectively.

There may be many systematic methods for generating these trees. In [6], D. B. Reid called hypothesis tree generation using each measurement  $y_{kj}$  as a level variable<sup>45</sup> the *measurement-oriented approach*, from which the term *measurement-oriented MHT* originated, in contrast to the *target-oriented approach* in which a target-to-measurement assignment tree is generated using each target index as a level variable<sup>46</sup> (e.g., for PDA and JPDA algorithms) with a fixed known number  $n$  of targets.

The algorithm described in [5] recursively generates and evaluates tracks (including the track likelihood defined later in this section), in effect, building a track tree. Using a batch-processing form of hypothesis evaluation, it then selects the single best association hypothesis on  $(y_k)_{k=1}^K$  based on the a posteriori probability  $P(\lambda | (y_k)_{k=1}^K)$  (defined in Section IV-B) for each hypothesis, using a zero–one integer programming technique, where a set of association hypotheses is formed as feasible solutions to a system of binary linear equations. Over the years, it has become customary to call any MHT algorithm using this approach, which originated from [5], a *track-oriented MHT*.

It is well known that the numbers,  $\#(\Lambda_K)$  and  $\#(\mathcal{T}_K)$ , of hypotheses and tracks generally grow very rapidly, at exponential rates in many cases, so that any practical MHT implementation must have reasonable means of controlling the growth. Common methods for controlling the growth of the number of association hypotheses include *gating*, *pruning*, *combining*, and *clustering*, as outlined in [6]. The single best hypothesis selection of [5] over sliding windows of consecutive frames has been widely used as means for pruning track trees in a variety of ways for many track-oriented MHT algorithms. Many heuristic methods to control the numbers,  $\#(\Lambda_K)$  and  $\#(\mathcal{T}_K)$ , generally known as *hypothesis management methods*, have been devised in the past 40 years or so, as described in [8].

<sup>45</sup>Assigning each measurement to tracks in hypotheses at each expansion.

<sup>46</sup>Assigning each target to measurements at each expansion.

## B. Hypothesis Evaluation: Independence Assumptions

As mentioned in Remark 6 in Section III-C, in any of the three formalisms, an immediate consequence of Assumptions A1–A3 and the definition (13) of data association is as follows: Given the data association  $\lambda_K \in \Lambda_K$  on cumulative frame  $(y_k)_{k=1}^K$ , and given the number  $n$  of targets such that  $n \geq \#(\lambda_K)$ , any one of the equally possible  $n!/(n - \#(\lambda_K))!$  track assignments  $\alpha$ 's in  $\mathcal{A}(\lambda_K, \{1, \dots, n\})$  will define uniquely a multiframe target assignment  $(a_k)_{k=1}^K \in \prod_{k=1}^K \bar{\mathcal{A}}(\{1, \dots, n\}, \{1, \dots, m_k\})$ . Hence, if (13) holds, we have  $P(\lambda_K | n, (y_k)_{k=1}^K, (a_k)_{k=1}^K) = 1$  and  $P((a_k)_{k=1}^K | n, (y_k)_{k=1}^K, \lambda_K) = (n - \#(\lambda_K))!/n!$ . Both are zero otherwise. Hence, we have

$$P(\lambda_K, n | (y_k)_{k=1}^K) = P((y_k)_{k=1}^K)^{-1} \frac{n!}{(n - \#(\lambda_K))!} P((y_k, a_k)_{k=1}^K, n). \quad (16)$$

On the right-hand side of (16),  $(a_k)_{k=1}^K \in \prod_{k=1}^K \bar{\mathcal{A}}(\{1, \dots, n\}, \{1, \dots, m_k\})$  is any one of the  $n!/(n - \#(\lambda_K))!$  multiframe target assignment hypotheses that supports  $\lambda_K$  (through (13)).

Since the sensor model defined in Section III-B allows us to have multiple sensors, the sequence of measurement frame times,  $(t_k)_{k=1}^K$ , may contain repeated time stamps. We therefore need to consider a subset  $[K]$  of  $\{1, \dots, K\}$  to remove any repeated time, i.e.,  $[K] \subseteq \{1, \dots, K\}$ ,  $\#[K] = \#(\{t_k\}_{k=1}^K) \leq K$ , and  $K \in [K]$ , for hypothesis evaluation and target state estimation.

Under Assumptions A1–A4,  $P((y_k, a_k)_{k=1}^K, n)$  in (16) can be expanded by the target states, in RFSeq formalism, as

$$P((y_k, a_k)_{k=1}^K, n) = p_n \int_{E^{\#[K]n}} \left( \prod_{k=1}^K P(y_k, a_k | (x_i(t_k))_{i=1}^n) \right) f^{(n)} \left( ((x_i(t_k))_{\kappa \in [K]}^n)_{i=1}^n; (t_k)_{\kappa \in [K]} \right) \mu^{\#[K]n} \left( ((dx_i(t_k))_{\kappa \in [K]}^n)_{i=1}^n \right). \quad (17)$$

The product,  $n!p_n f^{(n)}(\cdot; (t_k)_{\kappa \in [K]})$ , which appears when we substitute (17) into (16), is nothing but the  $n$ -JD  $J^{(n)}(\cdot; (t_k)_{\kappa \in [K]})$ , and hence should be replaced by JMD  $\phi(\{((x_i(t_k))_{\kappa \in [K]}^n)_{i=1}^n\}; (t_k)_{\kappa \in [K]})$  in FPP formalism, and JMD  $\phi(\{(x_i(t_k))_{\kappa \in [K]}^n\}_{i=1}^n; (t_k)_{\kappa \in [K]})$  in RFSet formalism. Each frame-wise extended likelihood function  $P(y_k, a_k | \varphi((x_i(t_k))_{i=1}^n))$  (with  $\varphi(x) = x$ ,  $\varphi(x) = [x]$ , and  $\varphi((x_i)_{i=1}^n) = \{x_i\}_{i=1}^n$  for RFSeq, FPP, and RFSet formalisms, respectively) can then be expanded by the sensor model (10).

The a posteriori probabilities of each hypothesis  $\lambda_K \in \Lambda_K$  and of the number  $n$  of targets are obtained separately through marginalization of (16) with (17). To evaluate them in a practical and hence meaningful way, however, we need to divorce ourselves from target-to-measurement assignments,  $(a_k)_{k=1}^K$ , which would require a few more assumptions on the target and sensor models, including

**(A5) [i.i.d. Targets]:** Given the number  $n$  of targets, assume the joint probability distribution for the set of

targets is i.i.d. with the common single-target joint PD  $f_{\text{TGT}}$ , in the sense that, for any  $(s_\kappa)_{\kappa=1}^N \in [t_0, \infty)^N$  of distinct times, for any  $((x_i(s_\kappa))_{\kappa=1}^N)_{i=1}^n \in E^{Nn}$ , we have  $f^{(n)}(\{((x_i(s_\kappa))_{\kappa=1}^N)_{i=1}^n\}; (s_\kappa)_{\kappa=1}^N) = \prod_{i=1}^n f_{\text{TGT}}((x_i(s_\kappa))_{\kappa=1}^N; (s_\kappa)_{\kappa=1}^N)$  in RFSeq formalism, and  $\phi_{\text{TGT}}(\varphi(\{((x_i(s_\kappa))_{\kappa=1}^N)_{i=1}^n\}; (s_\kappa)_{\kappa=1}^N)) = n!p_n \prod_{i=1}^n f_{\text{TGT}}((x_i(s_\kappa))_{\kappa=1}^N; (s_\kappa)_{\kappa=1}^N)$  in FPP ( $\varphi(x) = [x]$ ) or RFSet ( $\varphi((x_i)_{i=1}^n) = \{x_i\}_{i=1}^n$ ) formalism.

Under this i.i.d. assumption, the target model can conveniently be expressed by the *intensity measure density* (IMD),<sup>47</sup>  $\gamma_{\text{TGT}}(\{(\xi_\kappa)_{\kappa=1}^N\}; (s_\kappa)_{\kappa=1}^N) = \nu f_{\text{TGT}}(\{(\xi_\kappa)_{\kappa=1}^N\}; (s_\kappa)_{\kappa=1}^N)$ , for any  $N$ , for any  $(\xi_\kappa, s_\kappa)_{\kappa=1}^N \in (E \times [t_0, \infty))^N$ , with a priori expected number of targets,  $\nu = \sum_{n=1}^\infty n p_n < \infty$ .

Another set of independence assumptions is concerned with our sensor model:

**(A6) [Independent Detections and i.i.d. False Alarms]:** For each measurement frame,  $y_k = (y_{kj})_{j=1}^{m_k}$ ,

1) the target detection is target-wise independent and determined by a common detection probability as a function  $p_{\text{Dk}}$  of the target state, 2) the target-state-to-measurement transition is also target-wise independent with a common transition probability density<sup>48</sup>  $p_{\text{Mk}}$ , and 3) each false alarm in the frame is independent from the target states and from other false alarms with a common PD,  $p_{\text{FAk}}$ , while the probability of the number of false alarms in the frame being  $m_{\text{FAk}}$  is given as  $p_{\text{NFAk}}(m_{\text{FAk}})$  with finite mean  $\nu_{\text{FAk}} = \sum_{m_{\text{FAk}}=1}^\infty m_{\text{FAk}} p_{\text{NFAk}}(m_{\text{FAk}}) < \infty$ .

By applying Assumption A6 to (10), for each  $k$ , we have

$$P\left((y_{kj})_{j=1}^{m_k}, a_k \mid \varphi((x_i(t_k))_{i=1}^n)\right) = \frac{L_{\text{FAk}}(\{1, \dots, m_k\} \setminus \text{Im}(a_k))}{m_k!} \left( \prod_{i \in \text{Dom}(a_k)} p_{\text{Mk}}(y_{ka_k(i)} | x_i(t_k)) p_{\text{Dk}}(x_i(t_k)) \right) \left( \prod_{\substack{i=1 \\ i \notin \text{Dom}(a_k)}}^n (1 - p_{\text{Dk}}(x_i(t_k))) \right) \quad (18)$$

<sup>47</sup>For an RFSeq  $(x_i)_{i=1}^n$ , an FPP  $[(x_i)_{i=1}^n]$ , or an RFSet  $\{x_i\}_{i=1}^n$  in  $(E^N, \mathcal{B}_N)$ , for any  $N = 1, 2, \dots$ , the intensity measure (IM)  $\Gamma$  is a finite measure on  $(E^N, \mathcal{B}_N)$  defined by  $\Gamma(B) = \mathbb{E}(\sum_{i=1}^n \mathbb{I}(x_i; B))$  (with the random measure representation  $\mathcal{N}$  of FPP formalism,  $\Gamma(B) = \mathbb{E}(\mathcal{N}(B))$ ), for each  $B \in \mathcal{B}_N$ , using the generic symbols,  $\mathbb{E}$  and  $\mathbb{I}$ , for mathematical expectation and indicator function. The IMD is its density, i.e., the Radon–Nikodym derivative with respect to the measure  $\mu^N$ . More commonly used name for IM is the *first-order moment measure* ([15, Sec. 5.4, p. 132], but we prefer IM and IMD because we only use the moment measure of the first order. Another synonym is *expectation measure*. A conditional version of IMD is called *probability hypothesis density* in [25]–[27].

<sup>48</sup>The use of a common  $p_{\text{Mk}}$ , equally for all the  $m_k$  measurements,  $y_{kj}$ 's, in frame  $k$ , may not be justified when each measurement  $y_{kj}$  has different measurement error characteristics from others. In that case, we should use the measurement-index-dependent  $p_{\text{Mkj}}$  in place of  $p_{\text{Mk}}$  (which we avoid for the sake of simplicity).

with the frame-wise false alarm likelihood, defined for each  $I_{\text{FA}k} \subseteq \{1, \dots, m_k\}$ , as

$$L_{\text{FA}k}(I_{\text{FA}k}) = L_{\text{NFA}k}(\#(I_{\text{FA}k})) \prod_{j \in I_{\text{FA}k}} \gamma_{\text{FA}k}(y_{kj}), \quad (19)$$

where  $\gamma_{\text{FA}k}(\eta) = v_{\text{FA}k} p_{\text{FA}k}(\eta)$  is the IMD of the false alarms in frame  $k$  at each  $\eta \in E_{Mk}$ , and  $L_{\text{NFA}k}(m_{\text{FA}k}) = (m_{\text{FA}k}! / (v_{\text{FA}k})^{m_{\text{FA}k}}) p_{\text{NFA}k}(m_{\text{FA}k})$  is the likelihood on the number  $m_{\text{FA}k}$  of false alarms in frame  $y_k = (y_{kj})_{j=1}^{m_k}$ .

As shown in Appendix A, Assumptions A1–A6 allow us to derive a batch-mode hypothesis evaluation formula, which we call *Morefield form*, in terms of the a posteriori probability of the data association  $\lambda_K$  on cumulative frame  $(y_k)_{k=1}^K$ , as

$$\begin{aligned} & P(\lambda_K | (y_k)_{k=1}^K) \\ &= C_{\text{MK}}^{-1} L_{\text{NDTK}}(\#(\lambda_K)) \left( \prod_{\tau \in \lambda_K} L_{\text{TRKK}}(\tau) \right) L_{\text{FA}}^{(K)}(\lambda_K) \end{aligned} \quad (20)$$

with

- 1) the normalizing constant (*Morefield constant*),  $C_{\text{MK}} = P((y_k)_{k=1}^K) (\prod_{k=1}^K m_k!)$ ;
- 2) track likelihood

$$\begin{aligned} L_{\text{TRKK}}(\tau) &= \int_{E^{(\{K\})}} \left( \prod_{k=1}^K q_{\text{MD}k}(\xi_k; \tau) \right) \\ & \gamma_{\text{TGT}}((\xi_\kappa)_{\kappa \in [K]}; (t_\kappa)_{\kappa \in [K]}) \prod_{\kappa \in [K]} \mu(d\xi_\kappa) \end{aligned} \quad (21)$$

defined for each track  $\tau \in \mathcal{T}_K$ , derived from the a priori joint IMD  $\gamma_{\text{TGT}}$ , and the *extended target-wise state likelihood function*  $q_{\text{MD}k}(\cdot; \tau)$ , defined by, for each  $\xi \in E$ ,

$$q_{\text{MD}k}(\xi; \tau) = \begin{cases} p_{Mk}(y_j | \xi) p_{Dk}(\xi), & \text{if } (k, j) \in \tau \text{ for some } j \in \{1, \dots, m_k\}, \\ 1 - p_{Dk}(\xi), & \text{if } (k, j) \notin \tau \text{ for any } j \in \{1, \dots, m_k\}; \end{cases} \quad (22)$$

- 3) likelihood  $L_{\text{NDTK}}(n_D)$  of the cumulative number  $n_D = \#(\lambda_K)$  of detected targets defined by

$$L_{\text{NDTK}}(n_D) = \sum_{n=n_D}^{\infty} p_n \frac{n!}{v^n} \frac{(\hat{v}_K)^{n-n_D}}{(n-n_D)!} \quad (23)$$

expressed by the a priori mean  $v$  of the number of the targets and the a posteriori expectation  $\hat{v}_K = L_{\text{TRKK}}(\emptyset)$  of the number of the targets that remain undetected through the cumulative frames  $(y_k)_{k=1}^K$ ;

- 4) *multiframe false alarm likelihood*  $L_{\text{FA}}^{(K)}$ , defined by

$$L_{\text{FA}}^{(K)}(\lambda) = \prod_{k=1}^K L_{\text{FA}k}(\{j \in \{1, \dots, m_k\} | (k, j) \notin \cup \lambda\}) \quad (24)$$

for each  $\lambda \in \Lambda_K$  through frame-wise false alarm likelihood  $L_{\text{FA}k}$  defined by (19).

As shown in [5], Morefield form (20) for evaluating hypotheses can be expressed as a form of zero–one integer programming problem, by enumerating the set  $\cup \Lambda_K = \mathcal{T}_K \setminus \{\emptyset\}$  of all the nonempty tracks as  $(\tau_i)_{i=1}^{N_T}$ , and

by mapping the set  $\Lambda_K$  of all the hypotheses into the space  $\{0, 1\}^{N_T}$  through  $(\xi_i)_{i=1}^{N_T} = (\mathbb{I}(\tau_i; \lambda))_{i=1}^{N_T} \in \{0, 1\}^{N_T}$  for each  $\lambda \in \Lambda_K$ .

- C. More on Hypothesis Evaluation: Markov and Poisson Assumptions

We will now introduce two more commonly used assumptions.

**(A7) [Markov Assumption]:** The targets are modeled as an RFSeq, an FPP, or an RFSet of independent stochastic processes, with a common a priori joint IMD  $\gamma_{\text{TGT}}$ , which is *Markovian*, in the sense that, for any  $N$ -tuple  $(s_\kappa)_{\kappa=1}^N \in [t_0, \infty)^N$  of distinct times, such that  $s_1 < s_2 < \dots < s_N$ , and for any  $(\xi_\kappa)_{\kappa=1}^N \in E^N$ , we have

$$\begin{aligned} & \gamma_{\text{TGT}}((\xi_\kappa)_{\kappa=1}^N; (s_\kappa)_{\kappa=1}^N) \\ &= \gamma_{\text{TGT}}(\xi_1; s_1) \prod_{\kappa=2}^N f_{\text{TRN}}(\xi_\kappa | \xi_{\kappa-1}; s_\kappa - s_{\kappa-1}, s_{\kappa-1}) \end{aligned} \quad (25)$$

with a given *state transition probability density* (STPD),  $f_{\text{TRN}}(\cdot | \cdot; \Delta s, s)$ , on  $(E, \mathcal{B}, \mu)$ , for each  $\Delta s > 0$  and  $s \in [t_0, \infty)$ .

Markov assumption (A7) enables us to calculate track likelihood  $L_{\text{TRKK}}(\tau)$  for each nonempty track  $\tau \in \cup \Lambda_K = \mathcal{T}_K \setminus \{\emptyset\}$  defined by (21), recursively as

$$L_{\text{TRKK}}(\tau|_k) = \begin{cases} \gamma_{\text{MND}k}(y_{kj}), & \text{if } k = k_0(\tau) \text{ with } (k, j) \in \tau, \\ L_{\text{TRK}(k-1)}(\tau|_{(k-1)}) L_{\text{MD}k}(\tau|_k), & \text{if } k > k_0(\tau) \end{cases} \quad (26)$$

for<sup>49</sup>  $k = k_0(\tau), k_0(\tau) + 1, \dots, K$ , with the measurement IMD  $\gamma_{\text{MND}k}$  from newly detected targets, and the measurement-or-no-detection likelihood  $L_{\text{MD}k}$ , which are defined by

$$\begin{cases} \gamma_{\text{MND}k}(y_{kj}) = \int_E p_{Mk}(y_{kj} | \xi) p_{Dk}(\xi) \tilde{\gamma}_k(\xi) \mu(d\xi) \\ L_{\text{MD}k}(\tau|_k) = \int_E q_{\text{MD}k}(\xi; \tau|_k) \tilde{f}_k(\xi | \tau|_{(k-1)}) \mu(d\xi) \end{cases} \quad (27)$$

for each  $k$ , any  $y_{kj} \in E_{Mk}$ , and any track  $\tau \in \mathcal{T}_K$  for any  $K \geq k$ . The recursive calculation (26) of track likelihood can be done in parallel to a recursive process for obtaining the *updated* track target state PD  $\hat{f}_k(\cdot | \tau|_k)$  from the *predicted*  $\tilde{f}_k(\cdot | \tau|_{(k-1)})$ , and generating the next *predicted*  $\tilde{f}_{k+1}(\cdot | \tau|_k)$ , for every  $\xi \in E$ , as

$$\begin{cases} \hat{f}_k(\xi | \tau|_k) = \begin{cases} \gamma_{\text{MND}k}(y_{kj})^{-1} p_{Mk}(y_{kj} | \xi) p_{Dk}(\xi) \tilde{\gamma}_k(\xi), & \text{if } k = k_0(\tau) \text{ with } (k, j) \in \tau, \\ L_{\text{MD}k}(\tau|_k)^{-1} q_{\text{MD}k}(\xi; \tau|_k) \tilde{f}_k(\xi | \tau|_{(k-1)}), & \text{otherwise } (\tau|_{(k-1)} \neq \emptyset), \end{cases} \\ \tilde{f}_k(\xi | \tau|_{(k-1)}) = \begin{cases} \int_E f_{\text{TRN}}(\xi | \xi'; t_k - t_{k-1}, t_{k-1}) \hat{f}_{k-1}(\xi' | \tau|_{(k-1)}) \mu(d\xi'), & \text{if } t_k > t_{k-1}, \\ \hat{f}_{k-1}(\xi | \tau|_{(k-1)}), & \text{if } t_k = t_{k-1}. \end{cases} \end{cases} \quad (28)$$

<sup>49</sup> $k_0(\tau) \stackrel{\text{def}}{=} \min\{k | (k, j) \in \tau \text{ for some } j\}$  is the index of the first frame where track  $\tau$  obtains a measurement, i.e., track initiation frame.

The *predicted* IMD  $\bar{\gamma}_k(\xi)$  of the undetected targets in (27) and (28) is obtained from the similar recursion, along the *updated* IMD  $\hat{\gamma}_k(\xi)$ , for each  $k = 1, 2, \dots$ , as

$$\begin{cases} \hat{\gamma}_k(\xi) = (1 - p_{\text{DK}}(\xi))\bar{\gamma}_k(\xi) \\ \bar{\gamma}_k(\xi) = \begin{cases} \int_E f_{\text{TRN}}(\xi|\xi'; t_k - t_{k-1}, t_{k-1})\hat{\gamma}_{k-1}(\xi')\mu(d\xi'), & \text{if } k > 1 \text{ and } t_k > t_{k-1}, \\ \hat{\gamma}_{k-1}(\xi), & \text{if } k > 1 \text{ and } t_k = t_{k-1}, \\ \gamma_{\text{TGT}}(\xi, t_1), & \text{if } k = 1 \end{cases} \end{cases} \quad (29)$$

for every  $\xi \in E$ .

For each  $k = 1, \dots, K$ , let  $\bar{v}_k = \int_E \bar{\gamma}_k(\xi)\mu(d\xi)$  and  $\hat{v}_k = \int_E \hat{\gamma}_k(\xi)\mu(d\xi)$ . Then, we have  $\bar{v}_k = \hat{v}_{k-1}$  for any  $k > 1$  (reflecting our no-birth-no-death target model),  $\bar{v}_1 = v$  is the a priori expectation of the number  $n$  of targets, and  $\hat{v}_K = L_{\text{TRKK}}(\emptyset)$  is the a posteriori expectation of the number of targets that are not detected in any of the  $K$  frames,  $(y_k)_{k=1}^K$ .

Under Markovian assumption (A7), we can *rewrite* Morefield form (20) in a recursive hypothesis evaluation form, as

$$P(\lambda|(y_{k'})_{k'=1}^k) = C_{\text{Rk}}^{-1} P(\lambda_{|(k-1)}|(y_{k'})_{k'=1}^{k-1}) \left( \prod_{\substack{\tau \in \lambda \\ \tau_{|(k-1)} \neq \emptyset}} L_{\text{MDk}}(\tau) \right) \cdot \frac{L_{\text{NDTk}}(\#\lambda)}{L_{\text{NDT}(k-1)}(\#\lambda_{|(k-1)})} \left( \prod_{\substack{j=1 \\ \{(k,j)\} \in \lambda}}^{m_k} \gamma_{\text{MNDk}}(y_{kj}) \right) \cdot L_{\text{FAk}} \left( \bigcup_{\substack{j=1 \\ (k,j) \notin \lambda}}^{m_k} \{j\} \right) \quad (30)$$

for each  $k$ , for every  $\lambda \in \Lambda_k$ , where

- 1)  $C_{\text{Rk}} = (m_k!)P(y_k|(y_{k'})_{k'=1}^{k-1}) = J_{\text{Mk}}^{(m_k)}(y_k|(y_{k'})_{k'=1}^{k-1})$  is the normalizing constant (*Reid constant*);
- 2)  $\lambda_{|(k-1)}$  is the unique predecessor<sup>50</sup> of  $\lambda \in \Lambda_k$  in  $\Lambda_{k-1}$ ;
- 3)  $\tau_{|(k-1)} \in \mathcal{T}_{k-1}$  is the unique predecessor of each track  $\tau$  in a given hypothesis  $\lambda$  (including the case where  $\tau_{|(k-1)} = \emptyset$ ; in that case,  $\tau$  is a singleton  $\{(k, j)\}$  for some  $j \in \{1, \dots, m_k\}$ , i.e., a new track at frame  $y_k$ );
- 4)  $L_{\text{MDk}}(\tau)$  is the track-to-measurement likelihood of *old track*  $\tau_{|(k-1)}$  and measurement  $y_{kj}$  if  $(k, j) \in \tau$ , and the missed detection likelihood otherwise (i.e., if  $(k, j) \notin \tau$ ), defined in (27);
- 5)  $L_{\text{NDTk}}$  and  $L_{\text{NDT}(k-1)}$  are the likelihoods of the cumulative numbers of detected targets, in  $(y_{k'})_{k'=1}^k$  and  $(y_{k'})_{k'=1}^{k-1}$ , with  $\hat{v}_k$  and  $\hat{v}_{k-1}$ , as defined by (23);
- 6)  $\gamma_{\text{MNDk}}$  is the new detection IMD defined in (27);
- 7)  $L_{\text{FAk}}(I_{\text{FAk}})$  is the false alarm likelihood defined by (19).

We call this recursive hypothesis evaluation formula (30), *Reid form*, which is the non-Poisson extension of

<sup>50</sup>For  $k = 1$ , we use the convention that  $\bar{\lambda}_0 = \{\emptyset\}$  and  $P(\bar{\lambda}|(y_{k'})_{k'=1}^0) = P(\bar{\lambda}) = 1$  for  $\bar{\lambda} = \emptyset$ .

the formulas in [6, eq. 16, p. 848] and [7, eq. 19, p. 405], and was presented in [43, Th. 2, p. 231].<sup>51</sup>

Another common assumptions are Poisson assumptions on the a priori PDist  $(p_n)_{n=0}^\infty$  of the number  $n$  of the targets, and on the PDist  $(p_{\text{NFAk}}(m_{\text{FAk}}))_{m_{\text{FAk}}=0}^\infty$  of the number  $m_{\text{FAk}}$  of false alarms in each frame  $y_k = (y_{kj})_{j=1}^{m_k}$ .

**(A8) [Poisson Assumptions]:** 1) The PDist  $(p_n)_{n=0}^\infty$  of the number of targets is Poisson with mean  $\nu$ , i.e.,  $p_n = e^{-\nu}\nu^n/n!$ , for each  $n = 0, 1, 2, \dots$ , and 2) for each frame  $k = 1, 2, \dots$ , the PDist  $p_{\text{NFAk}}$  of the number  $m_{\text{FAk}}$  of false alarms in frame  $y_k = (y_{kj})_{j=1}^{m_k}$  is Poisson with mean  $\nu_{\text{FAk}}$ , i.e.,  $p_{\text{NFAk}}(m_{\text{FAk}}) = e^{-\nu_{\text{FAk}}}\nu_{\text{FAk}}^{m_{\text{FAk}}}/m_{\text{FAk}}!$ , for each  $m_{\text{FAk}} = 0, 1, 2, \dots$

With this Poisson assumption (A8), the likelihood functions,  $L_{\text{NDTk}}$  for the number of detected targets defined by (23) and likelihood  $L_{\text{NFAk}}$  for the number of false alarms at each frame  $k$ , both become constants, as  $L_{\text{NDTk}} \equiv e^{-(\nu-\hat{v}_k)}$  and  $L_{\text{NFAk}} \equiv e^{-\nu_{\text{FAk}}}$ , respectively. It was proven in [31, Th. 2, p. 1136] that Poisson assumption (A8) is also a necessary condition for those likelihoods to be constants. With this assumption, Morefield form (20) of hypothesis evaluation can be transformed to a linear objective function of a zero-one linear integer programming problem, or equivalently to an objective function for a form of multidimensional assignment algorithm described in [32]. Any hypothesis selection algorithm using Morefield form (20) became the core algorithm for every so-called track-oriented MHT [8].

## D. Target State Estimation

Under Assumptions A1–A3, given cumulative frame  $(y_k)_{k=1}^K$ , for each assumed number  $n$  of targets and for each data association  $\lambda_K \in \Lambda_K$ , there are  $n!/(n - \#\lambda_K)!$  multiframe target assignments  $(a_k)_{k=1}^K$ 's, each of which *supports* association  $\lambda_K$  (i.e.,  $(\lambda_K, (a_k)_{k=1}^K)$  satisfies (13)) and is uniquely determined by one of the equally probable  $n!/(n - \#\lambda_K)!$  track assignments  $\alpha \in \mathcal{A}(\lambda_K, \{1, \dots, n\})$  as mentioned in Remark 6 of Section III. Hence, in RFSeq formalism, we have

$$\begin{aligned} f^{(n)} & \left( ((x_i(t_k))_{k \in [K]}_{i=1}^n; (t_k)_{k \in [K]} | (y_k)_{k=1}^K \right) P(n|(y_k)_{k=1}^K) \\ & = \sum_{\lambda_K \in \Lambda_K} f^{(n)} \left( ((x_i(t_k))_{k \in [K]}_{i=1}^n; (t_k)_{k \in [K]} | \lambda_K, (y_k)_{k=1}^K \right) \\ & = \sum_{\lambda_K \in \Lambda_K} P(\lambda_K, n|(y_k)_{k=1}^K) \frac{P(\lambda_K, n|(y_k)_{k=1}^K)}{((n - \#\lambda_K))!/n!} \\ & \quad \sum_{\alpha_K \in \mathcal{A}(\lambda_K, \{1, \dots, n\})} f^{(n)} \left( ((x_i(t_k))_{k \in [K]}_{i=1}^n; (t_k)_{k \in [K]} | (y_k, a_k)_{k=1}^K \right), \end{aligned} \quad (31)$$

where, within the second summation,  $(a_k)_{k=1}^K$  is the multiframe assignment that is uniquely determined by  $\lambda_K \in \Lambda_K$  and  $\alpha_K \in \mathcal{A}(\lambda_K, \{1, \dots, n\})$ , such that

<sup>51</sup>In [43], the statement of Theorem 2 (p. 231) contains a misstatement:  $L_{\text{NDTk}}(\#\lambda)$  in eq. (22) (p. 231) must be replaced by  $L_{\text{NDTk}}(\#\lambda)/L_{\text{NDT}(k-1)}(\#\bar{\lambda})$  where  $\bar{\lambda} = \lambda_{|(k-1)}$  is the unique predecessor of hypothesis  $\lambda$ , and accordingly,  $(\bar{v} - \hat{v}_k)$  in Corollary 2 of [43, p. 233] should be replaced by  $(\hat{v}_{k-1} - \hat{v}_k)$ .

$(k, a_k(\alpha_K(\tau))) \in \tau$  for each  $\tau \in \lambda_K$  and  $\alpha_K(\tau) \in \text{Dom}(a_k)$ . While  $P(\lambda_K, n | (y_k)_{k=1}^K)$  can be determined through (16) and (17),  $f^{(n)}(\cdot; (t_k)_{k \in [K]} | (y_k, a_k)_{k=1}^K)$  can be expressed by the standard Bayes formula, under conditional independence assumption (A4).

The target permutability of Assumption A1 implies that, once  $f^{(n)}((x_i(t_k))_{i=1}^n; (t_k)_{k \in [K]} | (y_k, a_k)_{k=1}^K)$  is evaluated for any particular  $(a_k)_{k=1}^K$  determined by an arbitrary  $(\lambda_K, n, \alpha)$ , each term of the second summation of (31) can be obtained by appropriate coordinate permutation defined by each  $\alpha \in \mathcal{A}(\lambda_K, \{1, \dots, n\})$ .

With additional independence assumptions (A5 and A6), in RFSeq formalism, (31) can be rewritten as

$$\begin{aligned} \hat{f}_K^{(n)}((x_i(t_k))_{i=1}^n) &= \sum_{\lambda \in \Lambda_K} P(\lambda | (y_k)_{k=1}^K) P(n | \lambda, (y_k)_{k=1}^K) \\ &\frac{(n - \#(\lambda))!}{(\hat{\nu}_K)^{n - \#(\lambda)}} \sum_{\alpha \in \mathcal{A}(\lambda, \{1, \dots, n\})} \left( \prod_{\tau \in \lambda} \hat{f}_K(x_{\alpha(\tau)}(t_k) | \tau) \right) \\ &\left( \prod_{\substack{i=1 \\ i \notin \text{Im}(\alpha)}}^n \hat{\gamma}_K(x_i) \right) \end{aligned} \quad (32)$$

with

$$p(n | \lambda_K, Y_K) = \begin{cases} (L_{\text{NDTK}}(\#(\lambda_K)))^{-1} \frac{(\hat{\nu}_K)^{n - \#(\lambda_K)}}{(n - \#(\lambda_K))!} \cdot \frac{n!}{\hat{\nu}^n} P_n, & \text{if } n \geq \#(\lambda_K), \\ 0, & \text{otherwise,} \end{cases} \quad (33)$$

where

1)  $\hat{f}_K^{(n)}((x_i(t_k))_{i=1}^n) = J^{(n)}((x_i(t_k))_{i=1}^n; t_k | (y_k)_{k=1}^K)$  is the conditional  $n$ -JD of the current state  $(x_i(t_k))_{i=1}^n$  conditioned by  $(y_k)_{k=1}^K$ ;

2)  $L_{\text{NDTK}}(n_D)$  is the likelihood of the hypothesized number  $\#(\lambda)$  of all the detected targets in the  $K$  frames being  $n_D$ , defined by (23);

3)  $\hat{\nu}_K = L_{\text{TRKK}}(\emptyset)$  is the expected number of targets remaining undetected throughout the  $K$  frames, defined by (21) through  $q_{\text{MDk}}$  as  $q_{\text{MDk}}(\cdot; \emptyset) = 1 - p_{\text{Dk}}(\cdot)$  for each  $k = 1, \dots, K$ ;

4) for nonempty track  $\tau \in \cup \Lambda_K = \mathcal{T}_K \setminus \{\emptyset\}$ ,  $\hat{f}_K(\cdot | \tau)$  is the track target (current) state PD defined by

$$\begin{aligned} \hat{f}_K(\xi_k | \tau) &= \left( \int_{E^{\#(\{K\})-1}} \left( \prod_{k=1}^K q_{\text{MDk}}(\xi_k; \tau) \right) \right. \\ &\left. \gamma_{\text{TGT}}((\xi_\kappa)_{\kappa \in [K]}; (t_\kappa)_{\kappa \in [K]}) \prod_{\kappa \in [K] \setminus \{K\}} \mu(d\xi_\kappa) \right) / \\ &\left( \int_{E^{\#(\{K\})}} \left( \prod_{k=1}^K q_{\text{MDk}}(\xi'_k; \tau) \right) \right. \\ &\left. \gamma_{\text{TGT}}((\xi'_\kappa)_{\kappa \in [K]}; (t_\kappa)_{\kappa \in [K]}) \prod_{\kappa \in [K]} \mu(d\xi'_\kappa) \right); \end{aligned} \quad (34)$$

5)  $\hat{\gamma}_K$  is the IMD of the targets remaining undetected after the  $K$  frames, defined by

$$\begin{aligned} \hat{\gamma}_K(\xi_K) &= \int_{E^{\#(\{K\})-1}} \left( \prod_{k=1}^K (1 - p_{\text{Dk}}(\xi_k)) \right) \\ &\gamma_{\text{TGT}}((\xi_\kappa)_{\kappa \in [K]}; (t_\kappa)_{\kappa \in [K]}) \prod_{\kappa \in [K] \setminus \{K\}} \mu(d\xi_\kappa) \end{aligned} \quad (35)$$

for each  $\xi_K \in E$ .

By dropping the most current target-wise extended track-to-measurement likelihood function  $q_{\text{MDK}}(\cdot; \tau)$  from both the denominator and the numerator of (34), we have the prediction PD  $\hat{f}_K(\cdot | \tau_{|(K-1)})$ , which can then be used for the recursive calculation of the track likelihood by (26), without Poisson (A8) or Markovian (A7) assumptions. Under Markov assumption (A7), with or without Poisson assumption (A8),  $\hat{f}_K(\cdot | \tau)$  and  $\hat{f}_K(\cdot | \tau_{|(K-1)})$  can be obtained through the familiar recursion of (28). Similarly, by taking out  $(1 - p_{\text{Dk}}(\xi_k))$  from the integrand of (35), we have the predicted IMD  $\bar{\gamma}_K$  of the undetected targets, while, with Markovian assumption (A7),  $\bar{\gamma}_k$  and  $\hat{\gamma}_k$  can be obtained recursively by (29).

With Poisson assumption (A8), with or without Markov assumption (A7), we can rewrite (32) as

$$\begin{aligned} \hat{f}_K^{(n)}((x_i(t_k))_{i=1}^n) &= e^{-\hat{\nu}_K} \sum_{\lambda \in \Lambda_K} P(\lambda | (y_k)_{k=1}^K) \\ &\sum_{\alpha \in \mathcal{A}(\lambda, \{1, \dots, n\})} \left( \prod_{\tau \in \lambda} \hat{f}_K(x_{\alpha(\tau)}(t_k) | \tau) \right) \left( \prod_{\substack{i=1 \\ i \notin \text{Im}(\alpha)}}^n \hat{\gamma}_K(x_i) \right) \end{aligned} \quad (36)$$

and<sup>52</sup>

$$p(n | \lambda_K, Y_K) = \begin{cases} e^{-\hat{\nu}_K} \frac{(\hat{\nu}_K)^{n - \#(\lambda_K)}}{(n - \#(\lambda_K))!}, & \text{if } n \geq \#(\lambda_K), \\ 0, & \text{otherwise.} \end{cases} \quad (37)$$

In FPP formalism, we have

$$\begin{aligned} \hat{\phi}_K(\{(x_i(t_k))_{i=1}^n\}) &\stackrel{\text{def}}{=} \phi(\{(x_i(t_k))_{i=1}^n\}; t_k | (y_k)_{k=1}^K) \\ &= \hat{f}_K^{(n)}((x_i(t_k))_{i=1}^n), \end{aligned}$$

while

$$\begin{aligned} \hat{\phi}_K(\{(x_i(t_k))_{i=1}^n\}) &\stackrel{\text{def}}{=} \phi(\{(x_i(t_k))_{i=1}^n\}, t_k | (y_k)_{k=1}^K) \\ &= \hat{f}_K^{(n)}((x_i(t_k))_{i=1}^n) \end{aligned}$$

in RFSet formalism, both being expressed by (32) (non-Poisson cases) and (36) (Poisson cases), as the a posteriori JMD.

## V. RELATION OF MHT TO RFSET-BASED MTT ALGORITHMS

We understand that the relation between MHT and RFSet-based MTT algorithms has been actively discussed recently, e.g., in [36]–[39]. It was even claimed in

<sup>52</sup>Thus, the a posteriori probability distribution of the number of undetected targets is Poisson.

[38] that MHT can be derived from an RFSet-based algorithm. This development is interesting, as we remember that RFSet-based algorithms started to be developed as *correlation-free*<sup>53</sup> algorithms [44]. As mentioned earlier, it is not our objective to conduct the literature survey. In this section, we will state our perspectives of RFSet-based MTT algorithms, from our MHT viewpoints presented in Sections I–IV. We will use what we consider as typical RFSet-based MTT target and sensor models.

## A. RFSet Target and Sensor Models

Throughout this section, we basically maintain all the assumptions made so far, i.e., Assumptions A1–A8. Instead of the RFSet-of-stochastic-processes assumption (A1), however, we assume a discrete-time Markov process  $(X_k)_{k=1}^K$  ( $K \leq \infty$ ) on an FICM-QMS  $(\mathcal{F}(E), \mathcal{B}(\mathcal{B}), \mathcal{M})$ , with the  $k$ th state  $X_k \in \mathcal{F}(E)$  at time  $t_k$  of the  $k$ th measurement frame, such that  $t_1 \leq t_2 \leq \dots$ , defined by a transition JMD<sup>54</sup>  $\phi_{\text{TRN}k}(X_{k+1}|X_k)$ , and a Poisson initial state JMD  $\phi(X_1) = e^{-\bar{v}_1} \prod_{x \in X_1} \bar{\gamma}_1(x)$  with IMD  $\bar{\gamma}_1$  and the expected number of targets,  $\bar{v}_1 = \int_E \bar{\gamma}_1(x) \mu(dx)$ , at time  $t_1$ .

As a “typical” RFSet-based model, let us assume that the transition JMD  $\phi_{\text{TRN}k}(X_{k+1}|X_k)$  (for  $t_{k+1} > t_k$ ) includes a birth–death term, as<sup>55</sup>  $\phi_{\text{TRN}k}(\cdot|X_k) = \phi_{\text{TS}k}(\cdot|X_k) \otimes \phi_{\text{B}k}(\cdot)$ , which is the convolution of 1) the *survival-transition* JMD  $\phi_{\text{TS}k}(\cdot|X_k)$  defined as a conditional *multiple Bernoulli* (MBe) (or *Poisson binomial*) JMD,

$$\phi_{\text{TS}k}(\cdot|\{x_{ki}\}_{i=1}^n) = \phi_{\text{TSBe}k}(\cdot|x_{k1}) \otimes \dots \otimes \phi_{\text{TSBe}k}(\cdot|x_{kn}) \quad (38)$$

for each  $X_k = \{x_{ki}\}_{i=1}^n$ , with each conditional *Bernoulli* (Be) JMD  $\phi_{\text{TSBe}k}(\cdot|x_{ki})$ , defined by, for any  $X \in \mathcal{F}(E)$ ,

$$\phi_{\text{TSBe}k}(X|x_{ki}) = \begin{cases} 1 - p_{\text{S}k}(x_{ki}), & \text{if } X = \emptyset, \\ f_{\text{T}k}(x_{k+1}|x_{ki}) p_{\text{S}k}(x_{ki}), & \text{if } X = \{x_{k+1}\}, \\ 0, & \text{if } \#(X) > 1 \end{cases} \quad (39)$$

assuming target-wise independent, target-state dependent *survival probability*  $p_{\text{S}k} : E \rightarrow [0, 1]$ , and a discrete-time STPD<sup>56</sup>  $f_{\text{T}k}(x_{k+1}|x_k) = f_{\text{TRN}}(x_{k+1}|x_k; t_{k+1} - t_k, t_k)$  that is target-wise independent, and 2) a *Poisson birth* JMD  $\phi_{\text{B}k}(X) = e^{-\nu_{\text{B}k}} \prod_{x \in X} \gamma_{\text{B}k}(x)$ , defined through the IMD  $\gamma_{\text{B}k}$  with  $\nu_{\text{B}k} = \int_E \gamma_{\text{B}k}(x) \mu(dx)$ , all generally depending on  $k = 1, 2, \dots$

In Section III-B, we modeled the  $k$ th frame as an RFSeq  $(y_{kj})_{j=1}^{m_k}$  with each measurement having a unique

label. The likelihood function (11) is, however, permutable with respect to both measurements  $(y_{kj})_{j=1}^{m_k}$  and the target states  $(x_i(t_k))_{i=1}^n$ . Therefore, we can consider each measurement frame as an RFSet  $Y_k = \{y_{kj}\}_{j=1}^{m_k}$  in an LCHC2 measure space<sup>57</sup>  $(E_{\text{M}k}, \mathcal{B}_{\text{M}k}, \mu_{\text{M}k})$ , having a conditional JMD  $\phi_{\text{M}k}(\cdot|X_k) = \phi_{\text{MD}k}(\cdot|X_k) \otimes \phi_{\text{FA}k}(\cdot)$  that is the convolution of 1) conditional JMD  $\phi_{\text{MD}k}(\cdot|X_k)$  of target detections and 2) Poisson JMD  $\phi_{\text{FA}k}(Y_{\text{FA}k}) = e^{-\nu_{\text{FA}k}} \prod_{\eta \in Y_{\text{FA}k}} \gamma_{\text{FA}k}(\eta)$  with  $\nu_{\text{FA}k} = \int_{E_{\text{M}k}} \gamma_{\text{FA}k}(\eta) \mu_{\text{M}k}(d\eta)$  for the set of false alarms.

With the independent detection assumption (A6), the target detections are modeled by a conditional MBe JMD,

$$\phi_{\text{MD}k}(\cdot|\{x_{ki}\}_{i=1}^n) = \phi_{\text{MDBe}k}(\cdot|x_{k1}) \otimes \dots \otimes \phi_{\text{MDBe}k}(\cdot|x_{kn}) \quad (40)$$

for  $X_k = \{x_{ki}\}_{i=1}^n$ , with each conditional Be JMD,  $\phi_{\text{MDBe}k}(\cdot|x_{ki})$ , defined as, for any  $Y \in \mathcal{F}(E_{\text{M}k})$ ,

$$\phi_{\text{MDBe}k}(Y|x_{ki}) = \begin{cases} 1 - p_{\text{D}k}(x_{ki}), & \text{if } Y = \emptyset, \\ p_{\text{M}k}(y|x_{ki}) p_{\text{D}k}(x_{ki}), & \text{if } Y = \{y\}, \\ 0, & \text{if } \#(Y) > 1. \end{cases} \quad (41)$$

For  $k = 1, 2, \dots$ , let  $\bar{\phi}_k(X_k)$  and  $\hat{\phi}_k(X_k)$  be the predicted and the updated state JMD, i.e.,

$$\begin{cases} \bar{\phi}_k(X_k) \mathcal{M}(dX_k) = \begin{cases} \text{Prob}\{X_k \in dX_k\}, & \text{if } k = 1, \\ \text{Prob}\{X_k \in dX_k | (Y_{k'})_{k'=1}^{k-1}\}, & \text{if } k > 1, \end{cases} \\ \hat{\phi}_k(X_k) \mathcal{M}(dX_k) = \text{Prob}\{X_k \in dX_k | (Y_{k'})_{k'=1}^k\}. \end{cases} \quad (42)$$

Then, as shown in Appendix B, with the target and sensor models described earlier, we can prove that predicted JMD  $\bar{\phi}_k(X_k)$  and updated JMD  $\hat{\phi}_k(X_k)$  can be expressed as convolutions  $\bar{\phi}_k = \bar{\phi}_{\text{D}k} \otimes \bar{\phi}_{\text{U}k}$  and  $\hat{\phi}_k = \hat{\phi}_{\text{D}k} \otimes \hat{\phi}_{\text{U}k}$ , respectively, where 1) conditional JMD  $\bar{\phi}_{\text{D}k}$  or  $\hat{\phi}_{\text{D}k}$  for the detected targets is written as<sup>58</sup>

$$\begin{cases} \bar{\phi}_{\text{D}k}(X) = \sum_{\substack{\bar{\lambda} \in \bar{\Lambda}_k \\ \#(\bar{\lambda}) = \#(X)}} \bar{p}_k(\bar{\lambda}) \sum_{\bar{\alpha} \in \mathcal{A}(\bar{\lambda}, X)} \left( \prod_{\bar{\tau} \in \bar{\lambda}} \bar{f}_k(\bar{\alpha}(\bar{\tau})|\bar{\tau}) \right) \\ \hat{\phi}_{\text{D}k}(X) = \sum_{\substack{\hat{\lambda} \in \hat{\Lambda}_k \\ \#(\hat{\lambda}) = \#(X)}} \hat{p}_k(\hat{\lambda}) \sum_{\hat{\alpha} \in \mathcal{A}(\hat{\lambda}, X)} \left( \prod_{\hat{\tau} \in \hat{\lambda}} \hat{f}_k(\hat{\alpha}(\hat{\tau})|\hat{\tau}) \right) \end{cases} \quad (43)$$

and 2) conditional JMDs  $\bar{\phi}_{\text{U}k}$  and  $\hat{\phi}_{\text{U}k}$  for the undetected targets are Poisson JMD as

$$\begin{cases} \bar{\phi}_{\text{U}k}(X) = e^{-\bar{\nu}_k} \prod_{x \in X} \bar{\gamma}_k(x) \text{ with } \bar{\nu}_k = \int \bar{\gamma}_k(\xi) \mu(d\xi) \\ \hat{\phi}_{\text{U}k}(X) = e^{-\hat{\nu}_k} \prod_{x \in X} \hat{\gamma}_k(x) \text{ with } \hat{\nu}_k = \int \hat{\gamma}_k(\xi) \mu(d\xi) \end{cases} \quad (44)$$

for each  $X \in \mathcal{F}(E)$ , with undetected target IMD  $\bar{\gamma}_k$  and  $\hat{\gamma}_k$ , where

<sup>53</sup>We understand that the “correlation” is a “traditional” U.S. Navy terminology for data association.

<sup>54</sup>We assume that the transition JMD  $\phi_{\text{TRN}k}$  is only defined for  $t_{k+1} > t_k$ , and that  $X_{k+1} = X_k$  if  $t_{k+1} = t_k$ .

<sup>55</sup>We assume, for Section V, that any diagonal set  $D_n$  in  $E^n$  has zero product measure  $\mu^n$ , i.e.,  $\mu^n(D_n) = 0$ .

<sup>56</sup> $f_{\text{TRN}}$  is the continuous time STPD of Assumption A7, assuming  $\Delta s = t_{k+1} - t_k > 0$ .

<sup>57</sup>We also assume, for Section V, that any diagonal set  $D_{\text{M}km}$  in each product measurement space  $E_{\text{M}k}^m$  has zero product measure  $\mu_{\text{M}k}^m$ , i.e.,  $\mu_{\text{M}k}^m(D_{\text{M}km}) = 0$  for each  $m$ .

<sup>58</sup>We understand that each JMD of (43), a probability-weighted sum of the symmetrized asymmetric PD products, is called generalized multi-Bernoulli (GMBe) in [33].

- 1)  $\bar{\Lambda}_k$  and  $\hat{\Lambda}_k$  are sets of association hypotheses, each hypothesis being as a collection of nonempty tracks, each of which is a subset of  $\bigcup_{k'=1}^{k-1} \{k'\} \times Y_{k'}$  or  $\bigcup_{k'=1}^k \{k'\} \times Y_{k'}$ ;
- 2)  $(\bar{p}_k(\bar{\lambda}))_{\bar{\lambda} \in \bar{\Lambda}_k}$  and  $(\hat{p}_k(\hat{\lambda}))_{\hat{\lambda} \in \hat{\Lambda}_k}$  are probabilistic weights;
- 3) each nonempty track,  $\bar{\tau} \in \bigcup \bar{\Lambda}_k$  or  $\hat{\tau} \in \bigcup \hat{\Lambda}_k$ , is accompanied by track PD,  $\bar{f}_k(\cdot|\bar{\tau})$  or  $\hat{f}_k(\cdot|\hat{\tau})$ , on the state space  $E$ .

Thus, the predicted  $\bar{\phi}_k$  is represented by *parameters*,  $((\bar{p}_k(\bar{\lambda}))_{\bar{\lambda} \in \bar{\Lambda}_k}, (\bar{f}_k(\cdot|\bar{\tau}))_{\bar{\tau} \in \bigcup \bar{\Lambda}_k}, \bar{y}_k)$ , the updated JMD  $\hat{\phi}_k$  by  $((\hat{p}_k(\hat{\lambda}))_{\hat{\lambda} \in \hat{\Lambda}_k}, (\hat{f}_k(\cdot|\hat{\tau}))_{\hat{\tau} \in \bigcup \hat{\Lambda}_k}, \hat{y}_k)$ , through (43) and (44). Those parameters, which we may call *sufficient statistics*,<sup>59</sup> are recursively calculated as shown in the next two sections.

## B. RFSet Filtering Update

The conditional JMD is updated, from  $\bar{\phi}_k$  to  $\hat{\phi}_k$ , by the *Bayes update formula*, as

$$\hat{\phi}_k(X_k) = \frac{\phi_{Mk}(Y_k|X_k)\bar{\phi}_k(X_k)}{\int_{\mathcal{F}(E)} \phi_{Mk}(Y_k|X)\bar{\phi}_k(X)\mathcal{M}(dX)}. \quad (45)$$

As proven in Appendix B, the updated parameter  $(\hat{p}(\hat{\lambda}))_{\hat{\lambda} \in \hat{\Lambda}_k}$  of the conditional JMD  $\hat{\phi}_k(X_k)$  is obtained from the parameters  $((\bar{p}(\bar{\lambda}))_{\bar{\lambda} \in \bar{\Lambda}_k}, (\bar{f}_k(\cdot|\bar{\tau}))_{\bar{\tau} \in \bigcup \bar{\Lambda}_k}, \bar{y}_k)$  of the predicted JMD  $\bar{\phi}_k(X_k)$  defined in (43) and (44), and from the sensor model defined by (40) and (41) with parameters  $(p_{Dk}, p_{Mk}, \gamma_{FAk})$ , as the Poisson version of Reid form,

$$\hat{p}_k(\hat{\lambda}) = C_{Rk}^{-1} \bar{p}_k(\bar{\lambda}) \left( \prod_{\substack{\hat{\tau} \in \hat{\lambda} \\ \hat{\tau}_{(k-1)} \neq \emptyset}} L_{MDk}(\hat{\tau}) \right) \left( \prod_{\substack{y \in Y_k \\ \{(k,y)\} \in \hat{\lambda}}} \gamma_{MNDk}(y) \right) \left( \prod_{\substack{y \in Y_k \\ (k,y) \notin \hat{\lambda}}} \gamma_{FAk}(y) \right) \quad (46)$$

for each updated hypothesis  $\hat{\lambda}$  in the set  $\hat{\Lambda}_k$  that is defined as<sup>60</sup>

$$\hat{\Lambda}_k = \left\{ \lambda_{OLDk}(\bar{\lambda}, \bar{a}) \cup \lambda_{NEWk}(Y_{Nk}) \left| \begin{array}{l} \bar{\lambda} \in \bar{\Lambda}_k, \\ \bar{a} \in \bar{\mathcal{A}}(\bar{\lambda}, Y_k) \text{ and} \\ Y_{Nk} \subseteq Y_k \setminus \text{Im}(\bar{a}) \end{array} \right. \right\} \quad (47)$$

with

$$\left\{ \begin{array}{l} \lambda_{OLDk}(\bar{\lambda}, \bar{a}) = \{\bar{\tau} \cup \{(k, \bar{a}(\bar{\tau}))\} | \bar{\tau} \in \text{Dom}(\bar{a})\} \\ \quad \cup (\bar{\lambda} \setminus \text{Dom}(\bar{a})), \\ \lambda_{NEWk}(Y_{Nk}) = \{k\} \times Y_{Nk}. \end{array} \right. \quad (48)$$

Equation (46) can be obtained by applying Poisson assumption (A8) to Reid form (30). The right-hand side of (46) consists of 1) Poisson version  $C_{Rk}'$  of Reid

constant, 2) the prior probability  $\bar{p}_k(\bar{\lambda})$  of the unique predecessor  $\bar{\lambda} = \hat{\lambda}_{|(k-1)}$  of each  $\hat{\lambda}$  in  $\bar{\Lambda}_k$ , 3) the extended track-to-measurement likelihood  $L_{MDk}(\hat{\tau})$  defined in (27) with  $\tau_{|k} = \hat{\tau}$ , 4) the newly detected target measurement IMD  $\gamma_{MNDk}(y)$  defined in (27), and 5) the false alarm IMD  $\gamma_{FAk}(y)$  of the Poisson false alarm JMD  $\phi_{FAk}$ . The rest of the parameters for the updated JMD  $\hat{\phi}_k(X_k)$  are updated to  $(\hat{f}_k(\cdot|\hat{\tau}))_{\hat{\tau} \in \bigcup \hat{\Lambda}_k}$  and  $\hat{y}_k$  in the first equations of (28) and (29) from  $(\bar{f}_k(\cdot|\bar{\tau}))_{\bar{\tau} \in \bigcup \bar{\Lambda}_k}$  and  $\bar{y}_k$ , respectively.

We should immediately note that (46) is the Reid form for evaluating association hypotheses recursively, shown in [6, eq. 16, p. 848], and that (47) expresses the recursive hypothesis expansion that corresponds almost exactly to the illustration in [6, Fig. 2, p. 846].

We should also note that, as seen in (48), each track (and hence each hypothesis) is defined through the value  $y \in Y_k$  of each measurement in each frame  $Y_k$  (that is defined as an RFSet), not through the measurement index, as having been done in Section III-C. Since we assume that the diagonal set  $D_{Mkm}$  in each order- $m$  product measurement space  $(E_{Mk})^m$  has zero product measure, we maintain the no-merged-or-split-measurement assumption (A2). Since every measurement frame is *data* or *observation*, we can reorder (or relabel) measurements in the RFSet-modeled frame in any arbitrary way (as we wish), and yet we obtain the same permutable target state likelihoods. For this reason, this difference in the definition of hypothesis is inconsequential, and in that sense, the hypothesis evaluation (46) is exactly the same as Reid form (30), except for the Poisson assumption (A8).

However, there is an important difference that we should note: In Section III-C, we define the hypotheses as possible realizations of an RFSet, which we call “association,” so that their evaluation is to calculate the conditional probabilities, while the hypotheses in this section appear only as *parameters* to define *weights* in (43). As shown in Appendix B, the fact that the set of weights,  $(\hat{p}_k(\hat{\lambda}))_{\hat{\lambda} \in \hat{\Lambda}_k}$ , is indeed in a *unit simplex* is a consequence of the evaluation of the denominator of the right-hand side of the update equation (45), i.e., the normalizing constant, under the induction assumption that  $(\bar{p}_k(\bar{\lambda}))_{\bar{\lambda} \in \bar{\Lambda}_k}$  is a set of probabilistic weights.

## C. RFSet Filtering Extrapolation

Since the Markov process  $(X_1, X_2, \dots)$  on measure space  $(\mathcal{F}(E), \mathcal{B}(B), \mathcal{M})$  is defined in Section V-A with the transition JMD  $\phi_{TRNk}$ , for each  $t_k < t_{k+1}$ , the *predicted* JMD  $\bar{\phi}_{k+1}$  of  $X_{k+1}$  conditioned on  $(Y_{k'})_{k'=1}^k$  is obtained by extrapolating the *previously updated* JMD  $\hat{\phi}_k$ , as

$$\bar{\phi}_{k+1}(X_{k+1}) = \int_{\mathcal{F}(E)} \phi_{TRNk}(X_{k+1}|X_k)\hat{\phi}_k(X_k)\mathcal{M}(dX_k). \quad (49)$$

<sup>59</sup>These *sufficient statistics* are not finite dimensional unless the track PDs and undetected target IMDs have finite-dimensional representations, which, most likely, exist only approximately.

<sup>60</sup>Using convention  $\bar{\mathcal{A}}(\emptyset, Y) = \{\emptyset\}$  with  $\text{Dom}(\emptyset) = \text{Im}(\emptyset) = \emptyset$ .

As shown in Appendix B, the representation (parameters)  $((\hat{p}_k(\hat{\lambda}))_{\hat{\lambda} \in \hat{\Lambda}_k}, (\hat{f}_k(\cdot|\hat{\tau}))_{\hat{\tau} \in \cup \hat{\Lambda}_k}, \hat{\gamma}_k)$  of the conditional JMD  $\hat{\phi}_k$  is extrapolated to  $((\bar{p}_{k+1}(\bar{\lambda}))_{\bar{\lambda} \in \bar{\Lambda}_{k+1}}, (\bar{f}_{k+1}(\cdot|\bar{\tau}))_{\bar{\tau} \in \cup \bar{\Lambda}_{k+1}}, \bar{\gamma}_{k+1})$  for the conditional JMD  $\bar{\phi}_{k+1}$  as

1) the extrapolated probabilistic weights

$$\bar{p}_{k+1}(\bar{\lambda}) = \sum_{\substack{\hat{\lambda} \in \hat{\Lambda}_k \\ \hat{\lambda} \supseteq \bar{\lambda}}} \hat{p}_k(\hat{\lambda}) \left( \prod_{\bar{\tau} \in \bar{\lambda}} P_{S_k}(\bar{\tau}) \right) \left( \prod_{\hat{\tau} \in \hat{\lambda} \setminus \bar{\lambda}} (1 - P_{S_k}(\hat{\tau})) \right) \quad (50)$$

for each *predicted* hypothesis  $\bar{\lambda}$  in

$$\bar{\Lambda}_{k+1} = \bigcup_{\hat{\lambda} \in \hat{\Lambda}_k} \mathcal{F}(\hat{\lambda}) = \{\bar{\lambda} \subseteq \hat{\lambda} | \hat{\lambda} \in \hat{\Lambda}_k\} \quad (51)$$

with the *track survival probability*  $P_{S_k}(\hat{\tau})$  defined by

$$P_{S_k}(\hat{\tau}) = \int_E p_{S_k}(x_k) \hat{f}_k(x_k|\hat{\tau}) \mu(dx_k) \quad (52)$$

for each  $\hat{\tau} \in \cup \hat{\Lambda}_k$ ;

2) the extrapolated target state PD  $\bar{f}_{k+1}(\cdot|\bar{\tau})$  for any surviving track  $\bar{\tau} \in \cup \bar{\Lambda}_{k+1} = \cup \hat{\Lambda}_k$  as

$$\bar{f}_{k+1}(x_{k+1}|\bar{\tau}) = P_{S_k}(\bar{\tau})^{-1} \int_E f_{Tk}(x_{k+1}|x_k) p_{S_k}(x_k) \hat{f}_k(x_k|\bar{\tau}) \mu(dx_k); \quad (53)$$

3) the predicted IMD of the undetected targets that are either surviving or newly born as

$$\bar{\gamma}_{k+1}(x_{k+1}) = \gamma_{Bk}(x_{k+1}) + \int_E f_{Tk}(x_{k+1}|x_k) p_{S_k}(x_k) \hat{\gamma}_k(x_k) \mu(dx_k). \quad (54)$$

Death of any previously detected target is *hypothesized* by  $\hat{\tau} \in \hat{\lambda} \setminus \bar{\lambda}$  through an *updated hypothesis*  $\hat{\lambda} \in \hat{\Lambda}_k$  and a *predicted hypothesis*  $\bar{\lambda} \in \bar{\Lambda}_{k+1}$  such that  $\bar{\lambda} \subseteq \hat{\lambda}$ , which may break the tree structure of the hypotheses described in Section IV-A. The extrapolation, as described earlier, should take place only when  $t_{k+1} > t_k$ . In case  $t_{k+1} = t_k$ , we should let  $\bar{\Lambda}_{k+1} = \hat{\Lambda}_k$ ,  $\bar{p}_{k+1} = \hat{p}_k$ , and  $\bar{f}_{k+1}(\cdot|\bar{\tau}) = \hat{f}_k(\cdot|\bar{\tau})$  for any  $\bar{\tau} \in \cup \bar{\Lambda}_{k+1} = \cup \hat{\Lambda}_k$ , to avoid any unwanted “jumps.”

#### D. Track Continuity

At least to the authors of this paper, it is rather surprising to see that, when we eliminate the birth–death model from the state transition described in Section V-A, i.e., with  $\gamma_{Bk} \equiv 0$  and  $p_{S_k} \equiv 1$ , a purely stochastic-process-on-FICM RFSet model of Section V-A regenerates Reid form (30), exactly by (46), and the state estimation of (36) by (43) and (44), in Section V-B, with Poisson assumption<sup>61</sup> (A8). We should remember that Reid form (30) was derived in Section IV, 1) with

<sup>61</sup>The RFSet filtering shown in Sections V-A to V-C should be easily extended to non-Poisson cases.

target model of an RFSeq (or FPP or RFSet) of stochastic processes and 2) with data association hypotheses defined as the set of all the possible realizations of a random element, called “data association.” This validates a claim made in [38]: “The MHT can be derived from an RFSet MTT algorithm.” We should note that, however, in the RFSet-based algorithm as described in this section, the hypotheses appear only as “indices,” with which probabilistic weights over the GMBer terms of (43) are expressed, not as the probabilistic evaluation of possible realizations of a random element as we defined as *association*.

The target transition model in RFSet formalism, described in Section V-A, does have an appearance that targets may *exchange* their states among them because the state transition is expressed as RFSet-state-to-RFSet transition. In fact, our motivation of using a set of stochastic processes, rather than a single stochastic process on an FICM, is to avoid the *target switches* of this kind, *through the most obvious and explicit way*. To the best of our knowledge, there are at least two known efforts to avoid these target switches. These two are based on two quite different approaches: 1) the introduction of the *labeled* RFSets in [33] and 2) the use of *trajectory states* in [39]. The former adds an extra state element, called a *label* to each single target state, to prevent target exchange during the extrapolation step, according to our interpretation. The latter extends<sup>62</sup> the individual target state to the consecutive series, from the target’s birth to the current state, again to prevent the “target exchange,” which is characterized as the maintenance of the track continuity in [39].

After having seen the re-creation of Reid form (30) by (46) in this section, sharing the same conclusion by [38], as we understand, we are not quite sure now if all those *precautions* to maintain track continuity are really necessary, or if they are mere *precauzione inutile*. It seems to us, at this point, that the track continuity issues are implicitly taken care of by the use of the concept of the tracks (and hypotheses), which is actually a core concept of the MHT.

## VI. CONCLUSIONS

We presented three mathematical formalisms, i.e., RFSeq, FPP, and RFSet formalisms, which provide us with theoretical foundations for MTT problems in general, and the basis for MHT in particular, when generally multiple sensors provide target detections with uncertain origins. MHT, as a concept for providing solutions to MTT problems, has been studied over the last 40 years extensively, as described in [8]. In this paper, using a general class of target and sensor models, we revisited the

<sup>62</sup>By this extension, the trajectory-state estimation may be considered as a variable-time-interval smoothing, i.e., estimation of each target trajectory from the moment of the birth to the current state or to the time when the target is killed.

generation and evaluation of data association hypotheses, and provided some new perspectives, by presenting them using, side by side, the three different formalisms. Those three may appear quite differently on the surface but are almost equivalent to each other except for subtle differences, e.g., those caused by *repeated elements* that are allowed in an RFSeq or an FPP but not in an RFSet.

Based on target models that use the concept of a set of stochastic processes, rather than a single stochastic process on FM (RFSeq), FCM (FPP), or FICM (RFSet), and sensor models with RFSeq outputs, we explicitly defined data association as a discrete-valued random element. We called all of its possible realizations data association hypotheses, as defined in Section III-C. The two well-known hypothesis evaluation forms, Morefield form and Reid form, were then derived in Section IV-B and IV-C, with a gradual introduction of commonly used assumptions, (A1–A8). Although hypotheses can be defined without the independence assumptions, the familiar hypothesis–track structure of MHT appeared only after the independence assumptions (A5 and A6) were introduced. The consequences of the other assumptions were rather predictable: the separation of evaluation of the probabilities of the number of newly detected targets and that of data association hypotheses was obtained by the Poisson assumption (A8), and the familiar extrapolation–update recursion structure appeared with the introduction of the Markov assumption (A7).

In Section V, we stated our perspectives on the recently developed RFSet-based MTT algorithms, for which intimate relations to MHT were claimed. We observed that not only the MHT hypothesis–track structure emerged as described in [36], but also the exact Reid form was *surprisingly* re-created from a *pure* RFSet model, which we think is consistent with the claim made by Brekke and Chitre [38]. Our conjecture on the reason for this reappearance of Reid form is the use of the hypothesis/track structure that forces the desired *continuity*, well within the context of MHT.

The MTT algorithm developments based on RFSet formalism, also known as FISST formalism [25]–[27], were relatively new, compared with the long history of FPP formalism, which is claimed to have started with [24]. The authors hope some *old* wisdom may benefit our efforts in advancing MTT technologies further.

#### APPENDIX A: DERIVATION OF HYPOTHESIS EVALUATION EQUATIONS

Under Assumptions A1–A3, for any cumulative frame  $(y_k)_{k=1}^K = ((y_{kj})_{j=1}^{m_k})_{k=1}^K$ , it follows from (16) that data association  $\lambda_K \in \Lambda_K$  on  $(y_k)_{k=1}^K$  can be evaluated as

$$\begin{aligned} P(\lambda_K | (y_k)_{k=1}^K) &= \sum_{n=\#(\lambda_K)}^{\infty} P(\lambda_K, n | (y_k)_{k=1}^K) \\ &= P((y_k)_{k=1}^K)^{-1} \sum_{n=\#(\lambda_K)}^{\infty} \frac{n!}{(n-\#(\lambda_K))!} P((y_k, a_k)_{k=1}^K, n), \end{aligned} \quad (\text{A.1})$$

where  $n$  is the number of targets and  $(a_k)_{k=1}^K \in \prod_{k=1}^K \bar{\mathcal{A}}(\{1, \dots, n\}, \{1, \dots, m_k\})$  is, for a given  $(\lambda_K, n)$ , any one of the  $n!/(n-\#(\lambda_K))!$  multiframe target assignment hypotheses that support  $\lambda_K$ , in the sense that the pair  $(\lambda_K, (a_k)_{k=1}^K)$  satisfies (13).

In the RFSeq formalism, with additional assumptions (A4–A6), substitute (18) into (17), and apply  $f^{(n)}(((x_i(t_k))_{\kappa \in [K]})_{i=1}^n; (t_k)_{\kappa \in [K]}) = \prod_{i=1}^n f_{\text{TGT}}((x_i(t_k))_{\kappa \in [K]}; (t_k)_{\kappa \in [K]})$ .

Then, we have

$$\begin{aligned} P((y_k, a_k)_{k=1}^K, n) &= P(((y_{kj})_{j=1}^{m_k}, a_k)_{k=1}^K | n) p_n \\ &= p_n v^{-n} \left( \prod_{k=1}^K \frac{L_{\text{FAk}}(\{1, \dots, m_k\} \setminus \text{Im}(a_k))}{m_k!} \right) \\ &\int_{E^{\#([K])^n}} \left( \prod_{k=1}^K \left( \prod_{i \in \text{Dom}(a_k)} p_{\text{Mk}}(y_{ka_k(i)} | x_i(t_k)) p_{\text{Dk}}(x_i(t_k)) \right) \right. \\ &\left. \left( \prod_{\substack{i=1 \\ i \notin \text{Dom}(a_k)}}^n (1 - p_{\text{Dk}}(x_i(t_k))) \right) \right) \\ &\prod_{i=1}^n \gamma_{\text{TGT}}((x_i(t_k))_{\kappa \in [K]}; (t_k)_{\kappa \in [K]}) \mu^{\#([K])}((dx_i(t_k))_{\kappa \in [K]}), \end{aligned} \quad (\text{A.2})$$

where the a priori target state IMD, over  $(t_k)_{\kappa \in [K]}$ , with a priori mean  $v = \sum_{n=1}^{\infty} n p_n < \infty$  of the number of targets, is  $\gamma_{\text{TGT}}((x_i(t_k))_{\kappa \in [K]}; (t_k)_{\kappa \in [K]}) = v f_{\text{TGT}}((x_i(t_k))_{\kappa \in [K]}; (t_k)_{\kappa \in [K]})$ , and  $L_{\text{FAk}}(I_{\text{FAk}})$  is the false alarm likelihood defined by (19).

Let the integral in (A.2) over the set  $E^{\#([K])^n}$  be  $L_{\text{TGTk}}((y_k, a_k)_{k=1}^K; n)$ . Then, when  $(a_k)_{k=1}^K$  supports  $\lambda_K$  (i.e., for which (13) holds) with  $\#(\lambda_K) \leq n$ , we have

$$\begin{aligned} L_{\text{TGTk}}((y_k, a_k)_{k=1}^K; n) &= \prod_{i=1}^n \int_{E^{\#([K])}} \left( \prod_{\substack{k=1 \\ i \in \text{Dom}(a_k)}}^K p_{\text{Mk}}(y_{ka_k(i)} | x_i(t_k)) p_{\text{Dk}}(x_i(t_k)) \right) \\ &\left( \prod_{\substack{k=1 \\ i \notin \text{Dom}(a_k)}}^K (1 - p_{\text{Dk}}(x_i(t_k))) \right) \\ &\gamma_{\text{TGT}}((x_i(t_k))_{\kappa \in [K]}; (t_k)_{\kappa \in [K]}) \\ &\mu^{\#([K])}((dx_i(t_k))_{\kappa \in [K]}) \\ &= \left( \prod_{\tau \in \lambda_K} \int_{E^{\#([K])}} \left( \prod_{k=1}^K q_{\text{MDk}}(\xi_k; \tau) \right) \gamma_{\text{TGT}}((\xi_k)_{\kappa \in [K]}; (t_k)_{\kappa \in [K]}) \right. \\ &\left. \mu^{\#([K])}((d\xi_k)_{\kappa \in [K]}) \right) \\ &\left( \int_{E^{\#([K])}} \left( \prod_{k=1}^K (1 - p_{\text{Dk}}(\xi_k)) \right) \right. \\ &\left. \gamma_{\text{TGT}}((\xi_k)_{\kappa \in [K]}; (t_k)_{\kappa \in [K]}) \mu^{\#([K])}((d\xi_k)_{\kappa \in [K]}) \right)^{n-\#(\lambda_K)} \\ &= \left( \prod_{\tau \in \lambda_K} L_{\text{TRKk}}(\tau) \right) L_{\text{TRKk}}(\emptyset)^{n-\#(\lambda_K)} \\ &= \left( \prod_{\tau \in \lambda_K} L_{\text{TRKk}}(\tau) \right) (\hat{v}_K)^{n-\#(\lambda_K)}, \end{aligned} \quad (\text{A.3})$$

where  $L_{\text{TRKK}}(\tau)$  is the track likelihood defined by (21) with (22), and  $\hat{v}_K = L_{\text{TRKK}}(\emptyset)$  is the a posteriori expected number of targets that remain undetected over the  $K$  frames. Then, substituting (A.3) into (A.2), and substituting (A.2) into (A.1), we obtain Morefield form (20), which completes the derivation of the hypothesis evaluation in RFSeq formalism.

In FPP or RFSet formalism, the integral in (17), and the  $n$ -PD  $f^{(n)}$  in its integrand, should be replaced by the set integral defined in (2) or (4), and by the JMD  $\phi(\cdot; (t_k)_{k \in (K)})$ . The constant  $n!$ , included in the JMD in either FPP or RFSet formalism, is cancelled out by  $1/n!$  included in the definition of the set integral in (2) or (4), resulting in the same expression as the one by (A.3), and hence, we have the same hypothesis evaluation equation, i.e., Morefield form (20).

The recursive form hypothesis evaluation equation, i.e., Reid form (30), can be readily derived from its batch-processing counterpart, Morefield form (20), with or without Markov assumption (A7), and vice versa (i.e., from Reid form to Morefield form).

## APPENDIX B : DERIVATION OF SOLUTION TO AN RFSET FILTER

This appendix provides a proof to our assertion that, under the assumptions made in Section V-A, the conditional JMDs,  $\bar{\phi}_k$  and  $\hat{\phi}_k$ , defined by (42), can be written as the convolutions of the GMBer JMDs,  $\bar{\phi}_{\text{D}k}$  and  $\hat{\phi}_{\text{D}k}$ , defined by (43), and the Poisson JMDs,  $\bar{\phi}_{\text{U}k}$  and  $\hat{\phi}_{\text{U}k}$ , of (44), respectively. Our proof is one by mathematical induction, giving a proof to all the update and extrapolation equations (46)–(48) and (50)–(54), together at the same time.

For  $k = 1$ , we have  $\bar{\Lambda}_1 = \{\emptyset\}$ , and  $\bar{\phi}_{U1} = \bar{\phi}_1$  is the Poisson initial-state JMD. For any  $k \geq 1$ , let assume, as the induction assumption, that  $\bar{\phi}_k$  is the convolution  $\bar{\phi}_k = \bar{\phi}_{\text{D}k} \otimes \bar{\phi}_{\text{U}k}$  of the GMBer  $\bar{\phi}_{\text{D}k}$  given in (43) and Poisson JMD  $\bar{\phi}_{\text{U}k}$  in (44). This convolution can be rewritten as

$$\bar{\phi}_k(\{x_i\}_{i=1}^n) = e^{-\bar{v}_k} \sum_{\bar{\lambda} \in \bar{\Lambda}_k} \bar{p}_k(\bar{\lambda}) \sum_{\bar{\alpha} \in \mathcal{A}(\bar{\lambda}, \{1, \dots, n\})} \left( \prod_{\bar{\tau} \in \bar{\lambda}} \bar{f}_k(x_{\bar{\alpha}(\bar{\tau})} | \bar{\tau}) \right) \left( \prod_{i \notin \text{Im}(\bar{\alpha})} \bar{\gamma}_k(x_i) \right). \quad (\text{B.1})$$

The JMD likelihood function  $\phi_{\text{M}k}$  for frame  $Y_k = \{y_{kj}\}_{j=1}^{m_k}$ , defined as the convolution of MBe JMD  $\phi_{\text{M}k}$ , defined by (40) and (41), and of Poisson JMD  $\phi_{\text{FA}k}$ , can be written as

$$\phi_{\text{M}k}(\{y_{kj}\}_{j=1}^{m_k} | \{x_i(t_k)\}_{i=1}^n) = e^{-v_{\text{FA}k}} \sum_{a \in \bar{\mathcal{A}}(\{1, \dots, n\}, \{1, \dots, m_k\})} \left( \prod_{i \in \text{Dom}(a)} p_{\text{M}k}(y_{ka(i)} | x_i(t_k)) p_{\text{D}k}(x_i(t_k)) \right) \left( \prod_{i \notin \text{Dom}(a)} (1 - p_{\text{D}k}(x_i(t_k))) \right) \left( \prod_{j \notin \text{Im}(a)} \gamma_{\text{FA}k}(y_{kj}) \right). \quad (\text{B.2})$$

It follows from (B.1) and (B.2) that

$$\begin{aligned} & \phi_{\text{M}k}(\{y_{kj}\}_{j=1}^{m_k} | \{x_i\}_{i=1}^n) \bar{\phi}_k(\{x_i\}_{i=1}^n) \\ &= e^{-v_{\text{FA}k} - \bar{v}_k} \sum_{\substack{\bar{\lambda} \in \bar{\Lambda}_k \\ \#(\bar{\lambda}) \leq n}} \bar{p}_k(\bar{\lambda}) \sum_{\bar{\alpha} \in \mathcal{A}(\bar{\lambda}, \{1, \dots, n\})} \sum_{a \in \bar{\mathcal{A}}(\{1, \dots, n\}, \{1, \dots, m_k\})} \\ & \left( \prod_{i \in \text{Im}(\bar{\alpha}) \cap \text{Dom}(a)} p_{\text{M}k}(y_{ka(i)} | x_i) p_{\text{D}k}(x_i) \bar{f}_k(x_i | \bar{\alpha}^{-1}(i)) \right) \\ & \left( \prod_{i \in \text{Im}(\bar{\alpha}) \setminus \text{Dom}(a)} (1 - p_{\text{D}k}(x_i)) \bar{f}_k(x_i | \bar{\alpha}^{-1}(i)) \right) \\ & \left( \prod_{i \in \text{Dom}(a) \setminus \text{Im}(\bar{\alpha})} p_{\text{M}k}(y_{ka(i)} | x_i) p_{\text{D}k}(x_i) \bar{\gamma}_k(x_i) \right) \\ & \left( \prod_{i \notin \text{Dom}(a) \cup \text{Im}(\bar{\alpha})} (1 - p_{\text{D}k}(x_i)) \bar{\gamma}_k(x_i) \right) \\ & \left( \prod_{\substack{j=1 \\ j \notin \text{Im}(a)}}^{m_k} \gamma_{\text{FA}k}(y_{kj}) \right), \end{aligned} \quad (\text{B.3})$$

where the five product factors, within the second summations over  $\bar{\mathcal{A}}(\{1, \dots, n\}, \{1, \dots, m_k\})$ , correspond to 1) targets detected before detected again, 2) targets detected before but not detected by frame  $k$ , 3) targets detected for the first time in frame  $k$ , 4) targets not detected before and remaining undetected, and 5) false alarms.

Each of the first three factors in (B.3) in the second summation can be written as the product of a particular assignment likelihood and the updated (or initiated) track PD obtained assuming that assignment. For example,  $p_{\text{M}k}(y_{ka(i)} | x_i) p_{\text{D}k}(x_i) \bar{f}_k(x_i | \bar{\tau})$  is the product of the likelihood  $\int_E p_{\text{M}k}(y_{ka(i)} | \xi) p_{\text{D}k}(\xi) \bar{f}_k(\xi | \bar{\tau}) \mu(d\xi)$  of track  $\bar{\tau}$  being assigned to measurement  $y_{ka(i)}$ , and the updated track PD  $\hat{f}_k(x_i | \bar{\tau} \cup \{(k, y_{ka(i)})\})$ .

When we calculate the denominator of (45) by the ‘‘set integral’’ defined in (4), because  $\phi_{\text{M}k}(\{y_{kj}\}_{j=1}^{m_k} | \{x_i\}_{i=1}^n) \bar{\phi}_k(\{x_i\}_{i=1}^n)$  is permutable with respect to  $(x_i)_{i=1}^n \in E^n$ , each term of the second summation over  $\bar{\alpha} \in \mathcal{A}(\bar{\lambda}, \{1, \dots, n\})$  of (B.3) becomes the same values in the integral, i.e.,  $n! / (n - \#(\bar{\lambda}))!$  times the one term obtained by any arbitrarily chosen  $\bar{\alpha} \in \mathcal{A}(\bar{\lambda}, \{1, \dots, n\})$ . Thus, rearranging the summations of (B.3) for the numerator of (45), the updated JMD is calculated as

$$\hat{\phi}_k(\{x_i\}_{i=1}^n) = e^{-\hat{v}_k} \sum_{\hat{\lambda} \in \hat{\Lambda}_k} \hat{p}_k(\hat{\lambda}) \sum_{\hat{a} \in \bar{\mathcal{A}}(\hat{\lambda}, \{1, \dots, n\})} \left( \prod_{\hat{\tau} \in \hat{\lambda}} \hat{f}_k(x_{\hat{a}(\hat{\tau})} | \hat{\tau}) \right) \left( \prod_{i \notin \text{Im}(\hat{a})} \hat{\gamma}_k(x_i) \right), \quad (\text{B.4})$$

which is nothing but the convolution  $\hat{\phi}_k = \hat{\phi}_{\text{D}k} \otimes \hat{\phi}_{\text{U}k}$  of  $\hat{\phi}_{\text{D}k}$  defined in (43) and of  $\hat{\phi}_{\text{U}k}$  defined in (44), with parameters  $(\hat{p}_k(\hat{\lambda}))_{\hat{\lambda} \in \hat{\Lambda}_k}$ ,  $(\hat{f}_k(\cdot | \hat{\tau}))_{\hat{\tau} \in \text{U}\hat{\Lambda}_k}$ ,  $\hat{\gamma}_k$  defined in (46), (28), and (29).

To derive the extrapolation formulas in Section V-C, we first should observe that  $\bar{\phi}_{k+1} = \bar{\phi}_{\text{D}(k+1)} \otimes \bar{\phi}_{\text{U}(k+1)}$

with  $\tilde{\phi}_{U(k+1)} = \tilde{\phi}_{U(k+1)} \otimes \phi_{Bk}$ , where

$$\begin{cases} \tilde{\phi}_{D(k+1)}(X_{D(k+1)}) = \int_{\mathcal{F}(E)} \phi_{\text{TSk}}(X_{D(k+1)}|X_{Dk}) \\ \quad \hat{\phi}_{Dk}(X_{Dk})\mathcal{M}(dX_{Dk}) \\ \tilde{\phi}_{U(k+1)}(X_{U(k+1)}) = \int_{\mathcal{F}(E)} \phi_{\text{TSk}}(X_{U(k+1)}|X_{Uk}) \\ \quad \hat{\phi}_{Uk}(X_{Uk})\mathcal{M}(dX_{Uk}) \end{cases} \quad (\text{B.5})$$

implying that  $\tilde{\phi}_{D(k+1)}$  and  $\tilde{\phi}_{U(k+1)}$  are independent<sup>63</sup> from each other, since  $\hat{\phi}_{Dk}$  and  $\hat{\phi}_{Uk}$  are independent from each other.  $\phi_{Bk}$  is independent from  $\tilde{\phi}_{D(k+1)}$  and from  $\tilde{\phi}_{U(k+1)}$  because  $\phi_{\text{TRNk}}(\cdot|X_k) = \phi_{\text{TSk}}(\cdot|X_k) \otimes \phi_{Bk}(\cdot)$ .

On the other hand, we can rewrite (38) and (39) as

$$\begin{aligned} \phi_{\text{TSk}}(\{x_i\}_{i=1}^n | \{x'_i\}_{i=1}^{n'}) &= \sum_{\substack{a' \in \tilde{\mathcal{A}}(\{1, \dots, n'\}, \{1, \dots, n\}) \\ \#(\text{Dom}(a'))=n}} \\ &\left( \prod_{i' \in \text{Dom}(a')} f_{\text{Tk}}(x_{a'(i')} | x'_{i'}) p_{\text{Sk}}(x'_{i'}) \right) \\ &\left( \prod_{\substack{i'=1 \\ i' \notin \text{Dom}(a')}}^{n'} (1 - p_{\text{Sk}}(x'_{i'})) \right). \end{aligned} \quad (\text{B.6})$$

By substituting the second equation of (43), and (B.6) into the first equation of (B.5), following the definition (4) of the ‘‘set integral,’’ we have

$$\begin{aligned} &\tilde{\phi}_{D(k+1)}(\{x_i\}_{i=1}^n) \\ &= \int_{\mathcal{F}(E)} \phi_{\text{TSk}}(\{x_i\}_{i=1}^n | \{x'_i\}_{i=1}^{n'}) \\ &\quad \hat{\phi}_{Dk}(\{x'_i\}_{i=1}^{n'}) \mathcal{M}(d\{x'_i\}_{i=1}^{n'}) \\ &= \sum_{n'=0}^{\infty} \frac{1}{n'!} \sum_{\substack{a' \in \tilde{\mathcal{A}}(\{1, \dots, n'\}, \{1, \dots, n\}) \\ \#(\text{Dom}(a'))=n}} \int_{E^{n'}} \\ &\quad \left( \prod_{i' \in \text{Dom}(a')} f_{\text{Tk}}(x_{a'(i')} | x'_{i'}) p_{\text{Sk}}(x'_{i'}) \right) \\ &\quad \left( \prod_{\substack{i'=1 \\ i' \notin \text{Dom}(a')}}^{n'} (1 - p_{\text{Sk}}(x'_i)) \right) \\ &\quad \left( \sum_{\substack{\hat{\lambda} \in \hat{\Lambda}_k \\ \#(\hat{\lambda})=n'}} \hat{p}_k(\hat{\lambda}) \sum_{\hat{\alpha} \in \hat{\mathcal{A}}(\hat{\lambda}, \{1, \dots, n'\})} \prod_{\hat{\tau} \in \hat{\lambda}} \hat{f}_k(x'_{\hat{\alpha}(\hat{\tau})} | \hat{\tau}) \right) \\ &\quad \prod_{i'=1}^{n'} \mu(dx'_{i'}) \\ &= \sum_{\hat{\lambda} \in \hat{\Lambda}_k} \hat{p}_k(\hat{\lambda}) \sum_{\substack{a' \in \tilde{\mathcal{A}}(\hat{\lambda}, \{1, \dots, n\}) \\ \#(\text{Dom}(a'))=n}} \frac{1}{\#(\hat{\lambda})!} \sum_{\hat{\alpha} \in \hat{\mathcal{A}}(\hat{\lambda}, \{1, \dots, \#(\hat{\lambda})\})} \\ &\quad \left( \prod_{\hat{\tau} \in \text{Dom}(a') \setminus E} \int f_{\text{Tk}}(x_{a'(\hat{\tau})} | x'_{\hat{\alpha}(\hat{\tau})}) p_{\text{Sk}}(x'_{\hat{\alpha}(\hat{\tau})}) \right. \\ &\quad \left. \hat{f}_k(x'_{\hat{\alpha}(\hat{\tau})} | \hat{\tau}) \mu(dx'_{\hat{\alpha}(\hat{\tau})}) \right) \\ &\quad \left( \prod_{\hat{\tau} \in \hat{\lambda} \setminus \text{Dom}(a') \setminus E} \int (1 - p_{\text{Sk}}(x'_{\hat{\alpha}(\hat{\tau})})) \right. \\ &\quad \left. \hat{f}_k(x'_{\hat{\alpha}(\hat{\tau})} | \hat{\tau}) \mu(dx'_{\hat{\alpha}(\hat{\tau})}) \right). \end{aligned} \quad (\text{B.7})$$

<sup>63</sup>More precisely, the RFsets represented by conditional JMT  $\tilde{\phi}_{D(k+1)}$  and  $\tilde{\phi}_{U(k+1)}$  are independent.

For given any  $\hat{\lambda} \in \hat{\Lambda}_k$ , the last summation of (B.7) is over all the enumerations of the tracks in  $\hat{\lambda}$ . The summation for all the  $a''$ 's in  $\tilde{\mathcal{A}}(\hat{\lambda}, \{1, \dots, n\})$  such that  $\#(\text{Dom}(a'')) = n$  is the summation over all the choices of subsets  $\bar{\lambda}$  of  $\hat{\lambda}$ , such that  $\#(\bar{\lambda}) = n \leq \#(\hat{\lambda}) = n'$ , plus all the possible enumerations of the tracks in the ‘‘decimated’’ hypothesis  $\bar{\lambda}$ . Hence, we have (51), and we can rewrite (B.7) in the form of first equation of (43) with the index  $k$  replaced by  $k+1$ , with the probabilistic weights  $(\bar{p}_{k+1}(\bar{\lambda}))_{\bar{\lambda} \in \bar{\Lambda}_{k+1}}$  defined by (50), and with the track PDs,  $(\hat{f}_{k+1}(\cdot | \hat{\tau}))_{\hat{\tau} \in U \cup \bar{\Lambda}_{k+1}}$ , defined by (53).

Since  $\hat{\phi}_{Uk}$  is Poisson and the transition PD  $\phi_{\text{TSk}}$  of (38) is target-wise independent,  $\tilde{\phi}_{U(k+1)}$  defined by the second equation of (B.5) is also Poisson with the IMD defined as the second term of the right-hand side of (54). Since  $\tilde{\phi}_{U(k+1)}$  is independent of  $\phi_{Bk}$ , we have the Poisson JMD  $\tilde{\phi}_{U(k+1)} = \tilde{\phi}_{U(k+1)} \otimes \phi_{Bk}$ , which completes the proof by mathematical induction for all the update and prediction formulas in Section V-B and V-C.

## REFERENCES

- [1] Y. Bar-Shalom, X. R. Li, and T. Kirubarajan *Estimation with Applications to Tracking and Navigation*. Hoboken, NJ: Wiley, 2001.
- [2] S. S. Blackman and R. Popoli *Design and Analysis of Modern Tracking Systems*. Norwood, MA: Artech House, 1999.
- [3] L. D. Stone, R. L. Streit, T. L. Corwin, and K. L. Bell *Bayesian Multiple Target Tracking*, 2nd ed. Norwood, MA: Artech House, 2014.
- [4] Y. Bar-Shalom ‘‘Tracking methods in a multitarget environment,’’ *IEEE Trans. Autom. Control*, vol. 23, no. 4, pp. 618–626, Aug. 1978.
- [5] C. L. Morefield ‘‘Application of 0–1 integer programming to multi-target tracking problems,’’ *IEEE Trans. Autom. Control*, vol. 23, no. 3, pp. 302–312, Jun. 1977.
- [6] D. B. Reid ‘‘An algorithm for tracking multiple targets,’’ *IEEE Trans. Autom. Control*, vol. 24, no. 6, pp. 843–854 Dec. 1979.
- [7] S. Mori, C.-Y. Chong, E. Tse, and R. P. Wishner ‘‘Tracking and classifying multiple targets without a priori identification,’’ *IEEE Trans. Autom. Control*, vol. 31, no. 5, pp. 401–409, May 1986.
- [8] C.-Y. Chong, S. Mori, and D. B. Reid ‘‘Forty years of multiple hypothesis tracking,’’ *J. Adv. Inf. Fusion*, vol. 14, no. 2, Dec. 2019; an earlier version appeared as C.-Y. Chong, S. Mori, and D. B. Reid ‘‘Forty years of multiple hypothesis tracking—A review of key developments,’’ in *Proc. 21st Int. Conf. Inf. Fusion*, Cambridge, UK, Jul. 2018.
- [9] S. Mori, C.-Y. Chong, and K. C. Chang ‘‘Three formalisms of multiple hypothesis tracking,’’ in *Proc. 19th Int. Conf. Inf. Fusion*, Heidelberg, Germany, Jul. 2016.
- [10] J. R. Munkres *Topology*, 2nd ed. London, U.K.: Pearson Education, 2015.
- [11] W. Rudin *Functional Analysis*. New York, NY: McGraw-Hill, 1973.

- [12] Y. Bar-Shalom and E. Tse  
“Tracking in a cluttered environment with probabilistic data association,”  
*Automatica*, vol. 11, pp. 451–460, Sep. 1975.
- [13] Y. Bar-Shalom  
“Extension of the probabilistic data association filter in multitarget tracking,”  
in *Proc. 5th Symp. Nonlinear Estimation*, San Diego, CA, Sep. 1974, pp. 16–21.
- [14] M. Lothaire  
*Combinatorics on Words*. Cambridge, U.K.: Cambridge University Press, 1997.
- [15] D. J. Daley and D. Vere-Jones  
*An Introduction to the Theory of Point Processes, vol. I: Elementary Theory and Methods*, 2nd ed. Berlin, Germany: Springer, 2003.
- [16] S. Mori and C.-Y. Chong  
“Point process formalism of multitarget tracking,”  
in *Proc. 5th Int. Conf. Inf. Fusion*, Annapolis, MD, Jul. 2002.
- [17] S. K. Srinivasan  
*Stochastic Theory and Cascade Processes*. New York, NY: Academic Elsevier, 1969.
- [18] L. Janossy  
“On the absorption of a nucleon cascade,”  
*Proc. R. Irish Acad. Sect. A: Math. Phys. Sci.*, vol. 53, pp. 181–188, 1950.
- [19] P. Blagojevic, V. Grujic, and R. Zivaljevic  
“Symmetric products of surfaces: a unifying theme for topology and physics,”  
in *Proc. Summer School Mod. Math. Phys., SFIN XV (A3)*, Institute of Physics, Belgrade, Serbia, 2002.
- [20] E. Michael  
“Topologies on spaces of subsets,”  
*Trans. Amer. Math. Soc.*, vol. 71, pp. 152–182, 1951.
- [21] S. Mori and E. Tse  
“A bargaining process modeled as an infinite dynamic non-cooperative game,”  
in *Proc. Amer. Control Conf.*, Arlington, VA, Jun. 1982.
- [22] A. F. Kaar  
*Point Processes and Their Statistical Inference*. New York, NY: Marcel Dekker, 1986.
- [23] J. E. Moyal  
“The general theory of stochastic population processes,”  
*Acta Math.*, vol. 108, pp. 1–31, 1962.
- [24] H. Wald  
“Sur les Processus Stationnaires Ponctuels,”  
in *Le Calcul des Probabilites et ses Applications*, no. 13. Paris, France: Centre National de la Recherche Scientifique, 1949.
- [25] R. P. S. Mahler  
*Statistical Multisource–Multitarget Information Fusion*. Norwood, MA: Artech House, 2007.
- [26] R. P. S. Mahler  
*Advances in Statistical Multisource–Multitarget Information Fusion*. Norwood, MA: Artech House, 2014.
- [27] I. R. Goodman, R. P. S. Mahler, and H. T. Nguyen  
*Mathematics of Data Fusion*. Dordrecht, The Netherlands: Kluwer Academic Publishers, 1997.
- [28] H. L. Royden  
*Real Analysis*, 3rd ed. Upper Saddle River, NJ: Prentice-Hall, 1988.
- [29] P. J. Daniell  
“A general form of integral,”  
*Ann. Math., Second Ser.*, vol. 19, no. 4, pp. 276–294, Jun. 1918.
- [30] K. Kastella  
“Joint multitarget probabilities for detection and tracking,”  
in *Proc. SPIE AEROSENSE '97 Conf. Acquisition, Tracking, Pointing XI*, Orlando, FL, Apr. 1997, vol. 3086, pp. 122–128.
- [31] S. Mori and C.-Y. Chong  
“Evaluation of data association hypotheses: Non-Poisson i.i.d. cases,”  
in *Proc. 7th Int. Conf. Inf. Fusion*, Stockholm, Sweden, Jul. 2004, pp. 1133–1140.
- [32] A. B. Poore and N. Rijavec  
“A new class of methods for solving data association problems arising from multitarget tracking,”  
in *Proc. Amer. Autom. Control Conf.*, Boston, MA, Jun. 1991, vol. 3, pp. 2302–2304.
- [33] B.-N. Vo, B.-T. Vo, and D. Phung  
“Labeled random finite sets and the Bayes multi-target tracking filter,”  
*IEEE Trans. Signal Process.*, vol. 62, no. 24, pp. 6554–6567, Dec. 2014.
- [34] S. Mori, K.-C. Chang, and C.-Y. Chong  
“Tracking aircraft by acoustic sensors—multiple hypothesis approach applied to possibly unresolved measurements,”  
in *Proc. Amer. Control Conf.*, Minneapolis, MN, Jun. 1987, pp. 1099–1103.
- [35] S. P. Coraluppi and C. A. Carthel  
“Multiple-hypothesis tracking for targets producing multiple measurements,”  
*IEEE Trans. Aerosp. Electron. Syst.*, vol. 54, no. 3, pp. 1485–1498, Jun. 2018.
- [36] J. Williams  
“Marginal multi-Bernoulli filters: RFS derivations of MHT, JIPDA, and association-based MeMBer,”  
*IEEE Trans. Aerosp. Electron. Syst.*, vol. 51, no. 3, pp. 1664–1687, Jul. 2015.
- [37] E. F. Brekke and M. Chitre  
“Relationship between finite set statistics and the multiple hypothesis tracker,”  
*IEEE Trans. Aerosp. Electron. Syst.*, vol. 54, no. 4, pp. 1902–1917, Jul. 2018.
- [38] E. F. Brekke and M. Chitre  
“The multiple hypothesis tracker derived from finite set statistics,”  
in *Proc. 20th Int. Conf. Inf. Fusion*, Xi’an, China, Jul. 2017.
- [39] K. Granström, L. Svensson, Y. Xia, J. Williams, and Á. F. García-Fernández  
“Poisson multi-Bernoulli mixture trackers: Continuity through random finite sets of trajectories,”  
in *Proc. Int. Conf. Inf. Fusion*, Cambridge, UK, Jul. 2018.
- [40] G. Mathéron  
*Random Sets and Integral Geometry*. Hoboken, NJ: Wiley, 1975.
- [41] D. B. Reid  
“A multiple hypothesis filter for tracking multiple targets in a cluttered environment,” Lockheed Report LMSC-D560254, Lockheed Palo Alto Research Laboratory, Palo Alto, CA, Sep. 1977.
- [42] D. Stoyan, W. S. Kendall, and J. Mecke  
*Stochastic Geometry and Its Applications*, 2nd ed. Hoboken, NJ: Wiley, 1995.
- [43] S. Mori and C.-Y. Chong  
“Data association hypothesis evaluation for i.i.d. but non-Poisson multiple target tracking,”  
in *Proc. SPIE Symp. Signal Data Process. Small Targets*, O. Drummond Ed. Orlando, FL, Apr. 2004, vol. 5428, pp. 224–236.
- [44] S. Mori  
“Random sets in data fusion,”  
in *Proc. SPIE Symp. Signal Data Process. Tracking Small Targets*, O. Drummond Ed. San Diego, CA, Aug. 1997, vol. 3163, pp. 278–289.
- [45] I. Molchanov  
*Theory of Random Sets*. Berlin, Germany: Springer, 2005.

- [46] H. A. P. Blom and Y. Bar-Shalom  
 “The interacting multiple model algorithm for systems with Markovian switching coefficients,”  
*IEEE Trans. Autom. Control*, vol. 33, no. 8, pp. 780–783, Aug. 1988.
- [47] M. Petrich  
*Introduction to Semigroups*. Durham, NC: Bell & Howell, 1973.



**Shozo Mori** received the B.S. degree in electric engineering from Waseda University, Tokyo, Japan, in 1970, the M.S. degree in control engineering from Tokyo Institute of Technology, Tokyo, Japan, in 1972, and the Ph.D. degree in engineering economic systems from Stanford University, Stanford, CA, in 1983. He is currently a Consultant with Systems & Technology Research (STR), Sacramento, CA, USA. He was with Advanced Decision & Information Systems (later acquired by Booz-Allen & Hamilton), Mountain View, CA, USA, from 1980 to 1991, Tiburon Systems (later acquired by Texas Instruments, and then by Raytheon Company), San Jose, CA, USA, from 1992 to 1999, Information Extraction & Transport, Arlington, VA, USA, from 2000 to 2003, ALPHATECH (later acquired by BAE Systems), Burlington, MA, USA, from 2003 to 2013, and STR, Woburn, MA, USA, from 2013 to present. His current research interests include multiple target tracking, particularly as applications of theories of random finite sets and finite point processes, distributed data fusion problems in various domains, and applications of theories of information processing and multiple-person decision-making systems to economic and social system analysis. He is an IEEE Life Member. He was a member of Program Committee for MSS National Sensor and Data Fusion Symposium, and was an Area/Assistant Editor for the IEEE TRANSACTIONS ON SYSTEMS, MAN, AND CYBERNETICS, IEEE TRANSACTIONS ON AEROSPACE AND ELECTRONIC SYSTEMS, and *Journal of Advances in Information Fusion* published by International Society of Information Fusion. He was the recipient of 2016 Joseph Mignogna Data Fusion Award.



**Chee-Yee Chong** received the S.B., S.M., and Ph.D. degrees in electrical engineering from the Massachusetts Institute of Technology, Cambridge, MA, USA, in 1969, 1970, and 1973, respectively. He was with the Electrical Engineering Faculty, Georgia Tech, Atlanta, GA, USA, until 1980, when he moved to Silicon Valley to join Advanced Decision Systems, which was acquired by Booz Allen Hamilton in 1991. In 2003, he joined ALPHATECH, which was acquired by BAE Systems, and stayed until 2013. He is currently an independent researcher and consultant. He has been involved in all levels of information fusion, including Bayesian multiple hypothesis tracking, optimal track fusion and association, close loop tracking with sensor resource management, analytical model to predict association performance, Bayesian networks for situation assessment, hard and soft data fusion, and graph approaches for data association. He is particularly interested in combining model-based and learning-based approaches for robust data fusion in mission critical systems. He co-founded the International Society of Information Fusion (ISIF), and served as its President in 2004. He was general Co-chair for the 12th International Conference on Information Fusion held in Seattle, WA, USA, in 2009. He was an Associate Editor for the IEEE TRANSACTIONS ON AUTOMATIC CONTROL and Information Fusion, and is currently an Associate Editor for *Journal of Advances in Information Fusion* published by ISIF. He was the recipient of the ISIF Yaakov Bar-Shalom Award for a Lifetime of Excellence in Information Fusion in 2016.



**Kuo-Chu Chang** received the M.S. and Ph.D. degrees in electrical engineering from the University of Connecticut, Storrs, CT, USA, in 1983 and 1986, respectively. From 1983 to 1992, he was a Senior Research Scientist with Advanced Decision Systems (ADS) Division, Booz-Allen & Hamilton, Mountain View, CA, USA. In 1992, he joined the Systems Engineering and Operations Research Department, George Mason University, Fairfax, VA, USA, where he is currently a Professor. His research interests include estimation theory, multisensor data fusion, Bayesian inference, machine learning, and financial engineering. He has more than 35 years of industrial and academic experience and authored or co-authored more than 200 papers in the areas of multitarget tracking, distributed sensor fusion, Bayesian network technologies, and financial engineering. He was an Associate Editor on Tracking/Navigation Systems from 1993 to 1996 and on Large Scale Systems from 1996 to 2006 for the IEEE TRANSACTIONS ON AEROSPACE AND ELECTRONIC SYSTEMS. He was also an Associate Editor for the IEEE TRANSACTIONS ON SYSTEMS, MAN, AND CYBERNETICS, from 2002 to 2007. He was the Technical Program Co-chair of the 2009 International Conference on Information Fusion, Seattle, WA, USA. He was elected as an IEEE Fellow for his contribution on “sensor data fusion and Bayesian probabilistic inference” in 2010.

# On Indistinguishability and Antisymmetry Properties in Multiple Target Tracking

WOLFGANG KOCH

**The notion of indistinguishable targets is well established in advanced target tracking. If no specific target attributes are sensed, indistinguishability is often unavoidable and sometimes even desirable, for example, to enable “privacy by design” in public surveillance. Conceptually, this notion is rooted in quantum physics where functions of joint quantum particle states are considered that are either symmetric or antisymmetric under permutation of the particle labels. This symmetry dichotomy explains why quite fundamentally two disjoint classes of particles exist in nature: bosons and fermions. Besides symmetry, also *antisymmetry* has a place in multiple target tracking as we will show, leading to well-defined probability density functions describing the joint target states. Inbuilt antisymmetry implies a target tracking version of Pauli’s *exclusion principle*: Real-world targets are “fermions” in the sense that cannot exist at the same time in the same state. This is of interest in dense tracking scenarios with resolution conflicts and split-off and may mitigate track coalescence phenomena, for example. We discuss the framework that is illustrated by an example.**

Manuscript received February 6, 2019; revised August 21, 2019; released for publication February 5, 2020

The author is with Fraunhofer FKIE, Wachtberg 53343, Germany. E-mail: wolfgang.koch@fkie.fraunhofer.de

1557-6418/19/\$17.00 © 2019 JAIF

## I. INTRODUCTION

*In grateful memory of Günther van Keuk (1940–2003), a pioneer in multiple target tracking.*

Since Donald B. Reid’s seminal paper, multiple target tracking has been a topic of intensive research [1]–[5]. It provides backbone algorithms for multisensor fusion engines [6] that transform data streams from a variety of sensors along with context knowledge into situation pictures, the basis for decision making in an ever-increasing range of applications. Examples are manned–unmanned teaming and autonomous platform management, use cases in manufacturing, process control, or supply chain management, in health or elderly care, as well as in public security and defense. Situational awareness is basic not only to reaching goals efficiently, but also to reaching them in an ethically acceptable and responsible way [7].

Tracks represent the available knowledge on time-varying quantities of interest that characterize the state of the targets to be tracked. Quantitative performance measures describing the quality of this knowledge are part of the tracks. The information obtained by tracking algorithms also includes the history of the targets. Ideally, a one-to-one association between all the targets in the sensors’ field of view and the produced tracks is to be established and to be preserved as long as possible. The achievable track quality depends not only on the performance of the sensors used, but also on the target properties, their kinematic behavior, and the environmental conditions within the scenario observed.

### A. Indistinguishable Targets

In the macrophysical world of target tracking, objects of interest, such as airplanes, vehicles, persons, ships, and so on, are mutually distinguishable physical objects in themselves. The information on them that is collected by sensors, however, covers a limited set of their properties only and is in many cases restricted to positional and kinematic properties. Let us call targets *identical* if two assumptions hold: (1) their *intrinsic* properties cannot be distinguished from each other by the measurements considered; and (2) they move according to the same dynamical model. Spatiotemporal target properties are *extrinsic* by definition.

From a systems engineering perspective, target tracking algorithms often have to obey certain nontechnical rules “by design” in order to make their use acceptable at all. Besides aspects formulated by rules of engagement in defense applications, surveillance systems for preserving public security are examples, where rule-constraint tracking systems are of growing interest. In particular, the “indistinguishability of the uninvolved” is a desired property in this context where multiple sensor assistance systems are to be designed that facilitate the assessment of the value of the additional security against the privacy lost by public surveillance. The proper and balanced

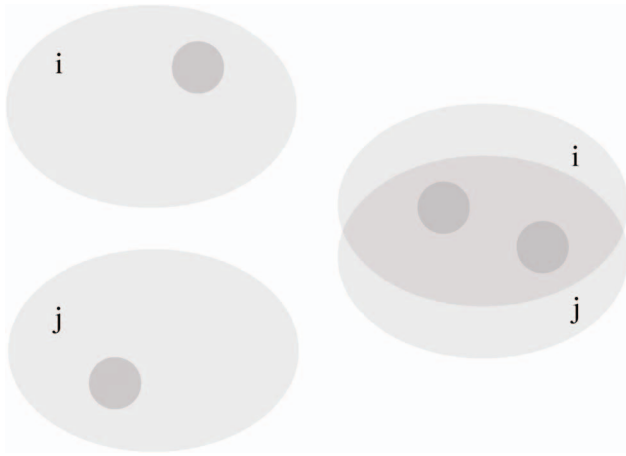


Fig. 1. Ellipses indicating imperfect knowledge on two mutually distinguishable (left) and indistinguishable (right) identical targets labeled by  $i$  and  $j$ .

relation between the emerging surveillance technology for public security and the notion of an individual human subject entitled to “inalienable fundamental rights,” for example, privacy, is of crucial importance.<sup>1</sup>

Within a conceptual framework that is inspired by classical mechanics, even identical objects in the previous sense can be distinguished from each other by their spatiotemporal behavior, since they move along well-defined trajectories. Let us consider, for example, a billiard game where all balls have the same color, their initial identity being known. Just by carefully watching, an observer could keep track of the balls as if they were individually colored. This changes even in classical mechanics in the case of “chaotic” dynamical systems according to sensitivity to initial conditions that are never known precisely. Even more so, this is valid in multiple target tracking problems where the temporal evolution has to be modeled stochastically and the measurements are inaccurate and ambiguous with respect to which object has produced which measurement, making a probabilistic description inevitable.

Fig. 1, left-hand side, illustrates the probabilistic representation of positional information on two well-separated identical targets. Even in case of imprecise positional information, each one of them occupies a clearly distinct spatial region, arbitrarily labeled by  $i$  and  $j$ , thus allowing us to distinguish between these identical targets just as previously discussed. The right-hand side of the figure shows two identical targets in a situation where the probability density functions representing imprecise positional information are overlapping. It is no longer unambiguous in which region each target is to be expected. They have become *indistinguishable* [8], [9, Ch. 3].

<sup>1</sup>“to which a person is inherently entitled simply because she or he is a human being.” *Human Rights*. In: Wikipedia, [http://en.wikipedia.org/wiki/Human\\_rights](http://en.wikipedia.org/wiki/Human_rights), last accessed August 26, 2019.

More precisely speaking, our knowledge of indistinguishable targets remains unchanged if their labels are changed. In other words, the labels of indistinguishable targets have no longer a physical meaning. The joint probability density functions describing the kinematic states of indistinguishable targets must therefore obey symmetry restrictions: if any permutation is applied to the target labels, the density function has to remain invariant. In an early paper with Günter van Keuk [10, Sec. IV-B], the concept of symmetry has been used in Bayesian multiple hypothesis tracking.

## B. Bosons and Fermions in Quantum Physics

In quantum physics where the notion of individual particle trajectories is abandoned altogether, we are confronted with a similar situation. Here, a complex-valued function, the multiple particle *wave function*  $\psi(\mathbf{x}_{1:n}, t)$ , completely describes a quantum system composed of  $n$  indistinguishable particles that at each instant of time  $t$  are characterized by their joint state  $\mathbf{x}_{1:n} = (\mathbf{x}_1, \dots, \mathbf{x}_n)$ . Knowledge of the wave function, together with the rules for the system’s temporal evolution, exhausts all that can be known on the quantum system. By taking the absolute square of the *complex* wave function,

$$p(\mathbf{x}_{1:n}, t) = |\psi(\mathbf{x}_{1:n}, t)|^2, \quad (1)$$

a probability density function is obtained for calculating the probable outcome of each possible measurement on the system. It has to be invariant under any permutation taken from the set  $S_n$  of all  $n!$  permutations of the  $n$  particle labels:

$$\forall \sigma \in S_n : p(\mathbf{x}_{1:n}, t) = p(\mathbf{x}_{\sigma(1:n)}, t). \quad (2)$$

Since only the absolute square of wave functions has a physically interpretable meaning, multiple particle quantum systems are characterized by a *symmetry dichotomy*: the wave function for a collection of indistinguishable particles must be either *symmetric* or *antisymmetric* when two particle labels are exchanged, that is, when the wave functions involved remain invariant under any permutation of the particle labels up to a factor of  $\pm 1$ . If a wave function is initially symmetric (or antisymmetric), it will remain symmetric (or antisymmetric) as the quantum system evolves in time. The symmetry dichotomy also claims that *asymmetric* multiple identical particle wave functions are forbidden. Quantum particles are either *bosons*<sup>2</sup> or *fermions*<sup>3</sup> characterized by symmetric or antisymmetric wave functions, respectively. For further details, see any standard

<sup>2</sup>Named after the Indian physicist and polymath Satyendra Nath Bose (1894–1974) who provided the foundation for Bose–Einstein statistics and the theory of the Bose–Einstein condensate.

<sup>3</sup>Named after the Italian physicist Enrico Fermi (1901–1954), who first applied Pauli’s exclusion principle to an ideal gas, employing a statistical formulation now known as Fermi–Dirac statistics.

textbook on quantum physics, such as [11, Ch. IX]. For historic aspects, see [12].

In the micro- and macrophysical world, the notions of *identity*, *individuality*, *distinguishability*, and their opposites are conceptually related, but to be distinguished carefully from each other in any philosophical reflections [8, Ch. 5], [13].

### C. Exclusion Principle in Target Tracking

A multiple target tracker extracts information on the kinematic properties of several moving targets from a time series of sensor data produced by a single sensor or multiple sensors; that is, target tracking provides information on the targets' position, velocity, and often also acceleration and related quantities.

As an example, let us consider a tracking problem with two targets, where probability density functions  $p(\mathbf{x}_1, \mathbf{x}_2)$  represent the information available on the kinematic target states  $\mathbf{x}_1$  and  $\mathbf{x}_2$ . In the case of indistinguishable targets,  $p(\mathbf{x}_1, \mathbf{x}_2)$  is symmetric under permutation of the target labels:  $p(\mathbf{x}_1, \mathbf{x}_2) = p(\mathbf{x}_2, \mathbf{x}_1)$ . In many cases,  $p(\mathbf{x}_1, \mathbf{x}_2)$  can be represented by a mixture with symmetric components:  $p(\mathbf{x}_1, \mathbf{x}_2) = \sum_v p_v p_v(\mathbf{x}_1, \mathbf{x}_2)$  and weighting factors  $p_v$ . No objection can be made if we are representing the component densities  $p_v(\mathbf{x}_1, \mathbf{x}_2)$  by the square of *real*-valued functions:

$$p_v(\mathbf{x}_1, \mathbf{x}_2) = (\psi_v(\mathbf{x}_1, \mathbf{x}_2))^2. \quad (3)$$

One can easily see that the functions  $\psi_v$  must be either

$$\text{symmetric } \psi_v^+(\mathbf{x}_1, \mathbf{x}_2) = \psi_v^+(\mathbf{x}_2, \mathbf{x}_1) \quad \text{or} \quad (4)$$

$$\text{antisymmetric } \psi_v^-(\mathbf{x}_1, \mathbf{x}_2) = -\psi_v^-(\mathbf{x}_2, \mathbf{x}_1) \quad (5)$$

under permutation of the target labels in order to guarantee that  $p(\mathbf{x}_1, \mathbf{x}_2)$  represents two indistinguishable targets. Since considering functions  $\psi_v^+$  does not add something substantially new to understanding the properties of symmetric densities  $p^+$ , we will be dealing with them as usual in the tracking literature. This is different, however, for densities  $p^-$  that are given by the square of antisymmetric components  $\psi_v^-$ .

As shown later, Bayesian multiple target tracking is equivalent to iteratively calculating the probability densities  $p^\pm$  of indistinguishable multiple targets. Of course, the “temporal propagation” of multiple target densities, driven by subsequent prediction and update steps, is mathematically quite different from the propagation of multiple particle wave functions in quantum physics. While the symmetric multiple target densities  $p^\pm$  remain symmetric if the same dynamics model is assumed for both targets in the prediction step and under wide and realistic assumptions on the sensor models to be used for the filtering update, the antisymmetric  $\psi^-$  components remain antisymmetric. Also in target tracking theory, we can therefore distinguish between *bosonic* and *fermionic* targets according to the symmetry properties of the functions  $\psi_v^\pm$  describing them. As in quantum physics, this

distinction is fundamental. Obviously, the macrophysical notion of bosonic and fermionic targets considered here is by no means related to the purely quantum physical concept of even or odd particle spin.

Real-world targets are fermions in the following sense: Due to the “fermionic” antisymmetry property of  $\psi_v^-$ , they cannot be characterized by the same state at the same instant of time:

$$p^-(\mathbf{x}, \mathbf{x}) = \sum_v (\psi_v^-(\mathbf{x}, \mathbf{x}))^2 = 0. \quad (6)$$

This is a target tracking version of the famous *exclusion principle*.<sup>4</sup>

### D. Contribution and Structure

In the tracking literature, indistinguishable targets have implicitly been considered as bosons; that is, no attention was given to antisymmetry. Attempts to broaden the methodological basis of point processes applied to target tracking, for example, do *not* use the concept of antisymmetry (see, e.g., the early and insightful paper by Soshio Mori and Chee-Yee Chong [14] or [15]). This is valid also for new trends in multitarget tracking such as labeled Random Finite Sets and message passing techniques to be mentioned [16]–[18]. Only a most recent paper, not yet published [19], points into the direction of “fermionic” multiple target tracking.

Since symmetric probability density functions are crucial building blocks for advanced trackers, see, for example, [3, pp. 239–244], also the notion of fermionic targets can quite naturally be introduced. In particular, the target tracking version of Pauli’s exclusion principle leads us to multiple target trackers that are better adapted to real-world phenomena since targets simply cannot exist at the same place at the same time. It is an open question what type of phenomena to be tracked might best be modeled by bosonic targets. Two collectively moving groups that may merge and split off again are candidates of two bosons, while extended target tracking is fermionic in nature. In this sense, fermionic point targets might be called somewhat provocatively “extended” point targets.

After more precisely stating the notions of symmetry and antisymmetry as well as reviewing some basics of multiple target tracking in Section II, we rigorously discuss the problem of tracking two indistinguishable targets using a realistic sensor model with possibly missing, false, and unresolved measurements (Section III). Via a simulated example based on a tracking vignette with road moving targets, Section IV illustrates some characteristics of “fermionic” target tracking and compares

<sup>4</sup>It was formulated in 1925 by Wolfgang Pauli (1900–1958) at the University of Hamburg, Germany. Nominated by Albert Einstein (1879–1955), Pauli received the 1945 Nobel Prize in Physics for his “decisive contribution through his discovery of a new law of Nature, the exclusion principle or Pauli principle” [20].

them with “bosonic” target tracking and more standard approaches. Since our focus here is on the methodological approach, a more comprehensive qualitative discussion of the advantages of the proposed approach in comparison to alternative tracking methodologies, although desirable, goes beyond the scope of this publication and will be provided by subsequent work. An evident and practically relevant benefit of “fermionic” trackers to be stated right now is the mitigation of track coalescence phenomena in dense target situations. In Section V, we discuss the relevance of indistinguishable target tracking in surveillance systems for public security. “Indistinguishability of the uninvolved” seems to be a fundamental principle for security systems design to be recognized as a certifiable means for preserving informational self-determination. Conclusions and some physics-inspired remarks for generalizing the formalism conclude the paper.

At the 21st International Conference on Information Fusion, the general idea underlying this paper and its potential relevance to tracking closely spaced targets were sketched [21]. We here provide a more comprehensive view and coherently consider the quantum physical background, which has guided our approach. In its present form, this contribution reflects also a series of discussions that were stimulated by the preliminary publication. The author in particular wishes to thank three anonymous reviewers for their insightful and inspiring comments.

As Wolfgang Pauli made clear himself, the fundamental symmetry dichotomy, tightly connected with the notion of indistinguishability, that is visible and relevant also in multiple target tracking as shown in this paper, still calls for a deeper understanding.<sup>5</sup>

## II. BAYESIAN MULTIPLE IDENTICAL TARGET TRACKING

Tracking systems extract kinematic target information from a time series of data  $Z_{k:1} = \{Z_k, Z_{k-1:1}\}$  produced by a single sensor or multiple sensors at certain instants of time  $t_l, l = 1, \dots, k$ , measuring positional and kinematic properties of the targets starting at an initial time  $t_1$ . The number of measurements  $m_k$  in each data set  $Z_k = \{\mathbf{z}_j\}_{j=1}^{m_k}$  produced at time  $t_k$  can be equal to, less than, or larger than the number  $n$  of targets to be tracked due to false, missing, and unresolved measurements. The targets’ position, velocity, and possibly also acceleration are described by kinematic state vectors  $\mathbf{x}_k^i, i = 1, \dots, n$ , at instants of time  $t_k$ , the *joint state* being denoted by  $\mathbf{x}_k^{1:n} = (\mathbf{x}_k^1, \dots, \mathbf{x}_k^n)$ . Identical targets obey the same dynamical model.

<sup>5</sup>“Already in my original paper I stressed the circumstance that I was unable to give a logical reason for the exclusion principle or to deduce it from more general assumptions. I had always the feeling, and I still have it today, that this is a deficiency.” [22].

The implications of antisymmetry in the formalism of multiple identical target tracking and its practical benefits are more clearly visible within the standard Bayesian framework where we assume independent targets along with a fixed and known number of targets than in more advanced tracking methodologies, such as Probability Hypothesis Density and intensity filtering, where antisymmetry can be embedded as well.

In Bayesian context, the problem of tracking well-separated targets or well-separated groups consisting of not too many targets or that of tracking some well-separated targets or groups joining and separating after a while can be solved more or less rigorously, that is, by explicitly enumerating data interpretation hypotheses. Since it seems unreasonable to deal with large groups by keeping track of each individual group member, we should rather track the centroid and the boundary of the group in this case until it splits off into smaller components to be tracked individually; see [6, Sec. 8.2] and [23], for example.

Our general line of argumentation is valid for nonlinear, non-Gaussian sensor and evolution models where the resulting probability densities and  $\psi$  functions can be calculated by numerical methods based on tensor decomposition methods, for example, those presented in [24]. For being able to discuss the impact of antisymmetry more analytically and in greater detail, however, we are assuming linear Gaussianity whenever to be justified and mathematically convenient.

### A. Antisymmetry in Mixture Densities

In the case of ambiguous sensor data, the time series  $Z_{k:1}$  is to be interpreted by *data interpretation histories*, series of possible interpretation hypotheses of the sensor data sets at different instants of time. The conditional probability density function  $p(\mathbf{x}_k^{1:n} | Z_{k:1})$  of the joint state  $\mathbf{x}_k^{1:n}$  that contains all information on the state vectors available at time  $t_k$  can thus be written as weighted sum of component densities  $p_v$  related to these interpretation histories:

$$p(\mathbf{x}_k^{1:n} | Z_{k:1}) = \sum_v p_v^v p_v(\mathbf{x}_k^{1:n} | Z_{k:1}). \quad (7)$$

If at one particular instant of time  $t_l$  the component densities  $p_v(\mathbf{x}_l^{1:n})$  are symmetric under permutation of the target labels,

$$\forall \sigma \in S_n : p_v(\mathbf{x}_l^{1:n} | Z_{k:1}) = p_v(\mathbf{x}_l^{\sigma(1:n)} | Z_{k:1}), \quad (8)$$

this property is preserved in the iterative calculation process of the densities that will become clear later. Symmetry in this sense can thus be imposed on the “noninformative” initial prior density as some structural information. As sketched in the introduction, the symmetric probability densities  $p_v$  can either be considered in themselves, that is, instead as a square of symmetric functions, this bosonic case being denoted by  $p_v^+(\mathbf{x}_k^{1:n} | Z_{k:1})$ , or be written as the square of func-

tions  $\psi_v$  that are antisymmetric under permutation of the target labels:

$$p_v^-(\mathbf{x}_k^{1:n}|Z_{k:1}) = \left( \psi_v(\mathbf{x}_k^{1:n}|Z_{k:1}) \right)^2. \quad (9)$$

With Dirac's<sup>6</sup> antisymmetrizing operator  $\mathcal{A}$ , see [11, p. 248],

$$\mathcal{A}f(\mathbf{x}_{1:n}) = \sum_{\sigma \in \mathcal{S}_n} (-1)^\sigma f(\mathbf{x}_{\sigma(1:n)}), \quad (10)$$

where the symbol  $(-1)^\sigma$  is 1 for even and  $-1$  for odd permutations  $\sigma$ . Let  $\psi_v$  be given by a weighted sum of Gaussians with positive and negative weighting factors:

$$\psi_v(\mathbf{x}_k^{1:n}|Z_{k:1}) = \sqrt{c_{k|k}^v} \mathcal{A} \mathcal{N}(\mathbf{x}_k^{1:n}; \mathbf{x}_{k|k}^v, \mathbf{P}_{k|k}^v) \quad (11)$$

$$=: \psi(\mathbf{x}_k^{1:n}; \mathbf{x}_{k|k}^v, \mathbf{P}_{k|k}^v) \quad (12)$$

that are characterized by joint state expectation vectors  $\mathbf{x}_{k|k}^v$ , corresponding covariance matrices  $\mathbf{P}_{k|k}^v$ , and a properly defined normalization constant (see Section A.1 in Appendix A):

$$1/c_{k|k}^v = \int d\mathbf{x}_k^{1:n} \left( \psi(\mathbf{x}_k^{1:n}; \mathbf{x}_{k|k}^v, \mathbf{P}_{k|k}^v) \right)^2. \quad (13)$$

Under these modeling assumptions, the fermionic component densities  $p_v^-$  are therefore given by correctly normalized, well-defined Gaussian mixture densities with possibly *negative* weighting factors that sum up to 1. More general non-Gaussian representations are possible.

With the symmetrizing operator  $\mathcal{S}$ ,

$$\mathcal{S}f(\mathbf{x}_{1:n}) = \sum_{\sigma \in \mathcal{S}_n} f(\mathbf{x}_{\sigma(1:n)}), \quad (14)$$

let the bosonic components be given by

$$p_v^+(\mathbf{x}_k^{1:n}|Z_{k:1}) = \frac{1}{n!} \mathcal{S} \mathcal{N}(\mathbf{x}_k^{1:n}; \mathbf{x}_{k|k}^v, \mathbf{P}_{k|k}^v). \quad (15)$$

With these definitions, the overall densities  $p^\pm(\mathbf{x}_k^{1:n}|Z_{1:k})$  are symmetric under permutation of the target labels. The symmetrizing and antisymmetrizing operators  $\mathcal{S}$  and  $\mathcal{A}$  are projectors into disjunct function subspaces.

## B. Fermionic Prediction

Let  $\mathbf{F}'_{k|k-1}$  and  $\mathbf{D}'_{k|k-1}$  denote the evolution and plant noise covariance matrices describing the temporal evolution of the identical targets as usual in the tracking literature. With  $\mathbf{F}_{k|k-1} = \mathbf{1}_n \otimes \mathbf{F}'_{k|k-1}$  and  $\mathbf{D}_{k|k-1} = \mathbf{1}_n \otimes \mathbf{D}'_{k|k-1}$ , where  $\mathbf{1}_n$  denotes the  $n$ -dimensional unity matrix and the Kronecker product is used, a Gauss–Markov

transition density for  $n$  identical independently moving targets is defined by

$$p(\mathbf{x}_k^{1:n}|\mathbf{x}_{k-1}^{1:n}) = \mathcal{N}(\mathbf{x}_k^{1:n}; \mathbf{F}_{k|k-1}\mathbf{x}_{k-1}^{1:n}, \mathbf{D}_{k|k-1}). \quad (16)$$

Since all identical targets obey the same evolution model, the multiple identical target transition density has the following property:

$$\forall \sigma \in \mathcal{S}_n : p(\mathbf{x}_k^{1:n}|\mathbf{x}_{k-1}^{1:n}) = p(\mathbf{x}_k^{\sigma(1:n)}|\mathbf{x}_{k-1}^{\sigma(1:n)}). \quad (17)$$

While the bosonic prediction update is quite straightforward, the fermionic version of it requires some care. The square root of the transition density is given by (see Section A.2 in Appendix A)

$$\pi(\mathbf{x}_k^{1:n}|\mathbf{x}_{k-1}^{1:n}) = |8\pi \mathbf{D}_{k|k-1}|^{1/4} \mathcal{N}(\mathbf{x}_k^{1:n}; \mathbf{F}_{k|k-1}\mathbf{x}_{k-1}^{1:n}, 2\mathbf{D}_{k|k-1}). \quad (18)$$

For modeling the prediction step in the tracking process, we consider predictive  $\psi$  functions defined by

$$\psi(\mathbf{x}_k^{1:n}|Z_{k-1:1}) = \sum_v p_k^v \psi(\mathbf{x}_k^{1:n}; \mathbf{x}_{k|k-1}^v, \mathbf{P}_{k|k-1}^v) \quad (19)$$

with mixture components given by

$$\psi(\mathbf{x}_k^{1:n}; \mathbf{x}_{k|k-1}^v, \mathbf{P}_{k|k-1}^v) = \sqrt{c_{k|k-1}^v} \mathcal{A} \mathcal{N}(\mathbf{x}_k^{1:n}; \mathbf{x}_{k|k-1}^v, \mathbf{P}_{k|k-1}^v) \quad (20)$$

with properly defined normalizing constants  $c_{k|k-1}^v$  and the standard, though “relaxed” Kalman prediction step:

$$\mathbf{x}_{k|k-1}^v = \mathbf{F}_{k|k-1}\mathbf{x}_{k-1|k-1}^v, \quad (21)$$

$$\mathbf{P}_{k|k-1}^v = \mathbf{F}_{k|k-1}\mathbf{P}_{k-1|k-1}^v\mathbf{F}_{k|k-1}^\top + 2\mathbf{D}_{k|k-1}. \quad (22)$$

The predicted fermionic density is thus given by

$$p^-(\mathbf{x}_k^{1:n}|Z_{k-1:1}) = \sum_v p_k^v \left( \psi(\mathbf{x}_k^{1:n}; \mathbf{x}_{k|k-1}^v, \mathbf{P}_{k|k-1}^v) \right)^2.$$

## C. Intrinsic Symmetry in Sensor Models

Likelihood functions represent imperfect and ambiguous information on the target states  $\mathbf{x}_k^{1:n}$  that is provided by a set of sensor data  $Z_k$  at time  $t_k$  as well as context knowledge on the sensor performance and the sensing environment. For identical targets, the likelihood functions necessarily have to be symmetric under permutation of the target labels, since otherwise the targets could be distinguished from each other via sensor data processing.

Likelihood functions  $\ell(\mathbf{x}_k^{1:n}; Z_k)$  are up to a multiplicative constant determined by the conditional densities  $p(Z_k|\mathbf{x}_k^{1:n})$ :

$$\ell(\mathbf{x}_k^{1:n}; Z_k) \propto p(Z_k|\mathbf{x}_k^{1:n}). \quad (23)$$

The potential origin of ambiguous sensor data  $Z_k$  is explained by a set of data interpretation hypotheses  $h_k \in H_k$ , which are assumed to be exhaustive and mutually exclusive, yielding a representation by a weighted

<sup>6</sup>Paul Adrien Maurice Dirac (1902–1984) shared the 1933 Nobel Prize in Physics with Erwin Schrödinger (1887–1961).

sum:

$$\ell(\mathbf{x}_k^{1:n}; Z_k) \propto \sum_{h_k \in H_k} p(h_k) p(Z_k | \mathbf{x}_k^{1:n}, h_k). \quad (24)$$

Following well-established and fairly general modeling assumptions for the sensors considered [6, Sec. 7.1], the likelihood functions can be rearranged as a sum of partial sums over classes  $H_k^\mu$  of data interpretation hypotheses that are similar in the sense that they differ only in a permutation of the target labels:

$$\ell(\mathbf{x}_k^{1:n}; Z_k) = \sum_{\mu} \ell_{\mu}(\mathbf{x}_k^{1:n}; Z_k) \quad (25)$$

$$\text{with } \ell_{\mu}(\mathbf{x}_k^{1:n}; Z_k) \propto \sum_{h_k \in H_k^\mu} p(h_k) p(Z_k | \mathbf{x}_k^{1:n}, h_k). \quad (26)$$

As a result, the component likelihood functions  $\ell_{\mu}$  related to  $H_k^\mu$  are symmetric under permutation of the target labels:

$$\forall \sigma \in S_n : \ell_{\mu}(\mathbf{x}_k^{1:n}; Z_k) = \ell_{\mu}(\mathbf{x}_k^{\sigma(1:n)}; Z_k). \quad (27)$$

This can be shown by assuming false measurements that are Poisson distributed in number with a spatial false measurement density  $\rho_F$  and uniformly distributed in the measurement space, missing measurements occurring according to a detection probability  $P_D$ , and the measurements  $\mathbf{z}_k \in Z_k$  being mutually independent. Moreover, let a *resolved* measurement  $\mathbf{z}_k^j$  related to target  $i$  be characterized by a Gaussian likelihood

$$p(\mathbf{z}_k^j | \mathbf{x}_k^i) = \mathcal{N}(\mathbf{z}_k^j; \mathbf{H}_k \mathbf{x}_k^i, \mathbf{R}_k^j) \quad (28)$$

with measurement and error covariance matrices  $\mathbf{H}_k$  and  $\mathbf{R}_k^j$ .

Inherently, antisymmetry and the exclusion principle it implies are only relevant for targets that may move closely spaced. Due to the finite resolution capabilities of real-world sensors, such targets are expected to transition from being resolved to unresolved and back again. It is thus inevitable to model the sensors' resolution capability appropriately and to take this phenomenon explicitly into account. In practical applications, only a small number of targets are expected to be jointly unresolved.

Let an *unresolved* measurement  $\mathbf{z}_k^u$  produced by a group of  $n$  closely spaced targets be modeled as a measurement of the group centroid that is characterized by the Gaussian likelihood

$$p(\mathbf{z}_k^u | \mathbf{x}_k^{1:n}) = \mathcal{N}(\mathbf{z}_k^u; \mathbf{H}_g \mathbf{x}_k^{1:n}, \mathbf{R}_g) \quad (29)$$

with  $\mathbf{R}_g$  denoting the measurement error of unresolved measurements and a measurement matrix given by

$$\mathbf{H}_g = (1, \dots, 1) \otimes \mathbf{H}_k. \quad (30)$$

The probability  $P_u(\mathbf{x}_k^{1:n})$  of  $n$  targets being jointly unresolved is modeled by pseudo-measurement "zero" of the distances between the targets [6, Sec. 7.1], where the sensor resolution in the measured quantities such as range and cross range,  $\alpha_r$  and  $\alpha_{xr}$ , can be considered as standard deviations entering a related pseudo-measurement

error covariance matrix  $\mathbf{A}_u$ :

$$P_u(\mathbf{x}_k^{1:n}) = |2\pi \mathbf{A}_u|^{1/2} \mathcal{N}(0; \mathbf{H}_d \mathbf{x}_k^{1:n}, \mathbf{A}_u), \quad (31)$$

where the corresponding pseudo-measurement matrix  $\mathbf{H}_d$  that describes mutual distances is given by

$$\mathbf{H}_d = \begin{pmatrix} 1 & -1 & 0 & \dots \\ 0 & \ddots & \ddots & 0 \\ \vdots & \ddots & 1 & -1 \\ -1 & 0 & \dots & 1 \end{pmatrix} \otimes \mathbf{H}_k. \quad (32)$$

Both Gaussians related to unresolved measurements are evidently symmetric under permutation of the target labels:

$$\forall \sigma \in S_n : \begin{aligned} \mathcal{N}(\mathbf{z}_k^u; \mathbf{H}_g \mathbf{x}_k^{1:n}, \mathbf{R}_g) &= \mathcal{N}(\mathbf{z}_k^u; \mathbf{H}_g \mathbf{x}_k^{\sigma(1:n)}, \mathbf{R}_g), \\ \mathcal{N}(0; \mathbf{H}_d \mathbf{x}_k^{1:n}, \mathbf{R}_u) &= \mathcal{N}(0; \mathbf{H}_d \mathbf{x}_k^{\sigma(1:n)}, \mathbf{R}_u). \end{aligned}$$

In order to pinpoint the effects of antisymmetry, a fully detailed discussion of this fairly general approach in the limiting case of two closely spaced targets is provided in Section III.

#### D. Fermionic Filtering

The data update of the fermionic density follows from Bayes' rule; that is, it is provided by normalizing the product of the sensor likelihood  $\ell(Z_k; \mathbf{x}_k^{1:n})$  and the predicted density  $p^-(\mathbf{x}_k^{1:n} | Z_{1:k-1})$ :

$$p^-(\mathbf{x}_k^{1:n} | Z_{k:1}) = c_{k|k} \ell(\mathbf{x}_k^{1:n}; Z_k) p^-(\mathbf{x}_k^{1:n} | Z_{k-1:1}) \quad (33)$$

$$\text{with } 1/c_{k|k} = \int d\mathbf{x}_k^{1:n} p(Z_k | \mathbf{x}_k^{1:n}) p^-(\mathbf{x}_k^{1:n} | Z_{1:k-1}).$$

We can therefore write the fermionic density function of the joint state as a mixture density:

$$p^-(\mathbf{x}_k^{1:n} | Z_{1:k}) = c_{k|k} \sum_{\mu, \nu} \ell_{\mu}(\mathbf{x}_k^{1:n}; Z_k) \times \left( \psi(\mathbf{x}_k^{1:n}; \mathbf{x}_{k|k-1}^{\nu}, \mathbf{P}_{k|k-1}^{\nu}) \right)^2. \quad (34)$$

If it is possible to rewrite the symmetric component likelihood functions  $\ell_{\mu}$  as squares of symmetric functions, the fermionic filtering update consists in updating the antisymmetric component  $\psi$  functions and squaring them. To keep the discussion simple, let us consider a tracking problem of reduced complexity that is still rich enough to be practically relevant.

### III. EXAMPLE WITH POSSIBLY UNRESOLVED TARGETS

While applicable for  $n$  targets, the effects of antisymmetry in identical target tracking can more easily be analyzed in the case of two targets that may move closely spaced for a while. Depending on the sensor-to-target geometry, the finite sensor resolution may even play a dominant role in target tracking.

In order to preserve antisymmetry of the fermionic  $\psi$  functions in the filtering update, the likelihood functions need to be modified appropriately. To do so, let us be guided by some sort of ‘‘correspondence principle’’ in the sense that for well-separated fermionic targets the effect of fermionically modified likelihood functions is the same as that for bosonic targets. If there is no need for any linear Gaussianity as in case of direct numerical calculation [24] where the square roots can be drawn directly, no modification is necessary.

#### A. Components of the Likelihood Function

For two targets moving in a cluttered environment, five different classes  $H_k^m$ ,  $m = 1, \dots, 5$ , of data interpretation hypotheses exist [6, Sec. 7.1]. The likelihood function for the bosonic and fermionic filtering update has thus a sum representation:

$$\ell^\pm(\mathbf{x}_k^{1:n}; Z_k) \propto \sum_{i=1}^5 \ell_i^\pm(\mathbf{x}_k^{1:2}; Z_k), \quad (35)$$

where the five component likelihood functions are symmetric under permutation of the target labels and correspond to the following data interpretation classes.

1)  $H_k^1$ —Both targets were resolvable, but not detected; all  $m_k$  measurements in  $Z_k$  are false (one interpretation): The component likelihood  $\ell_1$  is the same for bosonic and fermionic tracking and given by

$$\ell_1^\pm(\mathbf{x}_k^{1:2}; Z_k) = \rho_F^2 (1 - P_D)^2 (1 - P_u(\mathbf{x}_k^{1:2})). \quad (36)$$

2)  $H_k^2$ —Both targets were neither resolvable nor detected as a group; all measurements in  $Z_k$  are assumed to be false (one interpretation hypothesis): Also here, there is no difference between the bosonic and fermionic cases:

$$\ell_2^\pm(\mathbf{x}_k^{1:2}; Z_k) = \rho_F (1 - P_D^\mu) P_u(\mathbf{x}_k^{1:2}). \quad (37)$$

3)  $H_k^3$ —Both targets were not resolvable but detected as a group with probability  $P_D^\mu$ ,  $\mathbf{z}_k^j \in Z_k$  representing the centroid measurement; all remaining returns are false ( $m_k$  data interpretations): Up to constant factors, the corresponding component likelihood is equivalent to joint centroid and distance measurements; that is, the single unresolved group measurement  $\mathbf{z}_k^j$  provides under this hypothesis a measurement of the full joint position of the targets:

$$\ell_3^\pm(\mathbf{x}_k^{1:2}; Z_k) = \rho_F P_D^\mu P_u(\mathbf{x}_k^{1:2}) \sum_{j=1}^{m_k} \mathcal{N}(\mathbf{z}_k^j; \mathbf{H}_g \mathbf{x}_k^{1:2}, \mathbf{R}_g) \quad (38)$$

$$= \rho_F P_D^\mu |\mathbf{R}_u|^{1/2} \sum_{j=1}^{m_k} \mathcal{N}(\mathbf{z}_k^{j,1:2}; \mathbf{H}_u \mathbf{x}_k^{1:2}, \mathbf{R}_u), \quad (39)$$

$$\mathbf{z}_k^{j,1:2} = (\mathbf{z}_k^j, \mathbf{0}), \quad \mathbf{H}_u = \text{diag}[\mathbf{H}_g, \mathbf{H}_d], \quad \text{and} \quad \mathbf{R}_u = \text{diag}[\mathbf{R}_g, \mathbf{A}_u].$$

4)  $H_k^4$ —Both objects were resolvable but only one object was detected,  $\mathbf{z}_k^j$  is the measurement,  $m_k - 1$  measurements are false ( $2m_k$  interpretations): With the abbreviation

$$\lambda_4(\mathbf{z}_k^j; \mathbf{H}_k \mathbf{x}_k^{1:2}, \mathbf{R}_k^j) = \mathcal{N}(\mathbf{z}_k^j; \mathbf{H}_k \mathbf{x}_k^1, \mathbf{R}_k^j) + \mathcal{N}(\mathbf{z}_k^j; \mathbf{H}_k \mathbf{x}_k^2, \mathbf{R}_k^j), \quad (40)$$

the bosonic component likelihood is given by

$$\ell_4^+(\mathbf{x}_k^{1:2}; Z_k) = \rho_F P_D (1 - P_D) (1 - P_u(\mathbf{x}_k^{1:2})) \times \sum_{j=1}^{m_k} \lambda_4(\mathbf{z}_k^j; \mathbf{H}_k \mathbf{x}_k^{1:2}, \mathbf{R}_k^j). \quad (41)$$

For applying this component likelihood in the filtering update where the antisymmetric structure of  $\psi$  functions is to be preserved, we need a representation by appropriate ‘‘squares.’’ According to the introductory remarks, let us make an ‘‘ansatz’’:

$$\ell_4^-(\mathbf{x}_k^{1:2}; Z_k) = \rho_F P_D (1 - P_D) (1 - P_u(\mathbf{x}_k^{1:2})) \times \sum_{j=1}^{m_k} \lambda_4(\mathbf{z}_k^j; \mathbf{H}_k \mathbf{x}_k^{1:2}, 2\mathbf{R}_k^j)^2. \quad (42)$$

5)  $H_k^5$ —Both objects were resolvable and detected,  $\mathbf{z}_k^i$  and  $\mathbf{z}_k^j$  are the measurements,  $m_k - 2$  measurements are false ( $m_k(m_k - 1)$  interpretations): With the abbreviation

$$\lambda_5(\mathbf{x}_k^{1:2}; \mathbf{z}_k^{ij}, \mathbf{R}_k^{ij}) = \mathcal{S} \mathcal{N}(\mathbf{z}_k^{ij}; \mathbf{H}_k \mathbf{x}_k^{1:2}, \mathbf{R}_k^{ij}), \quad (43)$$

the bosonic component likelihood is given by

$$\ell_5^+(\mathbf{x}_k^{1:2}; Z_k) = P_D^2 (1 - P_u(\mathbf{x}_k^{1:2})) \sum_{i=1}^{m_k-1} \sum_{j=1}^{m_k-i} \lambda_5(\mathbf{x}_k^{1:2}; \mathbf{z}_k^{ij}, \mathbf{R}_k^{ij}), \quad (44)$$

while we assume for the fermionic component

$$\ell_5^-(\mathbf{x}_k^{1:2}; Z_k) = P_D^2 (1 - P_u(\mathbf{x}_k)) \sum_{i=1}^{m_k-1} \sum_{j=1}^{m_k-i} \left( \lambda_5(\mathbf{x}_k^{1:2}; \mathbf{z}_k^{ij}, \mathbf{H}_k \mathbf{x}_k^{1:2}, 2\mathbf{R}_k^{ij}) \right)^2. \quad (45)$$

Note the ‘‘relaxed’’ measurement error covariance matrix in the fermionic versions of the component likelihood functions  $\ell_4^-$  and  $\ell_5^-$ .

Each component likelihood is symmetric under permutation of the target labels. If an unresolved group is assumed, two measurements are to be processed: a real measurement of the group centroid and a pseudo-measurement ‘‘zero’’ of the distance between the objects. We can thus speak of a piece of *negative sensor information*, as the lack of a second target measurement conveys information on the target position, since in the case of a resolution conflict, the relative target distances must be smaller than the sensor resolution.

## B. Fermionic Filtering Update: Discussion

The general structure of the filtering update in case of two targets becomes visible even in the absence of clutter,  $\rho_F = 0$ , and in case of perfect detection,  $P_D = 1$ . This means that at a given instant of time  $t_k$  either two resolved measurements  $\mathbf{z}_k^1$  and  $\mathbf{z}_k^2$  or a single unresolved measurement  $\mathbf{z}_k$  has to be processed. Let the predictive  $\psi$  function be given by

$$\psi(\mathbf{x}_k^{1:2} | Z_{k-1:k}) = \psi(\mathbf{x}_k^{1:2}; \mathbf{x}_{k|k-1}, \mathbf{P}_{k|k-1}) \quad (46)$$

or by a weighted sum of such components.

1) *Unresolved measurement:* In this case, the bosonic and fermionic updates use the same component likelihood. Up to a constant, the square root of the likelihood is given by (see Section A.2 in Appendix A)

$$\lambda_3(\mathbf{x}_k^{1:2}; \mathbf{z}_k) \propto \mathcal{N}(\mathbf{z}_k^{u,1:2}; \mathbf{H}_u \mathbf{x}_k^{1:2}, 2\mathbf{R}_u). \quad (47)$$

The filtering update by a measurement that is assumed to be unresolved yields a  $\psi$  function  $\psi(\mathbf{x}_k^{1:2}; \mathbf{x}_{k|k}, \mathbf{P}_{k|k})$  characterized by a standard Kalman update based on the “relaxed” measurement error covariance matrix  $2\mathbf{R}_u$ :

$$\mathbf{x}_{k|k}^{1:2} = \mathbf{x}_{k|k-1}^{1:2} + \mathbf{W}_k(\mathbf{z}_k^{u,1:2} - \mathbf{H}_u \mathbf{x}_{k|k-1}^{1:2}), \quad (48)$$

$$\mathbf{P}_{k|k}^{1:2} = \mathbf{P}_{k|k-1}^{1:2} - \mathbf{W}_k \mathbf{S}_k \mathbf{W}_k^\top \quad (49)$$

with innovation covariance and gain matrices given by  $\mathbf{S}_k^u = \mathbf{H}_u \mathbf{P}_{k|k-1}^{1:2} \mathbf{H}_u^\top + 2\mathbf{R}_u$  and  $\mathbf{W}_k^u = \mathbf{P}_{k|k-1}^{1:2} \mathbf{H}_u^\top \mathbf{S}_k^{u-1}$ .

2) *Resolved measurements:* In this case, we obtain for the fermionic update (see Section A.3 in Appendix A)

$$\psi(\mathbf{x}_k^{1:2} | Z_{1:k}) \propto \lambda_5(\mathbf{x}_k^{1:2}; \mathbf{z}_k^{ij}, 2\mathbf{R}_k^{ij}) \psi(\mathbf{x}_k^{1:2}; \mathbf{x}_{k|k-1}, \mathbf{P}_{k|k-1}) \quad (50)$$

$$= p_k^{12} \psi(\mathbf{x}_k^{1:2}; \mathbf{x}_{k|k}^{12}, \mathbf{P}_{k|k}^{12}) + p_k^{21} \psi(\mathbf{x}_k^{1:2}; \mathbf{x}_{k|k}^{21}, \mathbf{P}_{k|k}^{21}), \quad (51)$$

where  $\mathbf{x}_{k|k}^{ij}$  and  $\mathbf{P}_{k|k}^{ij}$  result from the standard Kalman update equations with measurement vectors  $\mathbf{z}_k^{ij} = (\mathbf{z}_k^i, \mathbf{z}_k^j)$ . The weighting factors result from the corresponding innovation:

$$p_k^{ij} = \mathcal{N}(\mathbf{z}_k^{ij}; \mathbf{H}_k^{ij} \mathbf{x}_{k|k-1}, \mathbf{S}_k^{ij}) \quad (52)$$

with  $\mathbf{S}_k^{ij} = \mathbf{H}_k^{ij} \mathbf{P}_{k|k-1} \mathbf{H}_k^{ij\top} + \mathbf{R}_k^{ij}$ . Via symmetrized moment matching [10, Sec. IV-B], an increasing number of mixture components by the fermionic update can be avoided:

$$\psi(\mathbf{x}_k^{1:2} | Z_{1:k}) \approx \psi(\mathbf{x}_k^{1:2}; \mathbf{x}_{k|k}, \mathbf{P}_{k|k}). \quad (53)$$

## IV. EXAMPLE: GMTI TRACKING OF ROAD MOVING VEHICLES

Tracking of road moving targets using data from airborne GMTI (ground moving target indicator) radar is a relevant problem. Since here the state space has only one spatial dimension, the impact of antisymmetry can easily be visualized.

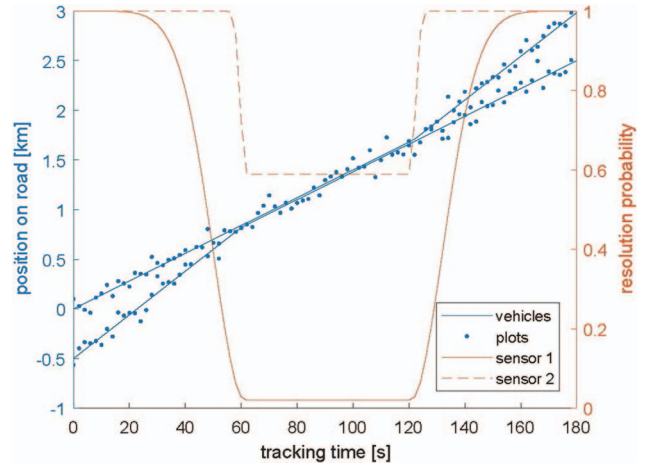


Fig. 2. Two road moving vehicles observed with GMTI radar.

### A. Description of a Characteristic Vignette

Let us therefore consider a straight road given by the  $x$ -axis of the chosen coordinate system with a road map error of 5 m. See [6, Sec. 9.1] for details and generalizations to winding roads. As a function of time, Fig. 2 shows the position of vehicle 1 moving uniformly with the speed  $v_1 = 14$  m/s. At time  $t_1 = 120$  s, it smoothly accelerates with  $a = 2$  m/s<sup>2</sup> over 4 s and continues to move uniformly with  $v_2 = 22$  m/s. Vehicle 2 approaches vehicle 1 with the initial speed  $v_2$ . At time  $t_2 = 58$  s, it decelerates with  $-a$  over 4 s and follows vehicle 1 at a distance of 20 m until vehicle 1 is accelerating.

Let this vignette be observed by a typical GMTI radar positioned at  $s_1 = (1, 40)$  km. For the sake of simplicity, we neglect the phenomenon of GMTI Doppler blindness [6, Sec. 7.2]. Moreover, we assume for resolved and unresolved measurements the same standard deviations of the measurement errors in range and cross range that are given by  $\sigma_r = 10$  m and  $\sigma_{xr} = 70$  m, respectively, while the sensor resolution parameters are  $\alpha_r = 15$  m and  $\alpha_{xr} = 100$  m.

Fig. 2 also shows the variation of the resolution probabilities in time and a time series of GMTI plots that are simulated according to these assumptions. Apparently, the vehicles are unresolved in the intermediate period of the vignette. The measurement and resolution capabilities of GMTI sensors strongly depend on the chosen sensor-to-target geometry. This is clearly indicated by the resolution probability of a second GMTI radar located at  $s_2 = (40, 0)$  km (dashed line).

### B. Comparison of Fermionic and Bosonic Densities

For the first sensor-to-target geometry previously discussed, we focus on four instants of time, shortly before the vehicles are becoming unresolvable (after 36 s), after processing a fairly long sequence of unresolved measurements (100 s), during the process of splitting off (140 s), and well after the vehicles have split off again (170). Figs. 3 (36, 100 s) and 4 (140, 170 s) show the

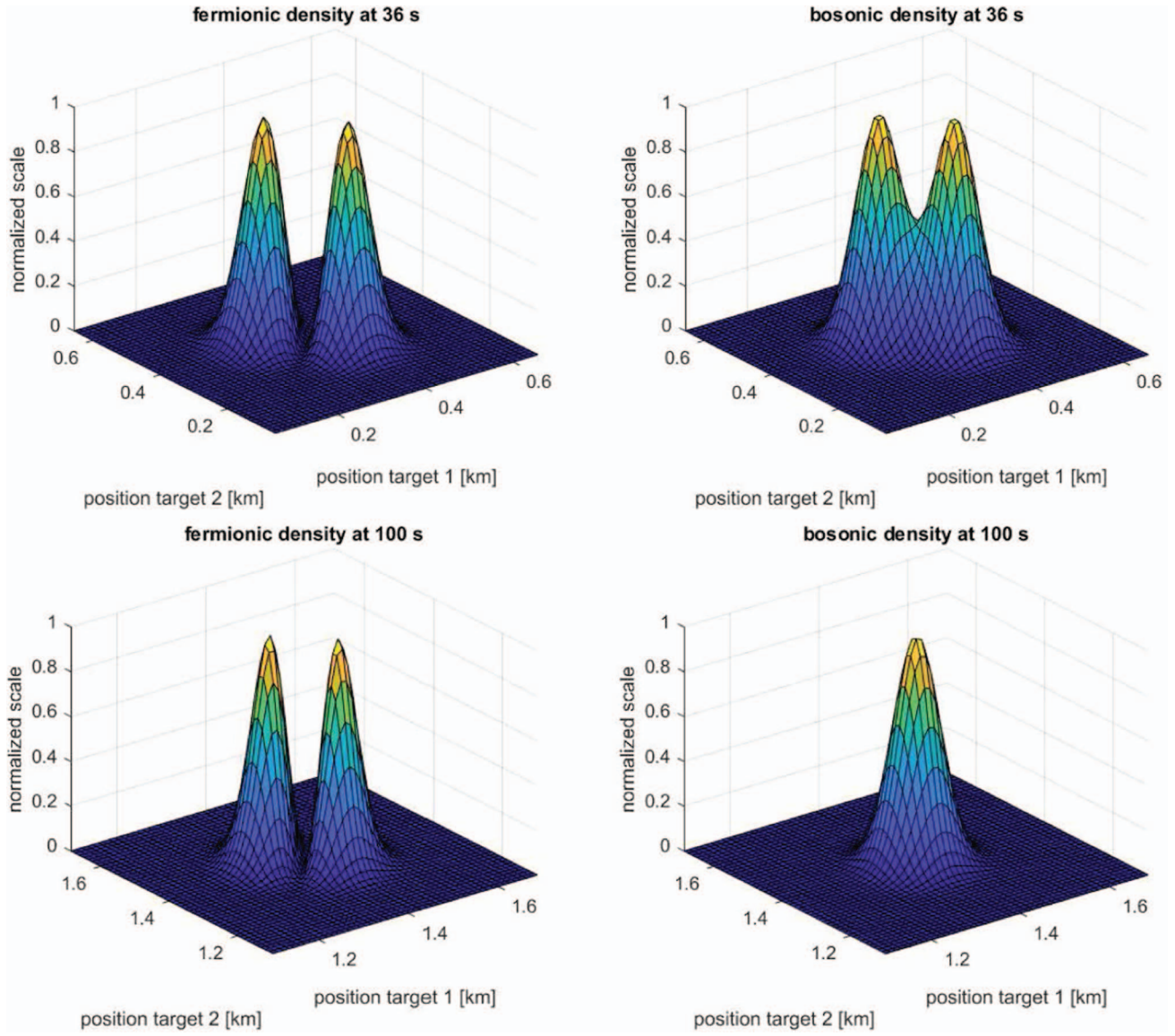


Fig. 3. Spatial projection of  $p^\pm(\mathbf{x}_k^{1:2}|Z_{k:1})$  at two different instants of time (36, 100 s).

spatial projections of the fermionic (left) and bosonic (right) joint densities representing the positional information on them for these instants of time. For about 30 s from the beginning of the vignette, the vehicles are well separated and characterized by two distinct Gaussian peaks that are the same in the fermionic and bosonic cases.

At time  $t_1 = 36$  s, however, the bosonic peaks are close to merging, while the peaks of the fermionic density are separated by a notch along the line where the vehicle positions are identical. This notch, which might be called the Pauli notch, is even more pronounced at time  $t_2 = 100$  s, when the bosonic peaks are completely merged for quite a long time. With “a smiling wink of the eye,” one might be tempted to speak of a Bose–Einstein condensate of the two tracks. At time  $t_3 = 140$  s, the bosonic tracks are beginning to be separated again, while at time  $t_4 = 170$  s, when the vehicles are well

separated again, the fermionic and the bosonic densities look identical.

Fig. 5 (left-hand side) shows the corresponding  $\psi$  function in a combined surface and contour plot where the Pauli notch is clearly visible. This phenomenon resembles the clutter notch in GMTI tracking [6, Sec. 7.2] that also “forbids” certain state characteristics. The Pauli notch vanishes when the vehicles become well separated again as shown for  $t_3 = 170$  s. The square of  $\psi$  function yields the fermionic density at this time (Fig. 4, left-hand side), which is essentially the same as in the bosonic case and in the beginning of the vignette.

In our simulations, we have observed that both fermionic and bosonic multiple identical target trackers mitigate the phenomenon of track coalescence, while fermionic trackers react significantly more agile to target split-off.

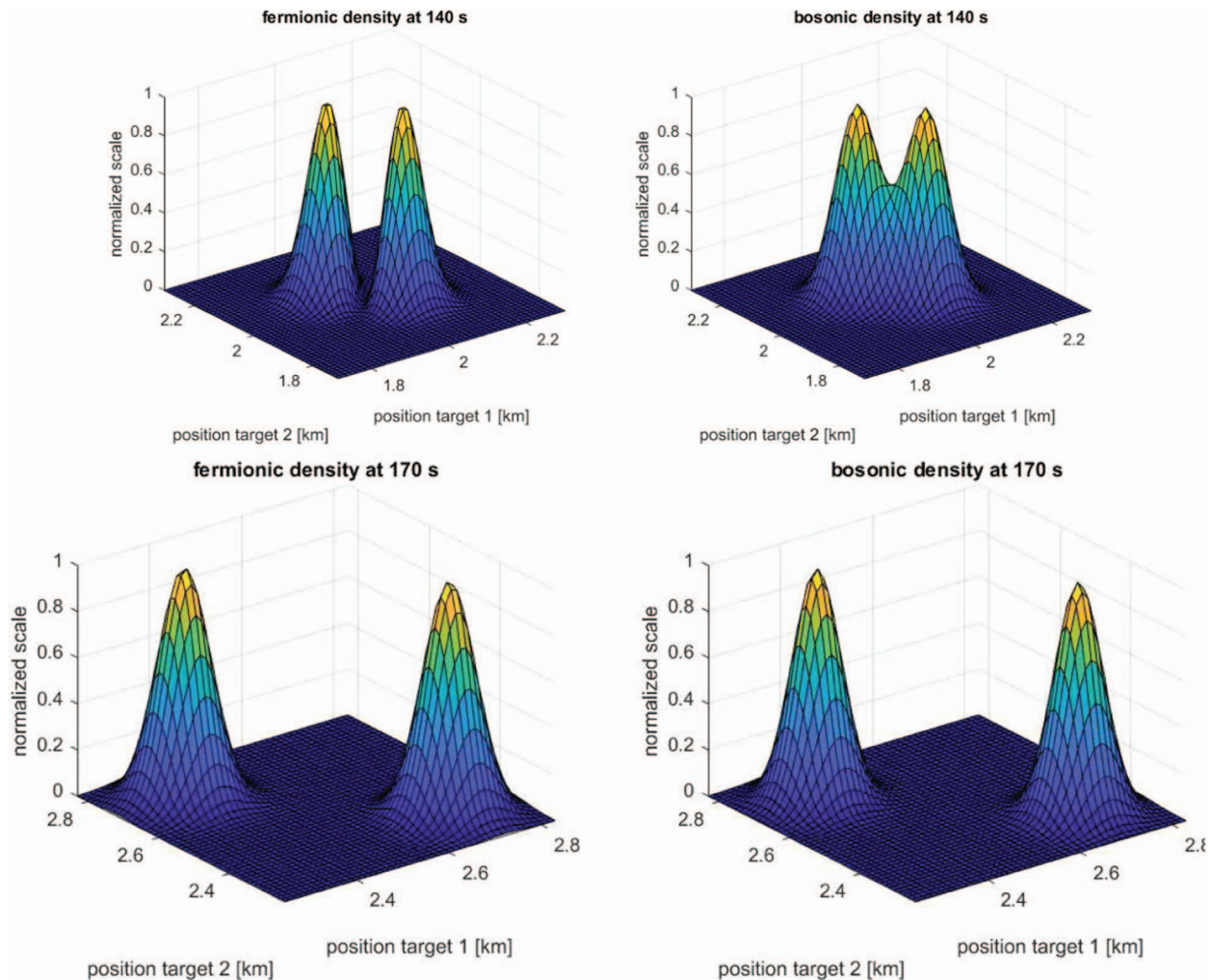


Fig. 4. Spatial projection of  $p^\pm(\mathbf{x}_k^{1:2}|Z_{k:1})$  at two different instants of time (134, 170 s).

## V. INDISTINGUISHABILITY AND PUBLIC SECURITY

Since security of public life is a basic human desire and a fundamental prerequisite of liberal societies,

its satisfaction raises an important question: How can public security be improved by morally and legally conformable and societally acceptable multiple sensor surveillance systems in public spaces? Perhaps rather

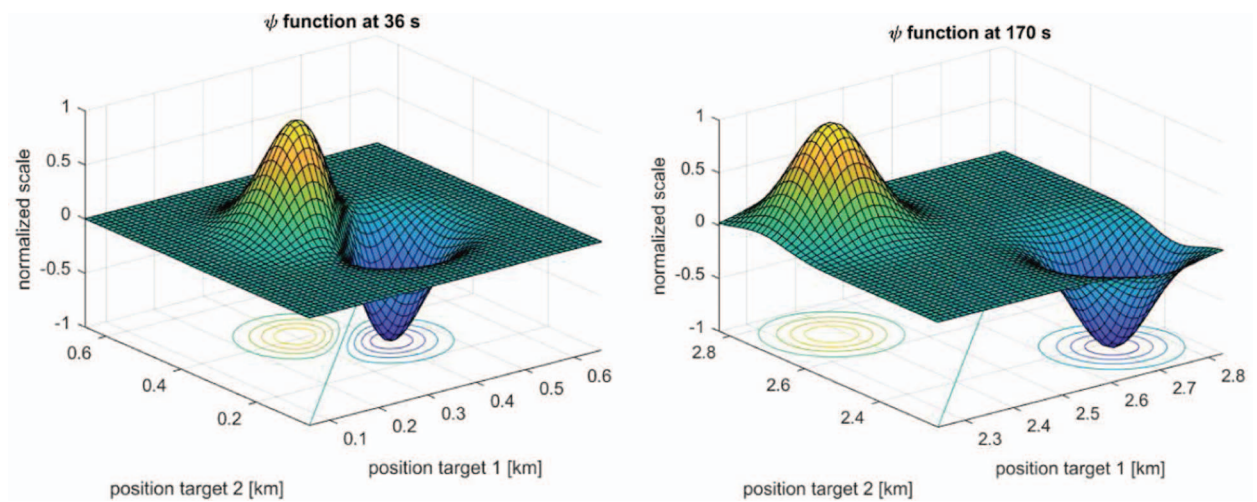


Fig. 5. Fermionic  $\psi$  function for closely spaced and well-separated vehicles (36, 170 s).

unexpectedly, bosonic and fermionic multiple target tracking, that is, *indistinguishable* target tracking, seems to play a key role seen from a systems engineering perspective whenever the problem of reconciling the values of greater security with the values of the liberality, freedom, personal dignity, or privacy that an individual foregoes is to be solved.

In the context of public surveillance, the tracking approach proposed here guarantees “indistinguishability of the uninvolved,” a notion that seems to play the role of a quite fundamental systems design principle. By considering persons to be tracked as indistinguishable targets, such security systems will be able to preserve the anonymity of the vast majority of persons until a certain level of suspicion is reached that may finally justify the identification of an individual, for example, by using the output of biometric sensors. From a systems engineering point of view, we conclude this paper discussing a prototypical realization that addresses security threats by hazardous materials in public infrastructures.

At the Nuclear Security Summit 2016,<sup>7</sup> radiological terrorism was identified as one of the greatest challenges to international security. Compared to nuclear weapons, improvised radiological dispersion devices (IRDDs) are relatively easy to produce, for which radioactive isotopes are used in many facilities, and often susceptible to theft. With the explicit constraint of not compromising the informational self-determination, an experimental public security system was developed to detect IRDDs in person streams and to make the security personnel aware of potential suspects. This research was part of a research project, which investigated the vulnerability of the transnational high-speed train systems [25]. While maintaining an open transport concept as far as possible, an analysis of the infrastructure usually available in and around railway stations shows that there are always areas suitable for continuous radiological monitoring. For details, see [26].

A spatially distributed network of gamma sensors records and classifies gamma radiation emitted by the materials used for building IRDDs. Any effective shielding by the perpetrators is impracticable. Such sensors provide data about the existence of a radiological hazard, the materials involved, the intensity, indications whether the material is incorporated for medical purposes or extracorporeal, and other attributes derivable from gamma spectra. The reliable localization of the source of gamma radiation, however, is not possible by considering spectrometers only.

The assignment of a radiological threat detected and classified to an individual is possible in a multiple sensor approach that exploits besides the spectra from spa-

tially distributed gamma sensors also the temporal dimension by tracking the persons while they are moving within the surveillance area. For tracking purposes, time-of-flight (ToF) cameras, cheap mass products, are used that are located in the ceiling above the surveillance area. These sensors provide additionally depth information in addition to the images. Person streams thus appear as “hilly landscapes” characterized by the moving heads of the people. Each individual can thus be tracked with high precision and without the risk of occlusions, even in dense crowds.

The demonstration of the experimental system shown in Fig. 6 shows persons walking around gamma sensors that in practical realizations may well be hidden in the walls or in the floor. The association of positive signatures provided by the gamma sensors with an individual and its track over time is produced by a track-while-classify (TwC) algorithm such as that described in [27]. Indistinguishable target tracking is essential in the TwC step that treats persons as fermionic targets. In other words, the overall system preserves in a certifiable sense personal privacy by the “indistinguishability of the uninvolved” principle that we would like to see recognized as a generally used principle of systems design in public surveillance applications.

The key benefit of indistinguishable target tracking in public security applications lies less in the fact that “better” tracks in a certain respect are produced, for example, in terms of accuracy or continuity, but to guarantee that no “uninvolved” person can be distinguished from another as long as it is not “uninvolved” any more, that is, until a sufficient level of “suspicion” has been accumulated, thus establishing *privacy by design*. In a crowd of persons, fermionic trackers may also provide a certain gain in track continuity as discussed in the example of the previous section.

## VI. CONCLUSIONS AND WAY AHEAD

Based on the fundamental observation that real-world targets cannot exist at the same time at the same place, we have introduced Pauli’s exclusion principle into multiple identical target tracking. Symmetry in target tracking, either in their fermionic variant or in their bosonic variant, inherently implies a multiple hypothesis structure where all measurements are associated with all targets that should conceptually be distinguished from classical enumeration of data interpretation hypotheses.

- Antisymmetry can seamlessly be embedded into the joint probability functions describing the kinematic properties of identical targets. Preliminary simulations indicate benefits in situation where targets may move closely spaced.
- In particular, antisymmetry leads to Gaussian sum representations with normalized weighting factors that are possibly negative. Such densities do

<sup>7</sup>Nuclear Security Summit, Washington, DC, USA, 2016, <http://www.nse2016.org>, last accessed August 26, 2019.



Fig. 6. Lab view of demonstrating IRDD localization in person streams using five gamma sensors on stabs and ToF cameras at the ceiling (invisible).

occur in target tracking for several reasons (see, e.g., [6, Sec. 7.4]).

- Extensive simulations will have to explore the properties and benefits of fermionic trackers quantitatively. In particular, the width of the Pauli notches has to be characterized and to be related to the targets' properties.
- Suitable approximations have to be developed as well and to be evaluated in view of practical implementations. Many-particle quantum physics has much more to offer to the tracking community as it would seem.
- Symmetry and antisymmetry can be embedded into group and extended target trackers, where the kinematics is described by random vectors and their shape by random matrices [6, Sec. 8.2]. While group targets might be dealt with as bosonic targets, extended targets are fermions.
- Antisymmetry is potentially present in *every* identical target tracking problem. Alternative methodologies are based on symmetric point processes [3, pp. 19, 240]. There are results for anti/skew-symmetric or “determinantal” point processes that are relevant to target tracking [19].
- Finally, symmetry and antisymmetry properties seem to be linked to “spooky action at a distance,” first observed in tracking by Dietrich Fränken, Michael Schmidt, and Martin Ulmke [28]. Apparently, entanglement is not restricted to the microphysical world. The physics literature may stimulate progress in understanding this paradox in target tracking [29].

## APPENDIX

### A.1 Normalizing $\psi$ Functions

With  $\Pi$  defined by  $\mathbf{x}_k^{1:2} = \Pi \mathbf{x}_k^{2:1}$ , we obtain

$$\begin{aligned} \int d\mathbf{x}_k^{1:2} (\mathcal{N}(\mathbf{x}_k^{1:2}; \mathbf{x}_{k|k}, \mathbf{P}_{k|k}) - \mathcal{N}(\mathbf{x}_k^{1:2}; \Pi \mathbf{x}_{k|k}, \Pi \mathbf{P}_{k|k} \Pi^\top))^2 \\ = \frac{2}{\sqrt{|4\pi \mathbf{P}_{k|k}|}} - 2\mathcal{N}(\mathbf{x}_{k|k}; \Pi \mathbf{x}_{k|k}, \mathbf{P}_{k|k} + \Pi \mathbf{P}_{k|k} \Pi^\top). \end{aligned} \quad (\text{A.1})$$

### A.2 Square Roots of Gaussians

According to the product formula for Gaussians, see [6, A.5], for example, we obtain

$$(\mathcal{N}(\mathbf{z}; \mathbf{x}, 2\mathbf{P}))^2 = \mathcal{N}(\mathbf{z}; \mathbf{z}, 4\mathbf{P}) \mathcal{N}(\mathbf{x}; \mathbf{z}, \mathbf{P}). \quad (\text{A.2})$$

### A.3 Fermionic Filtering Update

Since  $\mathbf{z}_k^1$  and  $\mathbf{z}_k^2$  are independent of each other,

$$\begin{aligned} \lambda_5(\mathbf{z}_k^{1:2}; \mathbf{H}_k^{1:2} \mathbf{x}_k^{1:2}, \mathbf{R}_k^{1:2}) \psi(\mathbf{x}_k^{1:2}; \mathbf{x}_{k|k-1}, \mathbf{P}_{k|k-1}) \\ = \mathcal{N}(\mathbf{z}_k^{1:2}; \mathbf{H}_k^{1:2} \mathbf{x}_k^{1:2}, \mathbf{R}_k^{1:2}) \mathcal{N}(\mathbf{x}_k^{1:2}; \mathbf{x}_{k|k-1}, \mathbf{P}_{k|k-1}) \\ - \mathcal{N}(\mathbf{z}_k^{2:1}; \mathbf{H}_k^{2:1} \mathbf{x}_k^{2:1}, \mathbf{R}_k^{2:1}) \mathcal{N}(\mathbf{x}_k^{2:1}; \mathbf{x}_{k|k-1}, \mathbf{P}_{k|k-1}) \\ + \mathcal{N}(\mathbf{z}_k^{2:1}; \mathbf{H}_k^{2:1} \mathbf{x}_k^{1:2}, \mathbf{R}_k^{2:1}) \mathcal{N}(\mathbf{x}_k^{1:2}; \mathbf{x}_{k|k-1}, \mathbf{P}_{k|k-1}) \\ - \mathcal{N}(\mathbf{z}_k^{1:2}; \mathbf{H}_k^{1:2} \mathbf{x}_k^{2:1}, \mathbf{R}_k^{1:2}) \mathcal{N}(\mathbf{x}_k^{2:1}; \mathbf{x}_{k|k-1}, \mathbf{P}_{k|k-1}). \end{aligned}$$

From the product formula [6, A.5], the update equations result.

## REFERENCES

- [1] S. Blackman  
*Design and Analysis of Modern Tracking Systems*. Norwood, MA, USA: Artech House Radar Library, 1999.
- [2] R. P. S. Mahler  
*Statistical Multisource–Multitarget Information Fusion*. Norwood, MA, USA: Artech House Information Warfare Library, 2007.
- [3] R. L. Streit  
*Poisson Point Processes. Imaging, Tracking, and Sensing (Electrical Engineering Series)*. Berlin, Germany: Springer, 2010.
- [4] Y. Bar-Shalom, P. K. Willett, and X. Tian  
*Tracking and Data Fusion. A Handbook of Algorithms*. Storrs, CT, USA: YBS Publishing, 2011.
- [5] L. D. Stone, R. L. Streit, Th. L. Corwin, and K. L. Bell  
*Bayesian Multiple Target Tracking*. Norwood, MA, USA: Artech House Radar Library, 2014.
- [6] W. Koch  
*Tracking and Sensor Data Fusion. Methodological Framework and Selected Applications (Mathematical Engineering Series)*. Berlin, Germany: Springer, 2014.
- [7] W. Koch  
“Towards cognitive tools: Systems engineering aspects for public safety and security,”  
*IEEE Aerosp. Electron. Syst. Mag.*, vol. 29, no. 9, pp. 14–26, Sep. 2014.
- [8] A. Bach  
*Indistinguishable Classical Particles (Lecture Notes in Physics)*. Berlin, Germany: Springer, 1997.
- [9] Y. Omar  
“Indistinguishable particles in quantum mechanics: An introduction,”  
*Contemp. Phys.*, vol. 46, no. 6, pp. 437–448, 2005.
- [10] W. Koch and G. van Keuk  
“Multiple hypothesis track maintenance with possibly unresolved measurements,”  
*IEEE Trans. Aerosp. Electron. Syst.*, vol. 33, no. 4, pp. 883–892, Jul. 1997.
- [11] P. A. M. Dirac  
*The Principles of Quantum Mechanics (International Series of Monographs on Physics, Book 27)*. Oxford, U.K.: Oxford University Press, 1st ed., 1930; 4th ed., 1958; 20th reprint, 2009.
- [12] L. Hoddeson, E. Braun, J. Teichmann, and S. Weart Eds.,  
*Out of the Crystal Maze. Chapters from the History of Solid-State Physics*. Oxford, U.K.: Oxford University Press, 1992.
- [13] S. French  
“Identity and individuality in quantum theory,”  
in *The Stanford Encyclopedia of Philosophy*, Fall 2015 ed., E. N. Zalta Ed., <https://plato.stanford.edu/archives/fall2015/entries/qt-idind/>.
- [14] S. Mori and C.-Y. Chong  
“Point process formalism for multiple target tracking,”  
in *Proc. 5th Int. Conf. Inf. Fusion*, 2002.
- [15] R. Mahler  
“Tracking ‘bunching’ multitarget correlations,”  
in *Proc. IEEE Int. Conf. Multisensor Fusion Integr. Intell. Syst.*, 2015.
- [16] B.-T. Vo and B.-N. Vo  
“Labeled random finite sets and multi-object conjugate priors,”  
*IEEE Trans. Signal Process.*, vol. 61, no. 13, pp. 3460–3475, Jul. 2013.
- [17] S. Reuter, B.-T. Vo, B.-N. Vo, and K. Dietmayer  
“The labeled multi-Bernoulli filter,”  
*IEEE Trans. Signal Process.*, vol. 62, no. 12, pp. 3246–3260, Jun. 2014.
- [18] F. Meyer, T. Kropfreiter, J. L. Williams, R. A. Lau, F. Hlawatsch, P. Braca, and M. Z. Win  
“Message passing algorithms for scalable multitarget tracking,”  
*Proc. IEEE*, vol. 106, no. 2, pp. 221–259, Feb. 2018.
- [19] N. Privault and T. Teoh  
“Second order multi-object filtering with target interaction using determinantal point processes,” arXiv:1906.06522, 2019.
- [20] “The Nobel Prize in Physics 1945,” Nobelprize.org, Nobel Media AB, 2014, [http://www.nobelprize.org/nobel\\_prizes/physics/laureates/1945/](http://www.nobelprize.org/nobel_prizes/physics/laureates/1945/).
- [21] W. Koch  
“On anti-symmetry in target tracking,”  
in *Proc. 21st Int. Conf. Inf. Fusion*, 2018.
- [22] W. Pauli  
“Exclusion principle and quantum mechanics” (Nobel Lecture on December 13, 1946, Stockholm),  
in *Nobel Lectures, Physics 1942–1962*. Amsterdam, the Netherlands: Elsevier, 1964, pp. 27–43.
- [23] W. Koch  
“Bayesian approach to extended object and cluster tracking using random matrices,”  
*IEEE Trans. Aerosp. Electron. Syst.*, vol. 44, no. 3, pp. 1042–1059, Jul. 2008.
- [24] M. A. Khan, M. Ulmke, B. Demissie, F. Govaers, and W. Koch  
“Combining log-homotopy flow with tensor decomposition based solution for Fokker–Planck equation,”  
in *19th Int. Conf. Inf. Fusion*, 2016.
- [25] REsilience of the Franco-German High Speed TRAIN Network (RE(H)STRAIN),  
<http://rehstrain.w3.rz.unibw-muenchen.de>, last accessed August 26, 2019.
- [26] F. Govaers, T. Fiolka, J. Heinskill, J. Biermann, and W. Koch  
“A detection system for dirty bombs in open environments,”  
in *Proc. Transport Res. Arena*, Vienna, 2018.
- [27] F. Govaers  
“A classify-while-track approach using dynamical tensors,”  
in *Proc. 7th IEEE Int. Workshop Comput. Adv. Multi-Sensor Adaptive Process.*, Curacao, 2017.
- [28] D. Fränken, M. Schmidt, and M. Ulmke  
“‘Spooky action at a distance’ in the cardinalized probability hypothesis density filter,”  
*IEEE Trans. Aerosp. Electron. Syst.*, vol. 45, no. 4, pp. 1657–1664, Oct. 2009.
- [29] A. Zeilinger, T. Herbst, M. Aspelmeyer, M. Barbieri, T. Jennewein, and A. Zeilinger  
“Anti-symmetrization reveals hidden entanglement,”  
*New J. Phys.*, vol. 11, p. 103052, 2009.



**Wolfgang Koch** born 1962, studied physics and mathematics at the Aachen Technical University RWTH, Aachen, Germany, where he received the Ph.D. degree in theoretical physics. For many years, he is Head of the Department “Sensor Data and Information Fusion SDF,” Fraunhofer FKIE, Bonn, Germany, primarily working for the German MoD and defense industry. This comprises ISTAR, electronic/navigation warfare, sensor/platform resources management, and manned–unmanned teaming. Within these areas, he has published a well-referenced monograph, 18 handbook chapters, and about 300 journal and conference articles. He is one of the co-editors of the recently published two-volume handbook “Novel Radar Techniques and Applications” (2017). Dr. Koch is a member of the Board of Directors of the International Society of Information Fusion (ISIF). Being a Fellow, Distinguished Lecturer, and Member of the Board of Governors of the IEEE, he is actively serving in the IEEE Aerospace and Electronics Systems Society (AESS). Moreover, he is member at large on the Sensors and Electronics Technology panel of NATO STO and has contributed to many STO activities. At Bonn University, he is a Professor for applied computer science and teaches on sensor data fusion and artificial intelligence. He has organized many scientific conferences and workshops.

# Multiscan Implementation of the Trajectory Poisson Multi-Bernoulli Mixture Filter

YUXUAN XIA  
KARL GRANSTRÖM  
LENNART SVENSSON  
ÁNGEL F. GARCÍA-FERNÁNDEZ  
JASON L. WILLIAMS

**The Poisson multi-Bernoulli mixture (PMBM) and the multi-Bernoulli mixture (MBM) are two multitarget distributions for which closed-form filtering recursions exist. The PMBM has a Poisson birth process, whereas the MBM has a multi-Bernoulli birth process. This paper considers a recently developed formulation of the multitarget tracking problem using a random finite set of trajectories, through which the track continuity is explicitly established. A multiscan trajectory PMBM filter and a multiscan trajectory MBM filter, with the ability to correct past data association decisions to improve current decisions, are presented. In addition, a multiscan trajectory MBM<sub>01</sub> filter, in which the existence probabilities of all Bernoulli components are either 0 or 1, is presented. This paper proposes an efficient implementation that performs track-oriented  $N$ -scan pruning to limit computational complexity, and uses dual decomposition to solve the involved multiframe assignment problem. The performance of the presented multitarget trackers, applied with an efficient fixed-lag smoothing method, is evaluated in a simulation study.**

Manuscript received January 2, 2019; revised May 6, 2019, September 3, 2019; released for publication February 5, 2020.

Refereeing of this contribution was handled by Chee-Yee Chong.

Y. Xia, K. Granström, and L. Svensson are with the Department of Electrical Engineering, Chalmers University of Technology, 41296, Göteborg, Sweden.

Á. F. García-Fernández is with the Department of Electrical Engineering and Electronics, University of Liverpool, Liverpool J69 3GJ, U.K.

J. L. Williams is with the Commonwealth Scientific and Industrial Research Organisation, Brisbane QLD 4006 and Queensland University of Technology, Brisbane QLD 4000, Australia.

1557-6418/19/\$17.00 © 2019 JAIF

## I. INTRODUCTION

Multitarget tracking (MTT) refers to the problem of jointly estimating the number of targets and their trajectories from noisy sensor measurements [1]. The number of targets and their trajectories can be time-varying due to targets appearing and disappearing. In a general MTT system, a multitarget tracker needs to tackle the modeling of births and deaths of targets, as well as the partitioning of noisy sensor measurements into potential tracks and false alarms; the latter is also referred to as data association. The major approaches to MTT include the joint probabilistic data association (JPDA) filter [2], the multiple hypothesis tracker (MHT) [3]–[5], and random finite set (RFS) [6] based multitarget filters [7, Ch. 6].

The JPDA filter [2] seeks to calculate the marginal distribution of each track. To accommodate for an unknown and time-varying number of targets, the joint integrated probabilistic data association [8] extends the basic JPDA [2] by incorporating target existence as an additional random variable to be estimated. It has recently been shown that the marginal data association probabilities can be efficiently approximated using message passing algorithms [9], [10].

MHT is described in a number of books; e.g., see [3, Ch. 16] and [4, Chs. 6 and 7]. The model was made rigorous in [11] through random finite sequences, under the assumption that the number of targets present is constant but unknown, with an a priori distribution that is Poisson. In MHT, multiple data association hypotheses are formed to explain the source of the measurements. Each data association hypothesis assigns measurements to previously detected targets, newly detected targets, or false alarms. Data association uncertainty is captured by the data hypothesis weight, and the target state uncertainty is captured by the target state density distribution conditioned on each hypothesis.

There are two types of MHT algorithms: the hypothesis-oriented MHT (HOMHT) [12] and the track-oriented MHT (TOMHT) [13], [14]. In HOMHT, multiple global hypotheses are formed and evaluated between consecutive time scans; the complete algorithmic approach was first developed by Reid [12]. The TOMHT operates by maintaining a number of single target hypothesis trees, each of which contains a number of single target hypotheses explaining the measurement association history of a potential target.

A TOMHT algorithm usually uses a deferred decision logic to consider the data associations of measurements from more than one scan, in the sense that the hypotheses are propagated into the future in anticipation that subsequent data will resolve the uncertainty [5]. Intuitively, measurements in more than one scan may provide more accurate data association than those in a single scan. The number of single target hypotheses can be limited by performing  $N$ -scan pruning [5], and the involved multiframe assignment problem is typi-

cally solved using Lagrangian relaxation-based methods [15]–[17]. Track management (target initiation and termination) is usually performed using some external procedures; see, e.g., [18].

RFSs and finite set statistics (FISST) were developed to provide a systematic methodology for dealing with MTT problems involving a time-varying number of targets [6]. The relationship between RFS-based approaches to MTT and MHT has been discussed in [19] and [20]. In the RFS formulation of MTT, the multitarget filtering density contains the information of the target states at the current time step. Exact closed-form solutions of RFS-based multitarget Bayes filter are given by multitarget conjugate priors. The concept of multitarget conjugate prior was defined in [21] as “If we start with the proposed conjugate initial prior, then all subsequent predicted and posterior distributions have the same form as the initial prior.”

Two well-established MTT conjugate priors for the standard point target measurement model are the Poisson multi-Bernoulli mixture (PMBM) [22] based on unlabeled RFSs and the generalized labeled multi-Bernoulli (GLMB) [21] based on labeled RFSs. The PMBM consists of a Poisson distribution representing targets that are hypothesized to exist but have not been detected and a multi-Bernoulli mixture (MBM) representing targets that have been detected at some stage. The resulting PMBM filter [23] is a computationally tractable filter for the standard point target dynamic model, where the birth model is a Poisson RFS. If the birth process is a multi-Bernoulli RFS, the multitarget conjugate prior is of the form MBM [23], [24]. A discussion regarding the differences between the use of a Poisson birth model and the use of a multi-Bernoulli birth model can be found in [24].

#### A. Track Continuity in MTT

In this section, we discuss how track continuity can be maintained in different MTT methodologies. Vector-type MTT methods, e.g., the JPDA filter and the MHT, describe the multitarget states and measurements by random vectors. They are able to explicitly maintain track continuity; i.e., they associate a state estimate with a previous state estimate or declare the appearance of a new target [10]. For multitarget filters based on unlabeled RFS, time sequences of tracks cannot be constructed easily due to the set representation of the multitarget states that are order independent. The PMBM filter (as well as the MBM filter) seemingly does not provide explicit track continuity between time steps,<sup>1</sup> although a hypothesis structure in analogy to MHT was observed in [22] and [23].

<sup>1</sup>The PMBM filter and the MBM filter are able to maintain track continuity implicitly, in a practical setting, based on information provided by metadata.

One approach to addressing the lack of track continuity is to add unique labels to the target states and estimate target states from the multitarget filtering density [21], [25], [26]. This procedure can work well in some cases, but it becomes problematic in challenging situations, for example, when target birth is independent and identically distributed, and when targets get in close proximity and then separate [27]. The  $\delta$ -GLMB filter [28] (and its approximation the labeled multi-Bernoulli (LMB) filter [29]) is an example of the resulting labeled filter when the birth model is an LMB (mixture) RFS. The  $\delta$ -GLMB density is similar in structure to labeled MBM using MBM<sub>01</sub> parameterization [23], in which Bernoulli components are uniquely labeled, and their existence probability is restricted to either 0 or 1. It was shown in [23] that the MBM parameterization has computational and implementational advantages over the MBM<sub>01</sub> parameterization.

#### B. Trajectory PMBM Filter and Its Relation to MHT

In this section, we give a brief introduction to the trajectory PMBM filter and discuss its relation to MHT. More details of the trajectory PMBM filter will be given in Section III.

Compared to augmenting target states with unique labels, a more appealing approach to ensuring track continuity for RFS-based multitarget filters is to generalize the concept of RFSs of targets to RFSs of trajectories. The theoretical background to perform MTT using RFS of trajectories was provided in [27] and [30]. Within the set of trajectories framework, the goal of MTT is to recursively compute the posterior density over the set of trajectories, which contains full information about the target trajectories, and can be used to estimate the best set of trajectories at each time step.

Closed-form PMBM filtering recursions based on the set of trajectories framework have been derived in [31], which enables us to leverage on the benefits of the PMBM filter recursion based on sets of targets, while also obtaining track continuity. Assuming standard point target dynamic [32, Sec. 13.2.4] and measurement models (defined in Section II-A), two different trajectory PMBM filters were proposed in [31]: one in which the set of current (i.e., alive) trajectories is tracked, and one in which the set of all trajectories (dead and alive) up to the current time step is tracked. In both cases, finite trajectories, i.e., trajectories of finite length in time, are considered.

The implementation of the trajectory PMBM filter in [31] considers the single-scan data association problem, and the best global hypotheses are found using Murthy’s algorithm [33]. As a complement to [31], an approximation to the exact trajectory PMBM filter that considers multiscan data association was developed in [34]. It operates by performing track-oriented  $N$ -scan pruning [5] to limit computational complexity, and using dual

decomposition [17] to solve the involved multiframe assignment problem. The proposed algorithm therefore shares some of the key properties of certain TOMHT algorithms [5], [17], but is derived using RFSs of trajectories and birth/death models. As a comparison, TOMHT algorithms typically use heuristics to take into account the appearance and disappearance of targets [4, Ch. 7].

Numerical results in [34] show that the proposed multiscan trajectory PMBM filter has better tracking performance than the fast implementation of the  $\delta$ -GLMB filter using Gibbs sampling [35] in terms of estimation error and computational time. These two filters use different birth models, Poisson RFS and multi-Bernoulli RFS, respectively. A multi-Bernoulli birth can be suitable if one is certain that a known maximum of targets will enter the area of interest and the targets appear around some known locations. With multi-Bernoulli birth, the PMBM conjugate prior becomes an MBM conjugate prior [23]. An implementation of the MBM filter for sets of targets was proposed in [24]. The case in which the probability distribution of the number of targets is not necessarily Poisson was discussed in [36] for the batch-processing formulation used for TOMHT; however, a practical implementation was not provided in [36].

The data association is explicitly represented in both the trajectory PMBM filter and the trajectory MBM filter, in a data structure analogous to TOMHT. Compared to conventional MHT formalism, as described in [5] and [14], one important difference is that the presented trajectory PMBM filters include a Poisson RFS that models undetected trajectories. The modeling of undetected targets allows for newly discovered targets to have been born at earlier time steps [20]. Therefore, the trajectory PMBM filters give a higher effective birth rate than general TOMHT. The modeling of undetected targets was incorporated into TOMHT in [37]. In comparison, in the trajectory PMBM filters the hypotheses are purely data-to-data assignments and they are more efficiently represented using Bernoulli RFSs with probabilistic target existence. More importantly, in the PMBM trajectory filters the estimates of the set of trajectories can be directly extracted from the multitarget densities in addition to the target current states.

### C. Contributions and Organization

This paper is an extension of [34]. In this paper, we present the trajectory PMBM and the trajectory MBM filter with multiscan data association. The main novelties of the proposed algorithms, compared to previous work based on sets of trajectories [27], [31], [38], [39], are that they consider the multiscan data association problem. The main novelties of the proposed algorithms, compared to TOMHT, are that they produce full trajectory estimates, i.e., smoothed estimates, upon receipt of each new set of measurements, and that the filters based on sets of trajectories model the targets that remain to

be detected and the target death subsequent to the final detection.

The contributions can be summarized as follows:

- 1) We present the filtering recursions for the trajectory MBM filter and the trajectory MBM<sub>01</sub> filter using a multi-Bernoulli birth model. Two variants are considered for each filter: the set of current trajectories and the set of all trajectories.
- 2) We show that the ideas from the efficient TOMHT in [17] can be utilized in trajectory filters based on PMBM, MBM, and MBM<sub>01</sub> conjugate priors, resulting in so-called multiscan trajectory filters.
- 3) We explain how to efficiently perform fixed-lag smoothing to extract smoothed trajectory estimates for the presented algorithms.
- 4) We evaluate the performance of the presented algorithms in a simulation study, in terms of target state/trajectory estimation error and computational time.

The paper is organized as follows. In Section II, we introduce the modeling assumption and background on sets of trajectories. In Section III, we review the PMBM conjugate prior on the set of trajectories. In Section IV, we present the filtering recursion for trajectory MBM filter. In Section V, we present implementations of the multiscan trajectory filters. In Section VI, we present how to efficiently perform fixed-lag smoothing when extracting trajectory estimates. Simulation results are presented in Section VII, and conclusions are drawn in Section VIII.

## II. MODELING

In this section, we first outline the modeling assumptions utilized in this work. Next, we give a brief introduction to RFSs of trajectories. Then, we introduce the generalized transition and measurement models in the framework of set of trajectories; the precise mathematical definitions can be found in [27]. The modeling is probabilistic, and the interested reader can find the necessary details about FISST, measure theory, probability generating functionals (PGFLs), and functional derivatives for sets of trajectories in Appendices A and D.

### A. Modeling Assumptions

We assume that for each discrete time  $k$  (a non-negative integer), a continuous time  $t_k$  is assigned, such that  $t_k > t_{k'}$  for  $k > k'$ . In the traditional formulation for RFSs of targets, target states and measurements are represented in the form of finite sets [6]. A random single target state  $x_k$  is a random element of the state (Euclidean) space  $\mathcal{X} = \mathbb{R}^n$ , and a random measurement  $z_k$  is a random element of the measurement space  $\mathcal{Z} = \mathbb{R}^m$ , all at discrete time  $k$ . The random set of measurements obtained by a single sensor, including clutter and target measurements with unknown origin, at time

step  $k$  is denoted as  $\mathbf{z}_k \in \mathcal{F}(\mathcal{Z})$ , where  $\mathcal{F}(\mathcal{Z})$  denotes the set of all the finite subsets of  $\mathcal{Z}$ .

We proceed by introducing two families of RFSs that will have prominent roles throughout the paper: the Poisson RFS [6, Sec. 4.3.1] and the Bernoulli RFS [6, Sec. 4.3.3]. A Poisson RFS  $\Psi$  has multi-object density distribution

$$f^{\text{PPP}}(\Psi) = e^{-\int \lambda(\Psi) d\Psi} \prod_{\Psi \in \Psi} \lambda(\Psi), \quad (1)$$

where  $\lambda(\cdot)$  is the intensity function and the number of objects is Poisson distributed. An RFS  $\Psi$  is a Bernoulli RFS if  $|\Psi| \leq 1$ , and a Bernoulli RFS has multi-object density distribution

$$f^{\text{ber}}(\Psi) = \begin{cases} 1 - r, & \Psi = \emptyset, \\ rf(\Psi), & \Psi = \{\Psi\}, \\ 0, & \text{otherwise,} \end{cases} \quad (2)$$

where  $f(\cdot)$  is a single object probability density and  $r$  is the probability of existence. A multi-Bernoulli RFS is the union of a finite number of independent Bernoulli RFSs.

In previous works [27], [31], [38], [39], two different birth models have been used. In this paper, we present multiscan trajectory filter implementations for both birth models: the Poisson birth model defined in Assumption 1 and the multi-Bernoulli birth model defined in Assumption 2. The standard point target measurement model is defined in Assumption 3.

**Assumption 1.** *The multitarget state evolves according to the following standard dynamic process with a Poisson birth model:*

- 1) *New targets appear in the surveillance area independently of any existing targets. Targets arrive at each time step according to a Poisson RFS with birth intensity  $\lambda_k^b(x_k)$  defined on the target state space  $\mathcal{X}$ .*
- 2) *Given a target with state  $x_k$ , the target survives with a probability  $P^S(x_k)$  and moves with a Markov state transition density  $\pi(x_{k+1}|x_k)$  defined on the target state space  $\mathcal{X}$ . The state transition density is the density of the target state at time step  $k+1$ , given that the target had state  $x_k$  at time step  $k$ .*

**Assumption 2.** *The multitarget state evolves according to the following modified dynamic process with a multi-Bernoulli birth model:*

- 1) *New targets appear in the surveillance area independently of any existing targets. Targets arrive at time step  $k$  according to a multi-Bernoulli RFS, which has  $n_k^b$  Bernoulli components. The  $l$ th Bernoulli component has existence probability  $r_k^{b,l}$  and state density  $f_k^{b,l}(x_k)$  defined on the target state space  $\mathcal{X}$ .*
- 2) *Same as Assumption 1, point 2.*

**Assumption 3.** *The multitarget measurement process is as follows:*

- 1) *Each target may give rise to at most one measurement, and each measurement is the result of at most one target. The probability of detection of a target with state  $x_k$  is  $P^D(x_k)$ , and the single measurement density is  $f(z_k|x_k)$  from the target space  $\mathcal{X}$  to the measurement space  $\mathcal{Z}$ , which is the probability density of the measurement  $z_k$ , given that there is a target with state  $x_k$  in the scene.*
- 2) *Clutter measurements arrive according to a Poisson RFS with intensity  $\lambda^{\text{FA}}(z_k)$  defined on the measurement space  $\mathcal{Z}$ , independently of targets and target-oriented measurements.*

## B. Random Finite Sets of Trajectories

In this section, we first explain how the single trajectory state and its density are defined. Then, we briefly introduce some basic types of RFSs of trajectories.

1) *Trajectory State:* We use the trajectory state model presented in [27] and [30], in which the trajectory state is a tuple

$$X = (\beta, \varepsilon, x_{\beta:\varepsilon}), \quad (3)$$

where  $\beta$  is the discrete time of the trajectory birth, i.e., the time the trajectory begins;  $\varepsilon$  is the discrete time of the trajectory's end time. If  $k$  is the current time,  $\varepsilon = k$  means that the trajectory is alive;  $x_{\beta:\varepsilon}$  is, given  $\beta$  and  $\varepsilon$ , the (finite) sequence of states

$$x_{\beta:\varepsilon} = (x_\beta, x_{\beta+1}, \dots, x_{\varepsilon-1}, x_\varepsilon), \quad (4)$$

where  $x_\kappa \in \mathcal{X}$  for all  $\kappa \in \{\beta, \dots, \varepsilon\}$ . This gives a trajectory of length  $l = \varepsilon - \beta + 1$  time steps.

The single trajectory state can be considered a hybrid state consisting of discrete states  $\beta$  and  $\varepsilon$  representing the start and end time indices, and a continuous state  $x_{\beta:\varepsilon}$  that evolves according to a stochastic model dependent on the discrete states.<sup>2</sup> The trajectory state space at time step  $k$  is [27]

$$\mathcal{T}_k = \uplus_{(\beta,\varepsilon) \in I_k} \{\beta\} \times \{\varepsilon\} \times \mathcal{X}^{\varepsilon-\beta+1}, \quad (5)$$

where  $\uplus$  denotes the union of (possibly empty) sets that are mutually disjoint,  $I_k = \{(\beta, \varepsilon) : 0 \leq \beta \leq \varepsilon \leq k\}$  is the set of all possible start and end times of trajectories up to time step  $k$ , and  $\mathcal{X}^l$  denotes  $l$  Cartesian products of  $\mathcal{X}$ , i.e., the Cartesian products of spaces of different sizes. A trajectory state density  $p(\cdot)$  of  $X$  factorizes as follows:

$$p(X) = p(x_{\beta:\varepsilon} | \beta, \varepsilon) P(\beta, \varepsilon), \quad (6)$$

where, if  $\varepsilon < \beta$ , then  $P(\beta, \varepsilon)$  is zero. Integration for single trajectory densities is performed as follows [27]:

<sup>2</sup>We remark that the use of such a hybrid state, i.e., a combination of one (or more) discrete state and one (or more) continuous state, is not uncommon in MTT: a typical example is the interacting multiple model [40], in which the identification of multiple models, which can be of different dimensionality [41], is governed by a discrete stochastic process.

$$\begin{aligned} & \int p(X)dX \\ &= \sum_{(\beta, \varepsilon) \in I_k} \left[ \int \cdots \int p(x_{\beta:\varepsilon} | \beta, \varepsilon) dx_{\beta} \cdots dx_{\varepsilon} \right] P(\beta, \varepsilon). \end{aligned} \quad (7)$$

2) *Sets of Trajectories:* A set of trajectories is denoted as  $\mathbf{X}_k \in \mathcal{F}(\mathcal{T}_k)$ , where  $\mathcal{F}(\mathcal{T}_k)$  is the set of all the finite subsets of  $\mathcal{T}_k$ . Let  $g(\mathbf{X}_k)$  be a real-valued function on a set of trajectories, then the set integral is

$$\begin{aligned} & \int g(\mathbf{X}_k) \delta \mathbf{X}_k \\ & \triangleq g(\emptyset) + \sum_{n=1}^{\infty} \frac{1}{n!} \int \cdots \int g(\{X_k^1, \dots, X_k^n\}) dX_k^1 \cdots dX_k^n. \end{aligned} \quad (8)$$

A trajectory Poisson RFS has (multitrajectory) density of the form (1), where the trajectory Poisson RFS intensity  $\lambda(\cdot)$  is defined on the trajectory state space  $\mathcal{T}_k$ ; i.e., realizations of the Poisson RFS are trajectories with a birth time, a time of the most recent state, and a state sequence [38]. A trajectory Bernoulli RFS has density of the form (2), where  $f(\cdot)$  is a single trajectory density (6). Trajectory multi-Bernoulli RFS and trajectory MBM RFS are both defined analogously to target multi-Bernoulli RFS and target MBM RFS [27]: a trajectory multi-Bernoulli is the disjoint union of a multiple trajectory Bernoulli RFS; trajectory MBM RFS is an RFS whose density is a mixture of trajectory multi-Bernoulli densities.

### C. Transition Models for Sets of Trajectories

In the standard multitarget dynamic model with Poisson birth (see Assumption 1), target birth at time step  $k$  is modeled by a Poisson RFS, with intensity

$$\lambda_k^B(X) = \lambda_k^{B,x}(x_{\beta:\varepsilon} | \beta, \varepsilon) \Delta_k(\varepsilon) \Delta_k(\beta), \quad (9a)$$

$$\lambda_k^{B,x}(x_{k:k} | k, k) = \lambda_k^b(x_k), \quad (9b)$$

where  $\Delta(\cdot)$  denotes the Kronecker delta function. In the modified multitarget dynamic model with multi-Bernoulli birth (see Assumption 2), target birth at time step  $k$  is modeled by a multi-Bernoulli RFS, with the trajectory state density in the  $l$ th Bernoulli component

$$f_k^{B,l}(X) = f_k^{B,l,x}(x_{\beta:\varepsilon} | \beta, \varepsilon) \Delta_k(\varepsilon) \Delta_k(\beta), \quad (10a)$$

$$f_k^{B,l,x}(x_{k:k} | k, k) = f_k^{b,l}(x_k), \quad (10b)$$

and the existence probability  $r_k^{b,l}$ .

We focus on two different MTT problem formulations: the set of current trajectories, where the objective is to estimate the trajectories of targets that are still present in the surveillance area at the current time, and the set of all trajectories, where the objective is to estimate the trajectories of both the targets that are still present in the surveillance area at the current time and

the targets that once were in (but have since left) the surveillance area at some previous time. The probability of survival as a function on trajectories at time step  $k$  is defined as

$$P_k^S(X) = P^S(x_{\varepsilon}) \Delta_k(\varepsilon). \quad (11)$$

The transition density for the trajectories depends on the problem formulation.

1) *Transition Model for the Set of Current Trajectories:* The Bernoulli RFS transition density for a single potential target without birth is

$$\begin{aligned} & f_{k|k-1}^c(\mathbf{X} | \mathbf{X}') \\ &= \begin{cases} 1, & \mathbf{X}' = \emptyset, \mathbf{X} = \emptyset, \\ 1 - P_{k-1}^S(X'), & \mathbf{X}' = \{X'\}, \mathbf{X} = \emptyset, \\ P_{k-1}^S(X') \pi^c(X | X'), & \mathbf{X}' = \{X'\}, \mathbf{X} = \{X\}, \\ 0, & \text{otherwise,} \end{cases} \end{aligned} \quad (12a)$$

$$\pi^c(X | X') = \pi^{c,x}(x_{\beta:\varepsilon} | \beta, \varepsilon, X') \Delta_{\varepsilon'+1}(\varepsilon) \Delta_{\beta'}(\beta), \quad (12b)$$

$$\pi^{c,x}(x_{\beta:\varepsilon} | \beta, \varepsilon, X') = \pi^x(x_{\varepsilon} | x'_{\varepsilon'}) \delta_{x'_{\beta':\varepsilon'}}(x_{\beta:\varepsilon-1}), \quad (12c)$$

where  $\delta(\cdot)$  denotes Dirac delta function and  $X'$  denotes the single trajectory state at time step  $k-1$ . In this model,  $P^S(\cdot)$  is used as follows. If the target disappears, or “dies,” then the entire trajectory will no longer be a member of the set of current trajectories. If the trajectory survives, then the trajectory is extended by one time step.

2) *Transition Model for the Set of All Trajectories:* The Bernoulli RFS transition density for a single potential target without birth is

$$\begin{aligned} & f_{k|k-1}^a(\mathbf{X} | \mathbf{X}') \\ &= \begin{cases} 1, & \mathbf{X}' = \emptyset, \mathbf{X} = \emptyset, \\ \pi^a(X | X'), & \mathbf{X}' = \{X'\}, \mathbf{X} = \{X\}, \\ 0, & \text{otherwise,} \end{cases} \end{aligned} \quad (13a)$$

$$\pi^a(X | X') = \pi^{a,x}(x_{\beta:\varepsilon} | \beta, \varepsilon, X') \pi^{\varepsilon}(\varepsilon | \beta, X') \Delta_{\beta'}(\beta), \quad (13b)$$

$$\pi^{\varepsilon}(\varepsilon | \beta, X') = \begin{cases} 1, & \varepsilon = \varepsilon' < k-1, \\ 1 - P_{k-1}^S(X'), & \varepsilon = \varepsilon' = k-1, \\ P_{k-1}^S(X'), & \varepsilon = \varepsilon' + 1 = k, \\ 0, & \text{otherwise,} \end{cases} \quad (13c)$$

$$\begin{aligned} & \pi^{a,x}(x_{\beta:\varepsilon} | \beta, \varepsilon, X') \\ &= \begin{cases} \delta_{x'_{\beta':\varepsilon'}}(x_{\beta:\varepsilon}), & \varepsilon = \varepsilon', \\ \pi^x(x_{\varepsilon} | x'_{\varepsilon'}) \delta_{x'_{\beta':\varepsilon'}}(x_{\beta:\varepsilon-1}), & \varepsilon = \varepsilon' + 1. \end{cases} \end{aligned} \quad (13d)$$

In this model, the interpretation of the probability of survival is that it governs whether the trajectory ends or it is extended by one more time step. However, importantly, regardless of whether or not the trajectory ends,

the trajectory remains in the set of all trajectories with probability one.

The complete transition model for sets of trajectories is analogous to the complete transition model for sets of targets, by using sets of trajectories and the corresponding Bernoulli transition density for each problem formulation. Given the set  $\mathbf{X}_{k-1} = \{X_{k-1}^1, \dots, X_{k-1}^n\}$  of trajectories at time step  $k-1$ , the set  $\mathbf{X}_k$  of trajectories at time step  $k$  is  $\mathbf{X}_k = \mathbf{X}_k^b \uplus \mathbf{X}_k^1 \uplus \dots \uplus \mathbf{X}_k^n$ , where  $\mathbf{X}_k^b, \mathbf{X}_k^1, \dots, \mathbf{X}_k^n$  are independent sets,  $\mathbf{X}_k^b$  is the set of newborn trajectories, and  $\mathbf{X}_k^i$  is the set of trajectories resulting from  $X_{k-1}^i$ . Using the convolution formula for multi-object densities [6, eq. (4.17)], the resulting multitrajectory density  $f(\cdot|\cdot)$  of  $\mathbf{X}_k$  given  $\mathbf{X}_{k-1}$  can be written as

$$f(\mathbf{X}_k|\mathbf{X}_{k-1}) = \sum_{\mathbf{X}_k^b \uplus \mathbf{X}_k^1 \uplus \dots \uplus \mathbf{X}_k^n = \mathbf{X}_k} f_k^{\text{birth}}(\mathbf{X}_k^b) \times \prod_{i=1}^n f_{k|k-1}^{\text{persist}}(\mathbf{X}_k^i | \{X_{k-1}^i\}), \quad (14)$$

where  $f_k^{\text{birth}}(\cdot)$  is either a trajectory Poisson RFS or a trajectory multi-Bernoulli RFS, and  $f_{k|k-1}^{\text{persist}}(\cdot)$  is a Bernoulli transition density for a single potential target without birth, with the form  $f_{k|k-1}^a(\cdot)$  or  $f_{k|k-1}^c(\cdot)$ .

#### D. Single Trajectory Measurement Model

According to the point target measurement model in Assumption 3, the multi-object density of a target-generated measurement at time step  $k$  given a set of trajectories with 0 or 1 element is Bernoulli, with the form

$$\varphi_k(\mathbf{w}_k|\mathbf{X}) = \begin{cases} 1, & \mathbf{X} = \emptyset, \mathbf{w}_k = \emptyset, \\ 1 - P_k^D(X), & \mathbf{X} = \{X\}, \mathbf{w}_k = \emptyset, \\ P_k^D(X)\varphi(z_k|X), & \mathbf{X} = \{X\}, \mathbf{w}_k = \{z_k\}, \\ 0, & \text{otherwise,} \end{cases} \quad (15a)$$

$$P_k^D(X) = P^D(x_\varepsilon)\Delta_k(\varepsilon), \quad (15b)$$

$$\varphi(z|X) = f(z|x_\varepsilon). \quad (15c)$$

Note that trajectories that do not exist at the current time cannot be detected. The complete measurement model for sets of trajectories is similar to the measurement model for sets of targets by using the proper probability of detection and single measurement density for trajectories [27]. Given the set  $\mathbf{X}_k = \{X_k^1, \dots, X_k^n\}$  of trajectories at time step  $k$ , the set  $\mathbf{z}_k$  of measurements at time step  $k$  is  $\mathbf{z}_k = \mathbf{w}_k^c \uplus \mathbf{w}_k^1 \uplus \dots \uplus \mathbf{w}_k^n$ , where  $\mathbf{w}_k^c, \mathbf{w}_k^1, \dots, \mathbf{w}_k^n$  are independent sets,  $\mathbf{w}_k^c$  is the set of clutter measurements, and  $\mathbf{w}_k^i$  is the set of measurements produced by trajectory  $i$ . The resulting measurement set density  $f(\cdot|\cdot)$  of  $\mathbf{z}_k$  given  $\mathbf{X}_k$  can be written as

$$f(\mathbf{z}_k|\mathbf{X}_k) = \sum_{\mathbf{w}_k^c \uplus \mathbf{w}_k^1 \uplus \dots \uplus \mathbf{w}_k^n = \mathbf{z}_k} f_k^{\text{pppp}}(\mathbf{w}_k) \prod_i \varphi_k(\mathbf{w}_k^i | \{X_k^i\}). \quad (16)$$

### III. TRAJECTORY PMBM FILTER

The PMBM conjugate prior was developed for point targets in [22] and for extended targets in [42], and it was further generalized to trajectories in [31] and [43]. Given the sequence of measurements up to time step  $k'$  and Assumptions 1 and 3, the density of the set of trajectories at time step  $k \in \{k', k'+1\}$  is given by the PMBM density of the form

$$f_{k|k'}(\mathbf{X}_k) = \sum_{\mathbf{X}_k^u \uplus \mathbf{X}_k^d = \mathbf{X}_k} f_{k|k'}^{\text{pppp}}(\mathbf{X}_k^u) \sum_{a \in \mathcal{A}_{k|k'}} w_{k|k'}^a f_{k|k'}^a(\mathbf{X}_k^d), \quad (17a)$$

$$f_{k|k'}^{\text{pppp}}(\mathbf{X}_k^u) = e^{-\int \lambda_{k|k'}^u(X) dX} \prod_{X \in \mathbf{X}_k^u} \lambda_{k|k'}^u(X), \quad (17b)$$

$$f_{k|k'}^a(\mathbf{X}_k^d) = \sum_{\uplus_{i \in \mathbb{T}_{k|k'}} \mathbf{X}_k^i = \mathbf{X}_k^d} \prod_{i \in \mathbb{T}_{k|k'}} f_{k|k'}^{i,a}(\mathbf{X}_k^i), \quad (17c)$$

where the RFS of trajectories  $\mathbf{X}_k$  is an independent union of a Poisson RFS  $\mathbf{X}_k^u$  with intensity  $\lambda_{k|k'}^u$  and an MBM RFS  $\mathbf{X}_k^d$  with Bernoulli parameters  $r_{k|k'}^{i,a}$  and  $f_{k|k'}^{i,a}(\cdot)$ , cf. (2), and  $\mathcal{A}_{k|k'}$  is the set of all global hypotheses, which will be explained in the next section. A trajectory PMBM RFS can be defined by the parameters of the density,

$$\lambda_{k|k'}^u, \mathcal{A}_{k|k'}, \{\Theta_{k|k'}^a\}_{a \in \mathcal{A}_{k|k'}}, \quad (18a)$$

$$\Theta_{k|k'}^a = \{(w_{k|k'}^{i,a}, r_{k|k'}^{i,a}, f_{k|k'}^{i,a})\}_{i \in \mathbb{T}}. \quad (18b)$$

#### A. Structure of the Trajectory PMBM Filter

The structure of the trajectory PMBM (17) is in analogy to the structure of the target PMBM [22]. The Poisson RFS represents trajectories that are hypothesized to exist, but have never been detected; i.e., no measurement has been associated with them. In the track-oriented trajectory PMBM filter, a new track is initiated for each measurement received. In the MBM in (17),  $\mathbb{T}_{k|k'} = \{1, \dots, n_{k|k'}\}$  is a track table with  $n_{k|k'}$  tracks,  $a = (a^1, \dots, a^{n_{k|k'}}) \in \mathcal{A}_{k|k'}$  is a possible global data association hypothesis, and for each global hypothesis  $a$  and for each track  $i \in \mathbb{T}_{k|k'}$ ,  $a^i$  indicates which track hypothesis is used in the global hypothesis. For each track, there are  $h_{k|k'}^i$  single trajectory hypotheses.<sup>3</sup> The weight of global hypothesis  $a$  is  $w_{k|k'}^a \propto \prod_{i \in \mathbb{T}_{k|k'}} w_{k|k'}^{i,a^i}$ , where  $w_{k|k'}^{i,a^i}$  is the weight of single trajectory hypothesis  $a^i$  from track  $i$ .

Let  $m_k$  be the number of measurements at time step  $k \in \{1, \dots, \tau\}$  and  $j \in \mathbb{M}_k = \{1, \dots, m_k\}$  be an index to each measurement. Let  $\mathcal{M}_k$  denote the set of all measurement indices up to and including time step  $k$ ; the elements of  $\mathcal{M}_k$ , if not empty, are of the form  $(\tau, j)$ , where

<sup>3</sup>The ‘‘track’’ defined here is different from the convention used in MHT algorithms, where ‘‘track’’ is referred to as single trajectory hypothesis.

$j \in \{1, \dots, m_\tau\}$  is an index of a measurement at time step  $\tau \leq k$ . Further, let  $\mathcal{M}^k(i, a^i)$  denote the history of measurements that are hypothesized to belong to hypothesis  $a^i$  from track  $i$  at time step  $k$ . Under the standard point target measurement model assumption (see Assumption 3), there can be at maximum one measurement corresponding to the same time step in  $\mathcal{M}^k(i, a^i)$ .

For a global hypothesis to be correct, we have the following constraints. Each global hypothesis should explain the association of each measurement received so far. In addition, every measurement should be associated with one and only one track in each global hypothesis. In other words, the single trajectory hypotheses included in a given global hypothesis cannot have any shared measurement. Under these constraints, the set of global hypotheses at time step  $k$  can be expressed as

$$\mathcal{A}_{k|k'} = \left\{ a = (a^1, \dots, a^{n_{k|k'}}) \left| \bigcup_{i \in \mathbb{T}_{k|k'}} \mathcal{M}^k(i, a^i) = \mathcal{M}_k, \right. \right. \\ \left. \left. \mathcal{M}^k(i, a^i) \cap \mathcal{M}^k(j, a^j) = \emptyset \forall i \neq j, i, j \in \mathbb{T}_{k|k'} \right\}. \quad (19)$$

#### B. PMBM Filtering Recursion

The form of the PMBM conjugate prior on the sets of trajectories is preserved through prediction and update. The two different trajectory PMBM filters based on the two different transition models for sets of trajectories are both track-oriented. For each track, there is a hypothesis tree, where each hypothesis corresponds to different data association sequences for the track. The prediction step preserves the number of tracks and the number of hypotheses. By using a Poisson RFS birth model, the density of newborn trajectories  $\lambda_k^B(X_k)$  can be easily incorporated into the predicted density of Poisson distributed trajectories  $\lambda_{k|k-1}^u(X_k)$  that have never been detected. The two different trajectory PMBM filters have different prediction steps; the difference is that whether dead trajectories are still maintained in the set of trajectories. In the update step, a potential new track is initiated for each measurement, and additional hypotheses are created due to data association. The two different trajectory PMBM filters have the same update step. Explicit expressions for how the PMBM parameters (18) are predicted and updated, using the two different problem formulations, can be found in [31]; they are omitted here.

#### IV. TRAJECTORY MBM FILTER

It is shown in [23] that the MBM RFS of targets is a multitarget conjugate prior if the birth model is a multi-Bernoulli RFS, as in Assumption 2. In this section, we extend this result to RFS of trajectories. Given the

sequence of measurements up to time step  $k'$  and Assumptions 2 and 3, the density of the set of trajectories at time step  $k \in \{k', k' + 1\}$  is given by the MBM of the form

$$f_{k|k'}(\mathbf{X}_k) = \sum_{a \in \mathcal{A}_{k|k'}} w_{k|k'}^a \sum_{\substack{\cup_{j \in \mathbb{T}_{k|k'}} \mathbf{X}_j = \mathbf{X}_k \\ i \in \mathbb{T}_{k|k'}}} \prod f_{k|k'}^{i, a^i}(\mathbf{X}_k^i), \quad (20)$$

where the MBM RFS  $\mathbf{X}_k$  has Bernoulli parameters  $r_{k|k'}^{i, a^i}$  and  $f_{k|k'}^{i, a^i}(\cdot)$ , cf. (2). A trajectory MBM RFS can be defined by the parameters of the density

$$\mathcal{A}_{k|k'}, \{ \Theta_{k|k'}^a \}_{a \in \mathcal{A}_{k|k'}}, \quad (21a)$$

$$\Theta_{k|k'}^a = \{ (w_{k|k'}^{i, a^i}, r_{k|k'}^{i, a^i}, f_{k|k'}^{i, a^i}) \}_{i \in \mathbb{T}_{k|k'}}. \quad (21b)$$

#### A. Structure of the Trajectory MBM Filter

The structure of the trajectory MBM is similar to the MBM maintained in the trajectory PMBM. The difference lies in how tracks (i.e., Bernoulli components) are initiated. In the trajectory PMBM filter, a new track is initiated for each measurement, whereas in the trajectory MBM filter, a new track is initiated for each Bernoulli component in the multi-Bernoulli birth model; i.e., MBM hypotheses explicitly enumerate potential targets that remain to be detected. Both the trajectory PMBM filter and the trajectory MBM filter can explicitly represent trajectories that remain to be detected. In the PMBM representation, these trajectories are efficiently represented through the trajectory Poisson intensity  $\lambda_{k|k'}^u(\cdot)$ , whereas in the MBM representation, they are split across many single trajectory hypotheses (trajectory Bernoulli RFSs) with empty measurement association history, i.e.,  $\mathcal{M}^k(i, a^i) = \emptyset$ .

In each global hypothesis  $a \in \mathcal{A}_{k|k'}$ , each measurement, at each time step, is associated with at most one track, and each track is associated with at most one measurement. Measurements that are not associated with any tracks in a global hypothesis are considered to be clutter under this global hypothesis. Tracks that are not associated with any measurements in a global hypothesis are considered to be misdetected under this global hypothesis. Under these constraints, the set of global hypotheses at time step  $k$  can be expressed as

$$\mathcal{A}_{k|k'} = \left\{ a = (a^1, \dots, a^{n_{k|k'}}) \left| \bigcup_{i \in \mathbb{T}_{k|k'}} \mathcal{M}^k(i, a^i) \subseteq \mathcal{M}_k, \right. \right. \\ \left. \left. \mathcal{M}^k(i, a^i) \cap \mathcal{M}^k(j, a^j) = \emptyset \forall i \neq j, i, j \in \mathbb{T}_{k|k'} \right\}. \quad (22)$$

Compared to (19), here  $\mathcal{M}_k \setminus \bigcup_{i \in \mathbb{T}_{k|k'}} \mathcal{M}^k(i, a^i)$  consists of indices of measurements received so far that are clutter under global hypothesis  $a \in \mathcal{A}_{k|k'}$ . This is an important difference from the trajectory PMBM filter, in which the question whether a measurement corresponds to clutter, or to the initialization of a new target trajectory, is

captured by the existence probability of the created trajectory Bernoulli RFS.

In the rest of the section, we present the prediction and update steps for recursively computing (20) for the MBM parameterization. Similar to the trajectory PMBM filter, the two different trajectory MBM filters, based on the set of current trajectories formulation and the set of all trajectories formulation, have the same update step. For compactness, we denote the inner product of two functions  $h(\cdot)$  and  $g(\cdot)$  as  $\langle h; g \rangle = \int h(x)g(x)dx$ .

## B. MBM Filtering Recursion

We first present the prediction steps, respectively, for the two different problem formulations, and then we present the update step.

1) *Prediction Step for the Set of Current Trajectories:* The prediction step is given in the following theorem.

**Theorem 1.** *Assume that the distribution from the previous time step  $f_{k-1|k-1}(\mathbf{X}_{k-1})$  is given by (20), that the transition model is (12), and that the birth model is a trajectory multi-Bernoulli RFS with  $n_k^b$  Bernoulli components, each of which has density of the form (10). Then, the predicted distribution for the next step  $f_{k|k-1}(\mathbf{X}_k)$  is given by (20), with  $n_{k|k-1} = n_{k-1|k-1} + n_k^b$ . For tracks continuing from previous time ( $i \in \{1, \dots, n_{k-1|k-1}\}$ ), the parameters of the MBM are*

$$h_{k|k-1}^i = h_{k-1|k-1}^i, \quad (23a)$$

$$w_{k|k-1}^{i,a^i} = w_{k-1|k-1}^{i,a^i} \forall a^i, \quad (23b)$$

$$r_{k|k-1}^{i,a^i} = r_{k-1|k-1}^{i,a^i} \langle f_{k-1|k-1}^{i,a^i}; P_{k-1}^S \rangle \forall a^i, \quad (23c)$$

$$f_{k|k-1}^{i,a^i}(X) = \frac{\langle f_{k-1|k-1}^{i,a^i}; \pi^c P_{k-1}^S \rangle}{\langle f_{k-1|k-1}^{i,a^i}; P_{k-1}^S \rangle} \forall a^i. \quad (23d)$$

For new tracks ( $i \in \{n_{k-1|k-1} + l, l \in \{1, \dots, n_k^b\}\}$ ), the parameters of the MBM are

$$h_{k|k-1}^i = 1, \quad (24a)$$

$$\mathcal{M}^{k-1}(i, 1) = \emptyset, \quad (24b)$$

$$w_{k|k-1}^{i,1} = 1, \quad (24c)$$

$$r_{k|k-1}^{i,1} = r_k^{b,l}, \quad (24d)$$

$$f_{k|k-1}^{i,1}(X) = f_k^{b,l}(X). \quad (24e)$$

2) *Prediction Step for the Set of All Trajectories:* The prediction step is given in the following theorem.

**Theorem 2.** *Assume that the distribution from the previous time step  $f_{k-1|k-1}(\mathbf{X}_{k-1})$  is given by (20), that the transition model is (13), and that the birth model is a trajectory multi-Bernoulli RFS with  $n_k^b$  Bernoulli components, each of which has density given by (10). Then, the predicted distribution for the next step  $f_{k|k-1}(\mathbf{X}_k)$  is given by (20), with  $n_{k|k-1} = n_{k-1|k-1} + n_k^b$ . For tracks continuing from*

*previous time ( $i \in \{1, \dots, n_{k-1|k-1}\}$ ), the parameters of the MBM are*

$$h_{k|k-1}^i = h_{k-1|k-1}^i, \quad (25a)$$

$$w_{k|k-1}^{i,a^i} = w_{k-1|k-1}^{i,a^i} \forall a^i, \quad (25b)$$

$$r_{k|k-1}^{i,a^i} = r_{k-1|k-1}^{i,a^i} \forall a^i, \quad (25c)$$

$$f_{k|k-1}^{i,a^i}(X) = \langle f_{k-1|k-1}^{i,a^i}; \pi^a \rangle \forall a^i. \quad (25d)$$

For new tracks ( $i \in \{n_{k-1|k-1} + l, l \in \{1, \dots, n_k^b\}\}$ ), the parameters of the MBM are the same as (24).

3) *Update Step:* The update step is given in the following theorem.

**Theorem 3.** *Assume that the predicted distribution  $f_{k|k-1}(\mathbf{X}_k)$  is given by (20), that the measurement model is (15), and that the measurement set at time step  $k$  is  $\mathbf{z}_k = \{z_k^1, \dots, z_k^{m_k}\}$ . Then, the updated distribution  $f_{k|k}(\mathbf{X}_k)$  is given by (20), with  $n_{k|k} = n_{k|k-1}$ . For each track ( $i \in \{1, \dots, n_{k|k}\}$ ), a hypothesis is included for each combination of a hypothesis from a previous time and either a misdetection or an update using one of the  $m_k$  new measurements, such that the number of hypotheses becomes  $h_{k|k}^i = h_{k|k-1}^i(1 + m_k)$ . For misdetection hypotheses ( $i \in \{1, \dots, n_{k|k}\}$ ,  $a^i \in \{1, \dots, h_{k|k-1}\}$ ), the parameters of the MBM are*

$$\mathcal{M}^k(i, a^i) = \mathcal{M}^{k-1}(i, a^i), \quad (26a)$$

$$w_{k|k}^{i,a^i} = w_{k|k-1}^{i,a^i} (1 - r_{k|k-1}^{i,a^i} \langle f_{k|k-1}^{i,a^i}; P^D \rangle), \quad (26b)$$

$$r_{k|k}^{i,a^i} = \frac{r_{k|k-1}^{i,a^i} \langle f_{k|k-1}^{i,a^i}; 1 - P^D \rangle}{1 - r_{k|k-1}^{i,a^i} \langle f_{k|k-1}^{i,a^i}; P^D \rangle}, \quad (26c)$$

$$f_{k|k}^{i,a^i}(X) = \frac{(1 - P_k^D(X)) f_{k|k-1}^{i,a^i}(X)}{\langle f_{k|k-1}^{i,a^i}; 1 - P^D \rangle}. \quad (26d)$$

For hypotheses updating tracks ( $i \in \{1, \dots, n_{k|k}\}$ ,  $a^i = \tilde{a}^i + h_{k|k-1}^i j$ ,  $\tilde{a}^i \in \{1, \dots, h_{k|k-1}^i\}$ ,  $j \in \{1, \dots, m_k\}$ , i.e., the previous hypothesis  $\tilde{a}^i$ , updated with measurement  $z_k^j$ ), the parameters are

$$\mathcal{M}^k(i, a^i) = \mathcal{M}^{k-1}(i, \tilde{a}^i) \cup \{(k, j)\}, \quad (27a)$$

$$w_{k|k}^{i,a^i} = \frac{w_{k|k-1}^{i,\tilde{a}^i} r_{k|k-1}^{j,\tilde{a}^i} \langle f_{k|k-1}^{i,\tilde{a}^i}; \varphi(z_k^j | \cdot) P^D \rangle}{\lambda^{\text{FA}}(z_k^j)}, \quad (27b)$$

$$r_{k|k}^{i,a^i} = 1, \quad (27c)$$

$$f_{k|k}^{i,a^i}(X) = \frac{\varphi(z_k^j | X) P_k^D(X) f_{k|k-1}^{i,\tilde{a}^i}(X)}{\langle f_{k|k-1}^{i,\tilde{a}^i}; \varphi(z_k^j | \cdot) P_k^D \rangle}. \quad (27d)$$

The derivation here incorporates hypotheses updating every prior hypothesis with every measurement; however, in practical implementations, gating can be used to reduce the computational burden by excluding hypotheses with negligible weights.

### C. MBM<sub>01</sub> Filtering Recursion

The trajectory MBM<sub>01</sub> filter can be considered as a variant of the trajectory MBM filter, in which existence probabilities of Bernoulli components are either 0 or 1. The MBM<sub>01</sub> filtering recursion can be obtained from the MBM filtering recursions by expanding the MBM into its MBM<sub>01</sub> equivalent [23]. The filtering recursions for the trajectory MBM<sub>01</sub> filter are given in Appendix C.

### D. Discussion

All the trajectory filters presented above are track-oriented. For each Bernoulli component in the multi-Bernoulli birth density, a new track is initiated. Compared to the trajectory PMBM filter with Poisson RFS birth, tracks are created in the prediction step but not the update step of trajectory MBM/MBM<sub>01</sub> filter. In the trajectory MBM/MBM<sub>01</sub> filter for the set of all trajectories, the predictions (25d) and (66c) result in additional mixture component in Bernoulli densities  $f_{k|k'}^{i,a^i}(\mathbf{X}_k)$ , which are of the form

$$p(X) = \sum_j w^j p^j(x_{\beta:\varepsilon}|\beta, \varepsilon) \Delta_{e^j}(\varepsilon) \Delta_{b^j}(\beta), \quad (28)$$

where each mixture component is characterized by a weight  $w^j$ , a distinct birth time  $b^j$ , a distinct most recent time  $e^j$  where  $b^j \leq e^j$  for all  $j$ ,<sup>4</sup> and a state sequence density  $p^j(\cdot)$ . This type of state density facilitates simple representations for the state sequence  $x_{\beta:\varepsilon}$  (either the state of a trajectory that is still present or the state of a dead trajectory), conditioned on  $\beta$  and  $\varepsilon$ .

The prediction steps, given by Theorems 5 and 6, in the trajectory MBM<sub>01</sub> filter, create more single trajectory hypotheses than the prediction steps, given by Theorems 1 and 2, in the trajectory MBM filter; this is a direct result of restricting the existence probability of Bernoulli components to either 0 or 1. The existence probability of trajectory Bernoulli RFS  $r$  has different meanings in the four different trajectory filters: in the trajectory MBM filter for the set of current trajectories,  $r$  is the probability that the trajectory exists at the current time and has not ended yet; in the trajectory MBM filter for the set of all trajectories,  $r$  represents the probability that the trajectory existed at any time before including the current time; in the trajectory MBM<sub>01</sub> filter for the set of current trajectories,  $r$  indicates whether the trajectory exists at the current time and has not ended yet; in the trajectory MBM<sub>01</sub> filter for the set of all trajectories,  $r$  indicates whether the trajectory existed at any time before and including the current time.

We remark that the labeled trajectory MBM and MBM<sub>01</sub> filters, which are defined over the set of labeled

<sup>4</sup>Neither the birth time  $\beta$  nor the most recent time  $\varepsilon$  is deterministic.

trajectories, can be obtained by augmenting label to single target state  $x$  [27, Sec. IV-A]. This does not affect the filtering recursion or the information in the computed posterior, compared to MBM and MBM<sub>01</sub>. Therefore, the corresponding multiscan implementations in Section V are analogous.

## V. IMPLEMENTATION OF MULTISCAN TRAJECTORY FILTERS

In this section, we present efficient multiscan implementations of the above trajectory filters.

### A. Hypothesis Reduction

The hypothesis reduction techniques for the trajectory PMBM, MBM, and MBM<sub>01</sub> are quite similar, so we first explain the general formulation and then highlight the differences. As a first step, we identify the most probable global hypothesis, from which estimates of trajectories are also typically extracted. Conditioning on the most likely global hypothesis, we make use of track-oriented  $N$ -scan pruning [5], a conventional hypothesis reduction technique used in TOMHT, to prune global hypotheses with negligible weights.

We note that hypothesis reduction is not complicated by the fact that we are working with symmetric (unlabeled) distributions. Specifically, in (20), the quantities stored are the weight of hypothesis  $a$ , i.e.,  $w_{k|k'}^a$ , and the hypothesis-conditioned trajectory distributions  $f_{k|k'}^{i,a^i}(\mathbf{X}_k^i)$  for each target. Symmetry is ensured by the sum over  $\cup_{i \in \mathbb{T}_{k|k'}} \mathbf{X}_k^i = \mathbf{X}_k$ ; this sum is implicit, and terms never need to be explicitly represented. Therefore, hypothesis reduction achieved by either setting  $w_{k|k'}^a = 0$  for some subset of hypotheses (and renormalizing the weights of remaining hypotheses to sum to 1) or removing a subset of multi-Bernoulli components  $f_{k|k'}^{i,a^i}(\mathbf{X}_k^i)$  for some hypotheses always results in valid symmetric distributions. Likewise, if the existence probability of a Bernoulli component is close to zero in all the considered global hypotheses, pruning is equivalent to setting this existence probability equal to zero, which does not affect the symmetry of the posterior.

Given the most likely global hypothesis  $a^*$  at current time step  $k$ , we trace the single trajectory hypotheses included in  $a^*$  back to their local hypotheses at time step  $k - N$ . The assumption behind the  $N$ -scan pruning method is that the data association ambiguity is resolved before scan  $k - N$  [5]. In other words, global hypotheses that do not coincide with  $a^*$  up until and including time step  $k - N + 1$  are assumed to have negligible weights; these global hypotheses can then be pruned. In addition, tracks (local hypothesis trees) that, after pruning, have a single nonexistence local hypothesis, i.e.,  $r = 0$ , can be pruned. In what follows, we show that the most likely global hypothesis  $a^*$  can be obtained as the solution of a multiframe assignment problem.

## B. Data Association Modeling and Problem Formulation

As indicated in the previous section, the posterior global hypothesis probability  $w_{k|k}^a$  is proportional to the product of the weights of different single trajectory hypotheses  $w_{k|k}^{i,a^i}$ , one from each track:

$$w_{k|k}^a \propto \prod_{i \in \mathbb{T}_{k|k}} w_{k|k}^{i,a^i}, \quad (29)$$

where the proportionality denotes that normalization is required to ensure that  $\sum_{a \in \mathcal{A}_{k|k}} w_{k|k}^a = 1$ . Omitting time indices and introducing the notation  $c^a = -\log(w^a)$  and  $c^{i,a^i} = -\log(w^{i,a^i})$  yields

$$c^a = \sum_{i \in \mathbb{T}} c^{i,a^i} + C, \quad (30)$$

where  $C$  is the logarithm of the normalization constant in (29). The most likely global hypothesis is the collection of single trajectory hypotheses that minimizes the total cost, i.e.,

$$a^* = \arg \min_{(a^i) \in \mathcal{A}} \sum_{i \in \mathbb{T}} c^{i,a^i}. \quad (31)$$

Let  $\mathcal{H}^i$  denote the set of single trajectory hypotheses for the  $i$ th track, and let  $\mathbb{M}_\tau$  denote the set of measurement indices at time step  $\tau$ . Further, let  $\rho^{i,a^i} \in \{0, 1\}$  be a binary indicator variable, indicating whether single trajectory hypothesis  $a^i$  in the  $i$ th track is included in a global hypothesis or not, and let

$$\rho = \{\rho^{i,a^i} \in \{0, 1\} | a^i \in \mathcal{H}^i \forall i \in \mathbb{T}\} \quad (32)$$

be the set of all binary indicator variables. The minimization problem (31) can be further posed as a multiframe assignment problem by decomposing the constraint  $(a^i) \in \mathcal{A}$  into a set of smaller constraints [17, Sec. III], in the form of

$$\arg \min_{\rho \in \bigcap_{\tau=0}^k \mathcal{P}^\tau} \sum_{i \in \mathbb{T}} \sum_{a^i \in \mathcal{H}^i} c^{i,a^i} \rho^{i,a^i}, \quad (33)$$

with the constraint sets denoted as

$$\mathcal{P}^0 = \left\{ \rho \left| \sum_{a^i \in \mathcal{H}^i} \rho^{i,a^i} = 1, \forall i \in \mathbb{T} \right. \right\}, \quad (34a)$$

$$\mathcal{P}^\tau = \left\{ \rho \left| \sum_{i \in \mathbb{T}} \sum_{\substack{a^i \in \mathcal{H}^i: \\ (\tau, j) \in \mathcal{M}(i, a^i)}} \rho^{i,a^i} \leq 1, \forall j \in \mathbb{M}_\tau \right. \right\}, \quad (34b)$$

where  $k$  is the current time step and  $\tau = 1, \dots, k$ . The first constraint (34a) enforces that each global hypothesis should include one and only one single trajectory hypothesis from each track. The set of  $k$  constraints (34b) differs in the trajectory PMBM filter and the trajectory MBM/MBM<sub>01</sub> filter. In the trajectory PMBM filter, each measurement from each time should be associated with exactly one track, i.e., the  $\leq$  sign becomes an  $=$  sign in (34b), whereas in the trajectory MBM/MBM<sub>01</sub> filter,

each measurement from each time should be associated with at most one track, which explains the  $\leq$  sign.

## C. Multiframe Assignment via Dual Decomposition

The multidimensional assignment problem (33) is NP-hard for two or more scans of measurements. An effective approach to solving this problem is Lagrangian relaxation; this technique has been widely used to solve the multiscan data association problem in TOMHT algorithms; see, e.g., [15] and [16]. In this work, we focus on the dual decomposition formulation [44], i.e., a special case of Lagrangian relaxation, whose competitive performance, compared to traditional approaches [15], [16], in solving the multiframe assignment problem has been demonstrated in [17].

*1) Decomposition of the Lagrangian Dual:* We follow similar implementation steps as in [17]. The original (primal) problem (33) is separated into  $k$  subproblems, one for each time step, and for each subproblem a binary variable is used. The subproblem solutions

$$\rho_\tau = \{\rho_\tau^{i,a^i} \in \{0, 1\} | a^i \in \mathcal{H}^i \forall i \in \mathbb{T}\} \quad (35)$$

must be equal for all  $\tau$ ; this is enforced through Lagrange multipliers that are incorporated into the subproblems acting as penalty weights. The  $\tau$ th subproblem can be written as [17]

$$\arg \min_{\rho_\tau \in \mathcal{P}^0 \cap \mathcal{P}^\tau} \sum_{i \in \mathbb{T}} \sum_{a^i \in \mathcal{H}^i} \left( \frac{c^{i,a^i}}{k} + \delta_\tau^{i,a^i} \right) \rho_\tau^{i,a^i} \\ \triangleq \arg \min_{\rho_\tau \in \mathcal{P}^0 \cap \mathcal{P}^\tau} \mathcal{S}(\rho_\tau, \delta_\tau), \quad (36)$$

where the Lagrange multipliers used for the  $\tau$ th subproblem are denoted by

$$\delta_\tau = \{\delta_\tau^{i,a^i} | a^i \in \mathcal{H}^i \forall i \in \mathbb{T}\}, \quad (37)$$

and the division by  $k$  in (36) comes from the fact that the summation of the objectives that each subproblem tries to minimize should be equal to the objective of the original problem. The Lagrange multipliers  $\delta_\tau^{i,a^i} \in \mathbb{R}$  have the constraint that, for each single trajectory hypothesis, they must add up to zero over different subproblems [44]. Thus, the set of Lagrange multipliers has the form

$$\Lambda = \left\{ \delta_\tau \left| \sum_{\tau=1}^k \delta_\tau^{i,a^i} = 0, \forall a^i \in \mathcal{H}^i \forall i \in \mathbb{T} \right. \right\}. \quad (38)$$

*2) Subproblem Solving:* After eliminating all the constraint sets except two, i.e.,  $\mathcal{P}^0$  and  $\mathcal{P}^\tau$ , we obtain a 2D assignment problem (36). The objective of the  $\tau$ th assignment problem (36) is to associate each measurement received at time step  $\tau \leq k$ , i.e.,  $j \in \mathbb{M}_\tau$ , with either an existing track or a new track<sup>5</sup> at the current time

<sup>5</sup>In the trajectory MBM/MBM<sub>01</sub>, “dummy” tracks are created to represent clutter.

step  $k$ , i.e.,  $i \in \mathbb{T}_k$ , such that the total assignment cost is minimized.

For a track that is created after time step  $\tau$ , no measurement from time step  $\tau$  should be assigned to it; therefore, the measurement-to-track assignment cost is infinity. For a track that existed before and up to time step  $\tau$ , i.e.,  $i \in \mathbb{T}_\tau$ , if measurement  $z_\tau^j$  was not associated with this track, let the measurement-to-track assignment cost be infinity; if otherwise, let the cost first be the minimum cost of the single trajectory hypothesis in this track that was updated by  $z_\tau^j$  [45, Ch. VII, eq. (7.24)], i.e.,

$$\min \sum_{\substack{a^i \in \mathcal{H}^i: \\ (\tau, j) \in \mathcal{M}(i, a^i)}} \left( \frac{c^{i, a^i}}{k} + \delta_\tau^{i, a^i} \right). \quad (39)$$

In order to keep the cost of a hypothesis that does not assign a measurement to a track the same for an existing track and a new track (trajectory PMBM filter) or clutter (trajectory MBM filter), the cost (39) should then have subtracted from it the minimum cost of hypotheses that this track is not updated by any of the measurements at time step  $\tau$ , i.e.,

$$\min \sum_{\substack{a^i \in \mathcal{H}^i: \\ (\tau, j) \notin \mathcal{M}(i, a^i), \forall j \in \mathbb{M}_\tau}} \left( \frac{c^{i, a^i}}{k} + \delta_\tau^{i, a^i} \right). \quad (40)$$

Note that, in the context of Lagrangian relaxation, the costs of single trajectory hypotheses refer to the costs that are penalized by the Lagrange multipliers.

After solving the 2D assignment problem, we can obtain the associations for each measurement at time step  $\tau$ . For tracks not being associated with any measurements at time step  $\tau$ , if the track is created before and up to time step  $\tau$ , i.e.,  $i \in \mathbb{T}_\tau$ , the single trajectory hypothesis

$$\arg \min_{a^i} \sum_{\substack{a^i \in \mathcal{H}^i: \\ (\tau, j) \notin \mathcal{M}(i, a^i), \forall j \in \mathbb{M}_\tau}} \left( \frac{c^{i, a^i}}{k} + \delta_\tau^{i, a^i} \right) \quad (41)$$

is included in the most likely global hypothesis; if otherwise, i.e.,  $i \in \mathbb{T}_k \setminus \mathbb{T}_\tau$ , we can choose the single trajectory hypothesis

$$\arg \min_{a^i} \sum_{a^i \in \mathcal{H}^i} \left( \frac{c^{i, a^i}}{k} + \delta_\tau^{i, a^i} \right) \quad (42)$$

to be included in the most likely global hypothesis.

*3) Subgradient Updates:* The objective of Lagrangian relaxation is to find the tightest lower bound of the summation of the cost of each subproblem (36). The dual problem can be expressed as [17]

$$\arg \max_{\{\delta_\tau\} \in \Lambda} \left( \sum_{\tau=1}^k \min_{\rho_\tau \in \mathcal{P}^0 \cap \mathcal{P}^\tau} \mathcal{S}(\rho_\tau, \delta_\tau) \right), \quad (43)$$

where the maximum can be found using subgradient methods [46]. The Lagrange multipliers  $\{\delta_\tau\}$  are updated using

$$\delta_\tau^{i, a^i} = \delta_\tau^{i, a^i} + \alpha_t \cdot g_\tau^{i, a^i}, \quad (44)$$

where  $g_\tau^{i, a^i}$  is the projected subgradient that can be calculated as

$$g_\tau^{i, a^i} = \rho_\tau^{i, a^i} - \frac{1}{k} \sum_{\tau'=1}^k \rho_{\tau'}^{i, a^i}, \quad (45)$$

and  $\alpha_t$  is the step size at iteration  $t$ . There are many rules to set the step size; see [44]. In this work, we choose to use the same setting as in [17], which has the form

$$\alpha_t = \frac{C_t^{\text{BP}} - C_t^{\text{D}}}{\|\{g_\tau\}\|^2}, \quad (46)$$

where  $C_t^{\text{BP}}$  is the best (minimum) feasible primal cost so far obtained,  $C_t^{\text{D}}$  is the dual cost calculated at iteration  $t$  from (43), and  $\{g_\tau\}$  denotes the concatenation of all the projected subgradients  $g_\tau^{i, a^i}$ . The optimal solution is assumed to be attained when the relative gap between the primal cost and the dual cost  $(C_t^{\text{BP}} - C_t^{\text{D}})/C_t^{\text{BP}}$  is less than a specified threshold, e.g., 0.01 [44].

Each subproblem solution will, in general, be infeasible with respect to the primal problem (33); nevertheless, subproblem solutions will usually be nearly feasible since large constraint violations were penalized [44]. Hence, feasible solutions  $\rho$  can be obtained by correcting the minor conflicting binary elements on which subproblem solutions  $\rho_\tau$  disagree. For tracks for which we have not yet selected which single trajectory hypothesis to be included in the most likely global hypothesis, we use the branch and bound technique [47] to reconstruct the best feasible solution at each iteration of the Lagrangian relaxation. Note that there are many other ways to recover a feasible primal solution from subproblem solutions; see [44].

## D. Discussion

The objective of solving the multiframe assignment problem is to know which Bernoulli components are included in the multi-Bernoulli with the highest weight. Because the data association ambiguity is assumed to be resolved before time step  $k - N$ , obtaining the most likely global hypothesis at time step  $k$ , which explains the origin of each measurement from time step  $k - N$  to current time step  $k$ , requires the solution of an  $(N + 2)$ -dimensional assignment problem [5].

The computational complexity of filters can be further reduced by limiting the number of single target/trajectory hypotheses; see [23] and [31]. As for the multiscan trajectory PMBM and MBM filters, pruning single trajectory hypotheses with small existence probabilities besides  $N$ -scan pruning might sometimes harm the solvability of the multiframe assignment problem,

since the problem is formulated using the measurement assignment information contained in single trajectory hypotheses. Instead, we can choose single trajectory hypotheses  $a^i \in \mathcal{H}^i$ ,  $\forall i \in \mathbb{T}$ , with small Bernoulli existence probability  $r$  at current time step to be updated only by misdetection at next time step. Then, single trajectory hypotheses with several consecutive misdetections can be pruned using  $N$ -scan pruning. Also, to limit the number of mixture components in the trajectory Poisson RFS, components with negligible weights can be pruned.

## VI. EFFICIENT FIXED-LAG SMOOTHING

Multitarget filters based on sets of trajectories are able to estimate the full state sequence instead of appending the sequence of estimates at each time step. This is possible since the posterior density contains full trajectory information. The posterior density over the set of trajectories can be computed either off-line by applying fixed-interval smoothing or recursively as new measurements arrive by performing smoothing while filtering. Examples of the latter case include the Gaussian mixture trajectory (cardinalized) probability hypothesis density filter proposed in [38] and [39] and the trajectory MBM<sub>01</sub> filter proposed in [27] that use an accumulated state density representation [48], and the trajectory PMBM filter proposed in [31] that uses an information form [49], to represent the joint state density.

As time progresses, the lengths of the trajectories increase. Eventually, the length may be such that it is computationally beneficial to perform approximate smoothing while filtering. An  $L$ -scan implementation is proposed in [27] and [38] that propagates the joint density of the states of the last  $L$  time steps and independent densities for the previous states for each trajectory. Still, from the perspective of  $N$ -scan pruning, a lot of unnecessary calculations might be spent on obtaining the smoothed posterior density for each single trajectory hypothesis. More specifically, when the data association ambiguity is high (e.g., targets move in proximity), we might have hundreds or even thousands of single trajectory hypotheses, and at each time instance we only need to compute the posterior trajectory mean for those that are included in the most likely global hypothesis. However, note that the prediction and update of the hypotheses weights are the same as in the implementation using smoothing while filtering, e.g., [31].

We propose an efficient fixed-lag smoothing implementation of multiscan trajectory filters that solves the above-mentioned problem by combining the  $L$ -scan trajectory density approximation with  $N$ -scan pruning. After  $N$ -scan pruning, single trajectory hypotheses in the same track share the same measurement association history at all times up to time step  $k - N$ . Then, we can apply  $(N + L)$ -scan density approximation, such that all single trajectory hypotheses in the same track share the same posterior trajectory density up until time step  $k - N - L$ .

It is therefore sufficient to perform fixed-lag smoothing for  $N + L$  steps for the most likely global hypothesis, and then store the parameters of the smoothed target state densities at time step  $k - N - L + 1$  before proceeding. Following this approach, the extracted posterior trajectory mean from the most likely global hypothesis at time step  $k + 1$  consists of the newly computed smoothed estimates for the last  $N + L$  steps and the prestored smoothed estimates at all times up to  $k - N - L + 1$ .

## VII. SIMULATIONS

In this section, we show simulation results that compare five different filters<sup>6</sup>:

- 1) multiscan trajectory PMBM filter<sup>7</sup>;
- 2) multiscan trajectory MBM filter (footnote 7);
- 3) multiscan trajectory MBM<sub>01</sub> filter (footnote 7);
- 4) fast implementation of the  $\delta$ -GLMB filter using Gibbs sampling<sup>8</sup> [35];
- 5) fast implementation of the LMB filter using Gibbs sampling (footnote 8) [50].

For all the trajectory filters, we consider the set of all trajectories problem formulation.

### A. Parameter Setup

A 2D Cartesian coordinate system is used to define measurement and target kinematic parameters. The kinematic target state is a vector of position and velocity  $x_k = [p_{x,k}, v_{x,k}, p_{y,k}, v_{y,k}]^T$ . A single measurement is a vector of position  $z_k = [z_{x,k}, z_{y,k}]^T$ . Targets follow a linear Gaussian constant velocity model  $\pi_{k|k-1}(x_k|x_{k-1}) = \mathcal{N}(x_k; F_k x_{k-1}, Q_k)$ , with parameters

$$F_k = I_2 \otimes \begin{bmatrix} 1 & T \\ 0 & 1 \end{bmatrix}, \quad Q_k = 0.01 I_2 \otimes \begin{bmatrix} T^3/3 & T^2/2 \\ T^2/2 & T \end{bmatrix},$$

where  $\otimes$  is the Kronecker product,  $I_m$  is an identity matrix of size  $m \times m$ , and  $T = 1$ . The linear Gaussian measurement likelihood model has density  $f(z_k|x_k) = \mathcal{N}(z_k; H_k x_k, R_k)$ , with parameters  $H_k = I_2 \otimes [1, 0]$  and  $R_k = I_2$ .

The filters consider that there are no targets at time step 0. For multiscan trajectory filters, we use  $N$ -scan pruning ( $N = 3$ ) to remove unlikely global

<sup>6</sup>The TOMHT implementation developed in [17] can be considered as a special case of the multiscan trajectory PMBM filter for sets of current trajectories where the trajectory estimates consist of target state estimates that are extracted from the marginal densities over the current set of targets. Therefore, we choose not to include the TOMHT implementation in [17] in the simulation results.

<sup>7</sup>MATLAB code of the multiscan trajectory PMBM, MBM, and MBM<sub>01</sub> filters is available at <https://github.com/yuhsuansia/Multi-scan-trajectory-PMBM-filter>.

<sup>8</sup>We use the code that Prof. Ba-Ngu Vo and Prof. Ba-Tuong Vo share online: <http://ba-tuong.vo-au.com/codes.html>. The authors thank them for providing the code.

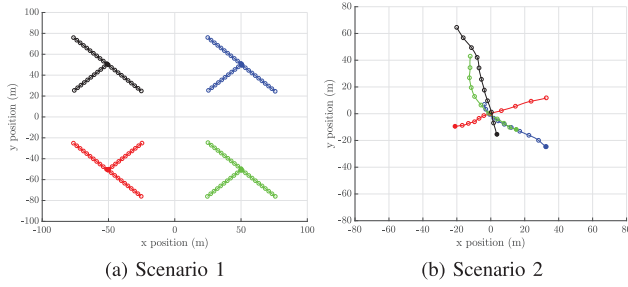


Fig. 1. True target trajectories for 81 time steps. In both scenarios, targets are born at times  $\{1, 11, 21, 31\}$  and are dead at times  $\{51, 61, 71, 81\}$ . Targets' positions every six time steps are marked with a circle, and their initial positions with a filled circle. In Scenario 1, there are 12 targets born at four different locations. In Scenario 2, targets move in close proximity around the midpoint.

hypotheses. In addition to filtering, we also perform fixed-lag smoothing for the latest four steps. Both filtering and smoothing performances are analyzed. For the trajectory PMBM filter and the trajectory MBM filter, Bernoulli components with existence probability smaller than  $10^{-3}$  are not updated by measurements (see Section V-D). For the trajectory PMBM filter, we remove mixture components in the trajectory Poisson RFS with weights smaller than  $10^{-3}$ . For the  $\delta$ -GLMB filter, the cap on the number of components  $H^{\max} = 2000$ . Ellipsoidal gating is used in all the compared filters; the gating size in probability is 0.999.

We consider two different scenarios with true trajectories shown in Fig. 1. In Scenario 1, targets are well spaced, and there is at most one target born at the same location per scan. In Scenario 2, for each trajectory, we initiate the midpoint from a Gaussian with mean  $[0, 0, 0, 0]^T$  and covariance matrix  $I_4$ , and the rest of the trajectory is generated by running forward and backward dynamics. This scenario is challenging due to the fact that all the four targets move in close proximity around the midpoint. In the simulation, we consider constant target survival probability  $P^S = 0.99$ , constant target detection probability  $P^D = 0.9$ , and Poisson clutter uniform in the region of interest with rate  $\lambda^{\text{FA}} = 10$ .

For the trajectory PMBM filter, the Poisson birth intensity has the form  $\lambda_k^b(x_k) = \sum_l 0.05 \mathcal{N}(x; \bar{x}_k^{b,l}, P_k^{b,l})$ . For the trajectory MBM filter, the trajectory MBM<sub>01</sub> filter, the  $\delta$ -GLMB filter, and the LMB filter, the  $l$ th Bernoulli component in the multi-Bernoulli birth has existence probability  $r_k^{b,l} = 0.05$  and single target state density  $\mathcal{N}(x; \bar{x}_k^{b,l}, P_k^{b,l})$ . In Scenario 1, we set  $\bar{x}_k^{b,1} = [50, 0, 50, 0]^T$ ,  $\bar{x}_k^{b,2} = [50, 0, -50, 0]^T$ ,  $\bar{x}_k^{b,3} = [-50, 0, 50, 0]^T$ ,  $\bar{x}_k^{b,4} = [-50, 0, -50, 0]^T$ , and  $P_k^{b,l} = \text{diag}([4, 1, 4, 1])$ . In Scenario 2, we set  $\bar{x}_k^{b,1} = [0, 0, 0, 0]^T$  and  $P_k^{b,1} = \text{diag}([100^2, 1, 100^2, 1])$ , which covers the region of interest. It should be noted that the multi-Bernoulli and Poisson birth models have the same intensity (probability hypothesis density) [6, eq. (4.129)].

This implies that birth models are as close as possible in the sense of Kullback–Leibler divergence.

## B. Performance Evaluation

For all the three multiscan trajectory filters, we estimate the full trajectories directly from the most likely global hypothesis. For the trajectory filters, we choose the most likely cardinality estimate  $n^*$  from the multi-Bernoulli of the most likely global hypothesis. We then report trajectory estimates from the  $n^*$  Bernoulli components with the highest existence probabilities. Given a Bernoulli state density (28), an estimate of the trajectory is obtained by selecting the most probable mixture component  $j^* = \arg \max_j w_{k|k'}^j$  and reporting its mean value [31]. For the  $\delta$ -GLMB filter and the LMB filter, we first obtain the maximum a posteriori estimate of the cardinality. We then find the global hypothesis with this cardinality with highest weight and report the mean of the targets in this hypothesis [28]. Trajectories are formed by connecting target estimates with the same label.

To evaluate the filtering performance, we used the generalized optimal subpattern assignment (GOSPA) metric [51], which can be decomposed into localization cost, missed target cost, and false target cost. The GOSPA metric is applied to the set of current target states at each time step. To evaluate the tracking performance, the trajectory metric in [52] based on linear programming (LP) was used, which can be decomposed into localization cost, missed target cost, false target cost, and track switch cost.

## C. Results

We perform 100 Monte Carlo runs and obtain the average root-mean-square (RMS) GOSPA error (order  $p = 2$ , location error cutoff  $c = 10$ , and  $\alpha = 2$ ), the average RMS trajectory estimation error (order  $p = 2$ , location error cutoff  $c = 10$ , switch cost  $\gamma = 2$ ), and the average running time, summed over 81 time steps. We apply the trajectory metric [52] at each time step  $k$ , and normalize it by  $\sqrt{k}$ . This normalization allows a comparison of how the RMS metric evolves over time in the scenario, as opposed to only computing the metric at the final time step.

The comparison of different filters by the RMS GOSPA error and by the average running time<sup>9</sup> is shown in Table I for Scenario 1 and in Fig. 2 for Scenario 2. We can see that the trajectory PMBM filter arguably has the best performance in terms of target state estimation error and computational complexity, especially in Scenario 2 with coalescence. By comparing the execution time of trajectory filters with and without fixed-lag smoothing

<sup>9</sup>MATLAB implementations on a desktop with 3.0 GHz Intel Core i5 processor.

TABLE I  
Simulation Results for Scenario 1: RMS GOSPA/LP Trajectory Metric Errors and Average Running Time (s)

Algorithm	Trajectory Without	PMBM With	Trajectory Without	MBM With	Trajectory Without	MBM <sub>01</sub> With	$\delta$ -GLMB (Gibbs) Without	LMB (Gibbs) Without
GOSPA	150.02	150.02	148.98	148.98	149.33	149.33	151.94	155.21
GOSPA—localization	120.73	120.73	120.76	120.76	120.74	120.74	120.82	120.93
GOSPA—missed	68.10	68.10	66.24	66.24	67.54	67.54	63.71	57.72
GOSPA—false	65.65	65.65	64.04	64.04	63.70	63.70	68.40	77.19
LP trajectory metric	141.91	128.25	141.02	127.15	141.04	127.16	167.50	168.85
LP—localization	123.23	101.72	123.40	101.87	123.35	101.72	123.01	123.01
LP—missed	98.10	98.10	93.81	93.81	93.89	93.89	131.80	128.21
LP—false	56.38	56.38	62.56	62.56	63.19	63.19	107.46	114.76
LP—track switch	9.68	9.68	7.73	7.73	6.00	6.00	22.73	30.79
Average running time (s)	4.41	4.61	8.57	8.90	10.29	10.50	12.87	2.27

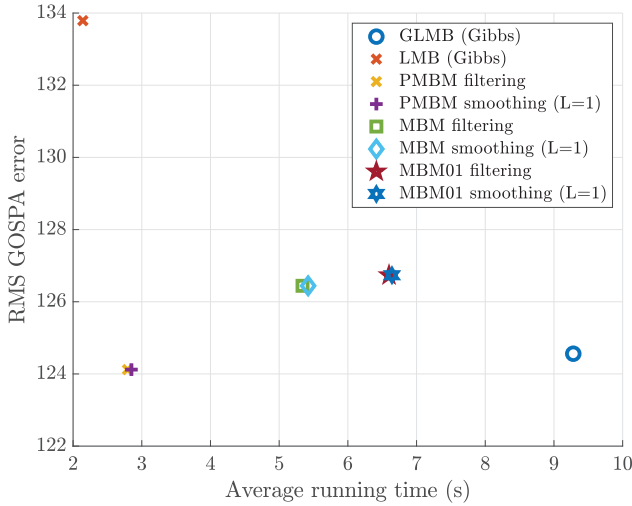


Fig. 2. Performance comparison among the  $\delta$ -GLMB (Gibbs) filter, the LMB (Gibbs) filter, the trajectory PMBM filter, the trajectory MBM filter, and the trajectory MBM<sub>01</sub> filter in Scenario 2: RMS GOSPA error versus average running time.

(for the latest four target states), we can find that the running time of the implemented filters is dominated by their filtering recursions.

For Scenario 1, the numerical values of the average RMS GOSPA and the trajectory estimation errors are given in Table I. For Scenario 2, the average RMS GOSPA error and its decomposed values over time are

illustrated in Fig. 3, and the average RMS trajectory estimation error and its decomposed values over time are illustrated in Fig. 4. Comparing the results of the two scenarios, we can find that when the birth process is less informative, i.e., a broad birth prior density, the trajectory PMBM filter exhibits lower estimation error than the trajectory MBM and MBM<sub>01</sub> filters.

While the differences in target state estimation error among different filters are not distinct in both scenarios, it is noticeable that trajectory filters yield much less trajectory estimation error than labeled RFS filters. The worse trajectory estimation performance of labeled RFS filters is a result of worse track continuity. There are two main drawbacks in forming trajectories by connecting target states with the same label: first, misdetections can lead to gaps in the trajectory formed by labeled estimates; second, physically unrealistic track switching; see [31, Fig. 2] for an example.

In addition, we can see that performing fixed-lag smoothing does not change the error due to missed/false detections and track switching; it mainly improves the localization error. This is expected since the choice of  $N + L$  has a direct effect on the estimation of past states of the trajectories. From the results of the simulation study, we can conclude that the trajectory PMBM filter has the best tracking performance, and that the trajectory MBM filter is more efficient than the trajectory MBM<sub>01</sub> filter.

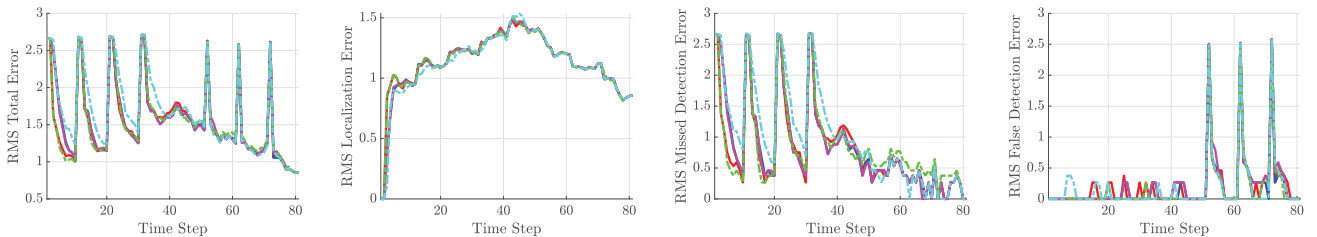


Fig. 3. Average target state estimation error in Scenario 2 evaluated using the GOSPA metric. The lines show the RMS error averaged over 100 Monte Carlo runs. Legend: trajectory PMBM filter (without smoothing) (red), trajectory MBM filter (without smoothing) (blue), trajectory MBM<sub>01</sub> filter (without smoothing) (magenta),  $\delta$ -GLMB (Gibbs) filter (green), and LMB (Gibbs) filter (cyan).

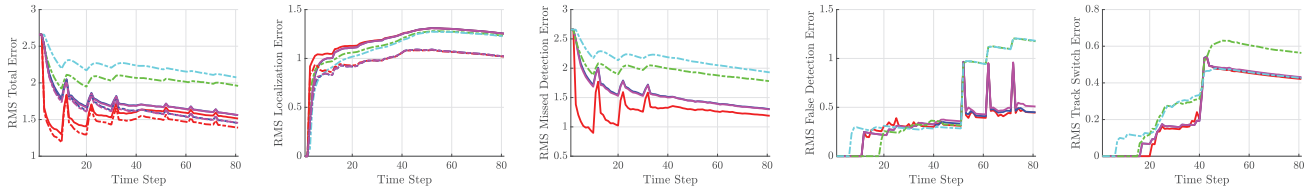


Fig. 4. Average trajectory state estimation error in Scenario 2 evaluated using the trajectory metric [52]. The lines show the RMS error averaged over 100 Monte Carlo runs. Legend: trajectory PMBM filter (without smoothing) (red solid line), trajectory PMBM filter (with smoothing) (red dash-dotted line), trajectory MBM filter (without smoothing) (blue solid line), trajectory MBM filter (with smoothing) (blue dash-dotted line), trajectory MBM<sub>01</sub> filter (without smoothing) (magenta solid line), trajectory MBM<sub>01</sub> filter (with smoothing) (magenta dash-dotted line),  $\delta$ -GLMB (Gibbs) filter (green), and LMB (Gibbs) filter (cyan).

## VIII. CONCLUSION

In this paper, we have presented the trajectory MBM filter. We have also presented an efficient implementation of multiscan trajectory PMBM, MBM, and MBM<sub>01</sub> filters using  $N$ -scan pruning and dual decomposition. The performance of the presented multitarget trackers, applied with an efficient fixed-lag smoothing method, is evaluated in a simulation study. The simulation results show that the multiscan trajectory PMBM filter has improved tracking performance over the trajectory MBM filter in terms of state/trajectory estimation error and computational time.

## APPENDIX A

In this appendix, we first review why FISST can be used for sets of trajectories. Then, we show how to define reference measures and measure theoretic integrals for sets of trajectories.

### A1. Use of FISST for Sets of Trajectories

In this section, we review why FISST can be used for sets of trajectories. The single trajectory space is locally compact, Hausdorff, and second countable (LCHS) [27, Appendix A], where second countable is also referred to as completely separable [53]. LCHS spaces are often used in random set theory [54], and LCHS is also the type of single object space required by Mahler's FISST [6, Sec. 2.2.2].

In particular, single object/measurement spaces that are the disjoint union of spaces of different dimensionalities, similarly to the single trajectory space, have previously been used in Mahler's FISST and RFS framework in [6, Sec. 2.2.2] and [6, Sec. 11.6] for variable state space cardinalized probability hypothesis density filters, and in [6, Ch. 18], [55], and [56] for RFS filters for unknown clutter. In addition, [6, Sec. 3.5.3] explicitly explains how the set integral is constructed for this type of space. Therefore, Mahler's FISST and RFS framework on its own enables us to perform inference on sets of trajectories. For completeness, we proceed to provide also the required measure theory to define probability densities.

### A2. Measure Theoretic Integrals

We begin by introducing some basic concepts in measure theory; for more details, see, e.g., [57] and [58, Appendix A]. Consider a nonempty set  $\mathcal{Y}$ , the pair  $(\mathcal{Y}, \sigma(\mathcal{Y}))$ , in which  $\sigma(\mathcal{Y})$  denotes a  $\sigma$ -algebra of subsets of  $\mathcal{Y}$ , is called a measurable space. Given a topology space  $\mathcal{Y}$ , the Borel  $\sigma$ -algebra is the smallest  $\sigma$ -algebra of the subsets of  $\mathcal{Y}$  containing the open sets of  $\mathcal{Y}$  (or equivalently, by the closed sets of  $\mathcal{Y}$ ). A set  $\mathcal{B}$  is said to be measurable if  $\mathcal{B} \in \sigma(\mathcal{Y})$ . A function  $f : \mathcal{Y} \rightarrow \mathbb{R}$  is said to be measurable if the inverse images of  $\mathbb{R}$  under  $f$  are measurable. The triple  $(\mathcal{Y}, \sigma(\mathcal{Y}), \mu)$  in which  $\mu$  is a measure on  $\sigma(\mathcal{Y})$  is called a measure space.

The integral of a measurable function  $f : \mathcal{Y} \rightarrow \mathbb{R}$ ,  $\int f(y)\mu(dy)$ , is defined as a limit of integrals of simple functions. The integral of  $f$  over any measurable  $\mathcal{B} \subset \mathcal{Y}$  is defined as

$$\int_{\mathcal{B}} f(y)\mu(dy) = \int \mathbf{1}_{\mathcal{B}}(y)f(y)\mu(dy), \quad (\text{A.1})$$

where  $\mathbf{1}_{\mathcal{B}}$  denotes the indicator function  $\mathbf{1}_{\mathcal{B}}(y) = 1$  if  $y \in \mathcal{B}$  and  $\mathbf{1}_{\mathcal{B}}(y) = 0$  otherwise.

### A3. Measure Theoretic Integrals for Single Object LCHS Spaces

In this section, we explain how to define measure theoretic integrals for RFSs whose single objects belong to LCHS spaces, following the steps in [58, Appendix B].

We denote an LCHS space as  $E$ . For instance,  $E$  could denote the single object space  $\mathcal{X}$  or the single trajectory space  $\mathcal{T}_k$ . We also let  $\mathcal{F}(E)$  denote the collection of finite subsets of  $E$ .<sup>10</sup>

A common class of RFSs is the Poisson point processes. A Poisson point process  $\Upsilon$  is an RFS that is characterized by the property that for any  $k$  disjoint Borel subsets  $S_1, \dots, S_k$  of  $E$ , the random variables  $|\Upsilon \cap S_1|, \dots, |\Upsilon \cap S_k|$  are independent and have a Poisson distribution. The mean of the Poisson random variables  $|\Upsilon \cap S_i|$  is denoted as  $v_{\Upsilon}(S_i)$ . The function  $v_{\Upsilon}(\cdot)$  is a (unitless) measure on the Borel subsets of  $E$  and is referred

<sup>10</sup>We would like to clarify that the topology on  $\mathcal{F}(E)$  is the myopic of Mathéron topology [59], for which we require an LCHS space. To be precise, second countability, not only separability as indicated in [58, Appendix B], is required in the Mathéron topology [59, Sec. 1.1], as it makes use of a countable base [59, p. 1].

to as the intensity measure of  $\Upsilon$ . If the mapping from vectors to finite sets is denoted as  $\chi : \uplus_{n=0}^{\infty} E^n \rightarrow \mathcal{F}(E)$ , we have that  $\chi((x_1, \dots, x_n)) = \{x_1, \dots, x_n\}$ . Then, the probability distribution of  $\Upsilon$  is [58, Appendix B]

$$P_{\Upsilon}(\mathcal{B}) = e^{-v_{\Upsilon}(E)} \sum_{n=0}^{\infty} \frac{v_{\Upsilon}^n(\chi^{-1}(\mathcal{B}) \cap E^n)}{n!}, \quad (\text{A.2})$$

where  $\mathcal{B}$  is a Borel subset of  $\mathcal{F}(E)$ ,  $\chi^{-1}$  is the inverse mapping of  $\chi$ , and  $v_{\Upsilon}^n(\cdot)$  is the  $n$ th product (unitless) Lebesgue measure of  $v_{\Upsilon}(\cdot)$ .

We define the measure  $\mu(\cdot)$ , on the Borel subsets of  $\mathcal{F}(E)$ , as

$$\mu(\mathcal{B}) = \sum_{n=0}^{\infty} \frac{v_{\Upsilon}^n(\chi^{-1}(\mathcal{B}) \cap E^n)}{n!}, \quad (\text{A.3})$$

which is proportional to the probability distribution  $P_{\Upsilon}(\cdot)$ . The integral of a measurable function  $f : \mathcal{F}(E) \rightarrow \mathbb{R}$  with respect to the measure  $\mu(\cdot)$  is then [58, Appendix B]

$$\begin{aligned} & \int_{\mathcal{B}} f(\mathbf{X}) \mu(d\mathbf{X}) \\ &= \sum_{n=0}^{\infty} \frac{1}{n!} \int_{\chi^{-1}(\mathcal{B}) \cap E^n} f(\{x_1, \dots, x_n\}) v_{\Upsilon}^n(dx_1 \cdots dx_n). \end{aligned} \quad (\text{A.4})$$

#### A4. Reference Measure for Sets of Trajectories

In the previous section, we explained how to define a measure theoretic integral with respect to a measure  $\mu(\cdot)$  on the Borel subsets of  $\mathcal{F}(E)$  in terms of a measure  $v_{\Upsilon}(\cdot)$  on the Borel subsets of  $E$ . We proceed to choose a specific measure  $v_{\Upsilon}(\cdot)$  when  $E$  is the single trajectory space  $\mathcal{T}_k = \uplus_{(\beta, \varepsilon) \in I_k} \{\beta\} \times \{\varepsilon\} \times \mathcal{X}^{\varepsilon-\beta+1}$  and  $\mathcal{X} = \mathbb{R}^n$ . This will allow us to write the measure theoretic integrals for sets of trajectories in terms of standard Lebesgue integrals and establish the correspondence with Mahler's set integral (8).

We first denote the units of the hypervolume in the single target space  $\mathcal{X}$  as  $K$ . For example, if the single target state is  $[p_x, v_x]$  with  $p_x$  being measured in meters ( $m$ ) and  $v_x$  being measured in meters per second (m/s), then  $K = m^2/s$ .

Given a Borel subset  $S$  of  $\mathcal{T}_k$ , which can be written as  $S = \uplus_{(\beta, \varepsilon) \in I_k} \{\beta\} \times \{\varepsilon\} \times S_{\varepsilon-\beta+1}$ ,  $S_{\varepsilon-\beta+1} \subset \mathcal{X}^{\varepsilon-\beta+1}$ , we choose the measure  $v_{\Upsilon}(\cdot)$  in the single trajectory space as

$$v_{\Upsilon}(S) = \sum_{(\beta, \varepsilon) \in I_k} \frac{\lambda_{K^{\varepsilon-\beta+1}}(S_{\varepsilon-\beta+1})}{K^{\varepsilon-\beta+1}}, \quad (\text{A.5})$$

where  $\lambda_{K^{\varepsilon-\beta+1}}(\cdot)$  represents the Lebesgue measure of  $S_{\varepsilon-\beta+1}$  (with units  $K^{\varepsilon-\beta+1}$ ). Therefore,  $\lambda_{K^{\varepsilon-\beta+1}}(\cdot)/K^{\varepsilon-\beta+1}$  represents the unitless Lebesgue measure on  $\mathcal{X}^{\varepsilon-\beta+1}$ . The normalization of each term in (A.5) by  $K^{\varepsilon-\beta+1}$  is needed so that we can perform the sum; otherwise, the

sum would consider terms with different units, which is erroneous. It is straightforward to check that (A.5) is a measure on the Borel subsets of  $\mathcal{T}_k$ . That is,  $v_{\Upsilon}(\cdot)$  meets the following three properties that define measures [60]:

- 1) For any  $S$ ,  $v_{\Upsilon}(S) \geq 0$ .
- 2)  $v_{\Upsilon}(\emptyset) = 0$ .
- 3) If  $S^1, S^2, \dots$  is a disjoint sequence, then  $v_{\Upsilon}(\sum_{j=1}^{\infty} S^j) = \sum_{j=1}^{\infty} v_{\Upsilon}(S^j)$ .

It is straightforward that the first two properties hold. For the third one, we have

$$\begin{aligned} v_{\Upsilon} \left( \sum_{j=1}^{\infty} S^j \right) &= \sum_{(\beta, \varepsilon) \in I_k} \frac{\lambda_{K^{\varepsilon-\beta+1}} \left( \sum_{j=1}^{\infty} S_{\varepsilon-\beta+1}^j \right)}{K^{\varepsilon-\beta+1}} \\ &= \sum_{j=1}^{\infty} \sum_{(\beta, \varepsilon) \in I_k} \frac{\lambda_{K^{\varepsilon-\beta+1}}(S_{\varepsilon-\beta+1}^j)}{K^{\varepsilon-\beta+1}} \quad (\text{A.6}) \\ &= \sum_{j=1}^{\infty} v_{\Upsilon}(S^j), \end{aligned}$$

where we have applied that  $\lambda_{K^{\varepsilon-\beta+1}}(\cdot)$  is a measure.

We substitute (A.5) into (A.4) and integrate over the whole space, which implies that  $\mathcal{B}$  satisfies that  $\chi^{-1}(\mathcal{B}) \cap \mathcal{T}_k^n = \mathcal{T}_k^n$ . We have that

$$\begin{aligned} & \int f(\mathbf{X}) \mu(d\mathbf{X}) \\ &= \sum_{n=0}^{\infty} \frac{1}{n!} \int_{\mathcal{T}_k^n} f(\{X_1, \dots, X_n\}) v_{\Upsilon}^n(dX_1 \cdots dX_n) \\ &= \sum_{n=0}^{\infty} \frac{1}{n!} \int_{\mathcal{T}_k} \cdots \int_{\mathcal{T}_k} f(\{X_1, \dots, X_n\}) v_{\Upsilon}(dX_1) \\ & \quad \cdots v_{\Upsilon}(dX_n) \\ &= \sum_{n=0}^{\infty} \frac{1}{n!} \sum_{(\beta_1, \varepsilon_1) \in I_k} \cdots \sum_{(\beta_n, \varepsilon_n) \in I_k} \int_{\mathcal{X}^{\varepsilon_1-\beta_1+1} \times \cdots \times \mathcal{X}^{\varepsilon_n-\beta_n+1}} \\ & \quad f(\{(\beta_1, \varepsilon_1, x_1^{1:\varepsilon_1-\beta_1+1}), \dots, (\beta_n, \varepsilon_n, x_n^{1:\varepsilon_n-\beta_n+1})\}) \\ & \quad \frac{\lambda_{K^{\varepsilon_1-\beta_1+1}}(dx_1^{1:\varepsilon_1-\beta_1+1})}{K^{\varepsilon_1-\beta_1+1}} \cdots \frac{\lambda_{K^{\varepsilon_n-\beta_n+1}}(dx_n^{1:\varepsilon_n-\beta_n+1})}{K^{\varepsilon_n-\beta_n+1}}. \end{aligned} \quad (\text{A.7})$$

If we further rewrite  $\lambda_{K^{\varepsilon_i-\beta_i+1}}(dx_i^{1:\varepsilon_i-\beta_i+1})$  as  $dx_i^{1:\varepsilon_i-\beta_i+1}$  and abbreviate  $\int_{\mathcal{X}^{\varepsilon_1-\beta_1+1} \times \cdots \times \mathcal{X}^{\varepsilon_n-\beta_n+1}}$  as  $\int$ , then we have that

$$\begin{aligned} \int f(\mathbf{X}) \mu(d\mathbf{X}) &= \sum_{n=0}^{\infty} \frac{1}{n!} \sum_{(\beta_1, \varepsilon_1) \in I_k} \cdots \sum_{(\beta_n, \varepsilon_n) \in I_k} \int \cdots \int \\ & \quad f(\{(\beta_1, \varepsilon_1, x_1^{1:\varepsilon_1-\beta_1+1}), \dots, (\beta_n, \varepsilon_n, x_n^{1:\varepsilon_n-\beta_n+1})\}) \\ & \quad \frac{dx_1^{1:\varepsilon_1-\beta_1+1}}{K^{\varepsilon_1-\beta_1+1}} \cdots \frac{dx_n^{1:\varepsilon_n-\beta_n+1}}{K^{\varepsilon_n-\beta_n+1}}. \end{aligned} \quad (\text{A.8})$$

Therefore, for the reference measure  $\mu(\cdot)$  in (A.3) and  $v_\gamma(\cdot)$  in (A.5), the measure theoretic integral corresponds to Mahler's set integral over sets of trajectories (8) but normalized by the units of the differential  $dx_1^{1:\varepsilon_1-\beta_1+1}, \dots, dx_n^{1:\varepsilon_n-\beta_n+1}$ , which are  $K^{\varepsilon_1-\beta_1+1}, \dots, K^{\varepsilon_n-\beta_n+1}$ . The relation between set integrals and measure theoretic integrals is similar in the single target case [58]. Therefore, if probability densities on sets of trajectories are defined with respect to the reference measure  $\mu(\cdot)$ , with  $v_\gamma(\cdot)$  given by (A.5), Mahler's multitrajectory densities are equivalent to measure theoretic densities, except for the normalizing units. Note that if the state space has no units, the measure theoretic integral and Mahler's set integral are alike.

## APPENDIX B

In this appendix, we proceed to explain how to use PGFLs, functional derivatives, and the fundamental theorem of multi-object calculus for RFSs of trajectories. These results are important as PGFLs are useful tools to derive filters. First, the prediction and update steps can be performed in the PGFL domain. Second, the fundamental theorem of multi-object calculus indicates how to recover the corresponding multi-object density from a PGFL, which requires functional derivatives. We explain PGFLs in Appendix E and functional derivatives in Appendix F. In Appendix G, we provide and prove the fundamental theorem of multi-object calculus for RFSs of trajectories.

### B1. Probability Generating Functionals

PGFLs for sets in LCHS spaces, such as the trajectory space, are defined in [6, Secs. 4.2.4 and 4.2.5]. Let  $h : \mathcal{T}_k \mapsto [0, 1]$  be a test function defined on the trajectory state space  $\mathcal{T}_k = \cup_{(\beta, \varepsilon) \in \mathcal{I}_k} \{\beta\} \times \{\varepsilon\} \times \mathcal{X}^{\varepsilon-\beta+1}$ . Let  $\mathbf{X}$  be an RFS of trajectories with multitrajectory density  $f(\cdot)$ , then its PGFL is

$$G_{\mathbf{X}}[h] = \mathbb{E}[h^{\mathbf{X}}] = \int h^{\mathbf{X}} f(\mathbf{X}) \delta \mathbf{X}, \quad (\text{B.1})$$

where

$$h^{\mathbf{X}} = \begin{cases} \prod_{X \in \mathbf{X}} h(X), & \mathbf{X} \neq \emptyset, \\ 1, & \mathbf{X} = \emptyset. \end{cases}$$

Note that both  $h(X)$  and the PGFL are unitless functions, i.e., functions whose output has no units.

### B2. Functional Derivatives

In this section, we explain (Volterra) functional derivatives for RFS of trajectories using FISST tools. We consider a unitless functional  $F[h]$  defined on unitless real-valued functions  $h(X)$  with  $X \in \mathcal{T}_k$ , e.g., a PGFL. Then, using FISST, the functional derivative of  $F[h]$  with respect to a finite subset  $\mathbf{Y} \in \mathcal{F}(\mathcal{T}_k)$  is defined to be [32,

Sec. 11.4]

$$\frac{\delta F}{\delta \mathbf{Y}}[h] = \begin{cases} F[h], & \mathbf{Y} = \emptyset, \\ \lim_{\varepsilon \rightarrow 0} \frac{F[h+\varepsilon \delta_Y] - F[h]}{\varepsilon}, & \mathbf{Y} = \{Y\}, \\ \frac{\delta^n F}{\delta Y_1 \cdots \delta Y_n}[h], & \mathbf{Y} = \{Y_1, \dots, Y_n\}, \end{cases} \quad (\text{B.2})$$

where the Dirac delta on the single trajectory space is

$$\begin{aligned} \delta_{(\beta', \varepsilon', y_{\beta': \varepsilon'})}(\beta, \varepsilon, x_{\beta: \varepsilon}) &= \begin{cases} \delta(x_{\beta: \varepsilon} - y_{\beta': \varepsilon'}), & \beta = \beta', \varepsilon = \varepsilon', \\ 0, & \beta \neq \beta', \varepsilon \neq \varepsilon', \end{cases} \end{aligned}$$

and we use the notational convention

$$\frac{\delta F}{\delta \{Y\}}[h] = \frac{\delta F}{\delta Y}[h].$$

Also, note that the Dirac delta on the single trajectory space meets the following identity:

$$\int \delta_Y(X) f(X) dX = f(Y).$$

We remark that the use of  $\delta_Y$  as the input of the functional is a tool of FISST that is not completely rigorous [6, p. 66], but admitted from a practical point of view. Set derivatives can be defined in terms of functional derivatives [6, p. 67].

### B3. Fundamental Theorem of Multi-Object Calculus

The fundamental theorem of multi-object calculus enables the recovery of a multi-object density from its PGFL [6, Sec. 3.5.1]. This result also applies to RFS of trajectories, and we provide a proof for completeness.

**Theorem 4.** *Given the PGFL  $G_{\mathbf{X}}[h]$  of an RFS  $\mathbf{X}$  of trajectories, we can recover its multitrajectory density  $f(\cdot)$  evaluated at  $\mathbf{Y}$  as*

$$f(\mathbf{Y}) = \left[ \frac{\delta G_{\mathbf{X}}}{\delta \mathbf{Y}}[h] \right]_{h=0}. \quad (\text{B.3})$$

The proof of this theorem is direct for  $\mathbf{Y} = \emptyset$  by substituting (B.2) into (B.1). For  $\mathbf{Y} \neq \emptyset$ , the theorem is a direct consequence of the following lemma.

**Lemma 1.** *The functional derivative of the PGFL  $G_{\mathbf{X}}[h]$  of an RFS  $\mathbf{X}$  of trajectories with respect to  $\mathbf{Y} = \{Y_1, \dots, Y_n\}$  is*

$$\frac{\delta^n G_{\mathbf{X}}}{\delta Y_1 \cdots \delta Y_n}[h] = \int h^{\mathbf{X}} f(\{Y_1, \dots, Y_n\} \cup \mathbf{X}) \delta \mathbf{X}, \quad (\text{B.4})$$

where  $f(\cdot)$  is its multitrajectory density.

The proof of Lemma 1 is given in Appendix G1. Then, by substituting  $h = 0$ , we directly obtain (B.3) for  $\mathbf{Y} \neq \emptyset$ . We also have

$$\left[ \frac{\delta G_{\mathbf{X}}}{\delta Y}[h] \right]_{h=1} = \int f(\{Y\} \cup \mathbf{X}) \delta \mathbf{X},$$

which represents the first-order moment, also called intensity and probability hypothesis density, as required.

### B3.1. Proof of Lemma 1

In this section, we prove (B.4) by using induction. In part I of the proof, we prove (B.4) for  $\mathbf{Y} = \{Y\}$ . Then, in part II, we prove the general case  $\mathbf{Y} = \{Y_1, \dots, Y_n\}$ .

#### B3.1.1. Part I of the proof

For  $\mathbf{Y} = \{Y\}$ , we proceed to prove that

$$\frac{\delta G_{\mathbf{X}}}{\delta Y} [h] = \int h^{\mathbf{X}} f(\{Y\} \cup \mathbf{X}) \delta \mathbf{X}.$$

For  $\mathbf{Y} = \{Y\}$ , we have

$$\begin{aligned} \frac{\delta G_{\mathbf{X}}}{\delta Y} [h] &= \lim_{\epsilon \rightarrow 0} \frac{G_{\mathbf{X}} [h + \epsilon \delta_Y] - G_{\mathbf{X}} [h]}{\epsilon} \\ &= \lim_{\epsilon \rightarrow 0} \frac{\int [h + \epsilon \delta_Y]^{\mathbf{X}} f(\mathbf{X}) \delta \mathbf{X} - \int [h]^{\mathbf{X}} f(\mathbf{X}) \delta \mathbf{X}}{\epsilon} \\ &= \lim_{\epsilon \rightarrow 0} \frac{\sum_{n=1}^{\infty} (1/n!) \int f(\{X_1, \dots, X_n\}) \times \dots}{\epsilon} \\ &\quad \times \frac{[\prod_{j=1}^n [h(X_j) + \epsilon \delta_Y(X_j)] - \prod_{j=1}^n h(X_j)] dX_{1:n}}{\epsilon}, \end{aligned}$$

where  $X_{1:n} = (X_1, \dots, X_n)$ . The limit can be computed by applying L'Hôpital's rule and taking derivatives with respect to  $\epsilon$ . This results in

$$\begin{aligned} \frac{\delta G_{\mathbf{X}}}{\delta Y} [h] &= \lim_{\epsilon \rightarrow 0} \sum_{n=1}^{\infty} \frac{1}{n!} \int \sum_{j=1}^n \left[ \delta_Y(X_j) \prod_{i=1, i \neq j}^n h(X_i + \epsilon \delta_Y(X_i)) \right] \\ &\quad \times f(\{X_1, \dots, X_n\}) dX_{1:n} \\ &= \sum_{n=1}^{\infty} \frac{1}{n!} \sum_{j=1}^n \int \left[ \delta_Y(X_j) \prod_{i=1, i \neq j}^n h(X_i) \right] \\ &\quad \times f(\{X_1, \dots, X_n\}) dX_{1:n}. \end{aligned}$$

The inner integral is the same for every  $j$ , so we can write

$$\begin{aligned} \frac{\delta G_{\mathbf{X}}}{\delta \{Y\}} [h] &= \sum_{n=1}^{\infty} \frac{1}{n!} n \int \left[ \delta_Y(X_1) \prod_{i=2}^n h(X_i) \right] \\ &\quad \times f(\{X_1, \dots, X_n\}) dX_{1:n} \\ &= \sum_{n=1}^{\infty} \frac{1}{(n-1)!} \int \left[ \prod_{i=2}^n h(X_i) \right] f(\{Y, X_2, \dots, X_n\}) dX_{2:n}. \end{aligned}$$

We further make the change of variables  $m = n - 1$  and  $X_{1:m}^* = X_{2:n}$  in the previous equation, which yields

$$\begin{aligned} \frac{\delta G_{\mathbf{X}}}{\delta \{Y\}} [h] &= \sum_{m=0}^{\infty} \frac{1}{m!} \int \left[ \prod_{i=1}^m h(X_i^*) \right] f(\{Y\} \cup \{X_1^*, \dots, X_m^*\}) dX_{1:m}^* \\ &= \int h^{\mathbf{X}} f(\{Y\} \cup \mathbf{X}) \delta \mathbf{X}. \end{aligned} \quad (\text{B.5})$$

#### B3.1.2. Part II of the proof

We proceed to prove (B.4) by induction. We assume that

$$\frac{\delta^{n-1} G_{\mathbf{X}}}{\delta Y_1 \dots \delta Y_{n-1}} [h] = \int h^{\mathbf{X}} f(\{Y_1, \dots, Y_{n-1}\} \cup \mathbf{X}) \delta \mathbf{X} \quad (\text{B.6})$$

holds and proceed to prove (B.4). Note that the relation holds for  $n = 1$ , as proved in the previous section. We denote

$$L[h] = \int h^{\mathbf{X}} l(\mathbf{X}) \delta \mathbf{X},$$

where

$$l(\mathbf{X}) = f(\{Y_1, \dots, Y_{n-1}\} \cup \mathbf{X}).$$

Then, by making use of (B.5), we obtain

$$\begin{aligned} \frac{\delta^n G_{\mathbf{X}}}{\delta Y_1 \dots \delta Y_n} [h] &= \frac{\delta}{\delta Y_n} L[h] \\ &= \int h^{\mathbf{X}} l(\{Y_n\} \cup \mathbf{X}) \delta \mathbf{X} \\ &= \int h^{\mathbf{X}} f(\{Y_1, \dots, Y_n\} \cup \mathbf{X}) \delta \mathbf{X}. \end{aligned}$$

This result completes the proof of Lemma 1.

## APPENDIX C

In this appendix, we present the MBM<sub>01</sub> filtering recursions for both the set of current trajectories and the set of all trajectories. The MBM<sub>01</sub> filtering recursions for the set of all trajectories were first given in [27]; they are presented here for completeness.

### C1. Prediction Step for the Set of Current Trajectories

The prediction step is given in the following theorem.

**Theorem 5.** Assume that the distribution from the previous time step  $f_{k-1|k-1}(\mathbf{X}_{k-1})$  is given by (20) with  $r_{k-1|k-1}^{i,a} \in \{0, 1\}$ , that the transition model is (12), and that the birth model is a trajectory multi-Bernoulli RFS with  $n_k^b$  Bernoulli components, each of which has density given by (10). Then, the predicted distribution for the next step  $f_{k|k-1}(\mathbf{X}_k)$  is given by (20) with  $r_{k|k-1}^{i,a} \in \{0, 1\}$  and  $n_{k|k-1} = n_{k-1|k-1} + n_k^b$ . For tracks continuing from previous time ( $i \in \{1, \dots, n_{k-1|k-1}\}$ ), a hypothesis is included for each combination of a hypothesis from a previous time and either a survival or a death. For new tracks

( $i \in \{n_{k-1|k-1} + l\}$ ,  $l \in \{1, \dots, n_k^b\}$ ), a hypothesis is included for each combination of a Bernoulli component in the multi-Bernoulli birth density and either born or not born. The number of hypotheses therefore becomes  $h_{k|k}^i = 2(h_{k-1|k-1}^i + n_k^b)$ .<sup>11</sup> For survival hypotheses ( $i \in \{1, \dots, n_{k-1|k-1}\}$ ,  $a^i \in \{1, \dots, h_{k-1|k-1}\}$ ), if  $r_{k-1|k-1}^{i,a^i} = 1$ , the parameters are

$$w_{k|k-1}^{i,a^i} = w_{k-1|k-1}^{i,a^i} \langle f_{k-1|k-1}^{i,a^i}; P_{k-1}^S \rangle, \quad (\text{C.1a})$$

$$r_{k|k-1}^{i,a^i} = 1, \quad (\text{C.1b})$$

$$f_{k|k-1}^{i,a^i}(X) = \langle f_{k-1|k-1}^{i,a^i}; \pi^c \rangle. \quad (\text{C.1c})$$

If  $r_{k-1|k-1}^{i,a^i} = 0$ , the parameters are

$$r_{k|k-1}^{i,a^i} = 0, \quad (\text{C.2a})$$

$$w_{k|k-1}^{i,a^i} = 0. \quad (\text{C.2b})$$

For death hypotheses ( $i \in \{1, \dots, n_{k-1|k-1}\}$ ,  $a^i = \tilde{a}^i + h_{k-1|k-1}^i$ ,  $\tilde{a}^i \in \{1, \dots, h_{k-1|k-1}^i\}$ ), the parameters are

$$w_{k|k-1}^{i,a^i} = w_{k-1|k-1}^{i,a^i} \langle f_{k-1|k-1}^{i,a^i}; 1 - P_{k-1}^S \rangle, \quad (\text{C.3a})$$

$$r_{k|k-1}^{i,a^i} = 0. \quad (\text{C.3b})$$

For birth hypotheses ( $i \in \{n_{k-1|k-1} + l\}$ ,  $l \in \{1, \dots, n_k^b\}$ ), the parameters are

$$\mathcal{M}^{k-1}(i, 1) = \emptyset, \quad (\text{C.4a})$$

$$w_{k|k-1}^{i,1} = r_k^{b,l}, \quad (\text{C.4b})$$

$$r_{k|k-1}^{i,1} = 1, \quad (\text{C.4c})$$

$$f_{k|k-1}^{i,1}(X) = f_k^{B,l}(X). \quad (\text{C.4d})$$

For nonbirth hypotheses ( $i \in \{n_{k-1|k-1} + l\}$ ,  $l \in \{1, \dots, n_k^b\}$ ), the parameters are

$$\mathcal{M}^{k-1}(i, 2) = \emptyset, \quad (\text{C.5a})$$

$$w_{k|k-1}^{i,2} = 1 - r_k^{b,l}, \quad (\text{C.5b})$$

$$r_{k|k-1}^{i,2} = 0. \quad (\text{C.5c})$$

Compared to the corresponding prediction steps (23) and (24) in the trajectory MBM filter, the MBM<sub>01</sub> parameterization entails an exponential increase in the number of global hypotheses.

## C2. Prediction Step for the Set of All Trajectories

The prediction step is given in the following theorem.

**Theorem 6.** Assume that the distribution from the previous time step  $f_{k-1|k-1}(\mathbf{X}_{k-1})$  is given by (20) with  $r_{k-1|k-1}^{i,a^i} \in \{0, 1\}$ , that the transition model is (13), and

<sup>11</sup>A hypothesis at the previous time with  $r_{k-1|k-1}^{i,a^i} = 0$  would be removed by setting its hypothesis weight to zero. For simplicity, the hypothesis numbering does not account for this exclusion.

that the birth model is a trajectory multi-Bernoulli RFS with  $n_k^b$  Bernoulli components, each of which has density given by (10). Then, the predicted distribution for the next step  $f_{k|k-1}(\mathbf{X}_k)$  is given by (20), with  $r_{k|k-1}^{i,a^i} \in \{0, 1\}$  and  $n_{k|k-1} = n_{k-1|k-1} + n_k^b$ . For tracks continuing from previous time ( $i \in \{1, \dots, n_{k-1|k-1}\}$ ), the number of hypotheses remains the same. For new tracks ( $i \in \{n_{k-1|k-1} + l\}$ ,  $l \in \{1, \dots, n_k^b\}$ ), a hypothesis is included for each combination of a Bernoulli component in the multi-Bernoulli birth density and either born or not born. The number of hypotheses therefore becomes  $h_{k|k}^i = h_{k-1|k-1}^i + 2n_k^b$ .

For hypotheses in tracks continuing from previous time ( $i \in \{1, \dots, n_{k-1|k-1}\}$ ,  $a^i \in \{1, \dots, h_{k-1|k-1}\}$ ), the parameters are

$$w_{k|k-1}^{i,a^i} = w_{k-1|k-1}^{i,a^i} \forall a^i, \quad (\text{C.6a})$$

$$r_{k|k-1}^{i,a^i} = 1, \quad (\text{C.6b})$$

$$f_{k|k-1}^{i,a^i}(X) = \langle f_{k-1|k-1}^{i,a^i}; \pi^a \rangle \forall a^i. \quad (\text{C.6c})$$

For new tracks ( $i \in \{n_{k-1|k-1} + l\}$ ,  $l \in \{1, \dots, n_k^b\}$ ), the parameters of MBM<sub>01</sub> parameterization are the same as (64) and (65).

## C3. Update Step

The update step is given in the following theorem.

**Theorem 7.** Assume that the predicted distribution  $f_{k|k-1}(\mathbf{X}_k)$  is given by (20) with  $r_{k|k-1}^{i,a^i} \in \{0, 1\}$ , that the measurement model is (15), and that the measurement set at time step  $k$  is  $\mathbf{z}_k = \{z_k^1, \dots, z_k^{m_k}\}$ . Then, the updated distribution  $f_{k|k}(\mathbf{X}_k)$  is given by (20), with  $r_{k|k}^{i,a^i} \in \{0, 1\}$  and  $n_{k|k} = n_{k|k-1}$ . For each track ( $i \in \{1, \dots, n_{k|k}\}$ ), a hypothesis is included for each combination of a hypothesis from a previous time with  $r_{k|k-1}^{i,a^i} = 1$  and either a misdetection or an update using one of the  $m_k$  new measurements, such that the number of hypotheses becomes  $h_{k|k}^i = h_{k|k-1}^i(1 + m_k)$ .<sup>12</sup> For misdetection hypotheses ( $i \in \{1, \dots, n_{k|k}\}$ ,  $a^i \in \{1, \dots, h_{k|k-1}\}$ ) with  $r_{k|k-1}^{i,a^i} = 1$ , the parameters are

$$\mathcal{M}^k(i, a^i) = \mathcal{M}^{k-1}(i, a^i), \quad (\text{C.7a})$$

$$w_{k|k}^{i,a^i} = w_{k|k-1}^{i,a^i} (1 - \langle f_{k|k-1}^{i,a^i}; P^D \rangle), \quad (\text{C.7b})$$

$$r_{k|k}^{i,a^i} = 1, \quad (\text{C.7c})$$

$$f_{k|k}^{i,a^i}(X) = \frac{(1 - P_k^D(X)) f_{k|k-1}^{i,a^i}(X)}{\langle f_{k|k-1}^{i,a^i}; 1 - P^D \rangle}. \quad (\text{C.7d})$$

For hypotheses updating tracks ( $i \in \{1, \dots, n_{k|k}\}$ ,  $a^i = \tilde{a}^i + h_{k|k-1}^i j$ ,  $\tilde{a}^i \in \{1, \dots, h_{k|k-1}^i\}$ ,  $j \in \{1, \dots, m_k\}$ , i.e.,

<sup>12</sup>A hypothesis at the previous time with  $r_{k|k-1}^{i,a^i} = 0$  must not be updated. For simplicity, the hypothesis numbering does not account for this exclusion.

the previous hypothesis  $\tilde{a}^i$ , updated with measurement  $z_k^j$  with  $r_{k|k-1}^{i,a^i} = 1$ , the parameters are

$$\mathcal{M}^k(i, a^i) = \mathcal{M}^{k-1}(i, \tilde{a}^i) \cup \{(k, j)\}, \quad (\text{C.8a})$$

$$w_{k|k}^{i,a^i} = \frac{w_{k|k-1}^{i,\tilde{a}^i} \langle f_{k|k-1}^{i,\tilde{a}^i}; \varphi(z_k^j | \cdot) P_k^D \rangle}{\lambda^{\text{FA}}(z_k^j)}, \quad (\text{C.8b})$$

$$r_{k|k}^{i,a^i} = 1, \quad (\text{C.8c})$$

$$f_{k|k}^{i,a^i}(X) = \frac{\varphi(z_k^j | X) P_k^D(X) f_{k|k-1}^{i,\tilde{a}^i}(X)}{\langle f_{k|k-1}^{i,\tilde{a}^i}; \varphi(z_k^j | \cdot) P_k^D \rangle}. \quad (\text{C.8d})$$

## REFERENCES

- [1] B.-N. Vo, M. Mallick, Y. Bar-Shalom, S. Coraluppi, R. Osborne, R. Mahler, and B.-T. Vo "Multitarget tracking," in *Wiley Encyclopedia of Electrical and Electronics Engineering*. Hoboken, NJ: Wiley, 2015.
- [2] T. Fortmann, Y. Bar-Shalom, and M. Scheffe "Sonar tracking of multiple targets using joint probabilistic data association," *IEEE J. Ocean. Eng.*, vol. 8, no. 3, pp. 173–184, 1983.
- [3] S. Blackman and R. Popoli *Design and Analysis of Modern Tracking Systems*. Norwood, MA: Artech House, 1999.
- [4] Y. Bar-Shalom, P. K. Willett, and X. Tian *Tracking and Data Fusion*. Storrs, CT: YBS Publishing, 2011.
- [5] S. S. Blackman "Multiple hypothesis tracking for multiple target tracking," *IEEE Aerosp. Electron. Syst. Mag.*, vol. 19, no. 1, pp. 5–18, 2004.
- [6] R. P. Mahler *Advances in Statistical Multisource–Multitarget Information Fusion*. Norwood, MA: Artech House, 2014.
- [7] S. Challa, M. R. Morelande, D. Mušicki, and R. J. Evans, *Fundamentals of Object Tracking*. Cambridge, U.K.: Cambridge University Press, 2011.
- [8] D. Musicki and R. Evans "Joint integrated probabilistic data association: JIPDA," *IEEE Trans. Aerosp. Electron. Syst.*, vol. 40, no. 3, pp. 1093–1099, 2004.
- [9] J. Williams and R. Lau "Approximate evaluation of marginal association probabilities with belief propagation," *IEEE Trans. Aerosp. Electron. Syst.*, vol. 50, no. 4, pp. 2942–2959, 2014.
- [10] F. Meyer, T. Kropfreiter, J. L. Williams, R. Lau, F. Hlawatsch, P. Braca, and M. Z. Win "Message passing algorithms for scalable multitarget tracking," *Proc. IEEE*, vol. 106, no. 2, pp. 221–259, 2018.
- [11] S. Mori, C.-Y. Chong, E. Tse, and R. Wishner "Tracking and classifying multiple targets without a priori identification," *IEEE Trans. Autom. Control*, vol. 31, no. 5, pp. 401–409, 1986.
- [12] D. Reid "An algorithm for tracking multiple targets," *IEEE Trans. Autom. Control*, vol. 24, no. 6, pp. 843–854, 1979.
- [13] C. Morefield "Application of 0–1 integer programming to multitarget tracking problems," *IEEE Trans. Autom. Control*, vol. 22, no. 3, pp. 302–312, 1977.
- [14] T. Kurien, "Issues in the design of practical multitarget tracking algorithms," in *Multitarget–Multisensor Tracking: Advanced Applications*. Norwood, MA: Artech House, 1990, pp. 43–87.
- [15] A. B. Poore and A. J. Robertson III "A new Lagrangian relaxation based algorithm for a class of multidimensional assignment problems," *Comput. Optim. Appl.*, vol. 8, no. 2, pp. 129–150, 1997.
- [16] S. Deb, M. Yeddanapudi, K. Pattipati, and Y. Bar-Shalom "A generalized SD assignment algorithm for multisensor–multitarget state estimation," *IEEE Trans. Aerosp. Electron. Syst.*, vol. 33, no. 2, pp. 523–538, 1997.
- [17] R. A. Lau and J. L. Williams, "Multidimensional assignment by dual decomposition," in *Proc. 7th Int. Conf. Intell. Sensors, Sensor Netw. Inf. Process.*, 2011, pp. 437–442.
- [18] S. Coraluppi and C. Carthel, "Modified scoring in multiple-hypothesis tracking," *J. Adv. Inf. Fusion*, vol. 7, no. 2, pp. 153–164, 2012.
- [19] S. Mori, C.-Y. Chong, and K.-C. Chang, "Three formalisms of multiple hypothesis tracking," in *Proc. 19th Int. Conf. Inf. Fusion*, 2016, pp. 727–734.
- [20] E. Brekke and M. Chitre "Relationship between finite set statistics and the multiple hypothesis tracker," *IEEE Trans. Aerosp. Electron. Syst.*, vol. 54, no. 4, pp. 1902–1907, 2018.
- [21] B.-T. Vo and B.-N. Vo "Labeled random finite sets and multi-object conjugate priors," *IEEE Trans. Signal Process.*, vol. 61, no. 13, pp. 3460–3475, 2013.
- [22] J. L. Williams "Marginal multi-Bernoulli filters: RFS derivation of MHT, JIPDA, and association-based member," *IEEE Trans. Aerosp. Electron. Syst.*, vol. 51, no. 3, pp. 1664–1687, 2015.
- [23] Á. F. García-Fernández, J. L. Williams, K. Granström, and L. Svensson "Poisson multi-Bernoulli mixture filter: Direct derivation and implementation," *IEEE Trans. Aerosp. Electron. Syst.*, vol. 54, no. 4, pp. 1883–1901, 2018.
- [24] Á. F. García-Fernández, Y. Xia, K. Granström, L. Svensson, and J. Williams, "Gaussian implementation of the multi-Bernoulli mixture filter," in *Proc. 22nd Int. Conf. Inf. Fusion*, 2019.
- [25] Á. F. García-Fernández, J. Grajal, and M. R. Morelande "Two-layer particle filter for multiple target detection and tracking," *IEEE Trans. Aerosp. Electron. Syst.*, vol. 49, no. 3, pp. 1569–1588, 2013.
- [26] E. H. Aoki, P. K. Mandal, L. Svensson, Y. Boers, and A. Bagchi "Labeling uncertainty in multitarget tracking," *IEEE Trans. Aerosp. Electron. Syst.*, vol. 52, no. 3, pp. 1006–1020, 2016.
- [27] Á. F. García-Fernández, L. Svensson, and M. R. Morelande, "Multiple target tracking based on sets of trajectories," *IEEE Trans. Aerosp. Electron. Syst.*, 2019. Available: <https://ieeexplore.ieee.org/document/8731733>.
- [28] B.-N. Vo, B.-T. Vo, and D. Phung "Labeled random finite sets and the Bayes multi-target tracking filter," *IEEE Trans. Signal Process.*, vol. 62, no. 24, pp. 6554–6567, 2014.
- [29] S. Reuter, B.-T. Vo, B.-N. Vo, and K. Dietmayer "The labeled multi-Bernoulli filter,"

- IEEE Trans. Signal Process.*, vol. 62, no. 12, pp. 3246–3260, 2014.
- [30] L. Svensson and M. Morelande, “Target tracking based on estimation of sets of trajectories,” in *Proc. 17th Int. Conf. Inf. Fusion*, 2014.
- [31] K. Granström, L. Svensson, Y. Xia, J. Williams, and Á. F. García-Fernández, “Poisson multi-Bernoulli mixture trackers: Continuity through random finite sets of trajectories,” in *Proc. 21st Int. Conf. Inf. Fusion*, 2018.
- [32] R. P. Mahler  
*Statistical Multisource–Multitarget Information Fusion*. Norwood, MA: Artech House, 2007.
- [33] K. Murthy  
“An algorithm for ranking all the assignments in order of increasing costs,”  
*Oper. Res.*, vol. 16, no. 3, pp. 682–687, 1968.
- [34] Y. Xia, K. Granström, L. Svensson, and Á. F. García-Fernández, “An implementation of the Poisson multi-Bernoulli mixture trajectory filter via dual decomposition,” in *Proc. 21st Int. Conf. Inf. Fusion*, 2018.
- [35] B.-N. Vo, B.-T. Vo, and H. G. Hoang  
“An efficient implementation of the generalized labeled multi-Bernoulli filter,”  
*IEEE Trans. Signal Process.*, vol. 65, no. 8, pp. 1975–1987, 2017.
- [36] S. Mori and C.-Y. Chong, “Evaluation of data association hypotheses: Non-Poisson iid cases,” in *Proc. 7th Int. Conf. Inf. Fusion*, 2004, pp. 1133–1140.
- [37] S. Coraluppi and C. A. Carthel  
“If a tree falls in the woods, it does make a sound: Multiple-hypothesis tracking with undetected target births,”  
*IEEE Trans. Aerosp. Electron. Syst.*, vol. 50, no. 3, pp. 2379–2388, 2014.
- [38] Á. F. García-Fernández and L. Svensson, “Trajectory probability hypothesis density filter,” in *Proc. 21st Int. Conf. Inf. Fusion*, IEEE, 2018, pp. 1430–1437.
- [39] Á. F. García-Fernández and L. Svensson  
“Trajectory PHD and CPHD filters,”  
*IEEE Trans. Signal Process.*, vol. 67, no. 22, pp. 5702–5714, 2019.
- [40] H. A. Blom and Y. Bar-Shalom  
“The interacting multiple model algorithm for systems with Markovian switching coefficients,”  
*IEEE Trans. Autom. Control*, vol. 33, no. 8, pp. 780–783, 1988.
- [41] K. Granström, P. Willett, and Y. Bar-Shalom  
“Systematic approach to IMM mixing for unequal dimension states,”  
*IEEE Trans. Aerosp. Electron. Syst.*, vol. 51, no. 4, pp. 2975–2986, 2015.
- [42] K. Granstrom, M. Fatemi, and L. Svensson  
“Poisson multi-Bernoulli mixture conjugate prior for multiple extended target filtering,”  
*IEEE Trans. Aerosp. Electron. Syst.*, 2019. Available: <https://ieeexplore.ieee.org/document/8730493>
- [43] Y. Xia, K. Granström, L. Svensson, Á. F. García-Fernández, and J. Williams, “Extended target Poisson multi-Bernoulli mixture trackers based on sets of trajectories,” in *Proc. 22nd Int. Conf. Inf. Fusion*, 2019.
- [44] N. Komodakis, N. Paragios, and G. Tziritas  
“MRF energy minimization and beyond via dual decomposition,”  
*IEEE Trans. Pattern Anal. Mach. Intell.*, vol. 33, no. 3, pp. 531–552, 2011.
- [45] Y. Bar-Shalom  
*Multitarget–Multisensor Tracking: Advanced Applications*. Norwood, MA, Artech House, 1990.
- [46] B. Polyak, “Subgradient methods: A survey of soviet research,” in *Proc. IIASA Workshop Nonsmooth Optim.*, 1978, pp. 5–30.
- [47] E. L. Lawler and D. E. Wood  
“Branch-and-bound methods: A survey,”  
*Oper. Res.*, vol. 14, no. 4, pp. 699–719, 1966.
- [48] W. Koch and F. Govaers  
“On accumulated state densities with applications to out-of-sequence measurement processing,”  
*IEEE Trans. Aerosp. Electron. Syst.*, vol. 47, no. 4, pp. 2766–2778, 2011.
- [49] R. M. Eustice, H. Singh, and J. J. Leonard  
“Exactly sparse delayed-state filters for view-based slam,”  
*IEEE Trans. Robot.*, vol. 22, no. 6, pp. 1100–1114, 2006.
- [50] S. Reuter, A. Danzer, M. Stübler, A. Scheel, and K. Granström  
“A fast implementation of the labeled multi-Bernoulli filter using Gibbs sampling,” in *Proc. Symp. Intell. Veh.*, IEEE, 2017, pp. 765–772.
- [51] A. S. Rahmathullah, Á. F. García-Fernández, and L. Svensson, “Generalized optimal sub-pattern assignment metric,” in *Proc. 20th Int. Conf. Inf. Fusion*, 2017, pp. 1–8.
- [52] A. S. Rahmathullah, Á. F. García-Fernández, and L. Svensson, “A metric on the space of finite sets of trajectories for evaluation of multi-target tracking algorithms,” arXiv:1605.01177, 2016.
- [53] G. F. Simmons, *Topology and Modern Analysis*. New York, NY: McGraw-Hill, 1963.
- [54] I. S. Molchanov, *Theory of Random Sets*. New York, NY: Springer, 2005.
- [55] R. Mahler and A. El-Fallah  
“CPHD and PHD filters for unknown backgrounds, part III: tractable multitarget filtering in dynamic clutter,” in *Signal and Data Processing of Small Targets 2010*, vol. 7698, O. E. Drummond, Ed., Bellingham, WA: SPIE, 2010, pp. 177–188.
- [56] R. P. Mahler, B.-T. Vo, and B.-N. Vo  
“CPHD filtering with unknown clutter rate and detection profile,”  
*IEEE Trans. Signal Process.*, vol. 59, no. 8, pp. 3497–3513, 2011.
- [57] G. Grimmett and D. Stirzaker  
*Probability and Random Processes*. Oxford, U.K.: Oxford University Press, 2001.
- [58] B.-N. Vo, S. Singh, and A. Doucet  
“Sequential Monte Carlo methods for multitarget filtering with random finite sets,”  
*IEEE Trans. Aerosp. Electron. Syst.*, vol. 41, no. 4, pp. 1224–1245, 2005.
- [59] G. Matheron, *Random Sets and Integral Geometry*. Hoboken, NJ: Wiley, 1975.
- [60] P. Billingsley, *Probability and Measure*. Hoboken, NJ: Wiley, 2008.



**Yuxuan Xia** was born in Wuhan, China, in 1993. He received the B.Sc. degree in engineering of Internet of Things from the Jiangnan University, Wuxi, China, in 2015, and the M.Sc. degree in communication engineering from Chalmers University of Technology, Gothenburg, Sweden, in 2017. He is currently working toward the Ph.D. degree at the Department of Electrical Engineering, Chalmers University of Technology. His research interests include Bayesian inference in general, and target tracking in particular.



**Karl Granström** (M'08) received the M.Sc. degree in applied physics and electrical engineering and the Ph.D. degree in automatic control from Linköping University, Linköping, Sweden, in 2008 and 2012, respectively. He is currently a Postdoctoral Research Fellow with the Department of Signals and Systems, Chalmers University of Technology, Gothenburg, Sweden. He previously held postdoctoral positions with the Department of Electrical and Computer Engineering, University of Connecticut, Storrs, CT, USA, from September 2014 to August 2015, and with the Department of Electrical Engineering, Linköping University, from December 2012 to August 2014. His research interests include estimation theory, multiple model estimation, sensor fusion, and target tracking, especially for extended targets. He was the recipient of paper awards at the Fusion 2011 and Fusion 2012 conferences. In 2018, the International Society of Information Fusion (ISIF) awarded him the ISIF Young Investigator Award for his contributions to extended object tracking and his service to the research community.



**Lennart Svensson** was born in Älvängen, Sweden, in 1976. He received the M.S. degree in electrical engineering and the Ph.D. degree from Chalmers University of Technology, Gothenburg, Sweden, in 1999 and 2004, respectively. He is currently a Professor of Signal Processing with Chalmers University of Technology. His main research interests include machine learning and Bayesian inference in general, and nonlinear filtering, deep learning, and tracking in particular. He has organized a massive open online course on multiple object tracking, available on edX and YouTube, and was the recipient of paper awards at the International Conference on Information Fusion in 2009, 2010, 2017, and 2019.



**Ángel F. García-Fernández** received the M.Sc. degree in telecommunication engineering and the Ph.D. degree from the Universidad Politécnica de Madrid, Madrid, Spain, in 2007 and 2011, respectively. He is currently a Lecturer with the Department of Electrical Engineering and Electronics, University of Liverpool, Liverpool, U.K. He previously held Postdoctoral positions with the Universidad Politécnica de Madrid, Chalmers University of Technology, Gothenburg, Sweden, Curtin University, Perth, WA, Australia, and Aalto University, Espoo, Finland. His main research activities and interests are in the area of Bayesian nonlinear inference, with emphasis on dynamic systems and multiple target tracking. He was the recipient of paper awards at the International Conference on Information Fusion in 2017 and 2019.



**Jason L. Williams** (S'01–M'07–SM'16) received BE (electronics)/BInfTech degree from Queensland University of Technology, Brisbane, Australia in 1999, the MSEE degree from the United States Air Force Institute of Technology, Wright-Patterson AFB, OH, USA in 2003, and the Ph.D. degree from Massachusetts Institute of Technology, Cambridge, MA, USA in 2007. He is currently a Senior Research Scientist in Robotic Perception with the Robotics and Autonomous Systems Group of Commonwealth Scientific and Industrial Research Organisation, Brisbane, Australia. His research interests include SLAM, computer vision, multiple object tracking, and motion planning. He is also an Adjunct Associate Professor with Queensland University of Technology. He previously worked in sensor fusion and resource management as a Senior Research Scientist with the Defence Science and Technology Group, Australia, and in electronic warfare as an Engineering Officer with the Royal Australian Air Force.



# INTERNATIONAL SOCIETY OF INFORMATION FUSION

ISIF Website: <http://www.isif.org>

## 2019 BOARD OF DIRECTORS\*

2017–2019	2018–2020	2019–2021
Wolfgang Koch	Fredrik Gustafsson	Kathryn Laskey
Simon Godsill	X. Rong Li	Felix Govaers
Murat Efe	Zhansheng Duan	Simon Maskell

\*Board of Directors are elected by the members of ISIF for a three year term.

## PAST PRESIDENTS

Lyudmila Mihaylova, 2018	Joachim Biermann, 2011	Chee Chong, 2004
Lyudmila Mihaylova, 2017	Stefano Coraluppi, 2010	Xiao-Rong Li, 2003
Jean Dezert, 2016	Elisa Shahbazian, 2009	Yaakov Bar-Shalom, 2002
Darin Dunham, 2015	Darko Musicki, 2008	Pramod Varshney, 2001
Darin Dunham, 2014	Erik Blasch, 2007	Yaakov Bar-Shalom, 2000
Wolfgang Koch, 2013	Pierre Valin, 2006	Jim Llinas, 1999
Roy Streit, 2012	W. Dale Blair, 2005	Jim Llinas, 1998

## SOCIETY VISION

The International Society of Information Fusion (ISIF) is the premier professional society and global information resource for multidisciplinary approaches for theoretical and applied information fusion technologies.

## SOCIETY MISSION

### Advocate

To advance the profession of fusion technologies, propose approaches for solving real-world problems, recognize emerging technologies, and foster the transfer of information.

### Serve

To serve its members and engineering, business, and scientific communities by providing high-quality information, educational products, and services.

### Communicate

To create international communication forums and hold international conferences in countries that provide for interaction of members of fusion communities with each other, with those in other disciplines, and with those in industry and academia.

### Educate

To promote undergraduate and graduate education related to information fusion technologies at universities around the world. Sponsor educational courses and tutorials at conferences.

### Integrate

Integrate ideas from various approaches for information fusion, and look for common threads and themes—look for overall principles, rather than a multitude of point solutions. Serve as the central focus for coordinating the activities of world-wide information fusion related societies or organizations. Serve as a professional liaison to industry, academia, and government.

### Disseminate

To propagate the ideas for integrated approaches to information fusion so that others can build on them in both industry and academia.

## Call for Papers

The Journal of Advances in Information Fusion (JAIF) seeks original contributions in the technical areas of research related to information fusion. Authors are encouraged to submit their manuscripts for peer review <http://isif.org/journal>.

## Call for Reviewers

The success of JAIF and its value to the research community is strongly dependent on the quality of its peer review process. Researchers in the technical areas related to information fusion are encouraged to register as a reviewer for JAIF at <http://jaif.msubmit.net>. Potential reviewers should notify via email the appropriate editors of their offer to serve as a reviewer.